Powered Lower Limb Prostheses

Angetriebene Prothesen für die untere Extremität
Zur Erlangung des Grades eines Doktors der Naturwissenschaften (Dr. rer. nat.)
genehmigte Dissertation von Dipl.-Sportwiss. Martin Grimmer aus Gera
Tag der Einreichung: 10. Dezember 2014, Tag der Prüfung: 05. Februar 2015
Darmstadt — D 17, Darmstadt 2015

1. Gutachten: Prof. Dr. André Seyfarth
2. Gutachten: Prof. Dr. Thomas Sugar

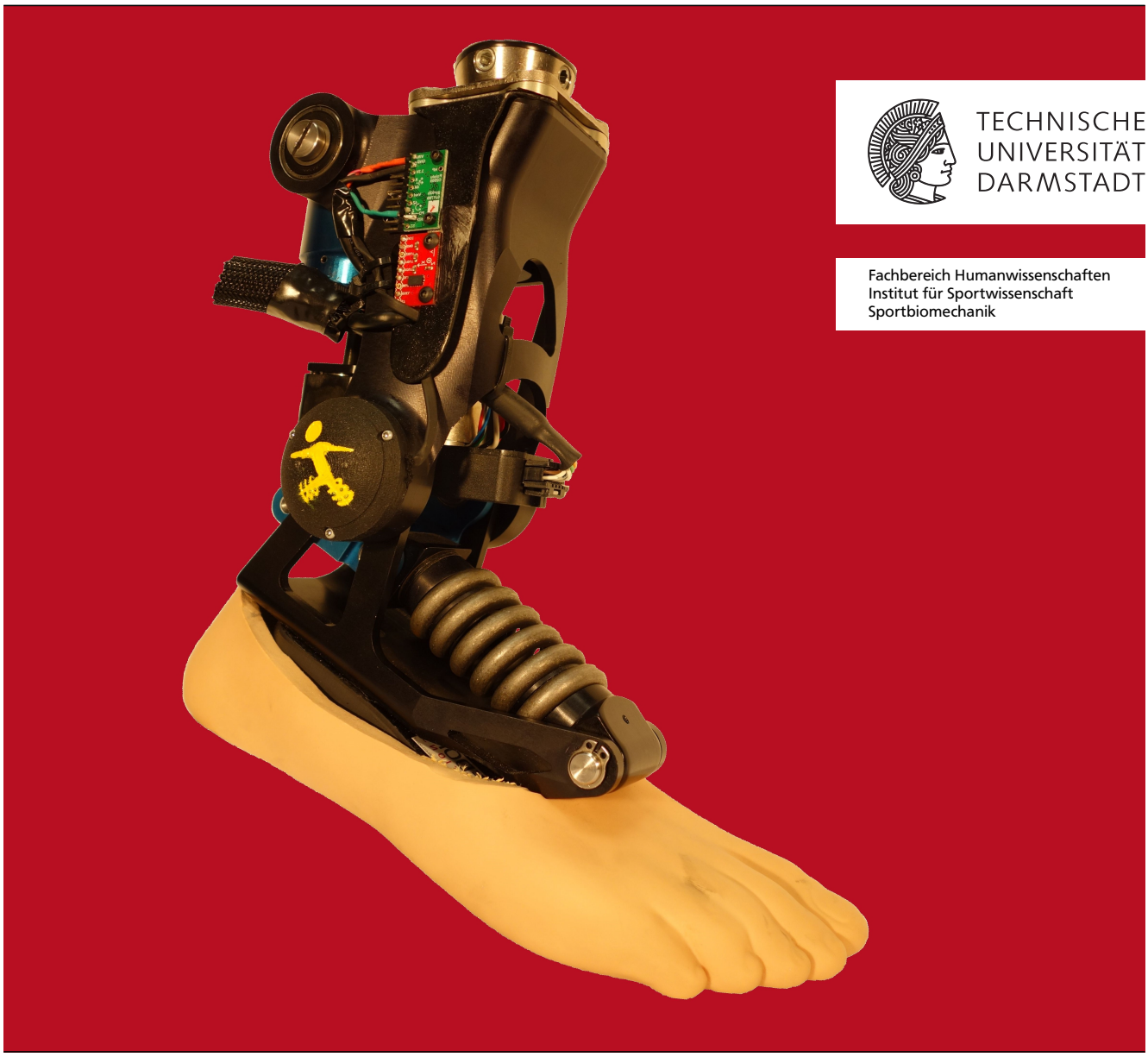

TECHNISCHE UNIVERSITÄT DARMSTADT

Fachbereich Humanwissenschaften
Institut für Sportwissenschaft
Sportbiomechanik

Powered Lower Limb Prostheses
Angetriebene Prothesen für die untere Extremität

Genehmigte Dissertation von Dipl.-Sportwiss. Martin Grimmer aus Gera

1. Gutachten: Prof. Dr. André Seyfarth
2. Gutachten: Prof. Dr. Thomas Sugar

Tag der Einreichung: 10. Dezember 2014
Tag der Prüfung: 05. Februar 2015

Darmstadt — D 17

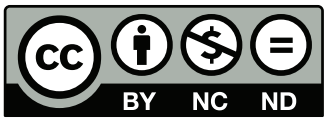

Erklärung zur Dissertation

Hiermit versichere ich, die vorliegende Dissertation ohne Hilfe Dritter nur mit den angegebenen Quellen und Hilfsmitteln angefertigt zu haben. Alle Stellen, die aus Quellen entnommen wurden, sind als solche kenntlich gemacht. Diese Arbeit hat in gleicher oder ähnlicher Form noch keiner Prüfungsbehörde vorgelegen.

Darmstadt, den 10. Dezember 2014

_____

Martin Grimmer

Zusammenfassung

Der aufrechte Gang des Menschen entstand vor etwa 6 Millionen Jahren. Er wird durch eine komplexe Interaktion von Körperaufbau und Gangkontrolle ermöglicht. Knochen, Muskeln, Sehen, zentralnervöse Befehle und Reflexmechanismen befähigen zu einer robusten und effizienten zweibeinigen Fortbewegung wie dem Gehen und Rennen. Neben diesen Arten der Fortbewegung sind dem Menschen auch komplexe Bewegungen wie Klettern, Tanzen oder Springen möglich. Die Identifikation der relevanten Grundprinzipien des Baus und der Kontrolle seines Bewegungsapparates kann bei der Konstruktion von zweibeinigen Robotern, Exoskeletten, Orthesen und Prothesen helfen. Krankheiten oder Unfälle können zum Verlust von Teilen der unteren Extremität oder deren Ansteuerung führen. Der älteste Bericht über ein künstliches Bein ist etwa 5000 Jahre alt und beschreibt den Verlust eines Beines von Königin Vishpla. Um auf das Schlachtfeld zurückzukehren, wurde sie mit einem eisernen Bein versorgt. Seit dieser Zeit haben Fortschritte den Aufbau, das Material und die Funktion prothetischer Versorgungen deutlich verbessert. Zunehmend werden biologische Wirkmechanismen durch technische Komponenten imitiert. Die Verwendung von Kohlefasern in Prothesenfüßen ermöglicht eine Unterstützung im Gang durch den elastischen Rückstoß vergleichbar einer Achillessehne. Dämpfer in Knieprothesen ermöglichen die Abbildung von exzentrischer Muskelarbeit im Gang. Kupplungsmechanismen werden zum Blockieren der Kniebeugung im Stand eingesetzt. Diese Funktion ist vergleichbar mit isometrischer Muskelarbeitsweise. Semi-aktive Kniegelenke erlauben eine Variation der Dämpfung und passen ihre Systemeigenschaften den Anforderungen an. Unter Zuhilfenahme der eingebauten Kraft- oder Inertialsensoren kann die Bewegungsabsicht identifiziert werden. So wird eine Anpassung der Dämpfung auf verschiedene Gehgeschwindigkeiten, auf Steigungen oder Treppen möglich.

All diese Entwicklungen haben das Gangbild der Amputierten näher an das natürliche Gangbild herangeführt. Jedoch war keines der Systeme in der Lage konzentrische Muskelarbeit abzubilden. Die bereitgestellte positive Muskelarbeit wird benötigt, um Energieverluste bei der Fortbewegung auszugleichen. Zum Steigen von Treppen und Begehen von Steigungen muss nicht nur das Sprunggelenk, sondern auch das Kniegelenk positive Arbeit zum Anheben des Körperschwerpunktes verrichten. Zur Umsetzung der angestrebten Gelenkbewegung ist ein Antrieb nötig, welcher einen Energieeintrag ermöglicht und damit die konzentrische Funktionsweise von Muskelfasern nachbilden kann.

Die Dissertation analysiert Gelenkanforderungen, evaluiert aktuelle prothetische Konzepte und entwickelt Modelle für künstliche Muskeln, um die Biomechanik der unteren Extremitäten beim Gehen und Rennen abzubilden. Die entwickelten Modelle sind biologisch inspiriert, wobei Motoren die Funktion von Muskelfasern und Federn die Funktion von Sehnen nachbilden. Die Systeme sind dabei nach Kriterien wie einer minimalen Motorleistung oder einem minimalen Energieverbrauch optimiert. Die Resultate zeigen, dass elastische Strukturen deutlich zur Reduzierung von Motoranforderungen beitragen können. Federn sind in der Lage, Energie in einer Phase des Gangzyklus aufzunehmen, um diese dann bei hohen Anforderungen wieder abzugeben. Ohne die elastische Unterstützung ist das Nachahmen des menschlichen Gelenkverhaltens mit aktueller Motorentechnologie nur eingeschränkt möglich. Die im Model optimierte Interaktion von Motor und Feder wird mit einer angetriebenen Fußprothese (Walk-Run ankle, Springactive) beim Gehen und Rennen untersucht. Neben Experimenten mit einem Nichtamputierten,

bei dem die Prothese parallel zu einem fixierten Sprunggelenk angebracht war (Bypass), wurden auch Studien mit einer einseitig Unterschenkelamputierten durchgeführt. Das optimierte Modellverhalten zeigt eine gute Übereinstimmung mit den experimentellen Daten. Ein Konzept zur Verbesserung eines optimierten Motorverhaltens wurde erfolgreich geprüft. Durch die Vereinfachung der Motortrajektorie auf grundlegende Verlaufsmerkmale (Filter) war es möglich die mechanische Energieabgabe und die Effizienz der Prothese zu steigern und den elektrischen Energieaufwand und die Geräuschemission zu reduzieren.

Um das Verhalten der Prothese weiter zu verbessern sollten das Timing für den Fußabdruck und Gründe für die Geräuschemission analysiert werden. Eine Gewichtsreduktion und psychoakustische Analysen können helfen die Akzeptanz bei Amputierten zu erhöhen. Zusätzlich müssen Trainingseffekte bei der Nutzung von aktiven Prothesen untersucht werden. Um den Leistungsbedarf und den Energieverbrauch zusätzlich zu reduzieren ist eine Steigerung der Effizienz von aktiven Prothesen sinnvoll. Dies kann durch effizientere Komponenten und durch eine Optimierung des Interaktionsverhaltens zwischen Prothese und Prothesennutzer erreicht werden. Die Mensch - Maschine Interaktion ist von der bereitgestellten Mechanik und dem Ansteuerungskonzept abhängig. Vergleichbar mit zweigelenkigen Muskeln könnte eine Kopplung von gesunden zu künstlichen Gelenken zusätzliche Vorteile bringen. Bei Oberschenkelamputierten wäre solch eine Kopplung auch zwischen dem künstlichen Knie- und dem künstlichen Sprunggelenk möglich. Muskeln von existierenden proximalen Gelenken wären in der Lage, Energie zu den distalen Gelenken zu übertragen. Durch die geometrisch bedingte Verspannung könnte der Aufwand für die grundlegende Beinkontrolle beim Gang reduziert werden.

Die Ergebnisse der Dissertation, zur effizienten Interaktion von Motoren und Federn, können zur Verbesserung vom Aufbau und der Ansteuerung angetriebener Prothesen beitragen. Vergleichbare Konzepte können aber auch zur Verbesserung von Exoskeletten eingesetzt werden. Diese könnten ältere Mitmenschen und Personen mit Mobilitätseinschränkungen bei der Fortbewegung unterstützen. Eine Verstärkung der menschlichen Physis für den Alltag oder das Arbeitsumfeld wäre denkbar. Neben der Unterstützung des Menschen könnten elastische Aktuatoren zudem das Gangverhalten, die Robustheit und die Laufzeit von zweibeinigen Robotern verbessern. Damit sind die Ergebnisse der Arbeit *Powered Lower Limb Prostheses - Angetriebene Prothesen für die untere Extremität* nicht nur auf das Anwendungsfeld der Prothetik limitiert sondern auch relevant für die Entwicklung von Exoskeletten und Robotern.

Abstract

Human upright locomotion emerged about 6 million years ago. It is achieved by a complex interaction of the biological infrastructure and the neural control. Bones, muscles, tendons, central nervous commands and reflex mechanisms interact to provide robust and efficient bipedal movement patterns like walking or running. Next to these locomotion tasks humans can also perform complex movements like climbing, dancing or jumping. Diseases or traumatic events may cause the loss of parts of the biological infrastructure or the ability to control the lower limbs. Thus an identification of the required framework helps to improve on the artificial lower limb design and the control for bipedal robots, exoskeletons, orthoses or prostheses. A first artificial leg design was reported about 5000 years ago. After losing one leg in a battle an iron leg was fitted to Queen Vishpla to get her back on the battlefield. Since this time major changes in the structure, the material and the functionality led to improved prosthetic restoration of physically disabled. The characteristics of the biological leg structure are imitated by technical components. Using carbon fiber for the design of prosthetic feet made it possible to benefit from the elastic recoil like in the Achilles tendon in stance phase. Dampers in prosthetic knee joints are able to mimic eccentric muscle work during the gait cycle. Clutch-like mechanisms are used to lock the knee during stance. Such a function is comparable to isometric muscle work. Semi-active knee joints allow changes in damping ratio to adapt the mechanical joint properties to the requirements. Using integrated force or inertial sensors, movement tasks can be identified. An adaptation of damping to different walking speeds and conditions, such as walking inclines, declines, or climbing stairs is possible.

All these developments permitted that amputees gait got closer to the natural human gait pattern. However, until the end of the 20th century prostheses were not able to reproduce concentric muscle work. External positive energy is required to compensate for energy losses during locomotion. For climbing stairs or walking inclines not only the ankle, but also the knee joint contributes net positive work to lift the body center of mass. To achieve desired joint motion, a power source like a motor would be required that can inject energy to mimic the concentric function of the muscle fascicles.

The thesis comprises an analysis of joint requirements, it evaluates the current prosthetic design approaches and develops models on artificial muscles to mimic lower limb biomechanics in walking and running. The developed models are biologically inspired, while motors represent the function of muscle fibers and springs represent the function of the tendons. These systems are optimized for criteria like minimum joint peak power or minimum required energy for the power source (motor). Results demonstrate that elastic elements can highly decrease the actuator requirements. The springs are able to store energy in one phase of the gait cycle and to release it later when high peak power is required. Without the elastic assistance the reproduction of human joint behavior is hardly possible using current motor technology. The optimized interaction of motor and elasticity is evaluated in walking and running, using a prototype of a powered ankle prosthesis (Walk-Run ankle, Springactive). Next to experiments with a non-amputee, where the prosthesis was fitted in parallel to the fixed healthy ankle joint (Bypass), also experiments with a female unilateral transtibial amputee were performed. The optimized model behavior was compared to experimental observations and showed good agreement.

Furthrmore, a concept on the improvement of an optimized walking motor pattern was successfully tested. By smoothening the motor curve to the main characteristics (low-pass filter) it was possible to increase the mechanical work output, to improve the system efficiency, and to decrease the electrical energy consumption and the noise.

To further improve the prosthetic performance, the push off timing and the causes for prosthesis noise should be analyzed. Weight reductions and psychoacoustic analysis can additionally help to improve on the amputees acceptance. In addition it must be evaluated how training can effect amputees gait patterns when using powered prostheses. To further reduce the power and the energy requirements, an improvement on the powered prosthesis efficiency is recommended. The efficiency can be further increased by using higher efficiency parts and improving the interaction of the prosthesis and the amputee. The human - machine interaction depends on the prosthesis mechanics and the control algorithm. Similar to the human biarticular muscles, couplings from biological to artificial joints may provide additional benefits for the amputee. The muscles from existing proximal joints would be able to transfer energy to the distal artificial joints. Also the inverse of this principle would be possible. A coupling between the hip and the knee (transfemoral amputees) and between the knee and the ankle (transfemoral and transtibial amputees) would be possible. Due to geometrical constraints, the elemental locomotion control might improve.

The results of the thesis, on the efficient cooperation of motors and springs, can be used to improve the design and the control of powered lower limb prostheses. Similar technologies can be used to improve on exoskeleton design to assist elderly and subjects with mobility impairments. Elastic exoskeletons may also augment human performance in daily life or workers environments. Next to assisting the human movement, the elastic actuators may advance the gait performance, the gait robustness, and the operation time of bipedal robots. Thus the results of the thesis *Powered Lower Limb Prostheses* are not limited to the specific field of prosthetics but may also be useful for applications like exoskeletons and legged robots.

Inhaltsverzeichnis

1 Introduction and Motivation

Current state of the art lower limb prosthetic technology allows amputees to master most daily life tasks. However, compared to non-amputees the metabolic energy consumption and thus the movement effort is increased (Waters and Mulroy, 1999). Studies on the locomotion patterns show clear differences between non-amputees and amputees (Schaarschmidt et al., 2012; Waters and Mulroy, 1999). The differences in joint kinematics and kinetics increase with the increased level of amputation (Waters and Mulroy, 1999). Long term sequelae like back pain or arthritis might be caused by asymmetric gait and the dominating use of the intact limb for unilateral amputees (Gailey et al., 2008; Robbins et al., 2009). At the end of the last century two major developments improved amputee walking performance. The development of passive elastic carbon feet (e.g. Seattle foot) in the early 80s, made it possible to recover stored elastic energy from the leaf spring during push off (Czerniecki et al., 1991). Especially for running, the elastic prosthetic feet like the Flex-Foot Cheetah (Ossur) enable achieving almost non-amputee running performance (Brüggemann et al., 2008).

Mechanical knee joints for transfemoral amputees made a huge step in performance and safety when introducing the semi-active devices like the C-Leg or the Genium knee (both Ottobock) (Blumentritt et al., 2012). Sensors and micro controllers allow gait detection and adaptations to walking speed by changing the rate of damping in the artificial knee. In addition, these prostheses can prevent falls that occured in the previous generation of passive knee joints (Blumentritt and Bellmann, 2010; Blumentritt et al., 2009). These completely passive systems required full knee extension before touch down to lock the knee for the stance phase. Too early touchdowns led to collapse. In more recent years, efforts have been made to develop semi-active ankle prostheses to similarly improve the artificial ankle performance (Meridium, Ottobock).

When analyzing the amputee gait kinematics and kinetics, differences in joint angles and torques can be identified (Schaarschmidt et al., 2012; Waters and Mulroy, 1999). For the artificial leg, deficiencies can be traced back to a missing power source, but also by limitations to the range of motion. To overcome both limitations, powered prostheses like the Power Knee, Sparky or the Power Foot were developed during the last years (Bellman et al., 2008; Highsmith et al., 2010; Au et al., 2009). All of them use a motor to provide external energy for joint actuation similar to the human muscle fibers. Next to the motor the Power Foot and Sparky use springs that are optimized to assist the motor to reduce peak power requirement and energy consumption. The springs are used to mimic the elastic function of the Achilles tendon. Only by including the elasticity it is possible to build compact powered ankles that can mimic the human ankle joint behavior for daily activities like walking with current motor technology.

Biomechanical gait analysis conducted in 2006 (Schaarschmidt et al., 2012) on multiple transfemoral unilateral amputees using passive and semi-active parts provided the scientific grounds for the thesis at hand. The differences between the residual and the intact limb clearly demonstrated that for level walking a major advancement in design and control is required at the prosthetic ankle joint to achieve similar amputee kinetics, kinematics, and symmetry in gait like non-amputees. Similar results were observed by other researchers too, when investigating the gait performance using different passive and semi-active prosthetic knee and foot components (Waters and Mulroy, 1999; Johansson et al., 2005; Segal et al., 2006).

Considering the outcome of these studies the following questions were deduced:

- What are the biomechanical requirements at the ankle joint to achieve human like gait?
- How can biomechanical ankle joint behavior be mimicked by an appropriate actuator design?
- How can artificial lower limb devices be controlled?

First studies on the improvement of amputee gait were done by the author in 2007 to 2008 (Grimmer, 2008; Grimmer and Seyfarth, 2009). It was proven if it is possible to improve the ankle push off by transferring energy from the intact knee of a transtibial amputee to the artificial foot using an elastic biarticular coupling. The study demonstrated that stiffness of mono- and biarticular springs, used to represent ankle function, clearly affects amputees gait performance. Thus it is an important design feature that should be exploited to provide maximum possible advantages for the amputee. An improved concept for choosing an optimal spring stiffness was required for further studies. It was not possible to achieve healthy ankle joint behavior due to limitations in push off energy injection and limitations in adjusting engagement timing of biarticular and monoarticular springs. As a consequence it was planned to include a series elastic actuator that can solve both issues by adjusting the resting length of the serial spring for further enhancement of artificial ankle performance.

When analyzing human ankle joint biomechanics for higher walking speeds and running, demanding requirements for the joint velocity, the torque and the acceleration can be identified. No off-the-shelf motor can match the required specifications. Therefore, a method to overcome the limitations of the current motor technology is required. As suggested by previous generations of prosthetic feet it might be possible that springs are able to assist the gait, to reduce the motor requirements. Such an arrangement of motors with springs was already used to actuate a powered ankle orthosis (Blaya and Herr, 2004). The arrangement is in line with the human muscle-tendon structure (Hill, 1938; Hof and Van den Berg, 1981). The series spring mimics the function of the Achilles tendon and the motor the function of the calf muscle fibers. Using the Sparky powered ankle prosthesis, Hitt et al. (2007) demonstrated that a series spring can clearly reduce the motor requirements. We used the same approach to determine the mechanical power requirements for the drive at multiple speeds in walking and running (Grimmer and Seyfarth, 2011). It was demonstrated that such a concept (motor assisted by a spring) is not limited to an average level walking speed. Especially for running the potential for assistance of elastic structures in a series elastic actuator (SEA) is enormous. To achieve the optimal assistance, gait and speed dependent variations in spring stiffness are required. A single compromising stiffness value for all speeds in walking and running is possible but reduces the system efficiency.

An open question was which optimization criteria are best suited to select the spring stiffness. The Sparky prosthesis was optimized to minimize peak power of the motor (Hitt et al., 2007; Hollander and Sugar, 2005). We introduced an alternative optimization criterion, namely minimizing the energy requirements (Grimmer and Seyfarth, 2011). The reduction of the necessary motor peak power makes it possible to use smaller motors and with that to reduce the system weight. The reduction of the energy consumption makes it possible to decrease the battery size and to increase the the runtime of an autonomous prosthetic system. For the ankle joint Grimmer and Seyfarth (2011) could demonstrate that the optimization for minimum peak power is the better choice as it results in almost the same energy consumption like the optimization for minimum energy. At the same time it reduces considerably the peak power. In contrast, the

energy minimization increased the required motor peak power but could not achieve major improvements in the energy consumption compared to the peak power optimization.

Next to the optimization approach, the alignment of the motor and the elastic components may be important for the powered ankle design. Similar to the Hill type muscle concepts (Hill, 1938; Hof and Van den Berg, 1981) parallel or combinations of parallel and series springs may be beneficial to reduce the actuator requirements.

Concepts for the alignment of motors and springs, including the criterion for an appropriate spring stiffness, are discussed in the theoretical part of the thesis (Manuscript II to IV). Later, these concepts are used to perform gait studies on amputees and non-amputees to prove the theoretical results (Manuscript V and VI). Manuscript I gives the reader a detailed introduction to the amputee and the non-amputee gait biomechanics, previous and state-of-the-art prosthetic technology and introduces various control approaches for different gait and terrain.

2 Overview

The dissertation contains six manuscripts. Manuscripts I to IV are published articles. Information on each publisher and the original publication can be found at each manuscripts cover page. Manuscripts V and VI are submitted to journals and are currently under review. Each manuscript contains its own summary of the references.

In the following paragraphs the contents of each manuscript is summarized. The relationships between the different publications are illustrated.

Manuscript I: Mimicking Human-like Leg Function in Prosthetic Limbs

The first chapter gives an introduction to the joint kinematics and the kinetics of the human gait. The presented data were recorded by Lipfert in 2005 in the Lauflabor Locomotion Laboratory. They are used as non-amputee subject reference for the whole thesis (Lipfert, 2010). The joint requirements for walking and running gait were distinguished using this data set. Subsequently, the chapter explains the state-of-the-art passive and semi-active lower limb prosthetic technology. The reasons and the prevalence for amputations are presented. Lower limb amputee walking biomechanics are described and limitations using unpowered devices are discussed. After focusing on previous generations of prosthetic limbs, the manuscript contains a summary of powered lower limb prosthetics systems which were developed until 2012. It explains design approaches and summarizes control approaches for different gaits and terrains.

The Manuscript I gives the reader an introduction to the state-of-the-art of lower limb prostheses, relevant problems, and ways to improve amputee gait performance. After introducing the overall topic in the first chapter, the following manuscripts II to VI will address different questions on powered joint biomechanics in more detail.

Manuscript II: A Comparison of Parallel- and Series Elastic Elements in an Actuator for Mimicking Human Ankle Joint in Walking and Running

The second chapter is based on the outcomes of the authors diploma thesis (Grimmer, 2008; Grimmer and Seyfarth, 2009) and the results of a first analysis of a series elastic actuator concept to improve artificial ankle push off performance (Grimmer and Seyfarth, 2011). It is shown that this concept can be further extended to include parallel elastic structures to reduce on the actuator peak power requirements but interestingly not the energy consumption.

Results of the first theoretical study on elastic structures to assist the motor (Grimmer and Seyfarth, 2011) were promising because the spring helps to overcome current limitations in the motor technology. As the simple concept of the series spring already had a huge effect it was planned to test possible extensions including also parallel springs. The previous concept for determining optimal stiffness to assist the motor (Hollander and Sugar, 2005) was used and extended in the Manuscript II to evaluate an actuator using a motor and a parallel spring (PEA). In addition a combination of parallel and series spring was evaluated (SE+PEA). Similar actuation concepts exist for the Hill type muscle model (Hill, 1938; Hof and Van den Berg, 1981) and might be beneficial to reduce the actuator requirements for a powered ankle prosthesis. The joint power is defined by joint velocity times joint torque. In contrast to the series spring that is

able to reduce actuator velocity, a parallel spring is able to reduce the torque. The Manuscript II demonstrates that there is a potential to decrease the peak power for multiple walking and running speeds when applying the parallel spring (PEA) compared to the SEA. To benefit from the torque reduction during push off, the parallel spring must be loaded during the flight phase. This loading requires energy. As a result, the energy consumption can not be reduced to levels achieved when using SEA. The combination of both structures (SE+PEA) combined the positive and the negative effects of the parallel and the series spring. The peak power is minimal, but the energy consumption is higher compared to an SEA. Next to the stiffness of each spring an additional constant, the parallel spring slack length, was introduced for the simulations. When keeping the stiffness and the slack length constant for all walking and running speeds, benefits for the peak power requirements and the energy consumption decrease. Thus for a special scenario (walking at a defined speed) such an approach might be worth to use. But for a versatile design performing multiple tasks like walking, running or stair climbing this approach might limit the required flexibility of the system. The additional weight for the mechanical structures for SE+PEA will decrease the system efficiency and reduce the possible advantages.

Manuscript III: Stiffness Adjustment of a Series Elastic Actuator in a Knee Prosthesis for Walking and Running: The Trade-off between Energy and Peak Power Optimization

After evaluating possible elastic motor assistance approaches for a powered prosthetic ankle joint in Grimmer and Seyfarth (2011) and the Manuscript II, it was analyzed whether similar effects are also possible for a powered knee joint.

To challenge urban environments, several movement tasks like level walking, walking inclines, climbing stairs or crossing obstacles are required. Also, while struggling with limitations, transtibial amputees can challenge most of the required tasks. Transfemoral amputees with passive artificial knee and ankle joint require increased hip effort, compared to non-amputees, but also additional compensating strategies. For example, they climb the stairs with the compensatory step-by-step lead-leg strategy where the healthy lead-leg always steps up the stair first. In addition they use the handrail for stabilization. A powered knee joint may enable amputees to reduce the user effort and to avoid compensating strategies. The first commercially available active knee joint is Ossurs Power Knee. It assists walking, climbing stairs, and standing up from a seated position. The Power Knee includes an elasticity to allow some degree of stance phase flexion. In contrast to the methods introduced by Hollander et al. (2005) the knee spring stiffness was here not optimized to assist the motor to reduce the peak power or the energy requirements. It is included in the design to allow some degrees of stance phase flexion under the amputees load.

The Manuscript III analyzes possibilities to decrease both the required motor peak power and the energy consumption in a powered knee prosthesis by optimizing spring stiffness. It is the first work that analyzes the effects of a series spring on the motor actuation for multiple walking and running speeds at the knee. It was found that especially running strongly benefits from a series knee elasticity. Almost no positive energy is required at the knee motor. A peak power reduction in walking can be achieved at higher speeds by a series spring. In contrast to the ankle joint, minimizing energy consumption was more useful than minimizing peak power in walking. Similar to the ankle joint it seems to be possible that a constant serial spring stiffness can be

used for all conditions (gaits and speeds). Compared to the gait and speed specific stiffness values, the constant stiffness will result in decreased efficiency for most of the conditions.

Manuscript IV: Energetic and Peak Power Advantages of Series Elastic Actuators in an Actuated Prosthetic Leg for Walking and Running

After analyzing the possible series elastic benefits to mimic the joint behavior of the ankle and the knee joint in Manuscripts II and III, the Manuscript IV investigates if also a powered hip joint might benefit from elasticity. In addition it should be answered which of leg joint is used to inject the most positive energy. Previous works used the overall joint positive work to answer this question. Here, we neglected the positive work that can be provided by passive elastic structures. The insights are relevant for the development of lower limb prostheses, but also for the construction of bipedal robots and exoskeletons. Finally, the chapter analyzes to which extent individual actuator optima (stiffness, peak power, energy) may differ from the subject group means. The results show the potential of the model approach and demonstrate chances for adapting a powered device to individual gait characteristics.

Methods used in Hollander and Sugar (2005) and Grimmer and Seyfarth (2011) were applied to a hip model including an SEA for actuation. The results demonstrate that, compared to the knee and the ankle joint, only minor reductions can be achieved regarding the peak power requirements and the energy consumption in walking. In running, no elastic benefits are predicted for the hip. The applied SEA is attached to the hip model in a monoarticular way. In contrast, humans have multiple biarticular muscles coupling the pelvis and the shank. It is assumed that the tendons of these structures are able to assist in actuation of the hip joint. Future studies should include these structures for coupling multiple joints including hip, knee and ankle.

The study showed that the positive energy supply during walking and running is reduced for the knee and the ankle joint when excluding the work of the series monoarticular springs. Thus the relevance to propel the legs for walking and running is shifted towards the hip joint. The authors guess that this shift will increase if also biarticular SEAs are included in the model. A major role of the hip joint to propel the legs in human locomotion can explain why transtibial and transfemoral amputees using passive knee and ankle joints are still able to walk and run.

The stiffness of a joint can be estimated using the slope of the torque-angle curve. Such a stiffness must not be optimal to assist the motor of an SEA. The methods used in Grimmer and Seyfarth (2011) and the Manuscripts II to IV have demonstrated that it is possible to determine optimal stiffness values minimizing the peak power requirements or the energy consumption. These methods should be preferred to design a powered artificial joint.

The optimal stiffness values that were determined in the Manuscripts II to IV base on the mean measurement data (joint tourque, angle, time for a gait cycle) of two groups of up to 21 subjects. Multiple steps of the left and right leg were averaged for each subject. These values were used to calculate a grand mean of all the subjects. The final part of Manuscript IV shows that individual optimal stiffness values for the ankle joint differ from the mean value. The standard deviation of the optimal stiffness for walking (29%) is almost twice that of running (16%). These results demonstrate that an individualization of the stiffness for each amputee might help to improve the powered prosthetic performance.

Manuscript V: A powered prosthetic ankle joint for walking and running

This chapter describes the first experiments of a powered prosthetic ankle joint for walking and running. It compares the model estimations of the spring and the motor behavior with the experimental observations. In the performed study, a control concept for changing gait and speed and the durability of the mechanical structure were tested.

Without performing experiments on a real powered prosthetic ankle the relevance of the model predictions of Manuscripts II to IV remain unclear. It might be possible that the user of a powered prosthesis is disturbed by the weight of the system, implemented motor patterns, or the stiffness of the included spring. If the ankle angle and the torque are not in line with the model assumptions (i.e. the torque-time and angle-time subject data underlying the optimization), the spring deflection and thus the elastic benefits might be reduced. The study performed in the Manuscript V should show how the user interacts with the artificial powered ankle. For the first evaluation, a healthy subject walked and ran on a treadmill with a powered prosthesis up to a speed of 4 m/s. The prosthesis was mounted at the subjects shank, using a bypass system that fixes the prosthesis in parallel to the blocked natural ankle joint.

The results demonstrate that the model assumption for the exchange of the power for the motor and the series spring are largely in line with the experimental observations for walking but not for running. The observed differences occur through the test setup and limitations in the motor power.

The non-amputee reference ankle angle and ankle torque tracings could be closely matched for 1.6 m/s walking with the powered ankle. In 2.6 m/s running the shapes of the joint angle and the torque patterns were roughly similar to the reference data. At 4 m/s running the peak ankle joint torque could not be achieved. As the stiffness of the powered ankle was optimized for 2.6 m/s running it was too soft for the 4 m/s. The simulated required mechanical peak motor power output was more than twice the motor continuous power. The low efficiency of the motor and the inertial effects of the mechanical parts will increase these requirements in addition. Model calculations predict that the optimal stiffness for 4 m/s running would decrease the mechanical peak power requirements to the half of the observed values. This highlights the importance of an adaptation of stiffness.

During the stance phase of 4 m/s running, the desired ankle kinematics (angle) could be achieved, the desired ankle kinetics (torque) were insufficient. Differences between the kinetics were mainly caused by limitations of the motor to follow the desired nut pattern. The authors assume that it may be possible to change the motor trajectories, predicted by the optimized model, to further improve the interaction of the powered and the passive joint movement if the motor power is limited. By this approach it may be possible to increase the powered ankle efficiency and the performance.

Manuscript VI: Simplified ankle control decreases powered prosthetic noise and improves performance and efficiency

The Manuscript VI describes experiments of transtibial amputee walking using the Walk-Run ankle. The study shows that the peak power optimized motor patterns can be simplified (by low-pass filtering) to improve the powered ankle performance. It is demonstrated that the system efficiency and the push off power can be improved while the noise of the prosthesis can be reduced. Next to the measured improvements the amputee reported to feel most comfortable

using the most simplified pattern.

In the Manuscript IV we demonstrated that individual optimal stiffness values differ in a certain range from the subject group mean. As a consequence, model assumptions of spring and motor interaction need not necessarily to represent users preferred patterns. In a certain range of stiffness values the main structure of the related optimal motor curve remains similar. This study was designed to test whether a simplification of the determined optimal motor pattern to the most prominent events of the structure can result in similar push off power. During amputee walking, the model assumptions for the power optimized motor and spring patterns show high agreement. Thus the principle concept to benefit from the elastic recoil was proved to work not only with the Bypass device (Manuscript V) but also for a unilateral transtibial amputee.

A zero-lag second order 4 Hz and a 2 Hz Butterworth filter were used to simplify applied motor patterns. The filter changes curves to avoid the high accelerations and reduces the changes in motor turning direction. Thus it was possible to reduce the electrical energy consumption for each step with the Walk-Run ankle. In addition, the positive mechanical power output of the spring and the motor increased. The overall system efficiency (mechanical output divided by electrical input) increased from 37% to 60.3%. The reduction in acceleration decreased the inertia and the friction effects. As a consequence, the prosthetic noise decreased with the increase of filter level.

Next to the observed potential of the applied methods the Manuscript VI leaves some questions open. Gait kinematics of the knee and the hip joint stayed almost equal for all applied motor patterns. Even the passive trial, where the motor did not change position, had almost similar kinematics. Training effects and the large passive push off may be a reason for the unchanged proximal joint behavior.

REFERENCES

Au, S., Weber, J., and Herr, H. (2009). Powered Ankle–Foot Prosthesis Improves Walking Metabolic Economy. *IEEE Transactions on Robotics*, 25(1):51–66.

Bellman, R. D., Holgate, M. A., and Sugar, T. G. (2008). Sparky 3: Design of an active robotic ankle prosthesis with two actuated degrees of freedom using regenerative kinetics. In *Biomedical Robotics and Biomechatronics, 2008. BioRob 2008. 2nd IEEE RAS & EMBS International Conference on*, pages 511–516. IEEE.

Blaya, J. A. and Herr, H. (2004). Adaptive control of a variable-impedance ankle-foot orthosis to assist drop-foot gait. *Neural Systems and Rehabilitation Engineering, IEEE Transactions on*, 12(1):24–31.

Blumentritt, S. and Bellmann, M. (2010). Potenzielle Sicherheit von aktuellen nicht-mikroprozessor-und mikroprozessorgesteuerten Prothesenkniegelenken. *Orthopädie-Tech nik*, 61:788–799.

Blumentritt, S., Bellmann, M., Ludwigs, E., and Schmalz, T. (2012). Zur biomechanik des mikroprozessorgesteuerten prothesenkniegelenks genium. *Orthopädie Technik*, 01:24–35.

Blumentritt, S., Schmalz, T., and Jarasch, R. (2009). The safety of c-leg: Biomechanical tests. *JPO: Journal of Prosthetics and Orthotics*, 21(1):2.

Brüggemann, G., Arampatzis, A., Emrich, F., and Potthast, W. (2008). Biomechanics of double transtibial amputee sprinting using dedicated sprinting prostheses. *Sports Technology*, 1(4-5):220–227.

Czerniecki, J., Gitter, A., and Munro, C. (1991). Joint moment and muscle power output characteristics of below knee amputees during running: the influence of energy storing prosthetic feet. *Journal of biomechanics*, 24(1):63–65.

Gailey, R., Allen, K., Castles, J., Kucharik, J., and Roeder, M. (2008). Review of secondary physical conditions associated with lower-limb amputation and long-term prosthesis use. *Journal of rehabilitation research and development*, 45(1):15.

Grimmer, M. (2008). Biomechanik des Ganges bei Ober- und Unterschenkelamputation - Analyse und mechanische Intervention. Diplomarbeit, Friedrich Schiller University Jena.

Grimmer, M. and Seyfarth, A. (2009). Biarticular structures to strengthen the push-off in lower leg prosthesis. *Dynamic Walking*.

Grimmer, M. and Seyfarth, A. (2011). Stiffness adjustment of a series elastic actuator in an ankle-foot prosthesis for walking and running: The trade-off between energy and peak power optimization. In *IEEE International Conference on Robotics and Automation (ICRA)*, pages 1439–1444. IEEE.

Highsmith, M. J., Kahle, J. T., Carey, S. L., Lura, D. J., Dubey, R. V., and Quillen, W. S. (2010). Kinetic differences using a power knee and c-leg while sitting down and standing up: a case report. *JPO: Journal of Prosthetics and Orthotics*, 22(4):237–243.

Hill, A. (1938). The heat of shortening and the dynamic constants of muscle. *Proceedings of the Royal Society of London. Series B, Biological Sciences*, pages 136–195.

Hitt, J. K., Bellman, R., Holgate, M., Sugar, T. G., and Hollander, K. W. (2007). The sparky (spring ankle with regenerative kinetics) project: Design and analysis of a robotic transtibial prosthesis with regenerative kinetics. In *Design Engineering Technology Conferences and Computers in Information and Engineering Conference (IDETC/CIE)*. ASME.

Hof, A. L. and Van den Berg, J. (1981). Emg to force processing i: an electrical analogue of the hill muscle model. *Journal of Biomechanics*, 14(11):747–758.

Hollander, K. and Sugar, T. (2005). Design of the robotic tendon. In *Design of Medical Devices Conference (DMD)*.

Johansson, J., Sherrill, D., Riley, P., Bonato, P., and Herr, H. (2005). A clinical comparison of variable-damping and mechanically passive prosthetic knee devices. *American Journal of Physical Medicine & Rehabilitation*, 84(8):563.

Lipfert, S. (2010). *Kinematic and dynamic similarities between walking and running*. Verlag Dr. Kovac, Hamburg. ISBN: 978-3-8300-5030-8.

Robbins, C., Vreeman, D., Sothmann, M., Wilson, S., and Oldridge, N. (2009). A review of the long-term health outcomes associated with war-related amputation. *Military medicine*, 174(6):588–592.

Schaarschmidt, M., Lipfert, S. W., Meier-Gratz, C., Scholle, H.-C., and Seyfarth, A. (2012). Functional gait asymmetry of unilateral transfemoral amputees. *Human movement science*, 31(4):907–917.

Segal, A., Orendurff, M., Klute, G., McDowell, M., Pecoraro, J., Shofer, J., and Czerniecki, J. (2006). Kinematic and kinetic comparisons of transfemoral amputee gait using C-Leg® and Mauch SNS® prosthetic knees. *Journal of rehabilitation research and development*, 43(7):857.

Waters, R. L. and Mulroy, S. (1999). The energy expenditure of normal and pathologic gait. *Gait & posture*, 9(3):207–231.

3 Manuscript I: Mimicking Human-like Leg Function in Prosthetic Limbs

Authors:

Martin Grimmer and André Seyfarth

Technische Universität Darmstadt

64289 Darmstadt, Germany

Published as a book chapter in

Neuro-Robotics, From Brain Machine Interfaces to Rehabilitation Robotics, Springer Science+Business Media Dordrecht, 2014

3.1 ABSTRACT

Human upright locomotion is a complex behavior depending on manifold requirements. Bones, muscles, cartilage and tendons provide mechanical infrastructure. Central nervous commands, reflex mechanisms from the spinal cord level or also preflexes defined by actuator properties provide input to create motion patterns like walking or running. Due to dysvascularity, infections or traumatic events parts of the biological framework can get lost. Until the end of the 20th century mostly passive structures were used to replace amputees lower limbs. Full functionality like in the biological system can not be provided because of missing sensory information and power source. Innovations in actuator, battery and micro electronics technology make it possible to improve prosthetic design. A first innovation was introduced with semi-active devices using microprocessor controlled dampers to modulate prosthetic joint behavior similar to isometric or eccentric muscle function. A further step is to power the joints to emulate concentric muscle function. Combined with ingenious control mechanisms this could potentially provide every possible movement task. 26 powered prosthetic systems and further passive prototypes are presented in this work. Mechanical and control solutions are introduced. Amputee gait in various daily life situations using passive, semi-active and powered prostheses is compared. Areas for improvements are discussed.

3.2 HUMAN LOCOMOTION

Upright humanoid locomotion emerged about 6 million years ago (Niemitz, 2010). The oldest humanoid footprints with evidence of bipedal locomotion are about 3.7 million years old (Crompton et al., 2012). As a result of evolutionary changes of the neural, the skeletal and the muscular system several upright human locomotion patterns were developed. In daily life commonly walking is performed. More dynamic gait patterns are skipping or running. A preferred walking speed is about 1.3 m/s (Dal et al., 2010). Running, especially sprinting gives the possibility to move faster (up to 12.27 m/s, Usain Bolt, (Sauren et al., 2010) compared to walking (4.3 m/s, Vladimir Kanaykin, mean value of World Record 20 km Race Walking). While walking with passive carbon fiber prosthetic ankle joints, amputees have still a lack in performance compared to healthy people. Whereas in running with passive carbon fiber feet international scientists and sport officials discussing about advantages for amputee sprinters compared to healthy athletes.

In the following pages requirements for mimicking healthy humanoid gait patterns are presented. Current state of the art lower limb prosthetic technology is discussed. Newest prototypes to improve amputee gait are introduced. Mechanical and control solutions are presented and fields for improvements are discussed.

3.3 PROSTHETICS

First lower limb prosthetics were reported in an Indian sacred book called the Rig Veda that was written between 3500 to 1800 B.C. There it is mentioned that the leg of Queen Vishpla was amputated in a battle. Afterwards an iron leg was fitted to her to walk and to get her back to the battlefield (Duraiswami et al., 1971). Still 2000 A.C. war is a reason for amputations. The Annual Report of the Red Cross (Verhoeff, 2002) reports 16,501 prosthetics manufactured in their 40 centers (14 selected countries) for 2001. 9,779 of them were made for mine victims. For the US Forces from 2000 to 2011, 6,144 traumatic amputations among 5,694 soldiers were realized. About 2,037 of them had major amputations like the loss of foot, hand or more (O'Donnell

et al., 2012). In comparison 185,000 amputations are estimated for the US in total each year. In total 1.6 million people with lost limbs were estimated for the U.S. for 2005 (Ziegler-Graham et al., 2008). Even higher numbers related to the population are documented in Germany. In the year 2003 about 61,000 amputations at 45,000 patients were made only for the lower extremity (Heller et al., 2005). These values are including all surgeries including toe to whole leg amputations. The main reason for lower limb amputations in the United Kingdom is dysvascularity (72%). Nearly half of it is related to diabetes mellitus. Also infections (8%), trauma (7%), neoplasia (3%) or neurological disorder (1%) can be a cause. In 4% of cases no specified cause was identified. Other reasons together account for 5% (NASDAB, 2009). Lower limb referrals accounting more than 90% of all new amputees. 53% of them were transtibial amputees in the UK. Another 39% are transfemoral amputees. The Amputee Statistical Database for the United Kingdom reports that over one half of the new amputees referred to prosthetics centers are aged over 65 and one fourth is over 75 years old. Only one fourth is younger than 54 years (Amputee statistical database UK, 2006).

The function of prosthetics is on the one hand to provide a cosmetic part to cover the loss of the limb. On the other hand it should provide functionalities of the lost limb. For example with a lower limb prosthesis the amputee should be able to perform at least standing and slow walking. Additional functionalities for daily life are required. Two strategies are used to provide them for the amputees. Special prostheses for specific purposes like swimming (Colombo et al., 2011) or running (Webster et al., 2001) were designed. A second way is to include more functions in existing prosthetic systems. For example, a special foot design with a manual ankle joint clutch makes it possible to use different kinds of shoes like sport shoes or high heels with one prosthetic foot (e.g. Runway, Freedom Innovations).

From an energetic point of view, prosthetics can be divided into three groups. Complete passive, semi-active and active devices. Complete passive devices are using passive clutch mechanisms, springs and dampers to mimic human gait behavior. They are the most common group. Semi-active devices are equipped with microprocessors to control the mechanical parts (e.g. hydraulic dampers) depending on gait phase. In the 3rd group, active prosthetics can provide positive net work, mostly by motors, to assist the amputee in walking or climbing stairs.

3.4 PASSIVE PROSTHETICS

3.4.1 Ankle Joint

Design characteristics

Passive prosthetic ankle joints can be classified by their functionality. A first group are the non-elastic feet (e.g. SACH feet - solid ankle cushioned heel). Materials like wood and plastics are used to design them. Low costs make them still attractive for amputees and paying authorities. In third world countries manufacturing costs of less than US$150 can be realized for an artificial limb. For example in Vietnam the ICRC (International Committee of the Red Cross) estimated manufacturing costs of between US$38 and US$64 per polypropylene prosthesis (Coupland, 1997).

A step further in functionality are ESAR (energy store and return) feet. They are able to store and release energy during the gait cycle by spring-like structures. Using the elastic capability of the forefoot they can mimic to some extend the function of the Achilles tendon which results in a more natural ankle joint behavior. For some prosthetic ankle joints one carbon heel part

with a different stiffness than the forefoot (e.g. Vari-Flex - Ossur) is used to mimic the eccentric tibialis anterior muscle function during touch down. After loading this leaf spring during loading response, energy from unloading for shank forward rotation is provided. Composite materials are mainly used for designing the elastic structures in ESAR feet.

Another difference between prosthetic feet can be made by the provided degrees of freedom. SACH feet have a solid ankle and a cushioned heel. No ankle joint rotation is possible. Single axis feet like the 1H38 (Ottobock) providing one degree of freedom limited by soft or rigid bumpers. Multi-axial feet (e.g. Multiflex DR - Endolite) can move in more than one plane. Inversion or eversion and adduction or abduction can be realized. Adaptations to ground while walking curves or uneven terrain are possible. Potentially torsional forces for higher joints can be reduced. Similar functions can be provided by prosthetic torsion adapters integrated between foot and socket or artificial knee joint.

Quite often a lot of these functionalities are combined in one prosthetic foot design. For example the Echolon VT (Endolite) provides a heel and a forefoot spring. In addition it has a shock absorbing torsional element. To improve ground contact while Eversion or Inversion the forefoot spring has a separate left and a right part.

Gait Biomechanics

Asymmetries in abled-bodied gait could be identified by various gait studies (Sadeghi et al., 2000). Even more pronounced are asymmetries for unilateral amputees. Transfemoral amputations cause higher biomechanical differences between affected and unaffected leg than for transtibial amputees (Nolan et al., 2003). For the second group only the missing biological ankle joint effects the gait pattern. Differences in kinematics and kinetics can be identified between affected and unaffected side. Various gait studies on amputee gait showing the effects for different prosthetic feet (Hafner, 2005; Prinsen et al., 2011; Rusaw and Ramstrand, 2011; van der Linde et al., 2004).

The natural Range of Motion (RoM) of the ankle joint while walking on a treadmill is between 20° to 38° increasing for speed from 0.5 m/s to 2.6 m/s (Fig. 1). For running the RoM is between 26° and 40° considering speeds from 0.5 m/s to 4 m/s (Fig. 3). For Sprinting values up to 50° are possible (Kuitunen et al., 2002).

Using a passive prosthetic foot the RoM is about 16.8° to 21.2° for 1.35 m/s walking (Postema et al., 1997; Vanicek et al., 2009). 11° to 23° were reported in (Hafner et al., 2002). Thereby ESAR feet could almost double RoM in comparison to SACH feet that provided only up to 14° dorsiflexion. Prosthetic feet with mechanical ankle joint (Lager or 1H38, Ottobock) can provide greater ROM than SACH or ESAR feet (Postema et al., 1997).

For amputees running with a Flex-foot (Ossur) at 2.7 m/s, a RoM of about 11° was achieved (Sanderson and Martin, 1996).

RoM is especially a topic on slopes or stairs. Limitations enforce compensating motion of the other leg joints. In (Vickers et al., 2008) 8° ankle RoM was identified for unilateral amputees walking up a slope of 5° (SACH foot). The control group had a RoM of about 24°. Descending the same slope the amputees had an ankle RoM of about 9°, while the control group had about 20°. In addition ankle angle at touch down differs significant between the control and the amputee group.

The lag for amputee ankle joint RoM is caused by rigid prosthetic foot mechanisms. Softer mechanisms like ESAR feet could improve performance and may also increase stride length of the residual limb (Hafner et al., 2002). On the other hand the plantarflexion of a prosthetic

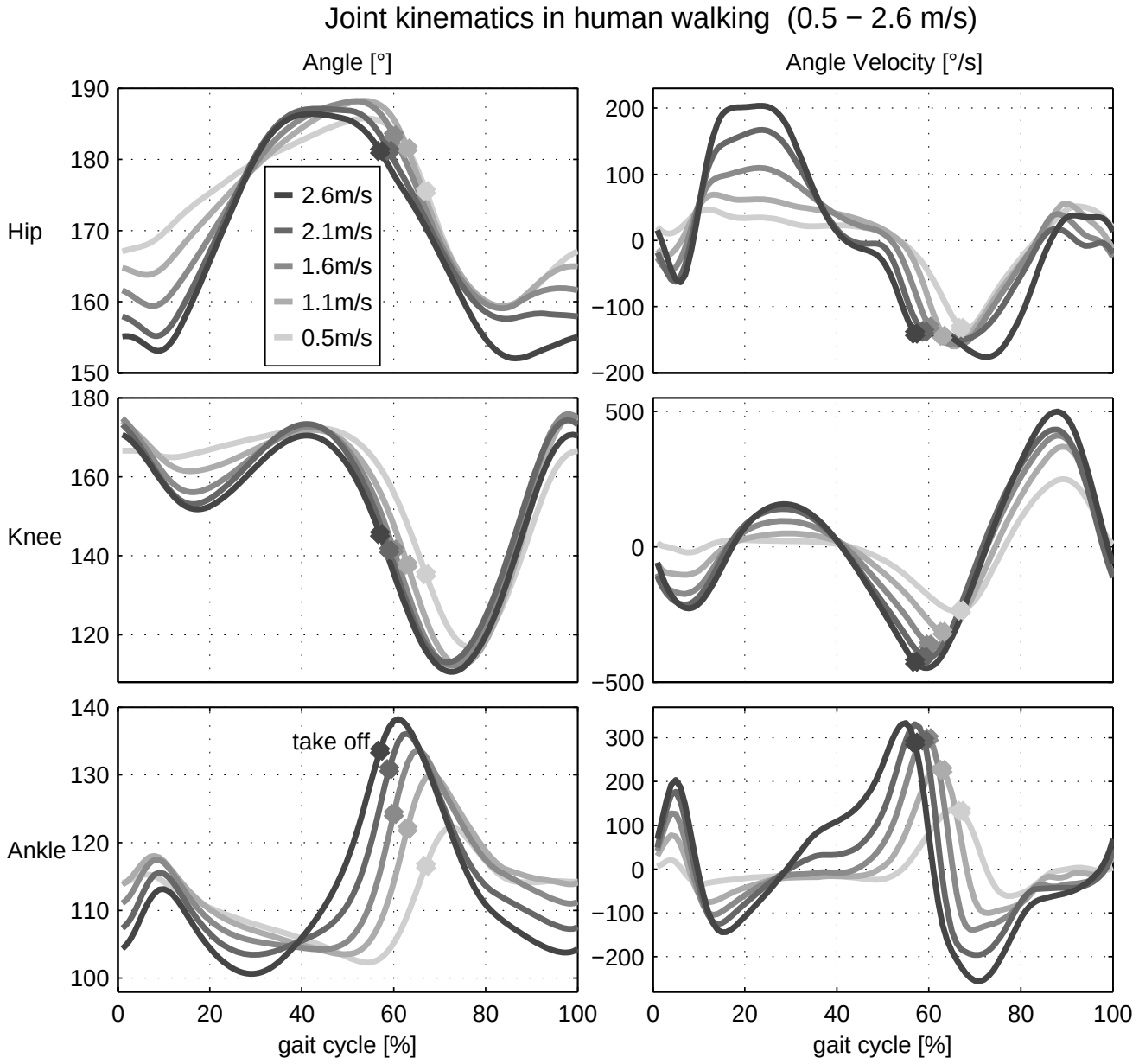

Figure 1: Angle and angle velocity of human hip, knee and ankle in treadmill walking. Hip ankle is calculated between the seventh spine bone, trochanter major and a assumed rotational point at the knee (two centimeter above the lateral meniscus at lateral femur condyle). Knee angle is calculated between trochanter major, the rotational point of the knee and the lateral malleolus. Ankle angle is calculated by the rotational point of the knee, the lateral malleolus and the fifth metartasal joint of the foot. Dots are indicating take off for the individual speeds. Mean values of 21 subjects (25.4 years, 1.73 m, 70.9 kg). Data from (Lipfert, 2010).

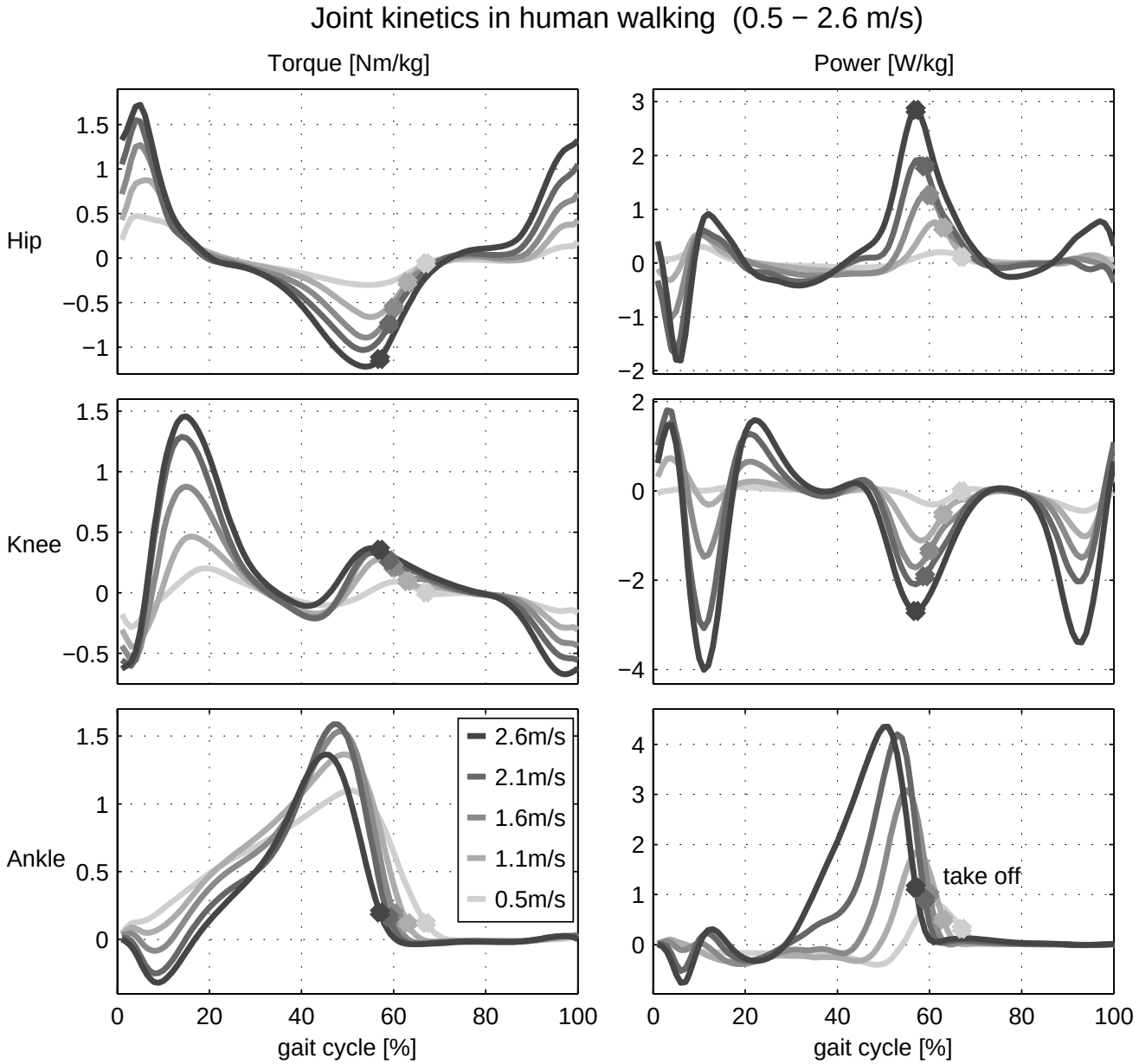

Figure 2: Joint torque and power for human hip, knee and ankle in treadmill walking. Joint torques are calculated using inverse dynamics. Power is the product of joint velocity and joint torque. Both values are normalized to body mass. Dots are indicating take off for the individual speeds. Mean values of 21 subjects (25.4 years, 1.73 m, 70.9 kg). Data from (Lipfert, 2010).

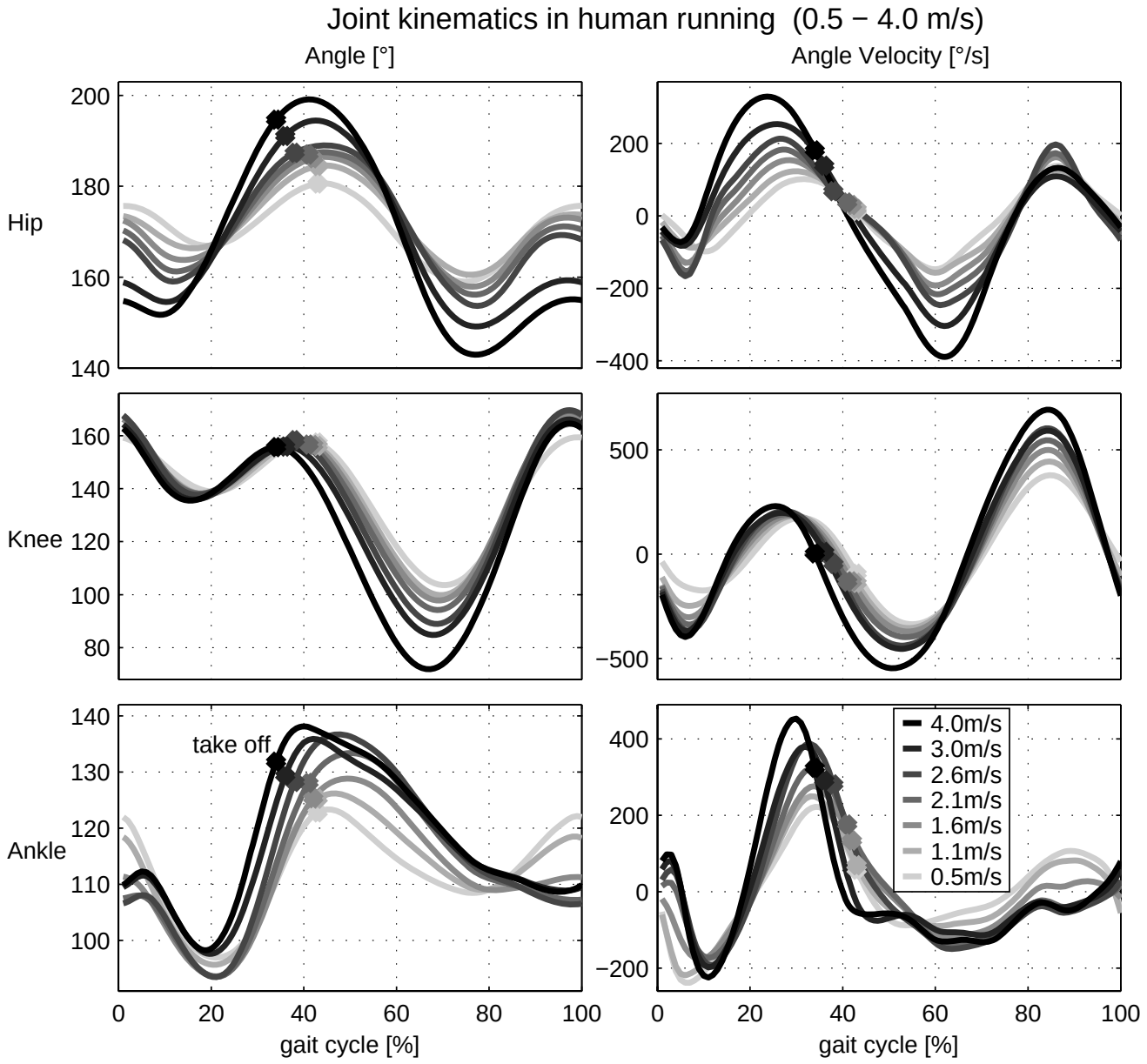

Figure 3: Angle and angle velocity of human hip, knee and ankle in treadmill running. Mean values of 21 healthy subjects for speeds 0.5 m/s to 2.6 m/s. Mean values of 7 subjects for 3 m/s and 4 m/s (23.7 years, 1.8 m, 77.5 kg). Data from (Lipfert, 2010). For more information see caption of Fig. 1.

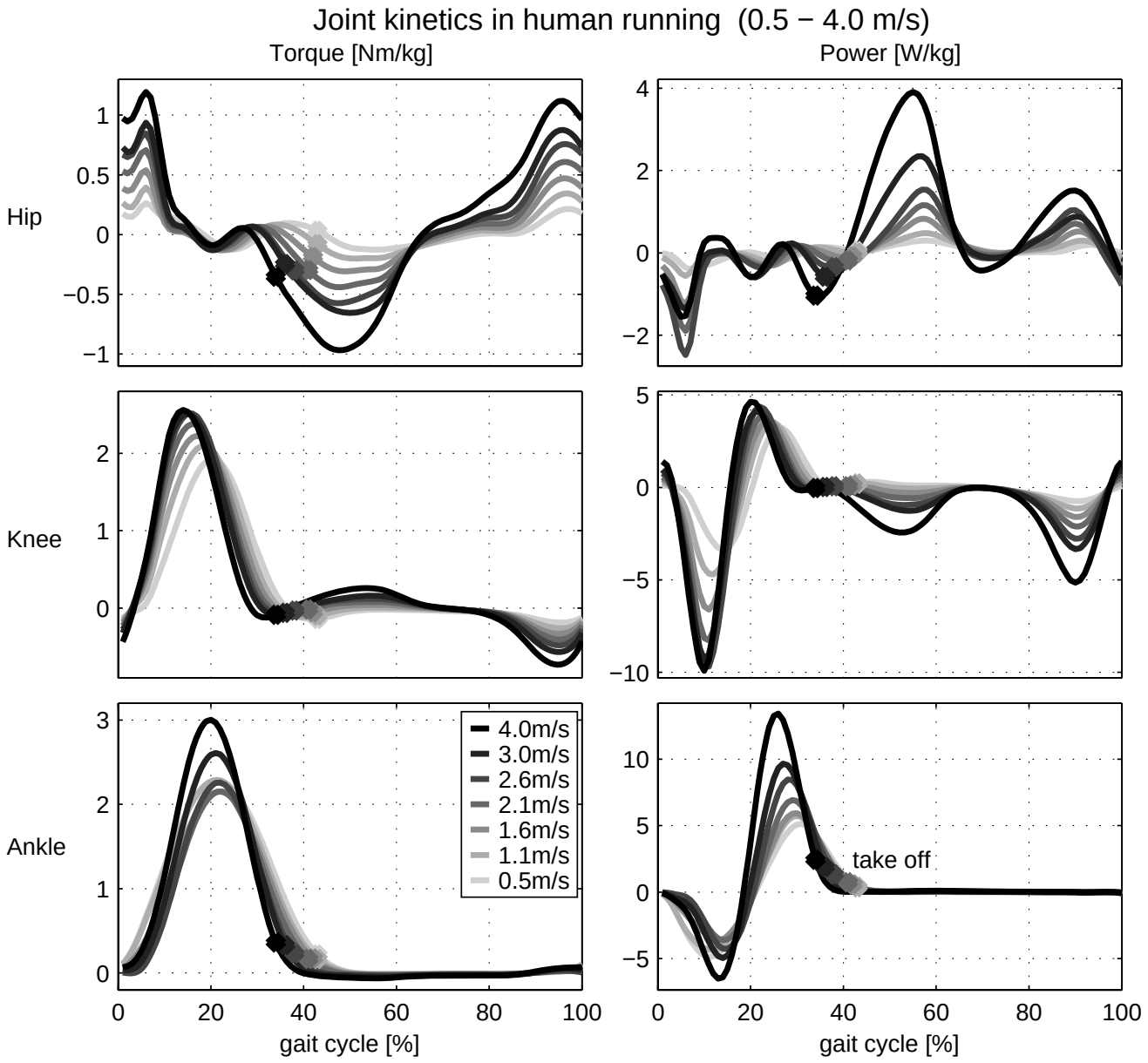

Figure 4: Joint torque and power for human hip, knee and ankle in treadmill running. Mean values of 21 healthy subjects for speeds 0.5 m/s to 2.6 m/s. Mean values of 7 subjects for 3 m/s and 4 m/s (23.7 years, 1.8 m, 77.5 kg). Data from (Lipfert, 2010). For more information see caption of Fig. 2.

Table 1: Positive and Negative Peak Power [W/kg] and work [J/kg] at the ankle joint during walking and running.

Gait	Walking					Running						
Speed [m/s]	0.5	1.1	1.6	2.1	2.6	0.5	1.1	1.6	2.1	2.6	3.0	4.0
Positive Peak Power	0.9	2.0	3.2	4.3	4.6	5.3	6.0	6.1	7.1	8.7	10.0	14.1
Negative Peak Power	0.5	0.4	0.4	0.5	0.8	4.8	4.3	3.6	3.7	4.4	5.1	7.0
Positive Work	0.12	0.20	0.29	0.45	0.54	0.54	0.60	0.60	0.64	0.70	0.80	0.98
Negative Work	0.14	0.13	0.07	0.04	0.05	0.48	0.42	0.31	0.27	0.29	0.32	0.39

ankle during push off is limited to the ankle rest position. Further changes in the ankle angle could only be realized by energy injecting systems. For realizing this in a passive device energy has to be stored first in another phase of the gait cycle.

In a novel semi-passive ankle prototype (Energy Recycling Foot, (Collins and Kuo, 2010)) energy storage is realized during heel contact. Afterwards it is used to support push off. For push off in walking at preferred speed (Dal et al., 2010) between 0.2 J/kg and 0.29 J/kg of positive ankle work is required (Tab. 1). For a 75 kg person this would be about 15 J to 22 J. In (Zelik et al., 2011) the system returned about 19 J to 25 J in unilateral amputees. The Energy Recycling Foot could double push of energy in comparison to a conventional prosthetic foot. Also net rate of metabolic consumption could be reduced from 23% above normal (conventional prosthesis) to 14% (Energy Recycling Foot) using a prosthetic simulator (Collins and Kuo, 2010). But more push off work not necessarily results in better gait performance. In (Zelik et al., 2011) it was shown that with the same device softer spring stiffness values could improve positive push off work. This outcome was different to the results for the metabolic rate. It was best for a medium stiffness condition. As reasons excessive heel displacement and center of mass (CoM) collision losses were assumed.

Lower stiffness values also seem to reduce efficiency of the ESAR feet (Fey et al., 2011). Similar tendencies could be identified by the hysteresis of different ESAR feet in a material testing machine (Geil, 2001).

Transtibial amputees can get between 0.04 J/kg to 0.26 J/kg positive ankle work from their prosthesis during walking (Tab. 2). Medium values for preferred walking speed are about 0.06 to 0.11 J/kg (Tab. 2). Energy storage and release is increasing with walking speed (Schneider et al., 1993; Silverman et al., 2008). SACH feet can store and release less energy in comparison to ESAR feet (Prince et al., 1998; Schneider et al., 1993; Gitter et al., 1991; Czerniecki et al., 1991). Efficiencies related to energy storage and dissipation and final push off recovery are between 39% and 89%. Calculation methods (Prince et al., 1998) and material properties contribute to the wide range (Geil, 2001). SACH feet seem to be less efficient than ESAR feet (Gitter et al., 1991; Czerniecki et al., 1991). However nearly similar values were identified in (Prince et al., 1998) when comparing both designs.

When running (2.8 m/s) using walking feet a similar range for prosthetic foot efficiency (31% - 84%) compared to walking (Tab. 2) was identified.

At the ankle joint PP around preferred walking speed in healthy subject gait is about 2.0 W/kg to 3.2 W/kg (Tab. 1, Fig. 2). In comparison 0.34 W/kg - 3.6 W/kg can be realized using prosthetic feet in transtibial amputees. Mean values for transfemoral amputees are about 0.6 W/kg

(Tab. 2). Comparing amputation level much higher values could be identified for transtibial amputees (Schneider et al., 1993; Gitter et al., 1991). Similar to increasing energy storage and return also PP is increasing with speed (Silverman et al., 2008).

Highest PP values could be identified in running (e.g. 5.5 W/kg at 2.8 m/s (Czerniecki et al., 1991)). At a similar speed healthy subjects would have a PP of about 9.4 W/kg (estimated from Tab. 1, Fig. 4).

Also when providing more positive work and higher PP, ambiguous outcomes for oxygen consumption with SACH feet in comparison to ESAR feet were identified by (Hafner et al., 2002). Only 3 out of 9 studies showed an improved energy expenditure when using ESAR feet. Benefits seem to be possible for higher walking speeds (Nielsen et al., 1988; Schmalz et al., 2002).

A reason for the discrepancy between oxygen consumption, positive work and PP could be a wrong timing and the wrong angular displacement of the leg segments at a certain event in comparison to non-amputees (Fig. 6 and 7). A primary contribution to the segment interaction could be created by biarticular structures coupling the joints. For example the gastrocnemius muscle has the potential for adjusting knee flexion and ankle plantarflexion during push off (van Ingen Schenau et al., 1987). By this it could be possible to set push off direction in an appropriate manner.

Ideas of biarticular structures, coupling the knee and the ankle joint, exist since the Hydra Cadence Knee in the late 1940's (Wilson, 1992). Already there the positive effects of the synchronized joints were reported. This concept is now used in a novel prototype to increase push off power in walking (Unal et al., 2012). While extending the knee in flight phase the biarticular design enables to load a spring passively. This energy is released during take off and helps to bend the knee and to extend the ankle (plantarflexion). As a disadvantage this feature excludes the possibility of knee stance phase flexion. Due to the design the amputee has to walk with an extended knee, which is in contrast to the natural bending behavior used for shock absorption.

To overcome missing positive net work at the prosthetic ankle joint a compensating motion of the body is required. This results in 23% higher oxygen consumption for speeds from 0.6 m/s to 1.4 m/s compared to non-amputees. Variations could be possible by different alignments of the foot (Schmalz et al., 2002). For the cost of transport (CoT) increased speed dependent (0.75 m/s to 1.75 m/s) values between 11% to 25% were identified for transtibial amputees (Herr and Grabowski, 2012).

In addition to no positive net work, higher metabolic rates, reduced RoM and reduced peak power further biomechanical characteristics could be identified caused by the artificial passive ankle joint.

Additional gait characteristics for transtibial amputees

- reduced first vertical ground reaction force peak at residual limb (RL) (Nolan et al., 2003)
- reduced impulse at RL (Nolan et al., 2003)
- increased impulse at intact limb (IL) (Nolan et al., 2003)
- reduced stance time at RL (Nolan et al., 2003)
- increased stance time at IL (Nolan et al., 2003)
- increased swing time at RL (Nolan et al., 2003)

- reduced swing time at IL (Nolan et al., 2003)
- reduced lower preferred walking speed (18%) (Herr and Grabowski, 2012)
- reduced stride length (Powers et al., 1998)
- increased EMG amplitude and duration for knee flexors and extensors at RL (Powers et al., 1998)
- increased EMG for hip extensor in early stance phase (Winter and Sienko, 1988)
- increased early stance hip peak power, work and moment for compensation (Silverman et al., 2008)

Further objects which are criticized by transtibial amputees testing ESAR and SACH feet can be found in (Hafner et al., 2002).

3.4.2 Knee Joint

Design characteristics

In contrast to the ankle joint, the knee joint performs more negative than positive work during level walking (Fig. 2). Thus it requires less actuation compared to the ankle joint. Dampers are able to modulate swing phase and by mechanical design the knee is locked to secure stance phase. Using these features passive prosthetic knee joints can perform level walking at a similar level compared to semi-active devices (Schaarschmidt et al., 2012).

There is a variety of mechanical features that differs between the passive joints. The number of axis (single, polycentric), the mechanism to lock the knee in stance phase or the way to provide damping during stance and swing are the most fundamental differences. First versions of hydraulic dampers were implemented in prosthetics in the late 1940's. A combination of hydraulic knee-ankle unit the Stewart-Vickers Hydraulic Above-Knee Leg, today known as the Hydra Cadence Knee, used a hydraulic mechanism to lock the knee at touch down. In addition it synchronized the behavior between the knee and ankle by a biarticular structure during the swing phase. In 1951 the Mauch S'n'S (Swing and Stance) system was developed by Henschke and Mauch. A hydraulic swing phase damper was introduced that worked together with a system to ensure stance phase (Wilson, 1992). In addition to hydraulics (e.g. 3R60, Ottobock) also pneumatics (e.g. ESK, Endolite) are used. Both joints the 3R60 and the ESK are using different locking mechanisms. The 3R60 uses a polycentric joint that secures stance by geometry. The ESK is a single axis knee that uses a drum brake that works progressively in relation to the applied load. Further differences are components that allow yielding (up to 15° in 3R60, Modular Knee Joint booklet, Ottobock) or to lock and unlock the knee joint manually for higher safety (e.g. 1M10, Proteor). A feasible set of knee components is offered for each level of activity by combining the required features in different combinations. As a result Ottobock provides over 40 different knee joints (Modular Knee Joint booklet).

Gait Biomechanics

Transfemoral amputees suffer not only from the missing natural knee function. In addition they have to deal with the artificial ankle function. As a result asymmetric behavior is much more pronounced than for transtibial amputees (Nolan et al., 2003). This requires an increased step width in walking to keep balance in comparison to non-amputees (Hof et al., 2007). Most

Table 2: Energy, efficiency and peak power values for different passive prosthetic feet in transtibial (TT) and transfemoral (TF) amputees for walking (W) and running (R). For authors marked with ∗ energy and peak power values are estimated from published figures. Various studies used self-selected preferred walking speed (PWS).

Article	Prosthesis	Energy absorbed / returned [J/kg]	Efficiency [%]	Peak Power absorbed / returned [W/kg]	Gait / Speed [m/s]	Subjects / Level of amputation
(Czerniecki et al., 1991)	Flex Foot Seattle Foot SACH Foot	0.45 / 0.38 0.49 / 0.25 0.26 / 0.08	84 52 31	6.7 / 5.5 8.2 / 4.1 5.3 / 1.5	R / 2.8	5x TT
(Gitter et al., 1991) ∗	Flex Foot Seattle Foot SACH Foot	0.29 / 0.26 0.15 / 0.11 0.1 / 0.04	89 71 39	1.4 / 3.6 0.8 / 1.6 0.5 / 0.7	W / 1.5	5x TT
(Seroussi et al., 1996) ∗	Seattle Light Foot Mauch SNS Knee	0.09 / 0.07	75	0.39 / 0.6	W / PWS	8x TF
(Silverman et al., 2008) ∗	SACH or ESAR Foot	0.11 / 0.05 0.148 / 0.06 0.149 / 0.068 0.152 / 0.074	45 41 46 49	0.3 / 0.23 0.48 / 0.47 0.67 /0.63 0.78 / 0.72	W / 0.6 W / 0.9 W / 1.2 W / 1.5	14x TT
(Prince et al., 1998)	Golden Foot Seattle Foot SACH Foot	0.27 / 0.11 0.17 / 0.064 0.15 / 0.057	41 39 37		W / 0.9 to 1.4	5x TT
(Schaarschmidt et al., 2012) (unpublished data)	C-Walk	0.11 / 0.065	59	0.36 / 0.53	W / 1.1	4x TF
(Schneider et al., 1993)	Flex Foot SACH Flex Foot SACH			0.98 / 1.29 0.57 / 0.29 1.51 / 1.94 0.78 / 0.34	W / 0.9 W / 1.3	12x TT (children)
(Nolan and Lees, 2000)	Multiflex or SACH Flex/Intelligent or Flex/Hydraulic			0.81 / 0.86 0.99 / 1.74	W / 1.2 W / 1.2	4x TT 4x TF
(Johansson et al., 2005)	Allurion Foot with Rheo Knee C-Leg Mauch SNS			 0.7 /0.75 0.7 /0.75 0.55 /0.75	W / PWS	8x TF
(Segal et al., 2006)	Dynamic Plus, C-Walk, LuXon Max with C-Leg Seattle Light, Flex Foot with Mauch SNS			0.6 / 0.6 0.8 / 0.66	W / 1.3 W / 1.3	8x TF
(Vanicek et al., 2009)	Multiflex, Variflex, Dynamic or Centerus Foot			Faller 0.55 / 0.4 Non Faller 0.4 / 0.45	W / PWS	11x TT

of the transtibial characteristics (Sect. 3.4.1) are even more pronounced. In comparison to the artificial ankle joints RoM is not restricted for the knee joint (Knee angle Fig. 6) during walking in swing phase. Depending on Mobility Grade and preferred walking speed an adequate module can be applied. Ottobock provides joints with a range of 110° to 175° (Modular Knee Joint booklet). Especially devices with lower RoM values can cause discomfort during daily activities like sitting.

Kinematic deficits for the knee joint are found in the stance phase (Seroussi et al., 1996; Johansson et al., 2005; Segal et al., 2006). In addition no positive work is provided for a knee flexion during swing leg retraction (Seyfarth et al., 2003). Various prosthetic knee joints are locking the knee in an extended position at touch down. As a result natural shock reduction (elastic or damping) by the knee is not possible. Subsequently no or only little knee flexion during stance is possible for the amputee. Advanced passive knee joint technology provides solutions for the missing shock absorption. Individual adaptive spring-damper systems like in the EBS system (Ottobock) allow stance phase flexion of up to 15°. Even though the technical feature to permit yielding is also implemented in the C-Leg, only a small part of the users is using it (Seroussi et al., 1996; Johansson et al., 2005; Segal et al., 2006), (Fig. 6). Missing yielding could be explained by already existing movement patterns used to handle previous versions of passive knee joints. Also missing positive work which could be introduced by elastic or active components could explain it. Why to reduce vertical hip position by knee flexion when there is no mechanism in the knee joint to extend it again. This limitation could be compensated by muscle work of hip extensors or monoarticular artificial ankle plantarflexors.

Interestingly forward propulsion is mainly generated by the prosthetic limb. This phenomenon can be explained by the CoM behavior. The intact limb is increasing CoM height and the potential energy. During the contact of the prosthetic limb this energy is transformed into horizontal kinetic energy. The height of the CoM is decreasing. By this interaction of both limbs the prosthetic limb creates a net forward impulse without providing positive work at the knee or net positive work at the ankle joint (Schaarschmidt et al., 2012).

The resulting preferred walking speed for transfemoral amputees (1.04 m/s) is lower than for amputees with knee disarticulation (1.19 m/s, (Boonstra et al., 1993)). 1.45 m/s (Boonstra et al., 1993) or 1.41 m/s (Herr and Grabowski, 2012) were identified for control groups. In comparison to the transtibial amputees (18% reduction) the preferred speed reduction would be about 27% for transfemoral amputees. Waters and Mulroy (Waters and Mulroy, 1999) showed the opposing trend of oxygen consumption and preferred speed for different levels of amputation (Fig. 5). When amputees are forced to walk at similar speeds like non-amputees higher oxygen consumption during walking can also be identified. For transfemoral amputees the additional expenses are increasing with speed (0.6 m/s to 1.4 m/s) by 55% to 64%. In comparison to transtibial amputees (23% higher than non-amputee) the increase is nearly tripled (Schmalz et al., 2002).

The reasons for this energetic increase are manifold. Compensating structures (muscles, tendons) to realize gait seem not to work at their most efficient operating point (e.g. muscle force - length relationship). Increased hip extensor torques were identified to be the reason for increased metabolic rates in different prosthetic alignments (Schmalz et al., 2002). Higher extensor muscle activity (Winter and Sienko, 1988) was mentioned as a reason in (Schmalz et al., 2002). In addition the elastic behavior of the artificial ankle and the knee joint is not used in an appropriate way. Optimal stiffness values can decrease energetic requirements dramatically (Grimmer and Seyfarth, 2011a,b). Also biarticular couplings are missing (e.g. gastrocnemius), which could

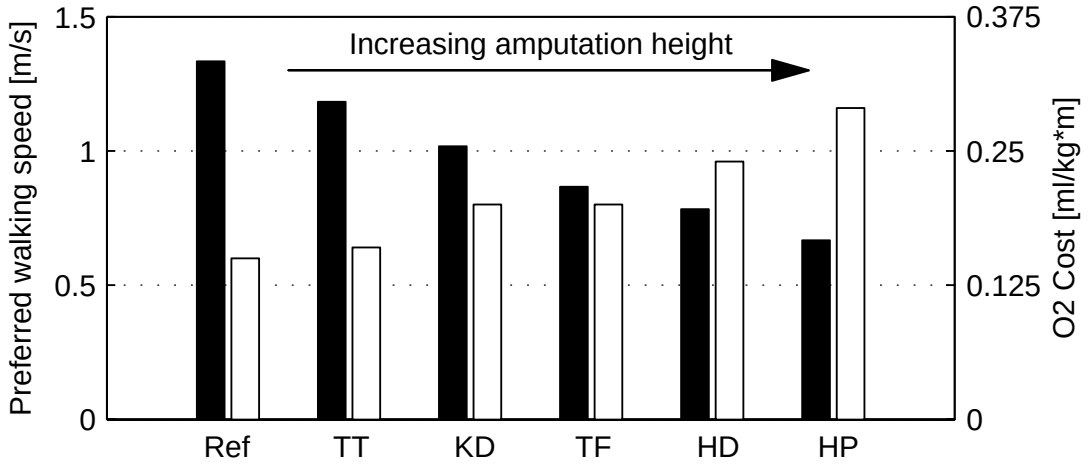

Figure 5: Preferred walking velocity (black) and oxygen consumption (white) for different levels of amputation. Ref, reference non amputee; TT, transtibial; KD, knee disarticulation; TF, transfemoral; HD, hip disarticulation; HP, hemi-pelvectomy : figure adapted from (Waters and Mulroy, 1999)

transfer energy between the joints. For saving energy, joint couplings seem to be highly beneficial (Van den Bogert, 2003). Without, also loading these tendons in one phase of the gait cycle and releasing this energy in other parts is not possible. This would directly influence energetic effort. Furthermore with such two-joint structures also the coordination between the joints could be facilitated. Co-contraction of antagonistic muscles at the prosthetic and also at the contra-lateral site could help to stabilize gait without these structures. Also this would result in increased metabolic rates.

3.5 SEMI-ACTIVE PROSTHETICS

3.5.1 Ankle Joint

Design characteristics

Compared to passive designs, semi-active feet provide an increased functionality. They are using passive mechanical principles controlled by active adjustable valves. Hydraulic concepts are used for the Raize ankle/foot system (Hosmer) or the élan foot (Endolite). The Raize ankle provides an adjustable planter/dorsiflexion range. In addition resistance is adaptable manually. Reduced damaging forces on the residual limb and greatly enhanced stability on slopes or slippery surfaces are promised (Hosmer). Both mechanisms should provide better ground adaptation especially at inclines and declines. The élan foot uses sensor feedback as an input for adaptive control depending on slope during walking. Foot characteristics should be adapted to the most comfortable and energy efficient response. For this the hydraulics allow adjustments of up to 6° plantarflexion and 3° dorsalextension which adds to the RoM of the carbon foot. 24 hours of operation should be possible.

Gait Biomechanics

The élan foot aims at supporting the push off while ascending slopes by stiffening the ankle damper at touch down. In addition, at descending slopes loading is reduced by a decreased ankle

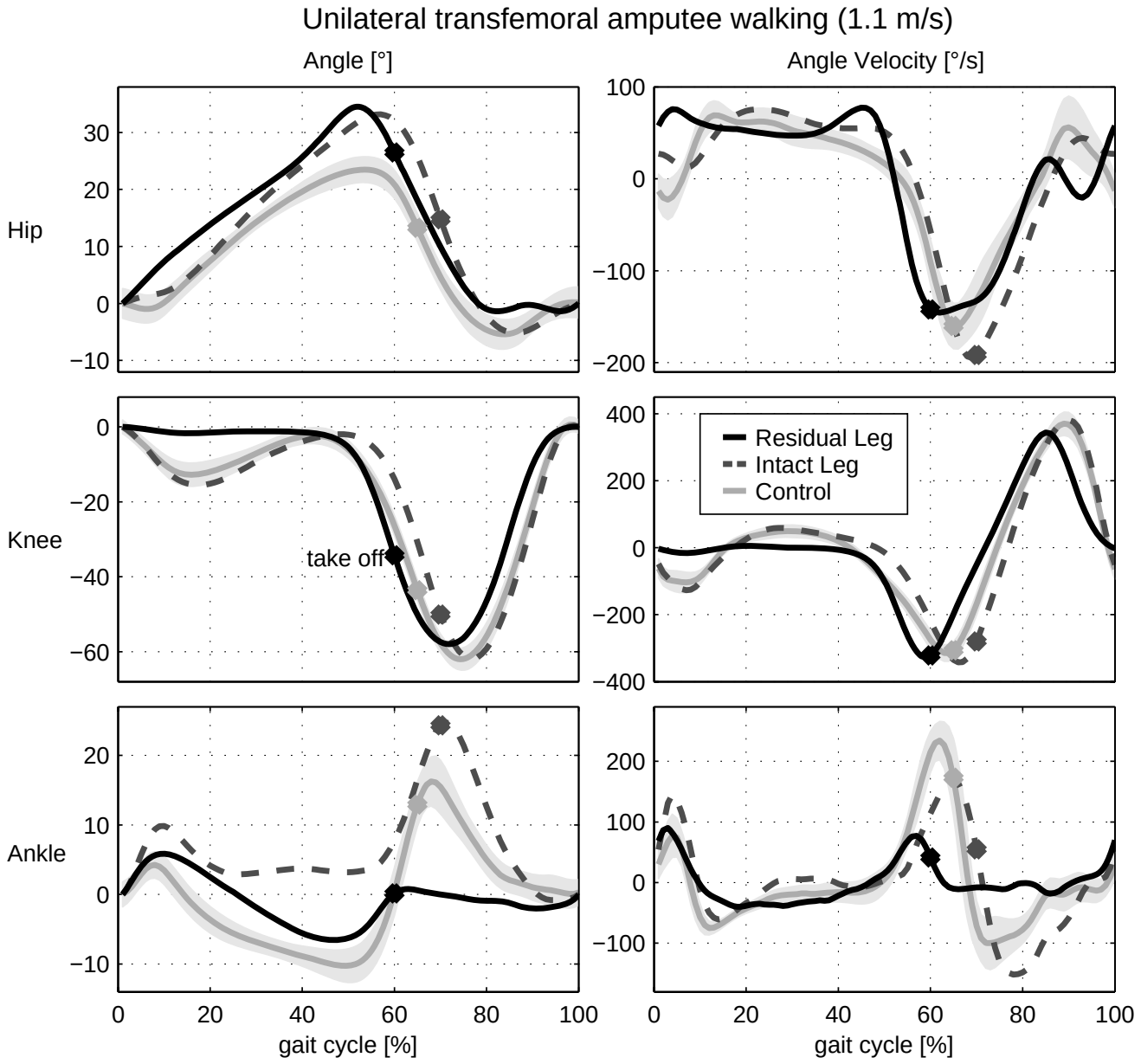

Figure 6: Angle and angle velocity of human unilateral, transfemoral amputees for the hip, knee and ankle in walking at 1.1 m/s. The solid black line indicates the residual prosthetic leg (C-Leg knee and C-Walk foot, Ottobock), the dashed grey line represents the intact amputee leg. Dots are indicating take off for the separate conditions. Reference data (grey solid, (Lipfert, 2010)) is presented with standard deviation. Amputee data is the mean value of 4 subjects taken from (Schaarschmidt et al., 2012), (42.3 years, 1.86 m, 91.3 kg).

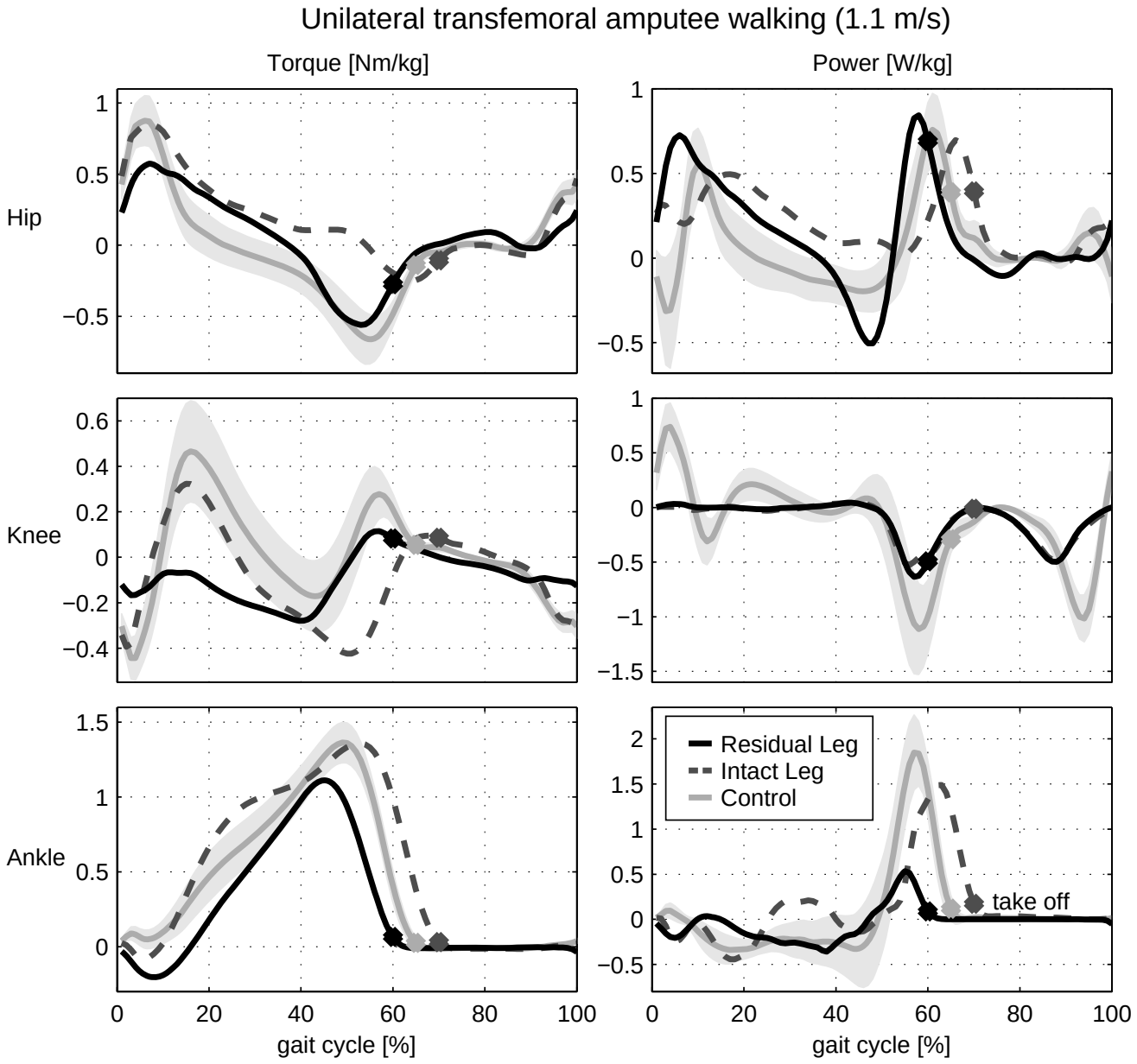

Figure 7: Joint torque and power for human human unilateral, transfemoral amputees for the hip, knee and ankle in treadmill walking at 1.1 m/s. Joint torques are calculated using inverse dynamics. Power is the product of joint velocity and joint torque. Both values are normalized to body mass. The solid black line indicates the residual prosthetic leg (C-Leg knee and C-Walk foot, Ottobock), the dashed grey line represents the intact amputee leg. Dots are indicating take off for the separate conditions. Reference data (grey solid, (Lipfert, 2010)) is presented with standard deviation. Amputee data is the mean value of 4 subjects taken from (Schaarschmidt et al., 2012), (42.3 years, 1.86 m, 91.3 kg).

damping. This results in an increased RoM compared to simple carbon fibre feet and provides more stability.

3.5.2 Knee Joint

Design characteristics

The most popular semi-active knee device is the C-Leg. After the introduction in 1997 over 40000 (Advanced Prosthetic Knee Technology booklet, Ottobock) of them were sold worldwide. Using different sensors (angle sensors, strain gauges) the knee joint can identify the gait phase. By this information and an individual patient depending gain adaptation of the prosthesis, the microprocessor can control the damping of a hydraulic joint. Primary targets like damping knee flexion or extension (negative knee power) in swing phase can be achieved (Fig. 7). However, the created patterns are only partially matching non-amputee data (Seroussi et al., 1996; Johansson et al., 2005; Segal et al., 2006).

Using the compensatory mechanism of the hip extensor muscles, the Genium knee (Ottobock) makes it possible to walk up stairs in an alternating stepping pattern. About two and five days of battery life are stated for the C-Leg and the Genium knee respectively. Up to two days of battery life are also envisioned for the Rheo Knee (Ossur). Damping is realized by a magnetorheological fluid. By varying the magnetic field intensity damping could be adapted comparable to the C-Leg. Similar technology is used in (Nandi et al., 2009; Nandy et al., 2012). Other examples for microprocessor controlled knee joints are the Plié 2.0 (Freedom Innovations) or the Orion knee (Endolite). Both knees are working with hydraulic mechanisms. In addition the Orion uses a pneumatic system to control swing phase.

Gait Biomechanics

A key advantage for microprocessor controlled knee joints to purely mechanical devices is the possibility to adapt to different conditions. For instance an adaptation for different slopes or speeds can be realized.

In a comparison for level walking only little differences between a passive (Mauch SNS) and a semi-active prosthesis (C-Leg) could be identified (Segal et al., 2006). Also when comparing 3R80 (passive) to the C-Leg at different speeds hardly any differences were observed (Schaarschmidt et al., 2012). Thus semi-active knee joints do not necessarily outperform passive mechanism at level walking in laboratory condition. More important seem to be non-steady daily life tasks as addressed in (Theeven, 2012). A daily activity test for amputees was used to compare passive with semi-active knee joints. Time was measured for different tasks. Using the semi active prosthesis all investigated scenarios were finished faster. A higher confidence of the users due to lower risk of falling could be a reason for this result (Blumentritt and Bellmann, 2010; Blumentritt et al., 2009).

Passive knee joints like the 3R80 need a sufficient knee extension to be capable of supporting load. If this angle is not reached like when tripping on uneven ground the amputee would fall. Sensors in the semi-active knee joints can detect such events and provide an increased damping e.g. by closing the corresponding hydraulic valve. Such a mechanism can to some extend prevent falling.

This can clearly increase the amputees confidence. It is of key importance since nearly 50% of amputees (including transfemoral and transtibial amputees) suffer from the fear of falling (Miller et al., 2001). About the same amount of amputees (50%) are indeed falling at least once a year (Greitemann and Bui-Khac, 2006; Kulkarni et al., 1996; Miller et al., 2001). Nearly

20% of the amputees needed medical care after falling (Miller et al., 2001). A maximum of 15 falls for one amputee in the last year (Greitemann and Bui-Khac, 2006) illustrates the relevance of improving preventing aspects like handling training or more secure technology. Technology improvement could decrease the 12% of falls that were reported to result from the prosthesis function alone and the 22% related to the environment (Kulkarni et al., 1996).

In (Kahle et al., 2008) various tests were made to compare passive knee joints with a microprocessor controlled knee joint (C-Leg). Stumbles decreased by 59% and falls by 64% when using the C-Leg. Due to the higher self confidence (stumble recovery) and the possibility to adapt to different speeds (Orendurff et al., 2006; Segal et al., 2006) improvements in walking speed on even and uneven terrain with semi-active knee prostheses are possible.

Benefits of microprocessor controlled knee joints

- stumbles decreased 59% (Kahle et al., 2008)
- falls decreased 64% (Kahle et al., 2008)
- higher potential for security (Blumentritt and Bellmann, 2010; Blumentritt et al., 2009)
- increased PWS 8% to 15% on even terrain (Kahle et al., 2008; Orendurff et al., 2006; Segal et al., 2006)
- similar oxygen costs for higher PWS (Orendurff et al., 2006)
- 3% to 5% reduced metabolic rate (Johansson et al., 2005)
- 75 m fastest possible walking speed (FPWS) on even terrain increased by 12% (Kahle et al., 2008)
- 38 m FPWS on uneven terrain increased by 21% (Kahle et al., 2008)
- 6 m FPWS on even terrain increased by 17% (Kahle et al., 2008)
- performance score for stair descent increased (Kahle et al., 2008)
- faster placing and picking up of objects (Theeven, 2012)
- faster on slopes, stairs (Theeven, 2012)
- faster slalom walking speed while carrying objects (Theeven, 2012)
- decrease in hip work (Johansson et al., 2005)
- lower peak hip flexion moment at terminal stance (Johansson et al., 2005)
- reduction in peak hip power generation at toe-off (Johansson et al., 2005)
- increased symmetry between limbs (Segal et al., 2006)
- less pronounced asymmetry between braking and propulsive impulses (Schaarschmidt et al., 2012)

Further improvements in semi-active knee joints can potentially close the gap between healthy and amputee gait. New designs like the Genium knee (Ottobock) mimic natural knee function better than the previous generations. Knee flexion angle during swing is independent of speed which is comparable to healthy gait (Fig. 1), (Blumentritt et al., 2012). A 4° preflexion of the Genium knee at touch down results in less asymmetry of step length. Increased stance phase flexion was found in 3 out of 11 subjects. Various additional benefits for daily life tasks like walking backwards, standing or walking on slopes or stairs were observed (Bellmann et al., 2012; Blumentritt et al., 2012).

3.6 POWERED PROSTHETICS

Microprocessor controlled spring-damper systems at the knee or at the ankle joint can improve prosthetic technology and amputee performance. However, kinematic and kinetic gait analyses still show more asymmetric gait and higher oxygen consumption than in non-amputees. Continuous asymmetries in gait can cause long term sequelae (Gailey et al., 2008; Robbins et al., 2009) which may result in even reduced living comfort and additional costs for the amputee or the health insurance company. To avoid this, further improvements in prosthetic technology are required.

Passive prosthetic devices can mimic eccentric or isometric muscle behavior (e.g. by dampers). They can also mimic elastic tendon like behavior by different kinds of springs. It is not possible to mimic concentric muscle behavior with passive systems. Including such an ability could provide additional functionality to a prosthetic system.

First steps toward powered prosthetics were realized with the Belgrade Above Knee Prosthesis (AKP) in the late 80's (Popovic et al., 1991). The system used external power supply and control. DC motor technology was used to drive the knee joint. By the active knee amputee energy consumption could be reduced and maximum walking speed could be increased.

25 years later still only a few commercialized systems provide the possibility to inject energy and to create joint torques actively. 26 systems including prototypes and commercialized systems are listed in Tab. 3 and 4 (appendix). Some of them have a couple of previous design generations. Non of the systems is addressing an active hip joint. So far only powered systems for ankle (Fig. 8, a-j, r) and knee (Fig. 8, k-r) are described in literature.

The first commercialized active foot is the Proprio Foot (Ossur, Fig. 8, i). It has the possibility to lift the toe during swing phase to adapt to terrain and to prevent trips or falling. Different sensors (accelerometer, angle sensor) detect the actual state (walking flat, stairs, slopes, sitting, standing) and set a linear actuator to the appropriate position corresponding to a defined ankle angle. For this motion events like take off or touch down are identified. To get a better pattern recognition also the last step is taken into account. A similar actuation concept was used for the prosthetic ankle concept introduced in (Svensson and Holmberg, 2006).

A further commercialized concept for an active foot is from iWalk (Fig. 8, f). They introduced the BiOM Power Foot, an active prosthesis to replace the ankle joint . Achilles tendon like elastic function (spring) is combined with a motor that mimics calf muscle behavior. By this method not only swing phase adaptations like in the Proprio Foot but also active powered push off becomes possible.

Active motor support for the knee joint is provided in the Power Knee (Ossur, Fig. 8, o). The first generation of the knee joint was launched in 2006. The second much more compact version is available since 2011. Knee extension while ascending stairs and slopes or also while standing up from sitting is supported by a motor. During sitting down or descending stairs and slopes the

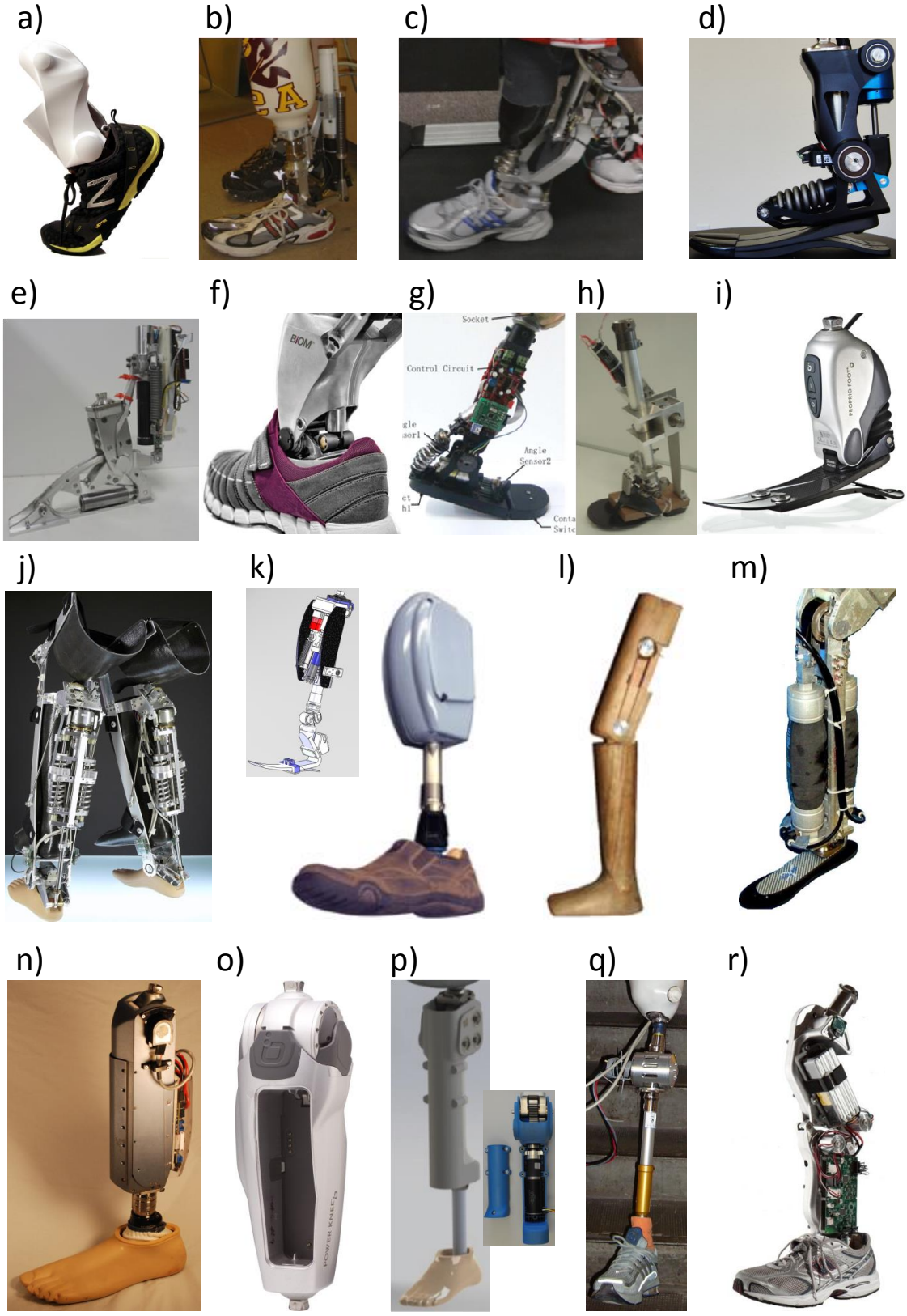

Figure 8: Active prosthetics for the ankle (a - j) the knee (k - q) and for both joints (r). For a more detailed description see Tab. 3 for the ankle and Tab. 4 for the knee joints (appendix).

motor can dissipate energy. During take off the motor rises the heel actively for swing flexion. In addition it assists at stairs or slopes for positioning the knee adequately for touch down. Like in the BiOM Foot a spring is assisting the motor to some extend by storing energy in a specific phase (yielding, stance phase flexion) and releasing it later. The same approach is used in (Martinez-Villalpando et al., 2011). A powered knee joint prototype with an antagonistic SEA design (Fig. 8, n) could increase amputee's average self-selected walking speed by 17% from 1.12 m/s to 1.31 m/s compared to a C-Leg. At fixed speed (1.3 m/s) metabolic costs decreased by 6.8% using the powered prototype in comparison to the semi-active knee joint.

Various powered prototypes (Tab. 3, 4) are in commercial or university development. Concepts are including single ankle and knee prosthetics but also approaches combining both joints actuated in one design. At the Vanderbilt University (Nashville) a combination of powered knee and ankle was developed (Sup et al., 2009), (Fig. 8, r). The concept will be further developed and commercialized by Freedom Innovations.

A concept using electrical motors to do cheap design knee prosthetics is introduced in (Islam et al., 2013; Latif et al., 2008), (Fig. 8, l). The motor should not replicate torque profiles of walking or stair climbing but it should enable the person to flex or extend the knee in low load or no load conditions.

Powered ankle joints for walking (Odyssey Ankle, Fig. 8, a) and running (Fig. 8, c and d) were developed at Springactive and Westpoint Military Academy (Hitt et al., 2010a) based on previous designs (Sparky, Fig. 8, b) from the Arizona State University (Bellman et al., 2008).

Walking should also be achieved with the PANTOE 1 (Fig. 8, g) foot prosthesis developed at the Peking University (Yuan et al., 2011; Zhu et al., 2010). In addition to the common concepts an activated toe joint is integrated in the design.

A mixture of prosthetic and orthotic design is developed at the TU Darmstadt. The Powered Ankle Knee Orthoprosthesis (PAKO, Fig. 8, j) should be used to evaluate elastic actuator design and control concepts for humanoid locomotion. Therefore a mechanism to change stiffness of a spring in the SEA is included in the design.

3.6.1 Mechanics

Actuator Concepts

All commercial available active prosthetics and the most of the prototypes use electrical motor technology for driving the ankle or the knee joint. In addition some of them include different kinds of elastic concepts. Series, parallel or unidirectional parallel alignments of motor and elastic element are used aiming at a reduction of motor requirements. Peak power (PP), which corresponds to motor size and energy requirements (ER), which defines battery size and operation time are characteristics to be decreased in comparison to direct drive (DD) systems.

Most of the active prosthetic prototypes try to mimic torque ankle profiles of the ankle and knee joint. Some of them are only acting with minimal power efforts (Fradet et al., 2010; Svensson and Holmberg, 2006) to change for example ankle angle for ground clearance in flight phase or to adapt ankle angle to slopes.

In order to get a higher power density than in electrical motors also hydraulic or pneumatic actuators could be used. In (Pillai et al., 2011) a design is introduced that provides energy injection for the ankle and the knee joint by linear hydraulic actuators driven by a single pump. So push off can be supported at the ankle, early swing at the knee and the ankle joint. During stair climbing and late swing the knee can be powered. A special feature of the prosthesis is to work in active mode or also as a semi-active device like the C-Leg.

Pneumatic actuation was demonstrated with the pleated pneumatic artificial muscles (PPAM) concept (Versluys et al., 2009). The system was able to produce required torques for an artificial ankle joint in walking. PPAM pressure was generated by a stationary compressor in the laboratory.

Using PPAM, a stiffness adaptation for different speeds was possible. Required stiffness was estimated by a linear regression on human ankle torque-angle curves.

Similar pneumatic concepts are used for experiments with orthotic structures (Ferris et al., 2005; Sawicki and Ferris, 2009).

Pneumatic actuation can also be found in a knee prosthesis (Waycaster et al., 2011), (Fig. 8, m). To become independent of external pneumatic supply this group investigates liquid propellants as energy source. The monopropellant, a reaction product of a catalytically decomposed liquid, should be able to provide large power output and long operation times. For a mobile solution the compact energy storage of the propellant will be beneficial (Shen and Christ, 2011).

The high power density of the pneumatic system (Waycaster et al., 2011) can help to improve prosthetic design. Similar advantages in power to weight ratio are identified for hydraulic solutions (Durfee et al., 2011).

Spring Configurations

For the different leg joints and also different tasks optimal elastic actuator configurations can be identified. The challenge is to identify a most multifunctional solution that can provide benefits in various daily life activities. In terms of energy consumption the primary focus should be on the most common daily life activities like walking or just standing in place. But also energy and power requirements in stair climbing, standing up, sitting down, walking slopes or running could be included in the choice for an elastic actuation concept.

Inspired by muscle modeling different actuator solutions can be considered. Solutions with series elastic elements (SE) were used in (Pierrynowski and Morrison, 1985). Parallel elements (PE) to the contractil element (CE) were omitted in this study because many authors reported only negligible passive parallel forces. In contrast the Hill Model includes a SE and a PE. Different solutions exist with the CE and the SE together in parallel to the PE (Zajac et al., 1989), (Fig. 9, e) or only the CE in parallel to the PE (Nigg et al., 1994), (Fig. 9, c). In addition to the conventional elastic concepts unidirectional springs, coming into action at a defined condition (kinematic, kinetic), can be considered.

Such an approach is used in (Sup et al., 2009) where the spring comes into action at an ankle angle of about five degrees of plantarflexion. The BiOM ankle prosthesis (Eilenberg et al., 2010) includes an SEA in addition, to extend the system to a scheme similar to Fig. 9, i. In an earlier version of the device the unidirectional spring is mentioned to be engaged at zero degrees (Au et al., 2009). A spring in series (Fig. 9, b) with a much smaller stiffness than in the BiOM ankle is included in the Robotic Tendon approach of Sparky. Stiffness is defined using power optimization calculations (Hollander and Sugar, 2005). Especially the long lever arm between ankle joint and actuator causes this design difference (Grimmer and Seyfarth, 2011b). In contrast, in the BiOM ankle series stiffness is chosen based on open-loop force bandwidth (Au et al., 2009). An extended version of the Robotic Tendon approach is introduced in (Hitt et al., 2010a; Schinder et al., 2011). For running two parallel elastic actuators were included in the design to achieve the required power demands.

A series spring approach is also used for the AMP foot 2.0 (Cherelle et al., 2012), (Fig. 8, e). In contrast to the approaches using motors with over 150 W the design requires only a 60 W motor. This solution is possible by combining two basic mechanisms. A series spring, which is decoupled from ankle motion, is loaded with a constant power by the small motor during the entire stance phase. A second spring is saving energy in a similar way like the forefoot part in ESAR feet. During push off the passive spring returns its energy. In addition a clutch is used to release the energy from the motor-spring combination (Fig. 9, f). On the one hand this approach provides the advantage of less peak power requirements for the motor. This could potentially save space and weight if the required clutch mechanism is small enough. In contrast to the mechanisms used in (Eilenberg et al., 2010) and (Hitt et al., 2010b) the energy return cannot be modulated in the same way. It is like a catapult that just releases the energy if the trigger is pulled. The interaction with the amputee must be programmed carefully to match desired patterns. To which extend this approach can handle different daily life situations like different speeds, slopes and stairs should be further investigated.

Two SEA's are used in the PANTOE 1 (Yuan et al., 2011; Zhu et al., 2010). The ankle prosthesis includes one SEA for ankle plantar and dorsiflexion. Another SEA modulates toe joint motion. It is envisioned that the active prosthetic toe joint can improve several biomechanical parameters for the foot like RoM, angle velocity and energy output. Higher walking speeds should be achieved in comparison to rigid foot design.

Systematic analysis on elastic actuator concepts that reduce energy requirements (ER) or peak power (PP) were published for the ankle (Grimmer and Seyfarth, 2011b; Wang et al., 2011; Eslamy et al., 2012; Grimmer et al., 2012), the knee (Grimmer and Seyfarth, 2011a; Wang et al., 2011) and the hip (Wang et al., 2011) joint. Methods for calculations base on (Hollander and Sugar, 2005). In order to decrease power, actuator velocity or actuator force could be reduced. A series spring has the capability to decrease motor velocity. A parallel spring has the capability to reduce motor force.

Especially for the ankle joint high benefits could be identified for the motor when using a series spring with optimal stiffness in comparison to a direct drive. In terms of ER the mean advantage for 5 different speeds between 0.5 m/s and 2.6 m/s was about 64.7% for running and 25.8% in walking using an SEA. A PEA (Fig. 9, c) could reduce ER to less extent. 45% and 12.2% were possible respectively. A combination of both elastic structures (SE+PEA, Fig. 9, d) results in an energetic advantage of 52.8% in running and 17.9% in walking for the elastic actuator.

In terms of peak power highest reductions were identified for the SE+PEA system (81.8%) in running. The force reduction by the parallel spring contributes most to reduce power requirements. A single PEA had already a mean advantage for the five speeds of 79%. An SEA could reduce PP by 68.5% in running.

For walking a similar trend was identified. An SE+PEA had highest benefits (70.4%). Lower advantages were identified for the PEA (62.5% and the SEA (48.3%).

Unidirectional parallel springs at the ankle joint (Fig. 9, g, h, i) can have similar power advantages like the PEA. In addition it is possible for some speeds to get lower ER than in PEA (Eslamy et al., 2012).

At the knee joint energetic benefits of 5% to 29% could be achieved by an SEA in comparison to a DD in walking (0.5 m/s to 2.6 m/s). Little or no PP (high speeds up to 31%) reductions were possible in walking, when considering that negative work has to be done by the motor (no

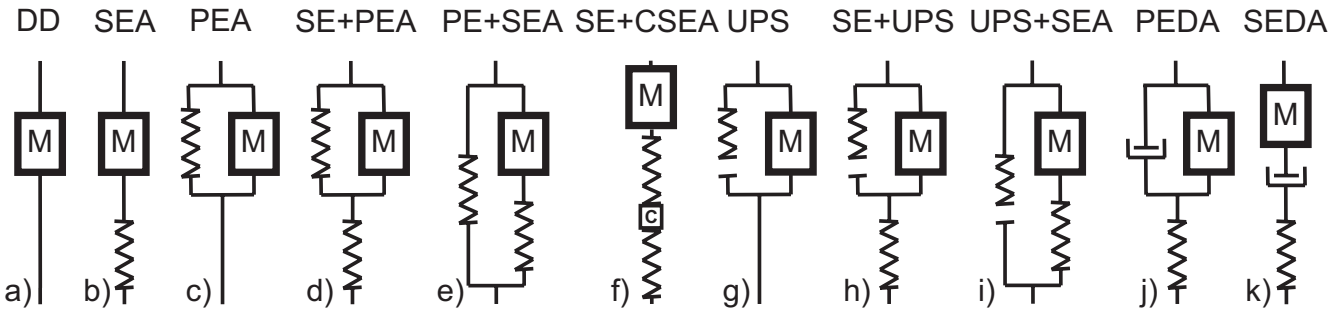

Figure 9: Various concepts for elastic actuators combining a motor (M) with series (SE), parallel (PE) and/or unidirectional parallel (UPS) springs. In addition it could be possible to include clutches (C) or damping elements (j and k).

passive damper or energy harvester to perform negative work). For running (0.5 m/s to 4 m/s) energetic reductions of 40% to 71% and PP reductions of 54% to 78% were identified.

For the hip joint calculations on possible reductions were done for walking at 0.8 m/s and 1.2 m/s. A PEA could reduce torque by 66% for flexion and extension. A reduction of 53% was identified at the hip for abduction and adduction (Wang et al., 2011). Using an SEA 60% reductions of torque could be identified for the same motion.

Damping

Next to springs also dampers can help to reduce actuator requirements in powered lower limb prosthetics. Negative joint power (Fig. 7) can be introduced by these passive prosthetic parts. Due to microprocessor controlled mechanisms damping ratio can be changed by semi-active prosthetic knee joints to adapt to variations in walking speed. Eccentric muscle function can be replaced. A similar function can be realized by a motor using energy for decelerating the motion. In contrast also energy harvesting could be possible for the same process. An energy harvester integrated in a single knee brace (Donelan et al., 2008) could generate about 2.4 W while generative braking in the late swing phase. In (Grimmer and Seyfarth, 2011a) it was shown that using an SEA setup at the knee joint needs nearly no positive work in walking and running. Thus it could be possible to generate electricity at the prosthetic knee joint to use it for powering the artificial ankle joint. A similar idea to use damping work, store it and release it later to support push of is realized in a prosthetic foot prototype (Collins and Kuo, 2010). Damping work from impact during touch down is used. A similar damping function is realized in biology by the heel pad (Gefen et al., 2001). Additionally to the heel pad also wobbling masses are damping impacts in locomotion (Pain and Challis, 2001). Similar systems are not included in current prosthetic designs. Partially shock absorbing elements are used to replace this function.

For a prosthetic ankle joint similar to the eccentric phases of the knee joint it is possible to reduce energy requirements for a motor when using a damper. Possible operation phases are when replacing tibialis anterior function after touch down. Also while descending stairs negative work could be realized by a damper to mimic eccentric plantar flexor work. Eslamy et al. (Eslamy et al., 2013) predicted benefits of up to 50% for PP and about 26% for energy requirements using an SEA combined with a damper in comparison to a pure SEA (Fig. 9, k). Similar concepts combining motors, springs and dampers for a powered ankle joint can be found in a patent from 2012 (Herr et al., 2012). In level walking no benefits of a continuous

acting damper could be identified for the evaluated systems (Eslamy et al., 2013). Controllable dampers that are active only for some gait phases might change the results.

If the damper that assists the motor is only required for some phases of the gait cycle it should be switchable to avoid negative effects for other phases. A damper mimicking heel pad or wobbling mass function can be active the entire gait cycle.

3.6.2 Control

Control of prosthetic devices can be classified by the source of input data. On the one hand computational intrinsic control (CIC) on the other hand interactive extrinsic control (IEC) are possible (Martin et al., 2010), (Fig. 10). CIC has no connection to the user, whereas IEC allows a communication between brain and user. This interaction can happen on the efferent command but also on the afferent feedback site. A commonly used signal in commercial arm prosthetics at the efferent site is EMG (electromyography). But also other signals could be possible for interfacing the peripheral and central nervous systems with the prosthetic system (Navarro et al., 2005). At the afferent feedback site up to now no sensor signals are transferred back to the brain from the prosthetic parts itself. Only sensory organs from the remaining parts of the limb provide information. For example mechanoreceptors of the skin can provide prosthetic socket pressure information or existing knee muscles in transtibial amputees can give information about force and position. A main benefit of IEC can be to provide intent control signals already before the movement occurs. In contrast CIC can only react on current motion where for example classification algorithms detect the intention of the user. A reaction on current motion like in the CIC is also found naturally. Reflex like mechanisms can create basic motion patterns without brain interaction. In cat (decerebrated) and dog (decapitated) experiments it was shown that the spinal cord is able to produce reflex stepping after suppression of all afferent inputs from the brain (Goltz et al., 1875; Sherrington, 1910).

Thus it seems to be useful to have both approaches CIC and IEC combined in prosthetic control to get advantages of decentralized primary locomotion functions and in addition intend based control. Especially for cyclic motions like walking less brain control effort would be required with independent reflex like mechanisms. Using CIC or IEC different levels of prosthetic control are required. Referring to (Sup et al., 2009) the highest level is the intent recognizer that detects the basic movement behavior of the amputee. Activities like standing, climbing stairs, level or inclined walking can be distinguished. On a mid-level the movement control is realized. Here movement phase is detected and an appropriate output for the powered joint is created. At the low level torque, speed or position control is used to generate required motor trajectory.

Various concepts are used to detect users intent and generate required motion patterns. In the following some of them are explained with a focus on unique parts of each approach.

Muscle reflex control

Muscle reflex control can be a way to control a system independent from central motor commands (Geyer et al., 2003). Sensory feedback from muscle spindles and Golgi tendon organs is used as an input for an appropriate control output. These organs can measure length, speed or force in the biological actuators. In (Geyer et al., 2003) it was shown that positive length and force feedback could be used to stabilize hopping in a computer simulation model. This basic idea is used and transferred to a complex multi-segmented bipedal muscle model (Geyer and Herr, 2010). The model is able to perform walking with human kinematics and dynamics, by

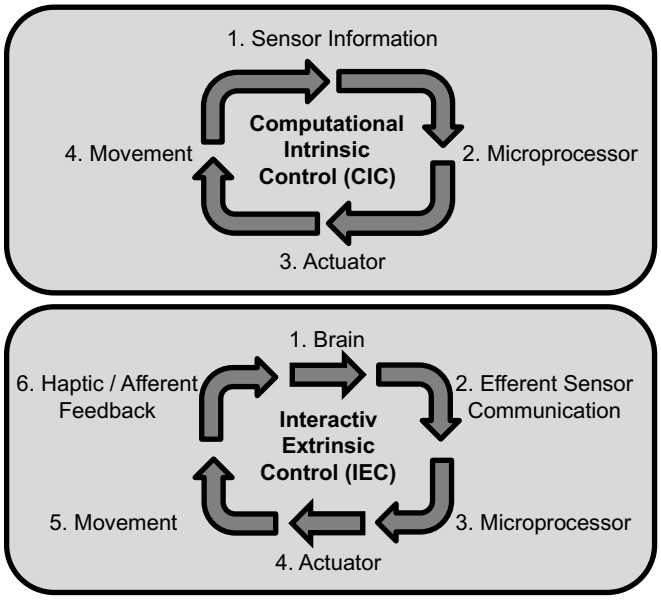

Figure 10: Components of computational intrinsic control (CIC) and interactive extrinsic control (IEC) for prosthetic devices (modified from (Martin et al., 2010))

using proprioreceptive feedback related to the body, muscle and ground interaction. Also it is able to deal with shallow slopes and small ground disturbances.

This concept is transferred to a powered ankle prosthesis (Eilenberg et al., 2010). An ankle angle sensor and an implemented spring force strain gauge can generate the input for the force and length feedback controller. Together with the strain gauge at the pyramid adapter the sensors detect also the gait phase and transitions to set a state machine (stance or swing). Joint torque is generated depending on torque delivered already by the mechanics (unidirectional parallel spring) to match human level walking. Using the neuromuscular model the intrinsic system characteristics will increase net work at the ankle when increasing speed (Markowitz et al., 2011).

Finite state impedance control

The finite state impedance control is used in a combined active knee and ankle prosthesis. A first version was implemented in a power-tethered pneumatically actuated prototype (Sup et al., 2008). Later the control was implemented in a brushless motor driven design (Sup et al., 2009). First an intent recognizer is detecting the amputees behavior. Prosthetic sensor data is compared to a database that classifies different activities like walking, sitting, standing or climbing stairs. For this classification a Gaussian Mixture Model is used (Varol et al., 2010). In addition for example in walking a state machine is separating different phases of the gait cycle. For these phases an impedance is created to match human reference joint torque trajectories. By generating torque instead of position trajectories the controller should provide a more natural performance. The output signal is generated by the amputee and the prosthesis and not only by the prosthesis like in a position based control (Sup et al., 2009).

Phase plane control

Phase plane control of a robotic ankle joint was introduced in (Holgate et al., 2009). Various prosthetic prototypes are using this concept (Hitt et al., 2010a,b). The controller needs a gyro

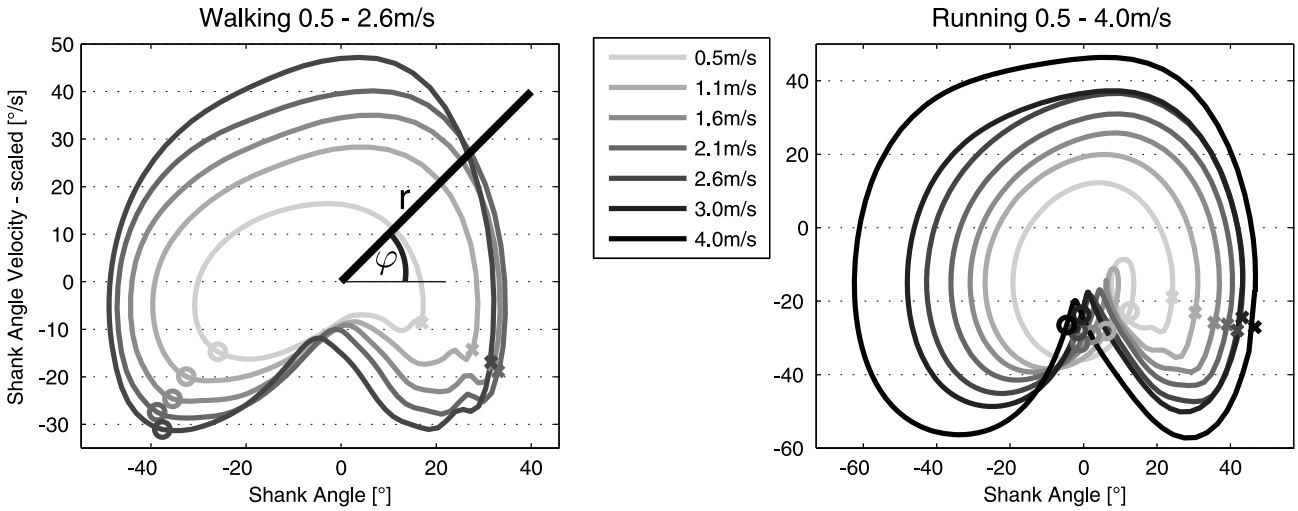

Figure 11: Phase plane trajectories of shank velocity and shank angle for walking and running. Shank velocities are scaled (divided by 10) to create more functional graphs for calculating the Polar angle phi and the Polar radius r. Polar angle is used for gait percent determination. Polar radius for speed determination. Touch down is visualized by a cross, take off by a circle for each speed.

sensor at the tibia to measure shank rotational velocity. By integration, shank angle in relation to the ground is determined. A transfer function is used to eliminate integration errors. Using shank velocity and shank angle a phase plot can be generated. This was made for different step lengths in (Holgate et al., 2009). Another possibility is to do it for different speeds (Fig. 11). The radius of the polar curves can determine step length or gait velocity. The angle phi is used to determine gait percent. Both information are required to set the right motor position calculated by the robotic tendon approach (Grimmer et al., 2012; Hollander and Sugar, 2005). An advantage of this control approach is the possibility for automatic speed or step length adaptation during the gait cycle. When stopping walking shank velocity gets zero and the motor stops automatically. No states are required. Also backwards walking is possible with such a control approach. Slopes, stairs and uneven terrain can be handled by the interaction of the controller and the spring integrated in the mechanical design of the Sparky prosthesis.

Control based on residual joints, segments or organs

In (Parsan and Tosunoglu, 2012) a control method is introduced that uses the knee motion of a transtibial amputee to control ankle motion. For this a rotary potentiometer is measuring the knee angle that is used to calculate knee angle velocity. In addition a force sensor at the heel is used for contact information. Based on the sensory signals 4 states related to positive or negative velocity and heel contact or heel in flight phase can be defined. Based on the state ankle angle is adjusted. Depending on amputation level also thigh (Thomas and Simon, 2012) or shank (Holgate et al., 2009) can be instrumented with sensors to control the prosthetic leg. In (Thomas and Simon, 2012) instead of a transfer function (Holgate et al., 2009) data from accelerometers and a Kalman filter is used to eliminate drift when calculating segment angle.

A method to determine knee and ankle motion by measured hip behavior is introduced in (Mutlu et al., 2011). Recursive Newton-Euler computation and inverse dynamics are used to obtain the joint behavior in walking.

Fuzzy logic as control approach is used for a motor driven knee joint (Alzaydi et al., 2011; Borjian, 2009; Lim, 2008). As an input a potentiometer at the knee and an accelerometer at the femur was used.

Prosthetic control on the basement of eye motion was proposed in (Duvinage et al., 2011). At the highest control level user intent like starting of walking, stopping or changing of speed can be transmitted to the prosthesis.

A neural network-based gait pattern classifier together with a rule-based gait phase detector was introduced in (Mai and Commuri, 2011). Inner socket forces of a transfemoral amputee were identified and used to establish a control scheme for a prosthetic foot.

EMG based control

EMG based control approaches for prosthetics are tested since the 40's for arms and legs (Battye et al., 1955; Childress, 1985; Dyck et al., 1975; Horn, 1972). Commercially available are so far only prosthetic arms. EMG signals of upper arm muscles are used to flex or extend the elbow, for closing of the hand or also pronation of the wrist (Cutti et al., 2007). Various research groups try to use this biological signal also for powered prosthetic control at the knee (Hargrove et al., 2011; Hoover et al., 2013; Islam et al., 2013) or also at the ankle (Au et al., 2005). EMG as a control signal for powered legs seems to be possible. Similar errors could be achieved while EMG based following of a trajectory with a prosthetic knee joint compared to a healthy knee (Ha et al., 2011).

A key problem in EMG control is safety. Especially with a prosthetic leg falls caused by measurement and classification errors could be possible. In (Zhang et al., 2012) it was tested to which extend intent recognition errors based on EMG will influence safety of gait. For this purpose 0.1 s, 0.2 s and 0.3 s lasting errors were applied in different phases of the gait. Errors applied used control signals for standing or ramp descent at level walking. For errors of 0.1 s no instability was reported. Also for longer error times during swing knee extension no critical safety issues were reported by the amputee. For 0.2 and 0.3 seconds during stance phase critical errors are reported. As a reason for the unsafe condition energetic differences between real and applied state were identified.

In (Hoover et al., 2013) an impedance control approach was combined with myoelectric control signals. Evaluation of a single subject with transfemoral amputation showed robust and repeatable performance for ascending stairs. Using also an EMG based control, combined with the active ankle and knee prosthesis described by (Lawson et al., 2013), in 2012 Zac Vawter climbed the 103 floors of Chicago's Willis Tower.

Neuromuscular - Mechanical Fusion

In addition to pure EMG based control also a fusion between biomechanical sensor signals (CIC) and EMG (IEC) could be possible. In (Huang et al., 2011) a classifier for gait was developed based on gluteal (2x) and residual thigh (9x) muscle EMG. Neuromuscular signals were combined with GRF and torques measured by a load cell on the prosthetic pylon. Insole pressure sensors were used for gait event detection. Using the combined method resulted in higher accuracy of gait mode prediction. 99% could be achieved in stance, 95% in swing phase. To increase swing phase accuracy authors propose to add kinematic sensors. Transitions between different gait modes (obstacle crossing) were recognized using the sensor fusion with a sufficient prediction time.

Sensor fusion was also used in (Delis et al., 2011). Here the desired knee angle was estimated based on gyro sensor and EMG data. The authors demonstrated that combining both signals could increase estimation precision and it reduces artifacts of purely EMG based control strategies (Delis et al., 2010).

Control with sound limb signals

Prosthetic control with the sound limb named "echo control" was already discussed in (Grimes et al., 1977). In (Au et al., 2005) it was tested if it is possible to generate motion patterns for a prosthetic foot by EMG signals of the residual limb. Both, a neural network based and a biomimetic based control approach could predict desired ankle movement patterns qualitatively. Using angle and angular velocity sensors of the sound limb (Vallery et al., 2011) it was possible to control a prosthetic knee in walking. Ascending stairs was possible but required balance assistance. Descending was anticipated to be insecure and was less smooth compared to the C-Leg.

Grimes described that asymmetric behavior of the legs can cause problems in this approach (Grimes, 1979). Especially the sound limb of the amputee that is doing a compensating motion cannot be the reference for the residual limb. To overcome this problem healthy subject data was used in (Vallery et al., 2011).

3.6.3 Prosthetic challenges

Wearing a lower limb prosthesis causes several challenges in daily life situations. Less RoM, no power support, no direct control but also things like water proofed design can be a reason. For a comparison of passive and semi-active microprocessor controlled knee joints a daily activity performance test was developed (Theeven, 2012). Special test situations were created to be executed by the subjects. Tasks like normal walking, walking sideways, sitting down, standing up, carrying loads or also picking up objects are included. In addition tasks like dressing, putting on or taking off the prosthetic device are tested. The complexity of the test shows the requirements for a prosthetic development. Some of the requirements are addressed in the following subsections.

Terrain

Most prosthetic prototypes are first designed to be capable of standing and level walking. Due to additional daily life requirements like slopes, stairs or rough terrain further functionality should be included. Also tasks like standing up, sitting down, driving a bicycle or a car could be achievements to take into account.

Level ground: Level ground walking is one of the primary achievements for prosthetic design. Healthy people realize about 6,500 walking steps per day (Tudor-Locke and Bassett, 2004) with a preferred walking speed of about 1.3 m/s (Dal et al., 2010). In comparison to passive prosthetic parts active ankle or knee joints should be able to reduce amputee metabolic costs, increase speed and reduce asymmetries in the gait pattern of the amputees.

With the BiOM ankle prosthesis ankle push off is supported. For a study of 11 amputees the ankle prosthesis generated significantly greater peak ankle power (35%) in comparison to healthy controls (Ferris et al., 2012). In comparison to passive ESAR feet an increase of 125% was possible. For a second study the increase of PP was about 54% compared to an ESAR foot (Mancinelli et al., 2011). Referring to (Zelik et al., 2011) higher peak power values, compared to normal condition, may not result in better gait performance. Using the motor also higher

RoM could be achieved in comparison to the ESAR feet (30%) (Ferris et al., 2012). However the control group was still 20% better. The difference is caused by the ankle motion shortly after push-off. Here the healthy ankle joint is highly accelerated when leaving the ground. The fast stretching of the dorsal extensors is possible for muscles but for a prosthesis doing dorsal extension and plantarflexion by one structure it is hard to realize. High power values and less inertia would be required for the motor. The prosthesis is maybe not capable to mimic human behavior at this event. Also it could be possible that the desired motor trajectory is on a compromise solution to save energy at this point. The change of motor turning direction shortly after this event is strengthening the argument for a compromise solution. Here again higher power demands depending on required braking and acceleration of motor must be considered.

In addition to the effects at the ankle joint differences at knee and hip joint were identified for the control group and the powered prosthetic leg. Effects of a missing biarticular structure between the ankle joint and the knee joint are mentioned as a possible reason. Also higher ankle PP of the BiOM foot, compared to healthy subjects, could be a reason for pattern differences. In comparison to (Herr and Grabowski, 2012; Au et al., 2009) (5% and 23% increase) an increase of about 6% in self-selected walking speed from 1.32 m/s to 1.4 m/s was identified using the powered foot compared to the ESAR foot (Ferris et al., 2012). Self selected walking speed also increased with the Sparky prototype compared to a passive foot (Hitt et al., 2010b) for one tested amputee. Desired ankle angle could be achieved in stance. In swing phase desired prosthetic ankle angle was reached too late. As a reason control properties can be assumed because electrical power consumption was not a limiting factor at this phase.

Typical amputee residual limb behavior with shorter stance and longer swing phases was not measured using the BiOM ankle. User recognition, reflected by the biomechanical data, resulted in higher user satisfaction using the powered foot.

Oxygen consumption in level walking could be reduced by 8.4% using the BiOM ankle compared to an ESAR foot (Mancinelli et al., 2011). 14% reduction could be achieved in a study with a previous ankle design (Au et al., 2009).

Self-selected walking speed was about 24% higher for one transfemoral amputee using an powered knee combined with a powered ankle joint (Sup et al., 2009). Level ground walking speed increased from 1.14 m/s to 1.41 m/s. Peak power at the ankle joint was at about 250 W, about 50 W were realized at the knee joint. At the ankle 0.2 J/kg of net energy is delivered each step which is very close to non-amputee data (0.22 J/kg Tab. 1). In total 66 Watts (45 ankle, 18 knee, 3 embedded system) were required doing one step with powered knee and ankle for a 70 kg amputee. Using the 0.62 kg (lipo 29.6 V, 4000 mAh) battery the prosthesis could be used over 9 km of powered level ground walking.

In comparison to most semi-active knee joints, stance phase flexion could be realized using the powered knee (Sup et al., 2009). Positive power could be delivered. In contrast to (Martinez-Villalpando et al., 2011) the system is not using springs at the knee joint to assist the motor. Partially negative joint power could be used to load the spring and to get positive power back to assist the motor. Additional reductions in energy requirements can potentially be achieved (see Sect. 3.6.1). Using an antagonistic SEA setup at the knee joint (Martinez-Villalpando et al., 2011) in combination with an ESAR foot already results in metabolic reductions of about 7%. Self-selected speed also increased with this setup from 1.12 m/s to 1.31 m/s (+ 17%) when using the active device compared to the C-Leg. Mean power consumption was about 11 W / gait cycle (Martinez Villalpando, 2012) for 4 subjects (mean weight 93.3 kg, mean speed 1.37 m/s). Even though the achieved knee angle - torque profiles are not similar to results achieved in (Sup

et al., 2009) mean power requirements for the device using springs are 0.12 W/kg compared to 0.26 W/kg - 0.3 W/kg (1.42 m/s, 70 kg) when using direct drive. Contrary results for walking speed and metabolic costs were identified in (Cutti et al., 2008) for the first version of the Power Knee. In a preliminary study with two amputees the powered device caused higher metabolics and reduced walking speed in comparison to the subjects with a semi-active prosthetic knee joint (C-Leg).

Slopes: Due to limited RoM and power generation amputees struggle to walk especially inclines (Vickers et al., 2008). Similar to level walking transtibial amputees show less deficits than transfemoral amputees (Vrieling et al., 2008). To improve gait performance authors propose to improve control of prosthetic knee flexion without stability reductions. Using active prosthetics this criterion can be addressed. In order to set the right control slope has to be detected. Slope estimation could be realized by an accelerometer at the prosthetic foot (Svensson and Holmberg, 2006). An accuracy of 0.5 to 1.0 degrees could be achieved for indoor experiments. Combining the accelerometer with a gyro sensor (at foot) resulted in an accuracy of about 1.5 degrees (Sabatini et al., 2005). Also strain sensors could be a possible solution. An error of about 1.5 degrees was identified when using these sensors to detect the slope at various speeds (Svensson and Holmberg, 2010). Instead of placing sensors at the foot segment also other locations were considered. In (Aminian et al., 1995) slope was estimated based on accelerometers placed at a waist belt. A neural network was trained and could predict slope with a standard deviation of about 2.3%. The possibility to adapt to slopes was shown for an active knee and ankle prosthesis (Sup et al., 2011). When a heel and a ball load sensors are detecting ground contact, slope angle is estimated by an accelerometer. 12, 15, and 17 J per stride were measured for the conditions level ground, 5° incline and 10° incline. For the active ankle-knee device 12.2 km of working range were estimated for level walking. Walking a slope of 5° or 10° would result in a decreased capability of 9.2 km and 7.7 km respectively. Compared to the semi-active C-Leg the authors identified various differences when using the powered device in upslope walking.

- stance knee flexion during heel strike and mid-stance
- ankle plantarflexion during heel strike
- ankle plantarflexion during push-off
- increased knee flexion with increased slope after heel strike
- net knee extension during stance phase
- increasing bias towards ankle dorsiflexion with increasing slope

Stairs: How many stairs people climb each day hardly depends on living and working conditions. For a study among 2,539 men (mean age, 57 years) on longevity (Lee and Paffenbarger, 2000) 31% of subjects reported less than 10 floors per week. Between 10 and 20 floors were reported by 20%. Between 20 and 30 by 19% and more than 35 floors by 30%. Assuming a mean of 22 floors a week and 15 stairs per floor this would result in about 47 stairs a day. This value is less than the value reported in (Purath et al., 2004). A group of 151 women (mean age, 43 years) reported 4.4 flights of stairs a day. At 15 stairs a flight this would be 66 stairs a day. In comparison to 6,500 walking steps per day (Tudor-Locke and Bassett, 2004) 47 to 66 stairs a day are only a very small amount. Ascending stairs requires a higher power effort than level

walking (Sup et al., 2011). Descending seems to need higher control effort because 76% of stair falls happen while descending (Svanström, 1974).

Stair ascent with a powered foot was analyzed in (Aldridge et al., 2012). In comparison to an ESAR foot the powered version could improve peak plantarflexion and push off power. It was found that peak power did not differ between the prosthetic foot and the ankle joint of a control group. Surprisingly the hip strategy to support stair ascent used by transtibial amputees with a passive foot is not influenced by additional RoM and push off power. Hip strategy is characterized by increased prosthetic limb hip extensor torque and power, reduced knee torque and power and a more extended residual limb knee in stance phase (Aldridge et al., 2012). A combination of powered knee and ankle was tested in stair ascent and descent (Lawson et al., 2013). The authors could show that using the powered prosthesis healthy gait was reflected better in comparison to a semi-active device (C-Leg). Similar characteristics were identified for the Power Knee in (Wolf et al., 2012). Without the possibility to inject energy knee extension at the semi-active knee joint in stair ascent is impossible. To ascend stairs a different strategy was used by the amputee including support of the hand rail (Lawson et al., 2013). Knee joint remained extended for the whole step. This causes high differences between healthy control, powered knee and the semi-active knee device. For stair descent less difference was identified for semi-active and powered knee joint whereas at the ankle joint the powered one showed much better performance in RoM.

Rough Terrain: Walking uneven terrain requires adaptation mechanisms for secure foot placement. This includes an angle adaptation to match ground slope that can vary with each step for example in rocky surfaces. Possible mechanisms for such adaptations could be active controlled or also passive like dampers or springs. To adapt contact area of the foot to the ground, a healthy foot can do inversion and eversion. For passive prosthetic feet this function could be partially represented by multiaxial joints or also splitted feet (Echolon VT). Powered solutions to increase amputee balance may provide additional benefits (Panzenbeck and Klute, 2012). In (Gates et al., 2013) it is shown, that an amputee wearing a powered foot prosthesis providing plantarflexion, has a 10% higher self-selected walking speed compared to an ESAR foot on a rocky surface. In comparison, on level ground a mean increase of about 5% (3 subjects) to 23% (7 subjects) was identified in (Herr and Grabowski, 2012; Au et al., 2009).

Sitting down - sitting - standing up

Semi-active prosthetic knee joints like the C-Leg are able to secure sitting down by the mechatronic hydraulic stance phase safety system. The knee joint is damped to avoid collapse. In comparison standing up can not be supported by the passive mechanics of these devices. Intelligent mechanisms with springs, storing energy while bending the knees during sitting down, similar to the mechanism in (Collins and Kuo, 2010), could potentially improve this. Standing up could be facilitated by powered knee devices. In (Varol et al., 2009) a finite state based impedance controller is designed to solve the specific task of sitting down and standing up. The subject reported easier standing up and he felt more support from the prosthesis compared to the C-Leg which he uses daily. Up to 0.7 W/kg of peak power was delivered by the powered knee during standing up and sitting down. Also the Power Knee (Ossur) can provide support in both sitting down and standing up. A comparison between C-Leg and Power Knee was made in (Highsmith et al., 2010). The authors analyzed hip torques, knee torques and vertical GRF for symmetry at one subject. While standing up for all conditions except for GRF the Power Knee showed improvements. However, still high asymmetries between the sound limb and the residu-

al limb exist. This outcome was approved in (Highsmith et al., 2011) where in addition to C-Leg and Power Knee also the Mauch-SNS was tested. Seven amputees for each joint were analyzed and compared to a seven subjects control group. While sitting down, a significant difference could only be identified for the prosthetics in GRF. The Power Knee showed best, the Mauch-SNS worst performance. While standing up a significant difference could only be identified for the hip torques. Also here, the Power Knee provides less asymmetric behavior. The authors concluded that with all three tested knee joints the transitional movement between sitting and standing is a one-legged task which probably increases the risk of injury or an accelerated degeneration to the sound limb.

A similar comparison with five C-Leg and five Power Knee users was done in (Wolf et al., 2013). The intact limb had higher average peak sagittal knee powers and vertical GRF for both prosthetic groups. During standing up peak knee power of the residual limb was greater for Power Knee users. In contrast to (Highsmith et al., 2010) but in line with (Highsmith et al., 2011) vertical GRF asymmetry was greater for the C-Leg. Few differences between both devices were identified.

As standing up is primary powered by the knee joint it is important to know that already significant differences between intact and residual limb exist for transtibial amputees (Agrawal et al., 2011). Intact limb body weight support was about 64% at seat off events. As a reason the authors assumed less muscular strength at the residual limb or limitations in ankle dorsal extension and plantar flexion.

While sitting it is important for the amputees to unlock the knee and move it freely. This provides higher comfort when choosing sitting position. Nearly all prosthetic knee devices include the feature to flex the knee joint within RoM.

Standing

While standing using a powered prosthesis the whole microcontroller - sensor system works to guarantee save changes in amputee behavior. This consumes about 3 W (Sup et al., 2009). In addition motors have to create isometric behavior in the knee and the ankle joint consuming each also about 3 W. In total about 10 W are required only for standing. To reduce energy consumption in standing it could be an option to switch to a semi-active mode like envisioned in (Lambrecht and Kazerooni, 2009) for the low battery situations. Here like in the C-Leg only the microcontroller would consume energy in standing.

Prosthesis mass

A design criterion for a prosthesis is its mass. Especially higher masses at the foot segment will increase hip joint torques during walking. In addition net metabolic rate will increase (Browning et al., 2007). To avoid these effects similar or smaller segment masses should be achieved. To estimate the mass of partially missing segments (m_{seg}) of the lower limb the formula provided below can be used. It relies on the assumption that the thigh and the shank have the shape of a frustum with a relationship of the upper to the lower circle of 0.75. This relationship is introduced because of the segmental center of mass which is at about 37% (Clauser et al., 1969; Robertson, 2004) of the segment length from the proximal site.

$$m_{seg} = \frac{h_a}{h_t} * \frac{(1-0.25*\frac{h_t-h_a}{h_t})^2 + (1-0.25*\frac{h_t-h_a}{h_t})*0.75 + \frac{9}{16}}{\frac{37}{16}} * m_s * m_b \quad (1)$$

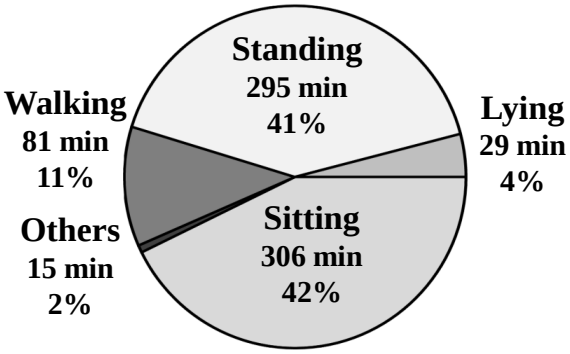

Figure 12: Daily activity of healthy retired people with a mean age of 66 years. Activity was measured for 12 hours after waking up (modified from (Pitta et al., 2005)).

The required constant for the relative segmental mass m_s is 0.0435 for the shank and 0.1027 for the thigh (Robertson, 2004). To get the mass of completely missing segments the segmental mass m_s is multiplied by the body mass m_b. h_t represents the unaffected length of the shank for transtibial or of the thigh for transfemoral amputees. h_a is the missing length of the affected segment.

We now estimate m_{seg} for a transtibial amputee (mass = 75 kg, body height = 1.8 m) that should fit to the BiOM ankle prosthesis which has a build height of about 0.22 m. Referring to (Winter, 2009) the segmental height of the foot is about 0.039 times the body height. This would result in about 0.07 m height for the foot. The height of the shank is 0.246 times the body height what would be about 0.44 m for h_t. An amputation height of about 0.3 m (measured from ground) would result in an amputation of about 0.23 m (h_a) for the shank segment. Using Eq. 1 a missing shank mass of 1.5 kg can be assumed. For the foot, which has a segmental mass of 0.0147 of body mass, 1.1 kg can be assumed. To fulfill the requirements of mimicking human like masses for the design a total prosthetic mass (including socket, adapters, prosthetic foot) of 2.6 kg is predicted. The weight of the BiOM foot is about 2.4 kg including battery and foot cover.

Sound level

Noise is one of the unsolved problems in powered prostheses. Electrical motors, ball screws and other mechanical parts produce motion related noise. Acoustical insulation of the mechanical system can decrease sound level. By this only the effect but not the cause would be addressed. Less system component friction and improvements in electrical motor design are design objects to address the reasons for sound level. On the other hand also different actuation mechanisms could be used. For example polymer artificial muscles (Mirfakhrai et al., 2007) could be a potential solution. When using current technology also a compromise between gait imitation and sound level can be targeted. High accelerations of the motor are necessary to match human gait patterns with SEA. In addition hard braking and turning of motor direction will increase loudness. If desired trajectories are smoothed less peak power and energy would be required. In addition this method could potentially reduce the sound level.

Battery runtime

Battery runtime is a limiting factor for powered prosthetics. The C-Leg and the Rheo Knee, both semi-active knee prostheses, have a runtime of one to two days depending on activity level. A similar runtime is envisioned with the partially powered Proprio Foot using a battery having

26.6 Wh. The Power Knee should provide a runtime of about five to seven hours using a battery capacity of 66.5 Wh (0.49 kg). All four systems use Lithium-Ion technology.

A former version of the BiOM Ankle is using a lithium polymer battery (0.22 kg) having an energy density of 165 Wh/kg. In a first study with 3 participants the prosthesis required about 31.4 Joule electrical energy per step to get 17.5 Joule per step net mechanical energy at 1.6 m/s walking speed (Au et al., 2009). This results in a system efficiency of 56%. Using a 36.3 Wh (130.68 kJ) battery (Eilenberg et al., 2010), about 4,162 steps could be realized consuming the 31.4 Joule (Au et al., 2009) used by MIT's PowerFoot.

In daily life people realize about 6,500 walking steps per day (Tudor-Locke and Bassett, 2004) with a preferred walking speed of about 1.3 m/s (Dal et al., 2010). As walking is one of the primary targets for powered prosthetics it can be a criterion for the dimensioning of a powered device. As the 6,500 steps are a result of two legs for unilateral amputees half of the steps need to be considered for the calculation of one day.

In addition ascending and descending of about 47 to 66 stairs and slopes should be considered. During these tasks ankle and knee joint behavior differs from level walking (DeVita et al., 2007). Thus it is required to estimate elastic actuator requirements similar to approaches used in (Grimmer and Seyfarth, 2011b) (ankle) and (Grimmer and Seyfarth, 2011a) (knee) for level walking and running.

Also while standing energy is required for a prosthetic device. For the electronics, the knee and the ankle motor a mean of 10 W was required in (Sup et al., 2009). Assuming the value of about 295 min of standing a day (Pitta et al., 2005), such a system needs 49.2 Wh only for this task. Less energy should be required while sitting or lying. Especially while lying motors require nearly no torque. About 3 W of electrical power consumption are measured for standing and walking for the electronics in (Sup et al., 2009). As between these two tasks is only little difference a similar value can be assumed for the sitting or laying down condition. These conditions are relevant because a huge amount of time (306 min) is spent for sitting (Fig. 12). Lying was executed for about 29 min. Both tasks together will need about 16.8 Wh at 3 W for 335 min. As level walking requires about 66 W for the powered knee and ankle joint and subjects performed about 81 min each day (Pitta et al., 2005), 89.1 Wh of battery is required for this task using a powered device at both legs. A single powered leg would require about 44.6 Wh. In total about 110.6 Wh are required to perform one day of a retired 66 years old person. This assumption is not including tasks like ascending or descending stairs or slopes which can increase requirements additionaly. Actually the device is using a 118 Wh lithium polymer battery which could be potentially enough to perform one day for a retired person based on this estimation.

3.7 TECHNOLOGY TRANSFER

The technology developed for leg prosthetics could potentially also be used in other robotic designs, including exoskeletons or rehabilitation platforms like the Lokomat (Hocoma). Exoskeletons are powered orthotic systems which can assist people with muscle weakness or other deficits that affect locomotion. But also healthy people can potentially benefit from assistance similar to pedelecs or e-bikes. They allow to set an percentage to amplify the own power introduced to the bicycle. Especially at inclines or stair but also while carrying heavy loads a powered system could be beneficial. Systems like the Lokomat can be used to train people with a neurological or orthopedic impairment with a robotic orthesis operating the legs on a treadmill. Basically walking can be performed. Exoskeleton technology could be a way to provide

flexible training conditions in each possible environment. A mobile device could also be used for locomotion training at home.

Also possible are combinations of powered or passive orthoses and prosthetics. This permits to include joint coupling structures that can transfer energy from a still existing to an artificial joint. With this, coordination in between the remaining limb and the artificial joints could be improved.

3.8 SUMMARY AND OUTLOOK

Based on advances in motor, battery and microprocessor technology there is an increasing effort in developments of powered lower limb prosthetics over the last years. First active devices for replacing the knee or the ankle joint are already commercialized. Powered prosthetics have the potential to increase amputee performance compared to passive or semi-active devices. When comparing them to natural movements a lack can still be identified. Especially when changing between movement tasks or during non steady state motions systems get to their limits.

These deficits can result from the technical system. Biologically inspired highly efficient elastic design approaches can improve actuator performance. In contrast to semi-active and passive devices most powered prostheses are so far not including passive dampers. They could further reduce requirements. Instead of wasting energy by dampers the energy could also be harvested. By this especially at the knee energy could be stored and reused at the ankle joint to support push off.

Next to the hardware design, also control has to be improved. Anticipation of the environment and the selected movement task are key aspects for an appropriate control. Prosthetic devices should at least handle all basic tasks like ascending and descending stairs or slopes, walking and standing. Multiple types of controllers were developed to address these conditions. Sudden events like stumbling should be detected and handled similar to the way used in semi-active systems. An improved level of control should recognize user intention. Thus voluntary motions, like flexing the knee while sitting, could be performed. Also adaptations to walking speed or level of slope could be possible. Changes in movement tasks (from walking to stair climbing) could be initiated intuitively by the amputee. In contrast to intrinsic control (CIC), that reacts on current motion, a kind of pre-positioning of the joint similar to pre-activation in muscles would be possible.

A feature that is less addressed in prosthetics so far are adaptable mechanical properties in the prosthesis. Stiffness of elastic elements could be changed to reduce actuator requirements or to improve stability. Increased weight while carrying loads, different movement tasks or speeds could benefit from a variable mechanical design. Damping ratio could also be considered as a controllable parameter. These features should be combined with an intelligent control that is finding the optimal mechanical adjustment (“sweet spot“) for the individual subject. As an optimization criteria energy requirements or symmetry for cyclical motions could be considered.

So far only limited user adjustment of the prosthesis are possible for commercial systems. Control and by this system behavior is pre-designed by the developers. Partially an individual gait can be configured while calibrating the system using software tools like in the C-Leg. Damping ratio for different phases of the gait cycle can be changed. Adaptations are made by the orthopedic technician. A further step could be to provide a software where each amputee could calibrate the system on his own. To ensure security only a safe region for possible changes in damping or power assistance should be considered. Exchange in internet communities could enhance user knowledge for creating their preferred personal settings. Even more potential would have an

open source library of prostheses software based on predefined standards. Universities but also private people could work on improved control algorithms for various daily life conditions.

Up to now a valid comparison of different powered but also passive prosthetics is difficult. Different subjects, measurement setups or also amputation condition and histories make it hard to compare systems. Results presented in different papers are using various biomechanical parameters, different units and also different normalization. To evaluate prosthetic systems it would be beneficial to have an institute that evaluates prosthetic systems under well-defined conditions similar to the TÜV, Germany. Such an independent institute could provide sufficient data to health insurance companies regarding the benefits of different prosthetic systems. With this it could be easier and better justified to select an adequate prosthesis matching users requirements.

3.9 AUTHOR CONTRIBUTIONS

Martin Grimmer is the main author of the book chapter. He was responsible for the conception and design, analysis and interpretation of data and writing of the manuscript. André Seyfarth assisted for the revision of the book chapter.

3.10 ABBREVIATIONS

CE contractile element

CIC computational intrinsic control

CoM center of mass

EMG electromyography

ER energy requirements

ESAR energy storage and return

FPWS fastest possible walking speed

GRF ground reaction force

IEC interactive extrinsic control

IL intact limb

PE parallel element

PEA parallel elastic actuator

PP peak power

PWS preferred walking speed

RL residual prosthetic limb

RoM range of motion

SACH solid ankle cushioned heel

SE series element

SEA series elastic actuator

TF transfemoral

TT transtibial

UPS unidirectional parallel spring

3.11 REFERENCES

Agrawal, V., Gailey, R., Gaunaurd, I., Gailey III, R., and O'Toole, C. (2011). Weight distribution symmetry during the sit-to-stand movement of unilateral transtibial amputees. *Ergonomics*, 54(7):656–664.

Aldridge, J. M., Sturdy, J. T., and Wilken, J. M. (2012). Stair ascent kinematics and kinetics with a powered lower leg system following transtibial amputation. *Gait & Posture*, 36(2):291–295.

Alzaydi, A. A., Cheung, A., Joshi, N., and Wong, S. (2011). Active Prosthetic Knee Fuzzy Logic-PID Motion Control, Sensors and Test Platform Design. *International Journal of Scientific & Engineering Research*, 2:1–17.

Aminian, K., Robert, P., Jequier, E., and Schutz, Y. (1995). Estimation of speed and incline of walking using neural network. *IEEE Transactions on Instrumentation and Measurement*, 44(3):743–746.

Au, S., Weber, J., and Herr, H. (2009). Powered Ankle–Foot Prosthesis Improves Walking Metabolic Economy. *IEEE Transactions on Robotics*, 25(1):51–66.

Au, S. K., Bonato, P., and Herr, H. (2005). An emg-position controlled system for an active ankle-foot prosthesis: an initial experimental study. In *9th International Conference on Rehabilitation Robotics (ICORR), Chicago*, pages 375–379. IEEE.

Battye, C., Nightingale, A., and Whillis, J. (1955). The use of myo-electric currents in the operation of prostheses. *Journal of Bone & Joint Surgery, British Volume*, 37(3):506–510.

Bellman, R. D., Holgate, M. A., and Sugar, T. G. (2008). Sparky 3: Design of an active robotic ankle prosthesis with two actuated degrees of freedom using regenerative kinetics. In *2nd IEEE RAS & EMBS International Conference on Biomedical Robotics and Biomechatronics (BioRob), Scottsdale*, pages 511–516. IEEE.

Bellmann, M., Schmalz, T., Ludwigs, E., and Blumentritt, S. (2012). Stair ascent with an innovative microprocessor-controlled exoprosthetic knee joint. *Biomed Tech*, 57:435–444.

Blumentritt, S. and Bellmann, M. (2010). Potenzielle Sicherheit von aktuellen nicht-mikroprozessor-und mikroprozessorgesteuerten Prothesenkniegelenken. *Orthopädie Technik*, 61:788–799.

Blumentritt, S., Bellmann, M., Ludwigs, E., and Schmalz, T. (2012). Zur Biomechanik des mikroprozessorgesteuerten Prothesenkniegelenks Genium. *Orthopädie Technik*, 01:24–35.

Blumentritt, S., Schmalz, T., and Jarasch, R. (2009). The safety of C-Leg: Biomechanical tests. *JPO: Journal of Prosthetics and Orthotics*, 21(1):2.

Boonstra, A., Fidler, V., and Eisma, W. (1993). Walking speed of normal subjects and amputees: aspects of validity of gait analysis. *Prosthetics and Orthotics International*, 17(2):78–82.

Borjian, R. (2009). Design, modeling, and control of an active prosthetic knee. Master's thesis, University of Waterloo.

Browning, R., Modica, J., Kram, R., and Goswami, A. (2007). The effects of adding mass to the legs on the energetics and biomechanics of walking. *Medicine & Science in Sports & Exercise*, 39(3):515.

Budaker, B. (2012a). Active driven prosthesis using a bevel helical gearbox in combination with a brushless DC-motor. In *Proceedings BMT 2012, 46. DGBMT Jahrestagung, Track R. Prevention and Rehabilitation Engineering, Jena*.

Budaker, B. (2012b). *Auslegung von Multidomänen-Systemen-Analyse, Modellierung und Realisierung von mechatronischen Systemen am Beispiel einer aktiven Knieprothese*. PhD thesis, Fraunhofer-Institut für Produktionstechnik und Automatisierung (IPA) Stuttgart.

Cherelle, P., Matthys, A., Grosu, V., Brackx, B., Van Damme, M., Vanderborght, B., and Lefeber, D. (2012). The AMP-Foot 2.0: a powered transtibial prosthesis that mimics intact ankle behavior. In *9th National Congress on Theoretical and Applied Mechanics, Brussels*.

Childress, D. S. (1985). Historical aspects of powered limb prostheses. *Clinical prosthetics and orthotics*, 9(1):2–13.

Clauser, C. E., McConville, J. T., and Young, J. W. (1969). Weight, volume, and center of mass of segments of the human body. Technical report, DTIC Document.

Collins, S. and Kuo, A. (2010). Recycling energy to restore impaired ankle function during human walking. *PloS one*, 5(2):e9307.

Colombo, C., Marchesin, E., Vergani, L., Boccafogli, E., and Verni, G. (2011). Design of an ankle prosthesis for swimming and walking. *Procedia Engineering*, 10:3503–3509.

Coupland, R. (1997). Assistance for victims of anti-personnel mines: needs, constraints and strategy. *Geneva: International Committee of the Red Cross*, 5:1–18.

Crompton, R., Pataky, T., Savage, R., D'Août, K., Bennett, M., Day, M., Bates, K., Morse, S., and Sellers, W. (2012). Human-like external function of the foot, and fully upright gait, confirmed in the 3.66 million year old laetoli hominin footprints by topographic statistics, experimental footprint-formation and computer simulation. *Journal of The Royal Society Interface*, 9(69):707–719.

Cutti, A., Raggi, M., Garofalo, P., Giovanardi, A., Filippi, M., and Davalli, A. (2008). The effects of the 'Power Knee' prosthesis on amputees metabolic cost of walking and symmetry of gait–preliminary results. *Gait & Posture*, 28:S38.

Cutti, A. G., Garofalo, P., Janssens, K., Davalli, A., Sacchetti, R., and Cutti, A. G. (2007). Biomechanical analysis of an upper limb amputee and his innovative myoelectric prosthesis: A case study concerning the otto bock dynamic arm. *Dynamic Arm, Orthopaedie-Technik Quarterly,(1) pp*, pages 6–15.

Czerniecki, J., Gitter, A., and Munro, C. (1991). Joint moment and muscle power output characteristics of below knee amputees during running: the influence of energy storing prosthetic feet. *Journal of Biomechanics*, 24(1):63–65.

Dal, U., Erdogan, T., Resitoglu, B., and Beydagi, H. (2010). Determination of preferred walking speed on treadmill may lead to high oxygen cost on treadmill walking. *Gait & Posture*, 31(3):366–369.

Delis, A. L., Carvalho, J., Seisdedos, C. V., Borges, G. A., and da Rocha, A. F. (2010). Myoelectric control algorithms for leg prostheses based on data fusion with proprioceptive sensors. In *Proceedings ISSNIP Biosignals and Biorobotics Conference 2010*, pages 137–142.

Delis, A. L., Carvalho, J. L., da Rocha, A. F., Nascimento, F. A., and Borges, G. A. (2011). Myoelectric knee angle estimation algorithms for control of active transfemoral leg prostheses. *Intechopen.com*.

DeVita, P., Helseth, J., and Hortobagyi, T. (2007). Muscles do more positive than negative work in human locomotion. *Journal of Experimental Biology*, 210(19):3361–3373.

Donelan, J., Li, Q., Naing, V., Hoffer, J., Weber, D., and Kuo, A. (2008). Biomechanical energy harvesting: generating electricity during walking with minimal user effort. *Science*, 319(5864):807–810.

Duraiswami, P., Orth, M., and Tuli, S. (1971). 5000 years of orthopaedics in India. *Clinical orthopaedics and related research*, 75:269.

Durfee, W., Xia, J., and Hsiao-Wecksler, E. (2011). Tiny hydraulics for powered orthotics. In *IEEE International Conference on Rehabilitation Robotics (ICORR), Zurich*, pages 1–6. IEEE.

Duvinage, M., Castermans, T., and Dutoit, T. (2011). Control of a lower limb active prosthesis with eye movement sequences. In *IEEE Symposium on Computational Intelligence, Cognitive Algorithms, Mind, and Brain (CCMB), Paris*, pages 1–7. IEEE.

Dyck, W., Onyshko, S., Hobson, D., Winter, D., and Quanbury, A. (1975). A voluntarily controlled electrohydraulic above-knee prosthesis. *Bulletin of prosthetics research*, 10(23-26):169.

Eilenberg, M., Geyer, H., and Herr, H. (2010). Control of a powered ankle–foot prosthesis based on a neuromuscular model. *IEEE Transactions on Neural Systems and Rehabilitation Engineering*, 18(2):164–173.

Endolite (2012). *www.endolite.com*.

Eslamy, M., Grimmer, M., Rinderknecht, S., and Seyfarth, A. (2013). Does it pay to have a damper in a powered ankle prosthesis? a power-energy perspective. In *IEEE International Conference on Rehabilitation Robotics (ICORR)*.

Eslamy, M., Grimmer, M., and Seyfarth, A. (2012). Effects of unidirectional parallel springs on required peak power and energy in powered prosthetic ankles: Comparison between different active actuation concepts. In *IEEE International Conference on Robotics and Biomimetics (ROBIO)*.

Ferris, A. E., Aldridge, J. M., Rábago, C. A., and Wilken, J. M. (2012). Evaluation of a powered ankle-foot prosthetic system during walking. *Archives of physical medicine and rehabilitation*, 93(11):1911–1918.

Ferris, D. P., Czerniecki, J. M., Hannaford, B., et al. (2005). An ankle-foot orthosis powered by artificial pneumatic muscles. *Journal of Applied Biomechanics*, 21(2):189.

Fey, N., Klute, G., and Neptune, R. (2011). The influence of energy storage and return foot stiffness on walking mechanics and muscle activity in below-knee amputees. *Clinical Biomechanics*, 26(10):1025–1032.

Fradet, L., Alimusaj, M., Braatz, F., and Wolf, S. I. (2010). Biomechanical analysis of ramp ambulation of transtibial amputees with an adaptive ankle foot system. *Gait & Posture*, 32(2):191–198.

Freedom Innovations (2012). *www.freedom-innovations.com*.

Gailey, R., Allen, K., Castles, J., Kucharik, J., and Roeder, M. (2008). Review of secondary physical conditions associated with lower-limb amputation and long-term prosthesis use. *Journal of Rehabilitation Research and Development*, 45(1):15.

Gates, D. H., Aldridge, J. M., and Wilken, J. M. (2013). Kinematic comparison of walking on uneven ground using powered and unpowered prostheses. *Clinical Biomechanics*, 28(4):467–472.

Gefen, A., Megido-Ravid, M., and Itzchak, Y. (2001). In vivo biomechanical behavior of the human heel pad during the stance phase of gait. *Journal of Biomechanics*, 34(12):1661–1665.

Geil, M. (2001). Energy loss and stiffness properties of dynamic elastic response prosthetic feet. *JPO: Journal of Prosthetics and Orthotics*, 13(3):70.

Geng, Y., Yang, P., Xu, X., and Chen, L. (2012). Design and simulation of active transfemoral prosthesis. In *24th Chinese Control and Decision Conference (CCDC), Taiyuan*, pages 3724–3728. IEEE.

Geyer, H. and Herr, H. (2010). A muscle-reflex model that encodes principles of legged mechanics produces human walking dynamics and muscle activities. *IEEE Transactions on Neural Systems and Rehabilitation Engineering*, 18(3):263–273.

Geyer, H., Seyfarth, A., and Blickhan, R. (2003). Positive force feedback in bouncing gaits? *Proceedings of the Royal Society of London. Series B: Biological Sciences*, 270(1529):2173–2183.

Gitter, A., Czerniecki, J., and DeGroot, D. (1991). Biomechanical analysis of the influence of prosthetic feet on below-knee amputee walking. *American Journal of Physical Medicine & Rehabilitation*, 70(3):142.

Goltz, F., Freusberg, A., and Gergens, E. (1875). Ueber gefässerweiternde Nerven. *Pflügers Archiv European Journal of Physiology*, 11(1):52–99.

Greitemann, B. and Bui-Khac, H. (2006). Wie haufig stürzen an der unteren Extremitat amputierte Patienten? *Medizinisch Orthopädische Technik*, 126(5):81.

Grimes, D., Flowers, W., and Donath, M. (1977). Feasibility of an active control scheme for above knee prostheses. *Journal of Biomechanical Engineering*, 99:215.

Grimes, D. L. (1979). *An active multi-mode above knee prosthesis controller*. PhD thesis, Massachusetts Institute of Technology.

Grimmer, M., Eslamy, M., Gliech, S., and Seyfarth, A. (2012). A comparison of parallel-and series elastic elements in an actuator for mimicking human ankle joint in walking and running. In *IEEE International Conference on Robotics and Automation (ICRA), St. Paul*, pages 2463–2470. IEEE.

Grimmer, M. and Seyfarth, A. (2011a). Stiffness adjustment of a series elastic actuator in a knee prosthesis for walking and running: The trade-off between energy and peak power optimization. In *IEEE/RSJ International Conference on Intelligent Robots and Systems (IROS), San Francisco*, pages 1811–1816. IEEE.

Grimmer, M. and Seyfarth, A. (2011b). Stiffness adjustment of a series elastic actuator in an ankle-foot prosthesis for walking and running: The trade-off between energy and peak power optimization. In *IEEE International Conference on Robotics and Automation (ICRA), Shanghai*, pages 1439–1444. IEEE.

Ha, K. H., Varol, H. A., and Goldfarb, M. (2011). Volitional control of a prosthetic knee using surface electromyography. *IEEE Transactions on Biomedical Engineering*, 58(1):144–151.

Hafner, B. (2005). Clinical prescription and use of prosthetic foot and ankle mechanisms: a review of the literature. *JPO: Journal of Prosthetics and Orthotics*, 17(4):S5.

Hafner, B., Sanders, J., Czerniecki, J., and Fergason, J. (2002). Energy storage and return prostheses: does patient perception correlate with biomechanical analysis? *Clinical Biomechanics*, 17(5):325–344.

Hargrove, L., Simon, A. M., Finucane, S. B., and Lipschutz, R. D. (2011). Myoelectric control of a powered transfemoral prosthesis during non-weight-bearing activities. In *Proceedings of the 2011 MyoElectric Controls/Powered Prosthetics Symposium, Fredericton, New Brunswick*. Myoelectric Symposium.

Heller, G., Günster, C., and Swart, E. (2005). Über die Häufigkeit von Amputationen unterer Extremitäten in Deutschland–About the frequency of lower limb amputations. *Dtsch Med Wochenschr*, 130(28/29):1689–1690.

Herr, H. and Grabowski, A. (2012). Bionic ankle–foot prosthesis normalizes walking gait for persons with leg amputation. *Proceedings of the Royal Society B: Biological Sciences*, 279(1728):457–464.

Herr, H. M., Au, S. K., Dilworth, P., and Paluska, D. J. (2012). Artificial ankle-foot system with spring, variable-damping, and series-elastic actuator components. US Patent App. 13/348,570.

Highsmith, M. J., Kahle, J. T., Carey, S. L., Lura, D. J., Dubey, R. V., Csavina, K. R., and Quillen, W. S. (2011). Kinetic asymmetry in transfemoral amputees while performing sit to stand and stand to sit movements. *Gait & Posture*, 34(1):86–91.

Highsmith, M. J., Kahle, J. T., Carey, S. L., Lura, D. J., Dubey, R. V., and Quillen, W. S. (2010). Kinetic differences using a power knee and c-leg while sitting down and standing up: a case report. *JPO: Journal of Prosthetics and Orthotics*, 22(4):237–243.

Hitt, J., Merlo, J., Johnston, J., Holgate, M., Boehler, A., Hollander, K., and Sugar, T. (2010a). Bionic running for unilateral transtibial military amputees. Technical report, DTIC Document.

Hitt, J., Sugar, T., Holgate, M., and Bellman, R. (2010b). An active foot-ankle prosthesis with biomechanical energy regeneration. *Journal of Medical Devices*, 4:011003.

Hitt, J. K., Bellman, R., Holgate, M., Sugar, T. G., and Hollander, K. W. (2007). The sparky (spring ankle with regenerative kinetics) project: Design and analysis of a robotic transtibial prosthesis with regenerative kinetics. In *Design Engineering Technology Conferences and Computers in Information and Engineering Conference (IDETC/CIE)*. ASME.

Hocoma (2012). *www.hocoma.com*.

Hof, A. L., van Bockel, R. M., Schoppen, T., and Postema, K. (2007). Control of lateral balance in walking: experimental findings in normal subjects and above-knee amputees. *Gait & Posture*, 25(2):250–258.

Holgate, M., Sugar, T., and Bohler, A. (2009). A novel control algorithm for wearable robotics using phase plane invariants. In *IEEE International Conference on Robotics and Automation (ICRA)*, pages 3845–3850. IEEE.

Hollander, K. and Sugar, T. (2005). Design of the robotic tendon. In *Design of Medical Devices Conference (DMD)*.

Hoover, C. and Fite, K. (2010). Preliminary evaluation of myoelectric control of an active transfemoral prosthesis during stair ascent. In *Proceedings ASME Dynamic Systems and Controls Conference, Cambridge, MA, Paper No. DSCC2010-4158*.

Hoover, C. D., Fulk, G. D., and Fite, K. B. (2013). Stair ascent with a powered transfemoral prosthesis under direct myoelectric control. *TRANSACTIONS ON MECHATRONICS*.

Horn, G. (1972). Electro-control: am EMG-controlled A/K prosthesis. *Medical and Biological Engineering and Computing*, 10(1):61–73.

Hosmer (2012). *www.hosmer.com*.

Huang, H., Zhang, F., Hargrove, L. J., Dou, Z., Rogers, D. R., and Englehart, K. B. (2011). Continuous locomotion-mode identification for prosthetic legs based on neuromuscular–mechanical fusion. *IEEE Transactions on Biomedical Engineering*, 58(10):2867–2875.

Islam, M. R., Haque, A. M., Amin, S., and Rabbani, K. (2013). Design and development of an emg driven microcontroller based prosthetic leg. *Bangladesh Journal of Medical Physics*, 4(1):107–114.

iWalk (2012). *www.iwalkpro.com*.

Johansson, J., Sherrill, D., Riley, P., Bonato, P., and Herr, H. (2005). A clinical comparison of variable-damping and mechanically passive prosthetic knee devices. *American Journal of Physical Medicine & Rehabilitation*, 84(8):563.

Kahle, J. T., Highsmith, M., and Hubbard, S. (2008). Comparison of nonmicroprocessor knee mechanism versus c-leg on prosthesis evaluation questionnaire, stumbles, falls, walking tests, stair descent, and knee preference. *Journal of Rehabilitation Research and Development*, 45(1):1.

Kuitunen, S., Komi, P., Kyröläinen, H., et al. (2002). Knee and ankle joint stiffness in sprint running. *Medicine and Science in Sports and Exercise*, 34(1):166.

Kulkarni, J., Wright, S., Toole, C., Morris, J., and Hirons, R. (1996). Falls in patients with lower limb amputations: prevalence and contributing factors. *Physiotherapy*, 82(2):130–136.

Lambrecht, B. G. and Kazerooni, H. (2009). Design of a semi-active knee prosthesis. In *Robotics and Automation, 2009. ICRA'09. IEEE International Conference on*, pages 639–645. IEEE.

Lambrecht, B. G. A. (2008). *Design of a Hybrid Passive-active Prosthesis for Above-knee Amputees*. ProQuest.

Latif, T., Ellahi, C., Choudhury, T., and Rabbani, K. (2008). Design of a cost-effective emg driven bionic leg. In *International Conference on Electrical and Computer Engineering (ICECE), Dhaka*, pages 80–85. IEEE.

Lawson, B., Varol, H. A., Huff, A., Erdemir, E., and Goldfarb, M. (2013). Control of stair ascent and descent with a powered transfemoral prosthesis. *Neural Systems and Rehabilitation Engineering, IEEE Transactions on*, 21(3):466–473.

Lee, I.-M. and Paffenbarger, R. S. (2000). Associations of light, moderate, and vigorous intensity physical activity with longevity the harvard alumni health study. *American Journal of Epidemiology*, 151(3):293–299.

Lim, J. (2008). The mechanical design and analysis of an active prosthetic knee. Master's thesis, University of Waterloo.

Lipfert, S. (2010). *Kinematic and dynamic similarities between walking and running*. Verlag Dr. Kovac, Hamburg. ISBN: 978-3-8300-5030-8.

Liu, M., Datseris, P., and Huang, H. H. (2012). A prototype for smart prosthetic legs-analysis and mechanical design. *Advanced Materials Research*, 403:1999–2006.

Mai, A. and Commuri, S. (2011). Gait identification for an intelligent prosthetic foot. In *IEEE International Symposium on Intelligent Control (ISIC), Denver*, pages 1341–1346. IEEE.

Mancinelli, C., Patritti, B. L., Tropea, P., Greenwald, R. M., Casler, R., Herr, H., and Bonato, P. (2011). Comparing a passive-elastic and a powered prosthesis in transtibial amputees. In *Annual International Conference of the IEEE Engineering in Medicine and Biology Society (EMBC) , Boston*, pages 8255–8258. IEEE.

Markowitz, J., Krishnaswamy, P., Eilenberg, M. F., Endo, K., Barnhart, C., and Herr, H. (2011). Speed adaptation in a powered transtibial prosthesis controlled with a neuromuscular model. *Philosophical Transactions of the Royal Society B: Biological Sciences*, 366(1570):1621–1631.

Martin, J., Pollock, A., and Hettinger, J. (2010). Microprocessor lower limb prosthetics: Review of current state of the art. *JPO: Journal of Prosthetics and Orthotics*, 22(3):183–193.

Martinez-Villalpando, E. and Herr, H. (2009). Agonist-antagonist active knee prosthesis: A preliminary study in level-ground walking. *J Rehabil Res Dev*, 46:361–374.

Martinez Villalpando, E. C. (2012). *Design and evaluation of a biomimetic agonist-antagonist active knee prosthesis*. PhD thesis, Massachusetts Institute of Technology.

Martinez-Villalpando, E. C., Mooney, L., Elliott, G., and Herr, H. (2011). Antagonistic active knee prosthesis. a metabolic cost of walking comparison with a variable-damping prosthetic knee. In *Annual International Conference of the IEEE Engineering in Medicine and Biology Society (EMBC), Boston*, pages 8519–8522. IEEE.

Miller, W. C., Speechley, M., and Deathe, B. (2001). The prevalence and risk factors of falling and fear of falling among lower extremity amputees. *Archives of Physical Medicine and Rehabilitation*, 82(8):1031–1037.

Mirfakhrai, T., Madden, J. D., and Baughman, R. H. (2007). Polymer artificial muscles. *Materials Today*, 10(4):30–38.

Mutlu, L., Uyar, E., Baser, O., and Cetin, L. (2011). Modelling of an under-hip prosthesis with ankle and knee trajectory control by using human gait analysis. In *18th IFAC World Congress Milano (Italy)*, pages 9672–9673.

Nandi, G., Ijspeert, A., Chakraborty, P., and Nandi, A. (2009). Development of adaptive modular active leg (amal) using bipedal robotics technology. *Robotics and Autonomous Systems*, 57(6):603–616.

Nandy, A., Mondal, S., Chakraborty, P., and Nandi, G. C. (2012). Development of a robust microcontroller based intelligent prosthetic limb. In *Contemporary Computing*, pages 452–462. Springer.

NASDAB (2009). The amputee statistical database for the united kingdom 2006/07.

Navarro, X., Krueger, T. B., Lago, N., Micera, S., Stieglitz, T., and Dario, P. (2005). A critical review of interfaces with the peripheral nervous system for the control of neuroprostheses and hybrid bionic systems. *Journal of the Peripheral Nervous System*, 10(3):229–258.

Nielsen, D. H., Shurr, D. G., Golden, J. C., and Meier, K. (1988). Comparison of energy cost and gait efficiency during ambulation in below-knee amputees using different prosthetic feet-a preliminary report. *JPO: Journal of Prosthetics and Orthotics*, 1(1):24.

Niemitz, C. (2010). The evolution of the upright posture and gait–a review and a new synthesis. *Naturwissenschaften*, 97(3):241–263.

Nigg, B. M., Herzog, W., and Herzog, W. (1994). *Biomechanics of the musculo-skeletal system*. Wiley New York.

Nolan, L. and Lees, A. (2000). The functional demands on the intact limb during walking for active trans-femoral and trans-tibial amputees. *Prosthetics and Orthotics International*, 24(2):117–125.

Nolan, L., Wit, A., Dudziński, K., Lees, A., Lake, M., and Wychowański, M. (2003). Adjustments in gait symmetry with walking speed in trans-femoral and trans-tibial amputees. *Gait & Posture*, 17(2):142–151.

O'Donnell, F., Brundage, J., Wertheimer, E., Olive, D., and Clark, L. (2012). Medical surveillance monthly report. volume 19, number 6. Technical report, DTIC Document.

Orendurff, M. S., Segal, A. D., Klute, G. K., McDowell, M. L., Pecoraro, J. A., and Czerniecki, J. M. (2006). Gait efficiency using the c-leg. *Journal of Rehabilitation Research and Development*, 43(2):239.

Ossur (2012). *www.ossur.com*.

Ottobock (2012). *www.ottobock.com*.

Pain, M. T. and Challis, J. H. (2001). The role of the heel pad and shank soft tissue during impacts: a further resolution of a paradox. *Journal of Biomechanics*, 34(3):327–333.

Panzenbeck, J. T. and Klute, G. K. (2012). A powered inverting and everting prosthetic foot for balance assistance in lower limb amputees. *JPO: Journal of Prosthetics and Orthotics*, 24(4):175–180.

Parsan, A. and Tosunoglu, S. (2012). A novel control algorithm for ankle-foot prosthesis. *Florida Conference on Recent Advances in Robotics*.

Pierrynowski, M. R. and Morrison, J. B. (1985). A physiological model for the evaluation of muscular forces in human locomotion: theoretical aspects. *Mathematical Biosciences*, 75(1):69–101.

Pillai, M. V., Kazerooni, H., and Hurwich, A. (2011). Design of a semi-active knee-ankle prosthesis. In *IEEE International Conference on Robotics and Automation (ICRA), Shanghai*, pages 5293–5300. IEEE.

Pitta, F., Troosters, T., Spruit, M. A., Probst, V. S., Decramer, M., and Gosselink, R. (2005). Characteristics of physical activities in daily life in chronic obstructive pulmonary disease. *American Journal of Respiratory and Critical Care Medicine*, 171(9):972–977.

Popovic, D., Tomovic, R., Tepavac, D., and Schwirtlich, L. (1991). Control aspects of active above-knee prosthesis. *International Journal of Man-Machine Studies*, 35(6):751–767.

Postema, K., Hermens, H., De Vries, J., Koopman, H., and Eisma, W. (1997). Energy storage and release of prosthetic feet part 1: Biomechanical analysis related to user benefits. *Prosthetics and Orthotics International*, 21(1):17–27.

Powers, C. M., Rao, S., and Perry, J. (1998). Knee kinetics in trans-tibial amputee gait. *Gait & Posture*, 8(1):1–7.

Prince, F., Winter, D., Sjonnensen, G., Powell, C., and Wheeldon, R. (1998). Mechanical efficiency during gait of adults with transtibial amputation: a pilot study comparing the SACH, Seattle, and Golden-Ankle prosthetic feet. *Development*, 35(2):177–185.

Prinsen, E. C., Nederhand, M. J., and Rietman, J. S. (2011). Adaptation strategies of the lower extremities of patients with a transtibial or transfemoral amputation during level walking: a systematic review. *Archives of Physical Medicine and Rehabilitation*, 92(8):1311–1325.

Proteor (2012). *www.proteor.com*.

Purath, J., Michaels, M. A., McCabe, G., and Wilbur, J. (2004). A brief intervention to increase physical activity in sedentary working women – une intervention ponctuelle en vue

daccroitre lactivite physique chez les travailleuses sedentaires. *CJNR: Canadian Journal of Nursing Research*, 36(1):76–91.

Robbins, C., Vreeman, D., Sothmann, M., Wilson, S., and Oldridge, N. (2009). A review of the long-term health outcomes associated with war-related amputation. *Military Medicine*, 174(6):588–592.

Robertson, D. G. E. (2004). *Research methods in biomechanics*. Human Kinetics Publishers.

Rusaw, D. and Ramstrand, N. (2011). Motion-analysis studies of transtibial prosthesis users: a systematic review. *Prosthetics and Orthotics International*, 35(1):8–19.

Sabatini, A. M., Martelloni, C., Scapellato, S., and Cavallo, F. (2005). Assessment of walking features from foot inertial sensing. *IEEE Transactions on Biomedical Engineering*, 52(3):486–494.

Sadeghi, H., Allard, P., Prince, F., and Labelle, H. (2000). Symmetry and limb dominance in able-bodied gait: a review. *Gait & Posture*, 12(1):34.

Sanderson, D. and Martin, P. (1996). Joint kinetics in unilateral below-knee amputee patients during running. *Archives of Physical Medicine and Rehabilitation*, 77(12):1279–1285.

Sauren, J., Lieby, B., et al. (2010). Motion analysis of the 2009 men's 100 m world record. *PhyDid B-Didaktik der Physik-Beiträge zur DPG-Frühjahrstagung*.

Sawicki, G. S. and Ferris, D. P. (2009). A pneumatically powered knee-ankle-foot orthosis (KAFO) with myoelectric activation and inhibition. *Journal of Neuroengineering and Rehabilitation*, 6(1):23.

Schaarschmidt, M., Lipfert, S. W., Meier-Gratz, C., Scholle, H.-C., and Seyfarth, A. (2012). Functional gait asymmetry of unilateral transfemoral amputees. *Human Movement Science*, 31(4):907–917.

Schinder, A., Genao, C., and Semmelroth, S. (2011). Methodology for control and analysis of an active foot-ankle prosthesis. *Proceedings of The National Conference on Undergraduate Research (NCUR) 2011 Ithaca College, New York*, pages 2011 –2018.

Schmalz, T., Blumentritt, S., Jarasch, R., et al. (2002). Energy expenditure and biomechanical characteristics of lower limb amputee gait: the influence of prosthetic alignment and different prosthetic components. *Gait & Posture*, 16(3):255.

Schneider, K., Hart, T., Zernicke, R., Setoguchi, Y., and Oppenheim, W. (1993). Dynamics of below-knee child amputee gait: SACH foot versus Flex foot. *Journal of Biomechanics*, 26(10):1191–1204.

Segal, A., Orendurff, M., Klute, G., McDowell, M., Pecoraro, J., Shofer, J., and Czerniecki, J. (2006). Kinematic and kinetic comparisons of transfemoral amputee gait using C-Leg® and Mauch SNS® prosthetic knees. *Journal of Rehabilitation Research and Development*, 43(7):857.

Seroussi, R., Gitter, A., Czerniecki, J., and Weaver, K. (1996). Mechanical work adaptations of above-knee amputee ambulation. *Archives of Physical Medicine and Rehabilitation*, 77(11):1209–1214.

Seyfarth, A., Geyer, H., and Herr, H. (2003). Swing-leg retraction: a simple control model for stable running. *Journal of Experimental Biology*, 206(15):2547–2555.

Shen, X. and Christ, D. (2011). Design and control of chemomuscle: A liquid-propellant-powered muscle actuation system. *Journal of Dynamic Systems, Measurement, and Control*, 133(2):021006–021006.

Sherrington, C. S. (1910). Flexion-reflex of the limb, crossed extension-reflex, and reflex stepping and standing. *The Journal of Physiology*, 40(1-2):28.

Silverman, A., Fey, N., Portillo, A., Walden, J., Bosker, G., and Neptune, R. (2008). Compensatory mechanisms in below-knee amputee gait in response to increasing steady-state walking speeds. *Gait & Posture*, 28(4):602–609.

Springactive (2012). *www.springactive.com*.

Sup, F., Bohara, A., and Goldfarb, M. (2008). Design and control of a powered transfemoral prosthesis. *The International Journal of Robotics Research*, 27(2):263–273.

Sup, F., Varol, H., Mitchell, J., Withrow, T., and Goldfarb, M. (2009). Self-contained powered knee and ankle prosthesis: Initial evaluation on a transfemoral amputee. In *IEEE International Conference on Rehabilitation Robotics (ICORR), Kyoto*, pages 638–644. IEEE.

Sup, F., Varol, H. A., and Goldfarb, M. (2011). Upslope walking with a powered knee and ankle prosthesis: initial results with an amputee subject. *IEEE Transactions on Neural Systems and Rehabilitation Engineering*, 19(1):71–78.

Suzuki, R., Sawada, T., Kobayashi, N., and Hofer, E. (2011). Control method for powered ankle prosthesis via internal model control design. In *International Conference on Mechatronics and Automation (ICMA)*, pages 237–242. IEEE.

Svanström, L. (1974). Falls on stairs: an epidemiological accident study. *Scandinavian Journal of Public Health*, 2(3):113–120.

Svensson, W. and Holmberg, U. (2006). An autonomous control system for a prosthetic foot ankle. In *4th IFAC Symposium on Mechatronic Systems (2006)*, pages 856–861. International Federation of Automatic Control (IFAC).

Svensson, W. and Holmberg, U. (2010). Estimating ground inclination using strain sensors with fourier series representation. *Journal of Robotics*, 2010.

Theeven, P. J. R. (2012). *Functional added value of microprocessor-controlled prosthetic knee joints*. PhD thesis, Maastricht University.

Thomas, G. and Simon, D. J. (2012). Inertial thigh angle sensing for a semi-active knee prosthesis. *Proceedings of the IASTED International Symposia Imaging and Signal Processing in Health Care and Technology (ISPHT 2012), Baltimore*.

Tudor-Locke, C. and Bassett, J. (2004). How many steps/day are enough?: Preliminary pedometer indices for public health. *Sports Medicine*, 34(1):1–8.

Unal, R., Carloni, R., Behrens, S., Hekman, E., Stramigioli, S., and Koopman, H. (2012). Towards a fully passive transfemoral prosthesis for normal walking. In *4th IEEE RAS & EMBS International Conference on Biomedical Robotics and Biomechatronics (BioRob), Rome*, pages 1949–1954. IEEE.

Vallery, H., Burgkart, R., Hartmann, C., Mitternacht, J., Riener, R., and Buss, M. (2011). Complementary limb motion estimation for the control of active knee prostheses. *Biomedizinische Technik/Biomedical Engineering*, 56(1):45–51.

Van den Bogert, A. J. (2003). Exotendons for assistance of human locomotion. *Biomedical Engineering Online*, 2(17):1–8.

van der Linde, H., Hofstad, C. J., Geurts, A. C., Postema, K., Geertzen, J. H., Van Limbeek, J., et al. (2004). A systematic literature review of the effect of different prosthetic components on human functioning with a lower-limb prosthesis. *Journal of Rehabilitation Research and Development*, 41(4):555–570.

van Ingen Schenau, G. v., Bobbert, M., and Rozendal, R. (1987). The unique action of bi-articular muscles in complex movements. *Journal of Anatomy*, 155:1.

Vanicek, N., Strike, S., McNaughton, L., and Polman, R. (2009). Gait patterns in transtibial amputee fallers vs. non-fallers: Biomechanical differences during level walking. *Gait & Posture*, 29(3):415–420.

Varol, H., Sup, F., and Goldfarb, M. (2009). Powered sit-to-stand and assistive stand-to-sit framework for a powered transfemoral prosthesis. In *IEEE International Conference on Rehabilitation Robotics (ICORR), Kyoto*, pages 645–651. IEEE.

Varol, H. A., Sup, F., and Goldfarb, M. (2010). Multiclass real-time intent recognition of a powered lower limb prosthesis. *IEEE Transactions on Biomedical Engineering*, 57(3):542–551.

Verhoeff, T. (2002). ICRC Physical Rehabilitation Programmes, Annual Report 2001. *Annual Report*.

Versluys, R., Lenaerts, G., Van Damme, M., Jonkers, I., Desomer, A., Vanderborght, B., Peeraer, L., Van der Perre, G., and Lefeber, D. (2009). Successful preliminary walking experiments on a transtibial amputee fitted with a powered prosthesis. *Prosthetics and Orthotics International*, 33(4):368–377.

Vickers, D. R., Palk, C., McIntosh, A., and Beatty, K. (2008). Elderly unilateral transtibial amputee gait on an inclined walkway: a biomechanical analysis. *Gait & posture*, 27(3):518–529.

Vrieling, A., Van Keeken, H., Schoppen, T., Otten, E., Halbertsma, J., Hof, A., and Postema, K. (2008). Uphill and downhill walking in unilateral lower limb amputees. *Gait and Posture*, 28(2):235–242.

Wang, S., van Dijk, W., and van der Kooij, H. (2011). Spring uses in exoskeleton actuation design. In *IEEE International Conference on Rehabilitation Robotics (ICORR)*, pages 1–6. IEEE.

Waters, R. L. and Mulroy, S. (1999). The energy expenditure of normal and pathologic gait. *Gait & Posture*, 9(3):207–231.

Waycaster, G., Wu, S.-K., and XIANGRONG, S. (2011). Design and control of a pneumatic artificial muscle actuated above-knee prosthesis. *Journal of Medical Devices*, 5(3).

Webster, J., Levy, C., Bryant, P., and Prusakowski, P. (2001). Sports and recreation for persons with limb deficiency. *Archives of Physical Medicine and Rehabilitation*, 82(3):S38–S44.

Wilson, A. B. (1992). History of amputation surgery and prosthetics. *At las of Limb Prosthetics: Surgical, Prosthetic, and Rehabilitation Principles. Mosby-Year Book*, pages 3–16.

Winter, D. A. (2009). *Biomechanics and motor control of human movement*. John Wiley & Sons, Inc., Hoboken, New Jersey.

Winter, D. A. and Sienko, S. E. (1988). Biomechanics of below-knee amputee gait. *Journal of Biomechanics*, 21(5):361–367.

Wolf, E. J., Everding, V. Q., Linberg, A. A., Czerniecki, J. M., and Gambel, C. (2013). Comparison of the power knee and c-leg during step-up and sit-to-stand tasks. *Gait & Posture*, 38(3):397–402.

Wolf, E. J., Everding, V. Q., Linberg, A. L., Schnall, B. L., Czerniecki, J. M., Gambel, J. M., et al. (2012). Assessment of transfemoral amputees using c-leg and power knee for ascending and descending inclines and steps. *Journal of Rehabilitation Research and Development*, 49(6):831–842.

Yuan, K., Zhu, J., Wang, Q., and Wang, L. (2011). Finite-state control of powered below-knee prosthesis with ankle and toe. In *Proc. 18th IFAC World Congress*, pages 2865–2870.

Zajac, F. E. et al. (1989). Muscle and tendon: properties, models, scaling, and application to biomechanics and motor control. *Critical Reviews in Biomedical Engineering*, 17(4):359.

Zelik, K., Collins, S., Adamczyk, P., Segal, A., Klute, G., Morgenroth, D., Hahn, M., Orendurff, M., Czerniecki, J., and Kuo, A. (2011). Systematic variation of prosthetic foot spring affects center-of-mass mechanics and metabolic cost during walking. *IEEE Transactions on Neural Systems and Rehabilitation Engineering*, 19(4):411–419.

Zhang, F., Liu, M., and Huang, H. (2012). Preliminary study of the effect of user intent recognition errors on volitional control of powered lower limb prostheses. In *Engineering in Medicine and Biology Society (EMBC), 2012 Annual International Conference of the IEEE*, pages 2768–2771. IEEE.

Zhu, J., Wang, Q., and Wang, L. (2010). Pantoe 1: Biomechanical design of powered ankle-foot prosthesis with compliant joints and segmented foot. In *IEEE/ASME International Conference on Advanced Intelligent Mechatronics (AIM)*, pages 31–36. IEEE.

Ziegler-Graham, K., MacKenzie, E., Ephraim, P., Travison, T., Brookmeyer, R., et al. (2008). Estimating the prevalence of limb loss in the united states: 2005 to 2050. *Archives of Physical Medicine and Rehabilitation*, 89(3):422.

Table 3: Overview on active prosthetic ankle developments

Item	Details
Device	ankle, Odyssey, Springactive, USA || Picture: a)
Actuator	motor-parallel spring complex
Battery	external battery
Sensors	motor encoder, gyro sensor
Control	continuous control without states
Device	ankle, Sparky, (Hitt et al., 2010b, 2007), Arizona State University and Springactive, USA || Picture: b)
Actuator	Robotic Tendon (SEA), Maxon RE-40, 150 W, lead screw, planetary gear box
Battery	external battery
Sensors	motor and ankle angle encoder, optical switch at heel or gyro sensor
Control	position control or phase plane control (Holgate et al., 2009)
Device	Bionic Foot, (Hitt et al., 2010a; Schinder et al., 2011), Military Academy West Point, USA || Picture: c)
Actuator	ankle, Robotic Tendon (SEA), 2x Maxon RE-40, lead screw
Battery	external battery
Sensors	motor encoder, gyro sensor
Control	phase plane control
Device	ankle, Walk-Run Ankle, Springactive, USA (design) and TU Darmstadt, Germany (control) || Picture: d)
Actuator	elastic motor spring combination
Battery	external battery
Sensors	motor encoder, gyro sensor, acceleration sensor
Control	for standing, walking, running and gait transitions
Device	ankle AMP-Foot 2.0, (Cherelle et al., 2012) Vrije Universiteit Brussel, Belgium, about 2.5 kg || Picture: e)
Actuator	series spring and clutched SEA, Maxon RE 30, 60 W, transmission, ball screw
Battery	external power supply
Sensors	force sensing resistor at toe and heel, strain gauges at two springs, two magnetic encoders at ankle joint,
Control	nothing stated
Device	ankle, BiOM - Power Foot (Eilenberg et al., 2010; Au et al., 2009), Massachusetts Institute of Technology and iWalk (iWalk, 2012), USA || Picture: f)
Actuator	SEA+UPS, Maxon EC-30, 200 W, 48 V at 24 V, belt drive transmission, ballscrew
Battery	0.22 kg lipo at 165 Wh/kg for 5000 steps, internal
Sensors	hall-effect ankle angle joint sensor, stain gauges for spring force, pyramid strain gauge for GRF, motor encoder
Control	neuromuscolar reflex model

Continued on next page

Table 3 – *Continued from previous page*

Item	Details
Device	ankle and toe, PANTOE 1, (Yuan et al., 2011; Zhu et al., 2010), Peking University, China, 1.47kg || Picture: g)
Actuator	ankle - 83 W Faulhaber brushed DC, toe - 45 W Faulhaber DC, ballscrew
Battery	Li, 1 kg, external
Sensors	motor angle encoder, touch and force sensor at heel and toe, potentiometer at ankle and toe joint, potentiometer for ankle spring displacement sensor
Control	finite state control (Yuan et al., 2011)
Device	ankle, (Suzuki et al., 2011), Kanazawa Institute of Technology, Japan 3.8kg including battery || Picture: h)
Actuator	unidirectional spring for controlling touch down plantarflexion with antagonistic unidirectional DD (assumed from figure), DC motor
Battery	internal
Sensors	ankle angle encoder
Control	internal model control including last step, ankle angle position control
Device	ankle, Proprio Foot, Ossur, Iceland, 1.5 kg with Pyramid and Foot cover || Picture: i)
Actuator	stepper motor
Battery	Lithium Ion 1800 mAh, 14.8 V
Sensors	Accelerometers, ankle angle sensor
Control	artificial intelligence including last step
Device	ankle, (Svensson and Holmberg, 2006), Halmstad University, Sweden || Picture: see publication
Actuator	DC motor, only powered in swing phase, ball screw
Battery	nothing stated
Sensors	accelerometer at foot for slope estimation and gait phase detection
Control	finite state control
Device	ankle, (Versluys et al., 2009), Vrije Universiteit Brussel, Belgium || Picture: see publication
Actuator	antagonistic pleated pneumatic artificial muscles (PPAM)
Battery	external power source
Sensors	ankle joint angle encoder, footswitch at forefoot, midfoot and hindfoot, pressure sensor
Control	feedforward torque control timed by foot switches
Device	ankle, PAKO - Orthoprosthesis, Technical University Darmstadt, Lauflabor - Locomotion Lab, Germany || Picture: j)
Actuator	SEA with variable stiffness, 1025 W Thingap 2320 brushless DC motor 80 V at 48 V
Battery	external power supply
Sensors	knee and ankle joint encoder, SEA force sensor, GRF sensor in foot, gyro and accelerometer at shank
Control	speed related phase plane control similar to (Holgate et al., 2009)

Table 4: Overview on active prosthetic knee developments

Item	Details
Device	knee, (Lambrecht and Kazerooni, 2009; Lambrecht, 2008; Pillai et al., 2011),University of California, USA || Picture: k)
Battery	12x 2000mAh 15C lipo cells 36 V - 51 V in early version (Lambrecht, 2008), 42 V to 48 V in new design, internal
Actuator	two linear hydraulic with one pump, Maxon EC-max 30 for pump - 40 W, low power valve motor
Sensors	accelerometer and gyroscope at thigh, magnetic knee and ankle angle encoder, pressure sensor in hydraulic units, force transducer for sagittal plane moments and axial shank forces
Control	finite state control
Device	knee, (Islam et al., 2013; Latif et al., 2008), Islamic University of Technology and University of Dhaka, Bangladesh || Picture: l)
Actuator	DD, 5 W DC motor for prototype, pulley
Battery	nothing stated
Sensors	EMG at thigh, motor sensor
Control	EMG control
Device	knee, (Waycaster et al., 2011), University of Alabama, USA, 3kg || Picture: m)
Actuator	antagonistic pneumatic artificial muscles
Battery	external pneumatic supply, research on liquid propellant
Sensors	force sensor (resistor) in foot for GRF, potentiometer knee, control valve and pressure sensors external
Control	finite state impedance control similar to (Sup et al., 2009)
Device	knee, (Martinez-Villalpando et al., 2011; Martinez-Villalpando and Herr, 2009), Massachusetts Institute of Technology, USA, 3 kg || Picture: n)
Actuator	two antagonistic SEA's, Maxon RE40 extension, Maxon RE 30 flexion, belt drive, ball screw
Battery	6 cell 22.2 V Lipo, 0.15 kg
Sensors	ankle angle encoder, motor encoder, spring compression by hall effect sensor, insole force resistor for heel and toe contact
Control	finite state control
Device	knee, Power Knee, Ossur, Iceland, 2.7 kg w/o battery || Picture: o)
Actuator	DC motor, harmonic drive gearing system
Battery	50.4 V, 1320 mAh, 66.5 Wh, 0.5 kg, 5-7 hours runtime
Sensors	Gyro, Accelerometers, Torque meter, Ground contact sensor
Control	state machine
Device	knee, (Budaker, 2012a,b), Fraunhofer Institut Stuttgart, Germany || Picture: p)
Battery	nothing stated
Actuator	Faulhaber 4490, 48 V, 200 W, bevel-helical gearbox

Continued on next page

Table 4 – *Continued from previous page*

Item	Details
Sensors	gyro sensor, accelerometers
Control	nothing stated
Device	knee, (Vallery et al., 2011), ETH Zurich, Switzerland || Picture: q)
Actuator	Maxon RE 40, 150W
Battery	external power supply
Sensors	optical quadrature motor encoder, contralateral hip and knee angle and angle velocity sensor (goniometer, gyroscope)
Control	complementary limb motion estimation (CLME)
Device	ankle and knee, 1st version (Sup et al., 2009), 2nd version (Lawson et al., 2013), Vanderbilt University, USA, 4.3 kg (2nd) || Picture: r)
Actuator	motor+UPS at ankle, DD at knee, Maxon EC-30, 200 W, ballscrew (1st)
Battery	29.6 V, 4000 mAh, 700 g, 115 Wh, internal (1st)
Sensors	series uniaxial load cell in each actuator unit, potentiometers at ankle and knee joint, strain based sagittal plane moment sensor between socket and knee, strain gauges at foot and heel for GRF (1st)
Control	finite state impedance control (1st)
Device	knee, (Liu et al., 2012; Zhang et al., 2012), University of Rhode Island Kingston, USA || Picture: see publication
Actuator	Motor with parallel torsion spring - clutch mechanism, variable damper, Maxon RE 40, ball screw
Battery	external power supply
Sensors	potentiometer for knee angle, motor encoder, 6 DOF load cell for GRF
Control	User intent recognition based on neuromuscular mechanical fusion, impedance control, finite state machine
Device	knee, APK, (Borjian, 2009; Lim, 2008), University of Waterloo, Canada || Picture: see publication
Actuator	DD, Maxon RE 40, ballscrew
Battery	external power supply
Sensors	potentiometer knee angle, accelerometer at femur, motor encoder
Control	intelligent Fuzzy logic based control
Device	ankle and knee proposed, (Mutlu et al., 2011), Dokuz Eylul University, Turkey || Picture: see publication
Actuator	DC motors
Battery	nothing stated
Sensors	nothing stated
Control	hip angle based knee and ankle joint control
Device	knee, (Geng et al., 2012), Hebei University of Technology, China || Picture: see publication
Actuator	hybrid linear step motor, Haydon model 57000,
Battery	nothing stated

Continued on next page

Table 4 – *Continued from previous page*

Item	Details
Sensors	nothing stated
Control	central pattern generator
Device	ankle and knee, (Delis et al., 2011),University of Brasilia and University of Oriente, Brazil and Cuba || Picture: see publication
Actuator	nothing stated
Battery	nothing stated
Sensors	EMG, Gyro
Control	nothing stated
Device	knee, (Hoover and Fite, 2010; Hoover et al., 2013), 3.5 kg including electronics and battery || Picture: see publication
Actuator	Maxon RE 40 150 W, ball screw
Battery	4x 11.1-V, 2000 mAh
Sensors	load cell at knee for torque, knee potentiometer, pneumatic pressure sensors at heel and toe for ground contact, surface EMG at thigh muscles
Control	finite-state linear impedance model based on EMG

4 Manuscript II: A Comparison of Parallel- and Series Elastic Elements in an Actuator for Mimicking Human Ankle Joint in Walking and Running

Authors:

Martin Grimmer, Mahdy Eslamy, Stefan Gliech and André Seyfarth

Friedrich Schiller Universität
07743 Jena, Germany
and
Technische Universität Darmstadt
64289 Darmstadt, Germany

Published as a paper at the

2012 IEEE International Conference on Robotics and Automation (ICRA)

4.1 ABSTRACT

Elastic elements in prosthetic devices can help to reduce peak power (PP) and energy requirements (ER) for the actuators. Calculations showed that it is impossible with current commercial motor technology to mimic human ankle behavior in detail for higher walking and running speeds with single motor solutions using a Serial Elastic Actuator (SEA). Concerning this result we checked the requirements of a parallel elastic actuator (PEA) and a combination of serial and parallel (SE+PEA) springs. We found that a PEA can reduce PP additionally in comparison to the SEA by pre-loading the spring in the flight phase. This reduces also peak torque. But this loading needs additional energy so that the ER increase in comparison to the SEA. The SE+PEA concept can further decrease PP. With that, the ER are less than the PEA but higher than for the SEA. The results show less benefit for the PEA and the SE+PEA when a constant stiffness and a fixed parallel spring slack length is used for both gaits and all speeds. All concepts show that mimicking human ankle joint behavior in running and walking at higher speeds is still challenging for single motor devices.

4.2 INTRODUCTION

Actual research shows that powered prosthetic feet, mimicking the human ankle angle-torque profile, are capable of improving amputees performance. Delivering positive net work at the ankle joint results in multiple advantages. In comparison to passive carbon fiber feet, lower cost of transport (Au et al., 2009) can be achieved for similar walking speeds. In unilateral amputees the biological leg can be unloaded and the preferred walking speed increased to values similar to non-amputees (Herr and Grabowski, 2011; Sup et al., 2009). In addition the more natural gait of the amputees, reflected in biomechanical parameters (Herr and Grabowski, 2011; Hitt et al., 2010; Sup et al., 2009), may provide advantages in terms of long-term sequelae.

To mimic the torque profile of the human ankle joint with a direct drive (DD) system for a 75 kg subject a peak power (PP) of 241 W in walking (1.6 m/s) and a PP of 651 W in running (2.6 m/s) is necessary (Fig. 5). Different approaches can help to reduce these requirements. A common solution is to use springs that can assist the motor by storing and releasing energy. Serial assemblies (Grimmer and Seyfarth, 2011; Hollander and Sugar, 2005) and unidirectional assemblies (Eilenberg et al., 2010; Sup et al., 2009) of the spring to the motor are used to reduce PP or ER. In (Grimmer and Seyfarth, 2011) it was shown how much an ankle prosthesis can benefit from a SEA in running and walking for a wide variation of speeds. The theoretical data showed that it is possible to get the desired ankle behavior with currently available motor technology but especially for higher speeds, mechanical couplings of two or more motors like in the Bionic Running Ankle (Hitt et al., 2010a) are required. To mimic human gait in detail with a single motor solution novel concepts for further reductions are essential.

In this paper we investigate if it is possible to get further reductions by using a Parallel Elastic Actuator (PEA) instead of a Series Elastic Actuator (SEA). Additionally, we want to check if a combination of both systems to a Series+Parallel Elastic Actuator (SE+PEA) can reduce additionally actuator requirements. The calculations for the parallel springs depending on system related model values like the spring stiffness and the slack length (when spring force is zero) of the parallel spring. In a first step we want to show the results for the case of optimized model parameters, which are partially restricted (partially restricted case, PRC). In a 2nd step we want to show which benefits can be achieved with constant model parameters (strict-restricted case, SRC).

4.3 METHODS

In an experiment (Tab. 1, (Lipfert, 2010)) healthy subjects walked and ran on a treadmill with integrated 3D force sensors (Kistler, 1000Hz). Kinematics were recorded by high-speed infrared cameras (Qualisys, 240Hz). Ankle angles and torques were calculated (Günther et al., 2003;

Table 1: Experimental and subject characteristics (mean ± std).

number of subj.	age [yrs]	body height [m]	body mass [kg]	speeds [m/s]	leg length [m]
21	25.4 ± 2.7	1.73 ± 0.09	70.9 ± 11.7	0.52, 1.04, 1.55,2.07,2.59	0.96 ± 0.08

Lipfert, 2010) and used to estimate SEA, PEA and SE+PEA length and force, corresponding to a lower limb orthoprosthetic model (Fig. 1). Ankle torques were normalized to a reference subject

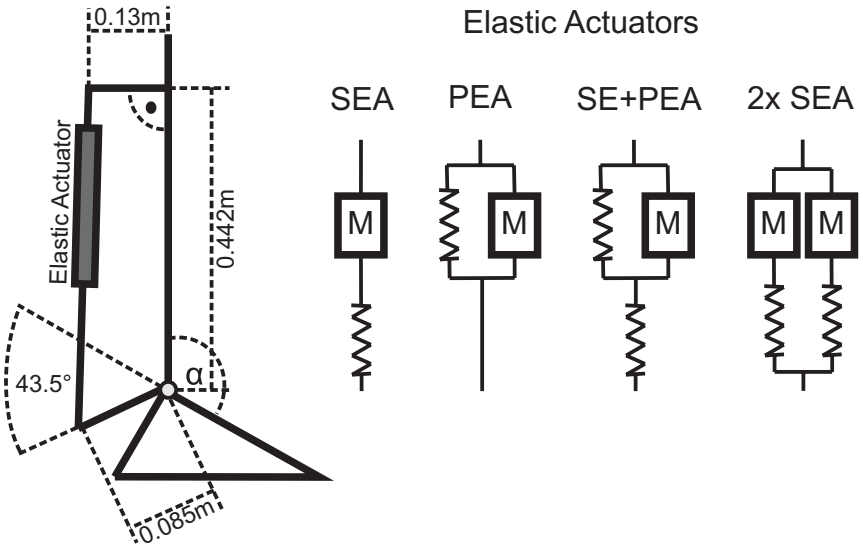

Figure 1: Orthoprosthetic model and four different kinds of elastic actuators that where used to calculate PP and ER for mimicking human ankle behavior

with body mass 75 kg and a resting leg length of 1m that is defined as the distance between the center of mass, COM, and the center of pressure, COP, in standing. PP and ER were derived based on length and force values using the model described in Fig. 1. For the PEA (Fig. 2) motor power P_m was derived according to equations 1 to 5.

$$P_m = F_m \cdot \dot{x}_g \tag{1}$$

F_m is the motor force and $\dot{x}_g$ is the system velocity.

$$F_m = F_{ex} + F_p \tag{2}$$

F_{ex} is the force applied to the PEA. F_p is the force of the parallel spring.

$$F_p = K_p \cdot \Delta x_g \tag{3}$$

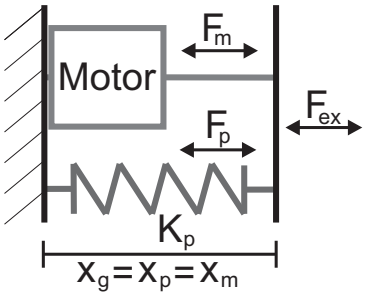

Figure 2: Schematic model of the PEA.

K_p is the stiffness of the parallel spring and Δx_g the length change of the PEA.

$$\Delta x_g = d_{0p} - x_g \tag{4}$$

Where d_{0p} is the slack length of the parallel spring. The system length x_g is equal to the spring length x_p and the length set by the motor x_m.

$$P_m = (F_{ex} + (K_p \cdot \Delta x_g)) \cdot \dot{x}_g \tag{5}$$

For the SE+PEA (Fig. 3) motor power was derived by the equations 6 to 12.

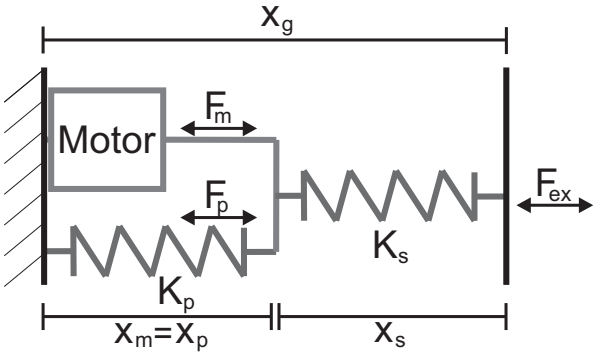

Figure 3: Schematic model of the SE+PEA.

Table 2: Predicted optimal SEA, PEA and SE+PEA stiffness values for minimizing PP at different walking and running speeds. For the SE+PEA the underlined SE represents the stiffness of the serial element, PE the parallel element.

Gait		Walking					Running				
Speed [m/s]		0.5	1.0	1.6	2.1	2.6	0.5	1.0	1.6	2.1	2.6
Stiffness in [kN/m]	SEA	78	61	80	115	143	70	74	77	77	77
	PEA	28	27	28	15	15	52	49	43	39	37
	SE+PEA	150	72	98	126	100	72	79	83	83	83
	SE+PEA	35	18	10	13	16	10	15	14	22	31

$$P_m = F_m \cdot \dot{x}_m \tag{6}$$

F_m is the motor force and $\dot{x}_m$ the motor velocity. F_m is influenced by the parallel and $\dot{x}_m$ by the serial element.

$$F_m = F_{ex} + F_p \tag{7}$$

F_{ex} is the force applied to the SE+PEA. F_p is the force of the parallel spring.

$$F_p = K_p \cdot \Delta x_m \tag{8}$$

K_p is the stiffness of the parallel spring and Δx_m the length change by the motor.

$$\Delta x_m = x_m - d_{0p} \tag{9}$$

Where x_m is the length set by the motor (position of ball screw nut) and d_{0p} is the slack length of the parallel spring. The length x_p is equal to x_m.

$$x_m = x_g + \frac{F_{ex}}{K_s} - d_{0s} \tag{10}$$

The derivation of equation 10 can be found in (Hollander and Sugar, 2005). The system length x_g is the sum of the serial (x_s) and the parallel spring length (x_p). K_s is the stiffness and d_{0s} the slack length of the serial spring.

$$\dot{x}_m = \dot{x}_g + \frac{\dot{F}_{ex}}{K_s} \tag{11}$$

Motor power is finally the product of motor force F_m and motor velocity $\dot{x}_m$.

$$P_m = (F_{ex} + (K_p \cdot \Delta x_m)) \cdot (\dot{x}_g + \frac{\dot{F}_{ex}}{K_s}) \tag{12}$$

All equations rely on the method and similar input data like for the calculation of PP in a SEA (Hollander and Sugar, 2005). ER was calculated as the sum of positive and the amount of negative work by integrating the positive and the negative power curve, respectively (Grimmer and Seyfarth, 2011). PP is the maximum of the absolute motor power. It is important to note, that the systems can introduce pushing and pulling forces to represent the function of both ankle extensors and flexors. Therefore, no antagonistic structure is required. The estimated PP and ER was normalized to body mass. Additionally ER was normalized to distance traveled during the gait cycle representing the cost of transport. By checking various settings optimal spring stiffness values (1 kN/m - 1000 kN/m, 1 kN/m step size) and parallel element slack length (0.3 m - 0.5 m, 1 mm step size) for minimal PP were determined for each walking and running speed. Finally PP was compared to the direct drive (DD) configuration.

The calculations were done for a strictly-restrictive (SRC) and a partially-restrictive case (PRC) to get only results that are mechanically feasible (space, parameter variability) for an ankle prosthesis.

In the PRC (Fig. 5) we set the maximum deflection of the parallel spring to 0.05 m (compression or elongation allowed) to limit system length. Solutions with very low stiffness values requiring high pretension to get the right force were excluded.

In the SRC (Fig. 6) the stiffness of the serial element (SE) and/or the parallel element (PE) was set to a constant value for all running and walking speeds. For this, we searched for the stiffness (by comparing PP values for a stiffness of 1 kN/m - 1000 kN/m, 1 kN/m step size) that results in minimum PP for both gaits up to 2.6 m/s. Additionally in this optimization a constant value for the slack length of the PE regarding both speeds was identified by checking a range of values around the optimum PRC slack length solutions. Also the maximum spring deflection is limited to 0.05 m like in the PRC.

4.4 RESULTS

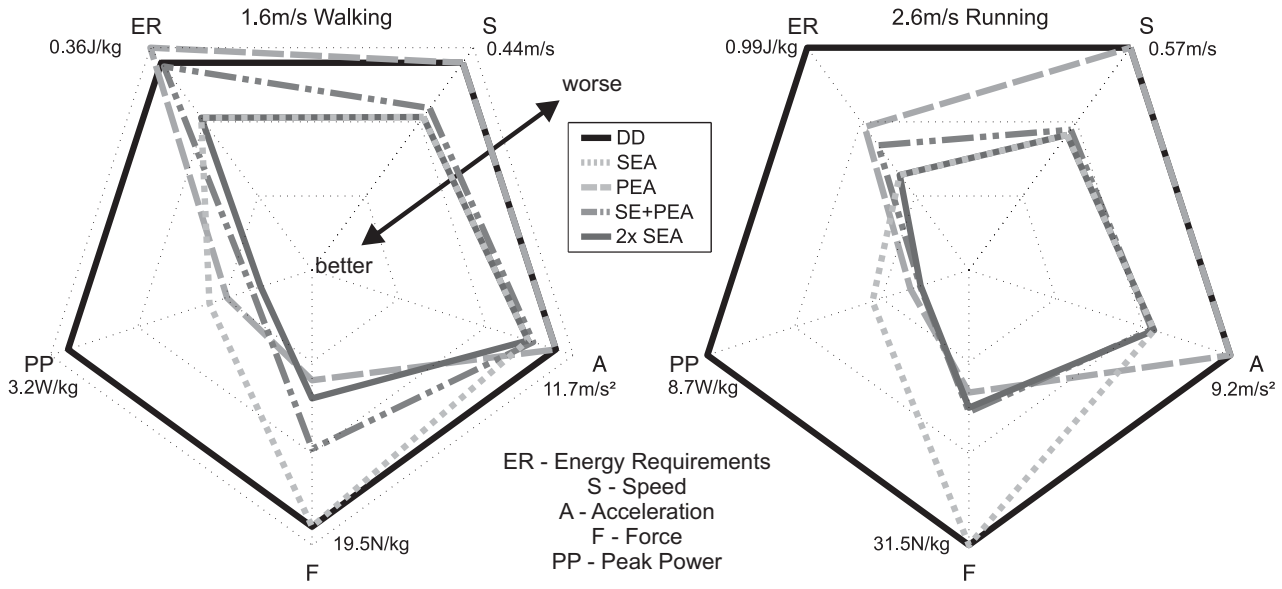

Figure 4: Motor requirements regarding peak power, energy, peak force, max. linear speed and max. linear acceleration to mimic human ankle behavior in walking (1.6m/s) and running (2.6m/s). The data is shown in relation to the requirements of a DD. Maximum speed and force must not occur at the same time. The results belong to the PRC.

4.4.1 Partial-restrictive case (PRC)

For this case we wanted to know which reductions in terms of PP and ER are possible by changing the slack length for the PE and the stiffness (PE and SE) in the calculation model.

Energy Requirements

For the SEA, PEA and the SE+PEA it is possible to reduce ER in comparison to the DD (Fig. 5, 7). With the SEA the mean benefit of all speeds in running (64.7%) is even higher than in walking (25.8%). For the PEA we got also higher reductions in running (45%) than in walking (12.2%). A SE+PEA can reduce the ER by 52.8% in running and 17.9% in walking compared to the DD.

Peak Power

Also the peak power can be reduced for all three systems compared to the DD (Fig. 5, 7) . In running we got the highest mean benefit by the SE+PEA (81.8%). The PEA system can reduce the PP by 79% and the SEA by a mean of 68.5%. A similar tendency is observed in walking (SE+PEA 70.4%, PEA 62.5% and SEA 48.3%).

Stiffness

The stiffness values of a SEA are higher compared to the PEA. Also the combination of both springs in one system (SE+PEA) shows this tendency (Tab. 2).

Slack Length

The elastic actuators change their length (range 0.44 m to 0.5 m) depending on the aimed ankle angle and the geometric model (Fig. 1). For the optimal slack length for a PEA we found speed and gait dependent values in a region of 0.438 m to 0.465 m system length. The optimal slack length decreased when increasing speed. In walking no PE compression was found before take-off (Fig. 8). In running just before take-off little compression occurs especially at lower speeds. After take-off PE compression occurred for walking and running in the PEA. For the SE+PEA the slack length occurs at a system length between 0.311 m and 0.345 m considering a serial spring rest-length of 0.12 m. No tendency was identified when changing speed or gait. Except 2.6m/s running and lower walking speeds than 1.6 m/s no compression of the PE was found (Fig. 8).

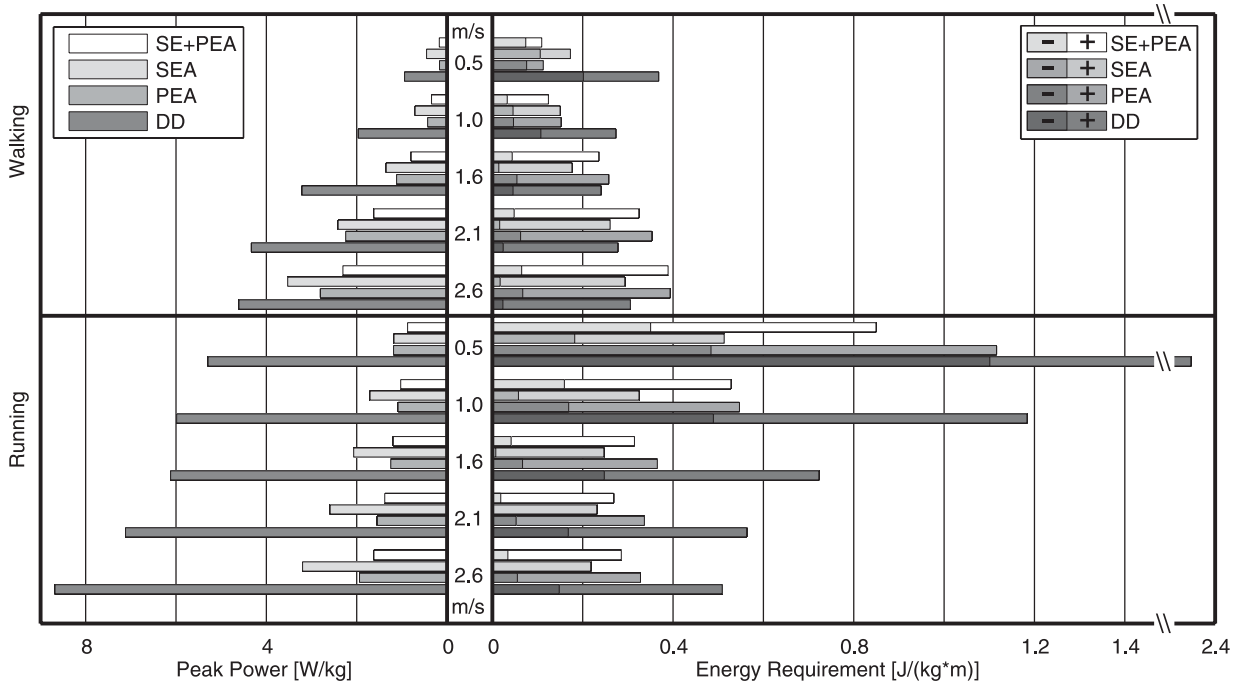

Figure 5: Ankle peak power (PP) and energy requirements (ER) for different walking and running speeds with stiffness optimized to minimize PP for a SEA, a PEA and the combination of SEA and PEA (SE+PEA). The amount of negative work (-) is indicated by the darker left part of the ER bars, positive work (+) is indicated by the brighter right part. The results belong to the partially restricted case (PRC).

4.4.2 Strict-restrictive case (SRC)

In order to keep the system design simple, a constant spring setup (stiffness, slack length) for all speeds and gaits is of advantage. For this case we asked which reductions in terms of PP and ER can be achieved if the slack length and the stiffness of the elastic system are constant.

Energy Requirements

The mean (throughout all speeds) energy reduction is highest with the SEA (27.1% walking, 62.5% running) compared to the DD. In running the ER can be reduced by 39.7% for the PEA

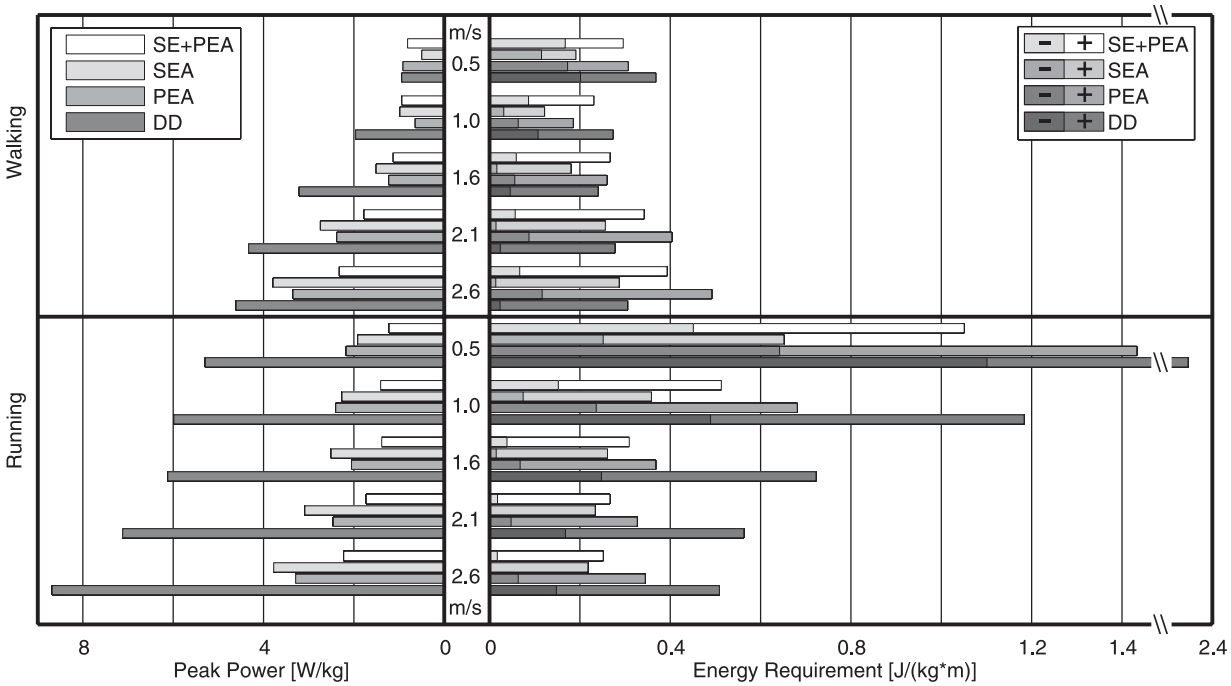

Figure 6: Ankle peak power (PP) and energy requirements (ER) for different walking and running speeds with a constant stiffness independent of speed and gait for each elastic system (SEA, PEA, SE+PEA). Additionally a constant parallel spring slack length is used in the PEA and SE+PEA. PP and ER are shown for the constants that minimize PP for both gaits up to 2.6 m/s most. The amount of negative work (-) is indicated by the darker left part of the ER bars, positive work (+) is indicated by the brighter right part. The results belong to the strict-restricted case (SRC).

and by 52.8% for the SE+PEA. In contrast the ER increases for walking by 9% for the PEA and 3.4% for the SE+PEA (Fig. 6).

Peak Power

For the PP we found the highest mean reductions compared to the DD in the SE+PEA (76.2% running, 48% walking). The PP reductions for the SEA and the PEA for running (59.7%, 62.6%) and walking (41%, 40.9%) are comparable. At the PP demanding higher speeds the PEA has advantages (Fig. 6).

Stiffness

The optimal stiffness of the SEA to reduce PP for all speeds in running and walking up to 2.6 m/s is 90 kN/m. As an optimal value for the PEA a stiffness of 29kN/m was identified. For the SE+PEA the serial stiffness was 95 kN/m and the parallel 17 kN/m.

Slack Length

The optimal slack length of the PE in the PEA was 0.455 m. At touch-down the spring is elongated. Just before and after take-off we found PE compression for speeds higher than 1 m/s. For the SE+PEA the optimal slack length is about 0.319 m with a serial spring rest-length of 0.12 m.

This length occurs for walking only at 2.6 m/s directly after take-off. For all other walking and running speeds the PE in the SE+PEA is always elongated.

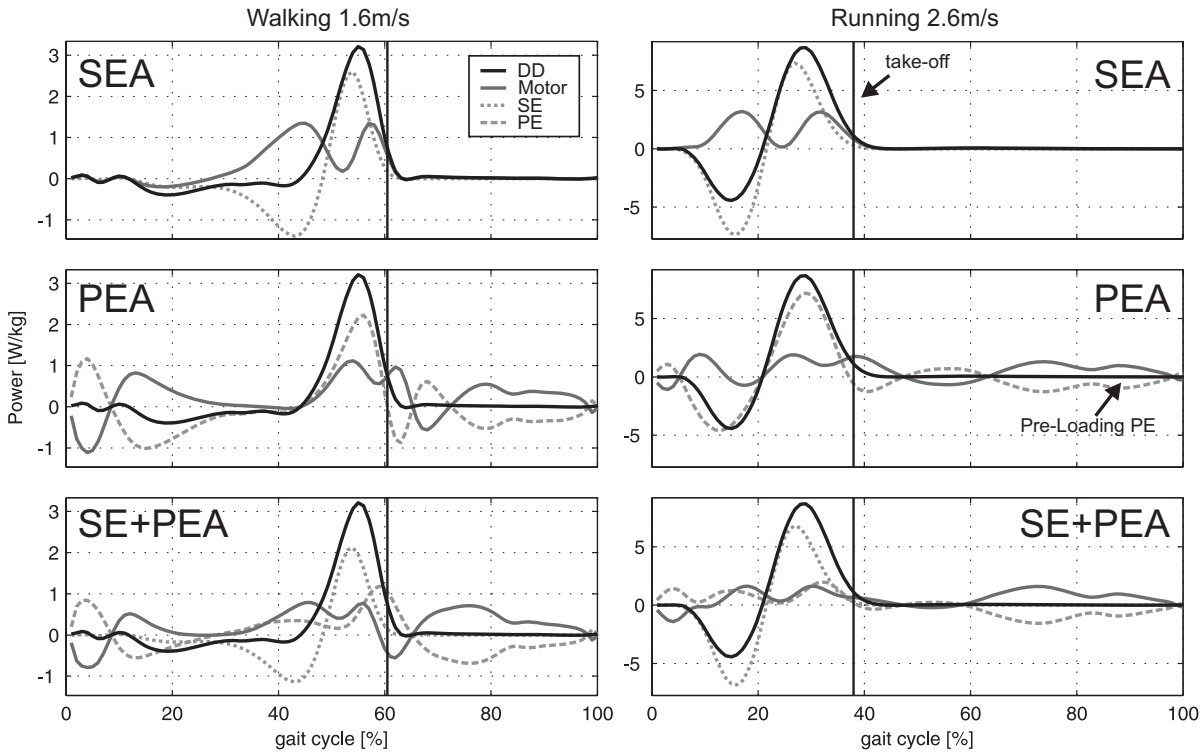

Figure 7: Power of the whole system (DD, solid black), the motor (Motor, solid dark grey), the serial element (SE, dotted grey) and/or the parallel element (PE, dashed grey) of the different elastic actuators SEA, PEA and SE+PEA for walking at 1.6 m/s and running at 2.6 m/s. The solid vertical lines represent the take-off. The results belong to the PRC.

4.5 DISCUSSION

4.5.1 Peak power and energy requirements.

We found that a SEA, a PEA and a SE+PEA can reduce PP and ER in comparison to a DD. A parallel element (PE) can decrease PP more than a serial element (SE) but a SE has the advantage to decrease ER more than a PE. A combination of serial and parallel element can give additional advantages in PP but lower benefits in ER than the single SE. By setting the stiffness and the PE slack length to a optimized constant value all the tested elastic actuators result in an increase of PP and partially in ER. For fast walking speeds the ER are higher than for the DD.

The reason for the decreased PP in the elastic systems can be the decrease of actuator force and/or actuator speed. Avoiding high forces and high speeds at the same time can also help to reduce the power requirements of a motor. Checking these parameters SE can only reduce motor-speed, PE the forces on the motor (Fig. 4, 9). So a combination (SE+PEA) provides both advantages (Fig. 4, 9).

In order to take advantage of the PE it must be pre-loaded in the swing-phase by the motor (Fig. 7, 8, 9). This energy can then be released later during push-off to support the motor plantarflexing the ankle-joint.

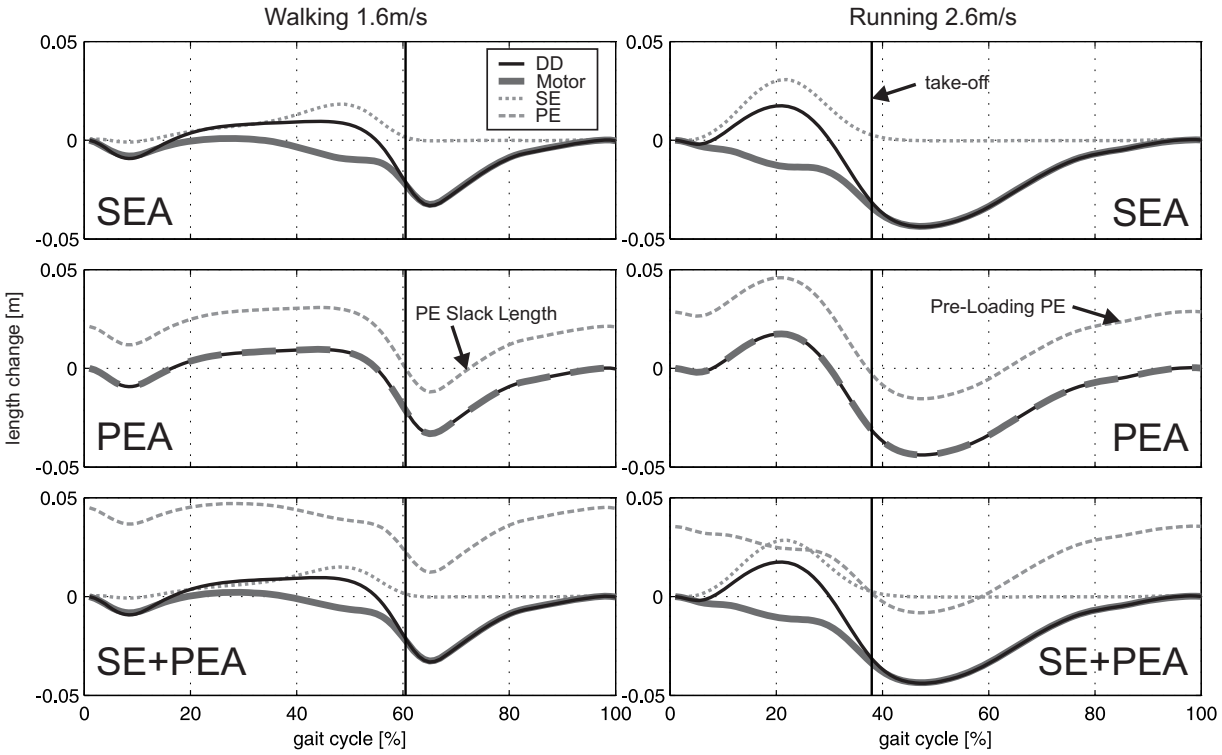

Figure 8: Length change of the whole system (DD, solid black), the motor (Motor, solid grey), the serial element (SE, dotted grey) and/or the parallel element (PE, dashed grey) for the different elastic actuators SEA, PEA and SE+PEA for walking at 1.6 m/s and running at 2.6 m/s. DD, Motor and SE are displayed in reference to be zero at touch-down. To get a better understanding of the PE that has the same length profile as the motor it is plotted in reference to the rest-length that is set as zero. The solid vertical lines represent the take-off. PE slack length occurs when the spring is unloaded and length change is 0. The results belong to the PRC.

4.5.2 Stiffness.

The stiffness values for the PE were predicted to be lower than for the SE. The reason is that the PE must follow the whole length change of the motor to mimic human ankle behavior. Too high stiffness would cause high forces for the motor and finally high power requirements.

A constant stiffness for all three elastic actuators is possible but it leads to speed and gait dependent increases in PP and ER.

4.5.3 PE slack length.

There is also compression for the parallel spring. We expected that a continuous elongation would give better results. But to set the slack length to have compression just before or mainly after take-off helps to reduce the PP during the PE loading process in flight phase or for mimicking ankle torque after touch-down (Fig. 7).

4.5.4 Partial- and Strict-restrictive case

We found that it is possible to have one constant PE slack length and one stiffness for the PE and/or the SE without increasing PP for the highest walking speed (2.6m/s, Fig. 5, 6). But

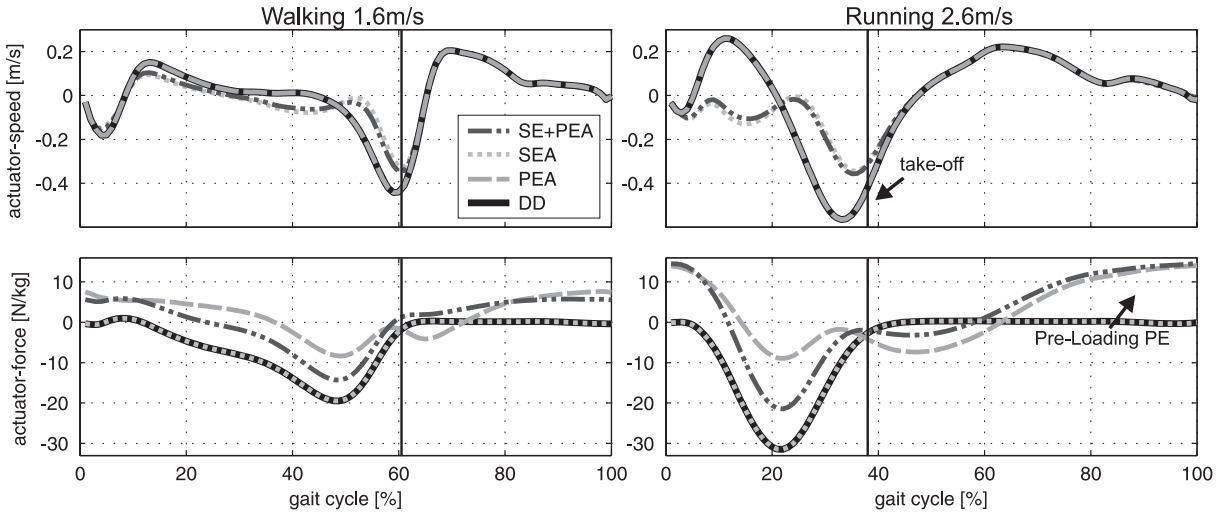

Figure 9: Calculated actuator speed and actuator force for the SE+PEA (dash + double dot, dark grey), the SEA (dotted, light grey), the PEA (dashed, grey) and the DD (solid black) to mimic human ankle joint behavior for walking (1.6 m/s, left) and running (2.6 m/s, right). The DD data for actuator speed is identical to the speed of the PEA actuator. The DD force is identical to the SEA actuator force. The results belong to the PRC.

by setting constant values the PP in all other conditions increases. ER only increasing for the actuators with PE at low speeds. In conclusion a change of stiffness and PE slack length can be avoided to get a simple mechanical system. A possibility to change the parameters can save energy for lower speeds and reduces the PP requirements almost for all conditions.

4.5.5 Motor selection

If we want to build a robotic ankle-joint that is capable of human like walking up to 1.6 m/s and running up to 2.6 m/s in a DD linear acceleration of 11.7 m/s^2, a linear speed of 0.57 m/s, a force of 31.5 N/kg and a power of 8.7 W/kg are necessary (Fig. 4). When we select a roller screw with a lead of 2 mm to transfer the linear to rotary motor motion the motor must have a speed of 1790 rad/sec. The acceleration should be 36757 rad/sec^2. Considering a roller-screw efficiency of 85% and a subject weight of 75 kg the motor must handle 0.88 Nm peak torque and a PP of 768 W for the DD.

Taking the same criteria into account (85%, 75 kg, 1.6 m/s walking and 2.6 m/s running) a parallel element can reduce the PP to 171 W and the peak torque to 0.39 Nm. The serial element can reduce PP to 282 W, acceleration to 32672 rad/sec^2 (10.4 m/s^2) and speed to 1037 rad/sec (0.33 m/s).

As an example the Maxon EC-4pole 30 (0.3 kg) can handle about 200 W and 0.12 Nm continuous. A nominal speed of about 1655 rad/sec and an acceleration of 36000 rad/sec^2 (continuous torque/rotor inertia) is possible. So the primary limitation for the inrunner Maxon motor is that it is not delivering sufficient torque. Outrunner motors (Sensinger et al., 2011) like the ThinGap TG2320 (0.48 kg) can provide higher torque. For a voltage of 48 V it can provide about 0.58 Nm and about 618 W. The nominal speed at 48 V is about 1025 rad/sec, the acceleration 3558 rad/sec^2. Especially the slow acceleration caused by the inertia would limit the function of the elastic actuator.

Both motor examples can not full-fill the estimated requirements of the elastic actuators in a single motor solution. To get a system that can handle the requirements given by human measurement data other or additional mechanical approaches are necessary.

Comparing the two motor solution 2x SEA with the SE+PEA (Fig. 4) shows that in running the requirements are nearly equal. Only the ER of the SE+PEA are higher because of the PE. In walking the ER and the force of the SE+PEA is higher than in the 2x SEA solution. From the mechanical point of view the 2x SEA solution has less complexity but maybe a higher weight. Higher complexity (PE+SE) can limit the variability and increases the sensitivity of the system. From this point of view especially a system like the Bionic Running Ankle (Hitt et al., 2010a) with two SEA's seems to be a good solution to achieve system requirements.

Taking heating into account, short time overloading of the motors can provide better feasibility. So two Maxon RE40, each rated at 150 W continious power, were able to handle about 550 W electrical peak power in running experiments with the Bionic Running Ankle (Hitt et al., 2010a). Considering the efficiency of the motor, a higher output power than the continuous power seems to be possible. If similar effects are possible for the continuous torque values of the Maxon EC-4pole motors, mentioned as an example, it could be a solution to achieve walking and running at higher speeds with a double motor system.

4.5.6 Further concepts

If two motors are used they can also be integrated in different locations to mimic human m. soleus and m. gastrocnemius function. Further improvements in leg control might also be achieved by this. Maybe the biological function of slow Type I fibers in the m. soleus and the fast Type II fibers in the m. gastrocnemius (Gollnick et al., 1974) can also be represented by the slow powerful ThinGap and the fast Maxon motors respectively. So a combination of the strengths of two motors could solve the desired requirements.

Other options to reduce the requirements can be to use non-linear springs which represent better the non-linear tendon function of the plantar-flexors (Alexander, 1992; Shin et al., 2008). This can also be realized by adding unilateral springs to the system. Another approach, to decrease the system requirements, is to mimic the measured human joint function not in detail. To which extend such a method works without clearly affecting the ankle function must be proofed in experiments.

In addition catapult like pre-loading (swing) and releasing (during push-off) similar to the parallel spring in the PEA or passive ankle-knee couplings (Unal et al., 2010) can help to improve ankle push-off performance.

Improvements in motor technology can also solve the limitations.

4.6 CONCLUSION

The theoretical calculations showed that a SEA, a PEA and a SE+PEA can reduce peak power and energy requirements in comparison to a DD. Parallel elements can give advantages in peak power in comparison to the serial elements. On the other hand serial elements having advantages in minimizing energy requirements. A combination of both elastic structures in an SE+PEA can further decrease peak power. With that, the energy requirements are less than the PEA but higher than for the SEA. The results show less benefit for the PEA and the SE+PEA when a constant stiffness and a fixed parallel spring slack length is used for all walking and running speeds. The proofed concepts show that mimicking human ankle joint behavior in running and walking

at higher speeds is still challenging for single motor devices. Improvements in motor technology or additional novel concepts for further reductions are required. As our investigation shows a double motor solution seems to be currently the best way to fully reproduce human ankle function for both gaits. For this, the best arrangement of mono- or biarticular elastic actuators has to be identified.

4.7 ACKNOWLEDGMENTS

This work was supported by the DFG grant SE1042/8. The authors acknowledge S.W. Lipfert for providing human data.

4.8 AUTHOR CONTRIBUTIONS

Martin Grimmer is the main author of the article. He was responsible for the conception and design, analysis and interpretation of data and writing of the manuscript. Mahdy Eslamy was contributing to the discussion of the results and for the revision of the article. Stefan Gliech assisted to perform first calculations on parallel elastic structures. André Seyfarth assisted for the revision of the article.

4.9 REFERENCES

Alexander, R. (1992). Exploring biomechanics. animals in motion. *Scientific American Library, New York*, 247.

Au, S., Weber, J., and Herr, H. (2009). Powered Ankle–Foot Prosthesis Improves Walking Metabolic Economy. *Robotics, IEEE Transactions on*, 25(1):51–66.

Eilenberg, M., Geyer, H., and Herr, H. (2010). Control of a powered ankle–foot prosthesis based on a neuromuscular model. *Neural Systems and Rehabilitation Engineering, IEEE Transactions on*, 18(2):164–173.

Gollnick, P., Sjödin, B., Karlsson, J., Jansson, E., and Saltin, B. (1974). Human soleus muscle: a comparison of fiber composition and enzyme activities with other leg muscles. *Pflügers Archiv European Journal of Physiology*, 348(3):247–255.

Grimmer, M. and Seyfarth, A. (2011). Stiffness adjustment of a series elastic actuator in an ankle-foot prosthesis for walking and running: The trade-off between energy and peak power optimization. In *IEEE International Conference on Robotics and Automation (ICRA)*, pages 1439–1444. IEEE.

Günther, M., Sholukha, V., Keßler, D., Wank, V., and Blickhan, R. (2003). Dealing with skin motion and wobbling masses in inverse dynamics. *Journal of Mechanics in Medicine and Biology*, 3(3-4):309–335.

Herr, H. and Grabowski, A. (2011). Bionic ankle–foot prosthesis normalizes walking gait for persons with leg amputation. *Proceedings of the Royal Society B: Biological Sciences*.

Hitt, J., Merlo, J., Johnston, J., Holgate, M., Boehler, A., Hollander, K., and Sugar, T. (2010a). Bionic running for unilateral transtibial military amputees.

Hitt, J., Sugar, T., Holgate, M., and Bellman, R. (2010b). An active foot-ankle prosthesis with biomechanical energy regeneration. *Journal of Medical Devices*, 4:011003.

Hollander, K. and Sugar, T. (2005). Design of the robotic tendon. In *Design of Medical Devices Conference (DMD 2005)*.

Lipfert, S. (2010). *Kinematic and dynamic similarities between walking and running*. Verlag Dr. Kovac, Hamburg. ISBN: 978-3-8300-5030-8.

Sensinger, J., Clark, S., and Schorsch, J. (2011). Exterior vs. interior rotors in robotic brushless motors. In *IEEE International Conference on Robotics and Automation (ICRA)*, pages 2764–2770. IEEE.

Shin, D., Finni, T., Ahn, S., Hodgson, J., Lee, H., Edgerton, V., and Sinha, S. (2008). In vivo estimation and repeatability of force–length relationship and stiffness of the human achilles tendon using phase contrast mri. *Journal of Magnetic Resonance Imaging*, 28(4):1039–1045.

Sup, F., Varol, H., Mitchell, J., Withrow, T., and Goldfarb, M. (2009). Self-contained powered knee and ankle prosthesis: Initial evaluation on a transfemoral amputee. In *Rehabilitation Robotics, 2009. ICORR 2009. IEEE International Conference on*, pages 638–644. IEEE.

Unal, R., Carloni, R., Hekman, E., Stramigioli, S., and Koopman, H. (2010). Conceptual design of an energy efficient transfemoral prosthesis. In *Intelligent Robots and Systems (IROS), 2010 IEEE/RSJ International Conference on*, pages 343–348. IEEE.

5 Manuscript III: Stiffness Adjustment of a Series Elastic Actuator in a Knee Prosthesis for Walking and Running: The Trade-off between Energy and Peak Power Optimization

Authors:

Martin Grimmer and André Seyfarth

Friedrich Schiller Universität

07743 Jena, Germany

Published as a paper at the

2011 IEEE International Conference on Intelligent Robots and Systems (IROS)

5.1 ABSTRACT

In ankle-foot prostheses a serial spring can assist the motor to reduce peak power (PP) and energy requirements (ER) during locomotion. Similar benefits can be expected for an active knee prosthesis. We compare the situation of a direct drive with a series elastic actuator optimized for minimal ER or for minimal PP. The simulations indicate that at the knee joint a serial spring can highly reduce ER and PP in running and fast walking. Around preferred walking speed (1.3 m/s) only a reduction in ER is found. The optimal stiffness changes with speed and gait. Still it is possible to use one constant stiffness for a huge range of walking and running speeds with only moderate increases of ER and PP in comparison to speed and gait optimized values.

5.2 INTRODUCTION

In comparison to a direct drive (DD), a Series Elastic Actuator (SEA) (Pratt and Williamson, 2002) or a Robotic Tendon (Hollander and Sugar, 2005) at the ankle joint can reduce peak power (PP) and the energy requirements (ER) for walking and running (Grimmer and Seyfarth, 2011; Hollander and Sugar, 2005). Several prototypes of ankle-foot prostheses are already using this mechanisms (Hitt et al., 2009; Sup et al., 2009; Au et al., 2009). There is one active knee joint prototype operated as an DD (Varol et al., 2009) and one with an antagonistic SEA-system (Martinez-Villalpando and Herr, 2009). The first commercial active knee (Power Knee, Ossur) uses a DD system. For a 75 kg subject walking at 1.6 m/s a PP of 127 W would be required with a DD at the knee joint (Fig. 5). For running at this speed the required PP increases to 490W (Fig. 5). Considering the limitations of current motor technology such high PP can be hardly realized in a prosthesis. Especially for running, it seems to be important to use springs at the knee to assist the motor to reduce PP (smaller motor) and ER (smaller battery) like at the ankle joint (Grimmer and Seyfarth, 2011). Such a knee spring could potentially also reduce the ER in walking as indicated in a recent study with a switchable knee spring (Endo et al., 2009).

Here, we aim at estimating to what extent a SEA knee spring can reduce PP and ER for walking and running over a large range of speeds. We want to compare both optimization goals and ask if it is possible to use one stiffness for all walking and running speeds without considerable increases in PP or ER. We expect that like at the ankle joint (Grimmer and Seyfarth, 2011) a spring can assist the motor in mimicking human knee behavior during different walking and running speeds. We expect different optimal stiffness values when changing speed and that the benefit for walking is not as high as in running.

Additionally we want to compare the human muscle tendon behavior with the knee SEA and current prosthetic knee joints. We aim at better understanding the limits of prosthetic knee joints and at defining the conditions (gait, timing) for which structures providing positive knee power are required.

5.3 METHODS

In two experiments (Tab. 1, (Lipfert, 2010)) subjects walked (Exp. I) and ran (Exp. I, II) on a treadmill with integrated 3D force sensors (Kistler, 1000Hz). Kinematics were recorded by high-speed infrared cameras (Qualisys, 240Hz).
Surface EMG (only Exp. I) was measured (Delsys) for the knee flexors m. biceps femoris (BCF), m. semitendinosus (SMT), m. gastrocnemius medialis (GSM) and knee extensors m. rectus femoris (RCF), m. vastus medialis (VSM). The raw EMG signals were band-pass filtered (20-450

Table 1: Experimental and subject characteristics (mean ± std).

	number of subj.	age [yrs]	body height [m]	body mass [kg]	speeds [m/s]	leg length [m]
Exp. I	21	25.4 ± 2.7	1.73 ± 0.09	70.9 ± 11.7	0.52, 1.04, 1.55,2.07,2.59	0.96 ± 0.08
Exp. II	7	23.7 ± 1.1	1.80 ± 0.10	77.5 ± 8.8	3.0, 4.0	1.02 ± 0.07

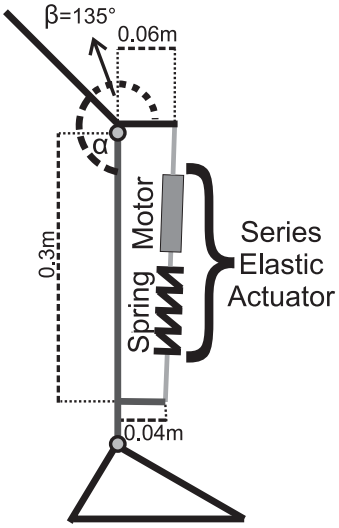

Figure 1: Concept of the active knee prosthesis used to estimate the minimal ER and PP requirements to mimic human locomotion. Lengths and forces of the SEA are estimated based on knee angle (α) and torque data for human walking and running. β is a constant angle (135°) between the thigh and the upper linkage of the SEA.

Hz), rectified and smoothed (40 Hz, 4th order Butterworth filter). Each individual trial then was normalized to the maximum value (100%) determined by the median of the top one per mille values. For both studies, knee angles and torques were calculated (Günther et al., 2003; Lipfert, 2010) and used to estimate SEA length and force, corresponding to a knee SEA concept (Fig. 1). Knee torques were normalized to a reference subject with body mass 75 kg and a resting leg length of 1m. The resting leg length is defined as the distance between the center of mass, COM, and the center of pressure, COP, in standing. Based on SEA length and force, actuator ER and PP are derived as described in (Hollander and Sugar, 2005) based on the prosthesis model concept described in Fig. 1. It is important to note, that the SEA can introduce pushing and pulling forces to represent the function of both knee extensors and flexors. Therefore, no antagonistic structure is required. ER was calculated as the sum of positive and the amount of negative work (Grimmer and Seyfarth, 2011). The estimated power and ER was normalized to body mass. Additionally ER was normalized to distance travelled during the gait cycle representing the cost of transport related to the SEA. Optimal spring stiffness values for minimal energy (SEA-E) and minimal peak power (SEA-P) were determined for each walking and running speed by checking the requirements for stiffness values between 1 kN/m and 1000 kN/m

(1 kN/m step size). The minimum ER and PP values were compared to the direct drive (DD) configuration (Fig. 5).

5.4 RESULTS

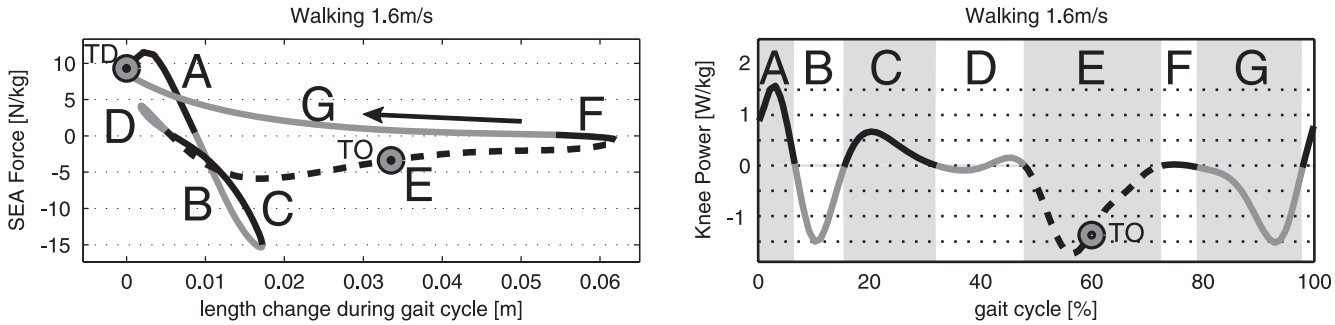

Figure 2: SEA force versus SEA length change (left) and knee power (right, similar to DD) during the gait cycle at 1.6 m/s walking. TD represents the touch down, TO the take off. A to G represent prominent phases during gait cycle in respect to knee power.

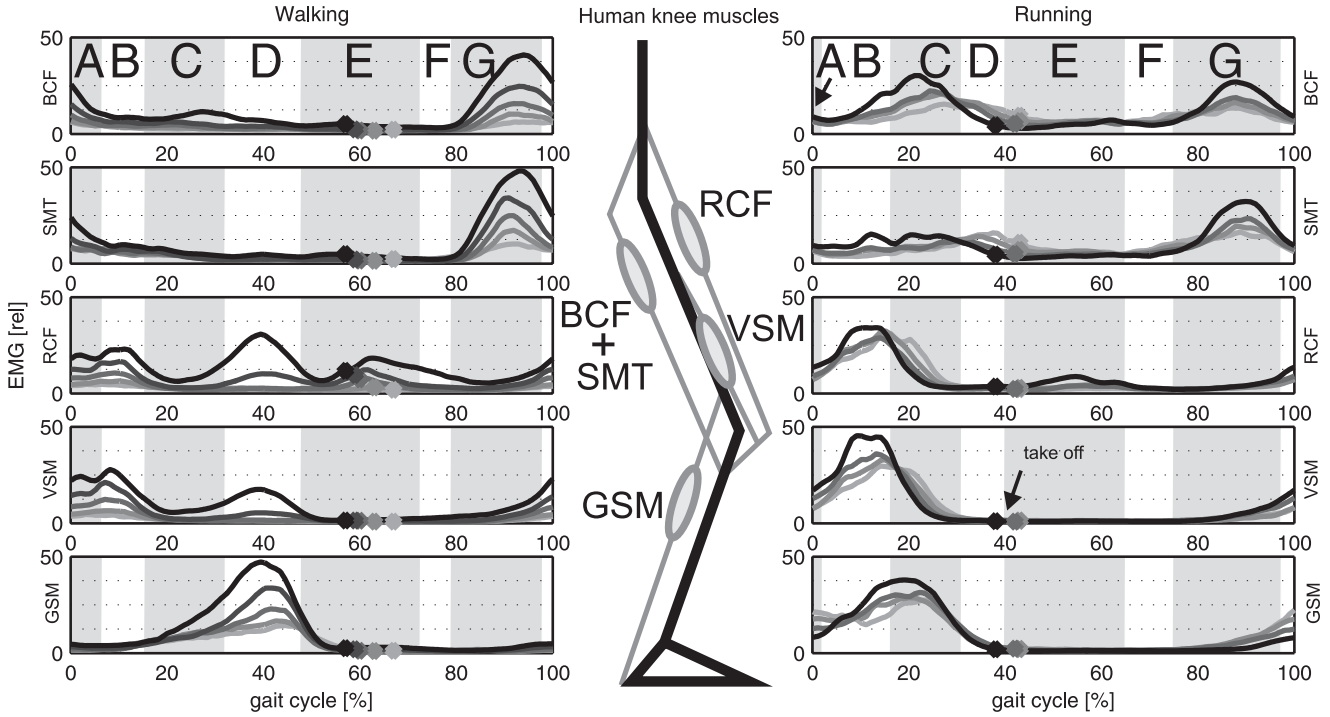

Figure 3: EMG of biarticular knee flexing muscles m. biceps femoris (BCF), m. semitendinosus (SMT), m. gastrocnemius medialis (GSM), the biarticular knee extending muscle m. rectus femoris (RCF) and the monoarticular m. vastus medialis (VSM) during gait cycle in walking and running at different speeds (light gray to black 0.5 m/s, 1 m/s, 1.6 m/s, 2.1 m/s, 2.6 m/s). The dots represent the take off at each speed. Phases A to G see Fig. 2 and 4.

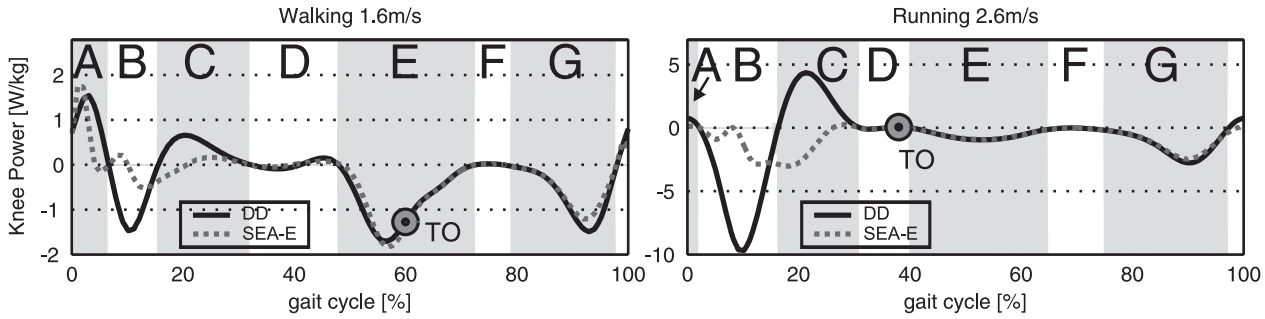

Figure 4: Knee power during gait cycle in walking (1.6 m/s) and running (2.6 m/s) for a direct drive system (black solid line) and the SEA motor (gray dotted line) optimized for SEA-E. TO represents the take off. A to G represent prominent phases during gait cycle in respect to knee power.

5.4.1 Knee joint and muscle function

Fig. 2 shows the calculated knee SEA force-length function and the required knee power to mimic human walking. During the gait cycle, phases A to G can be distinguished to explain the resulting knee function similar to Winter (Winter, 1983). The understanding may help for transferring the functionality to a technical system and to understand the limited performance of actual prosthetic knee joints. In phase A, swing-leg retraction (Seyfarth et al., 2003) is initiated by knee flexors (BCF, SMT, GSM only in running, Fig. 3) guaranteeing knee flexion for the Load Response (phase B). In phase B the energy is absorbed by eccentric work of knee extensors (RCF, VSM, Fig. 3). Similar to the patella tendon, part of this energy could be saved in the SEA spring (Fig. 4). Phase C (Mid Stance) is characterized by knee extension supported by a concentric shortening of the knee extensors (RCF, VSM, Fig. 3) and by release of elastic energy stored in phase B. For running, almost no positive work of the SEA motor is needed to assist the spring (Fig. 4). The motor even damps the spring to get human-like behavior. After reaching maximum knee extension in phase D, knee flexion restarts. The small negative and positive power could be generated by the biarticular knee flexor GSM (Fig. 3). Phase E is characterized by substantial negative work (eccentric operation of RCF, Fig. 3). During the Pre-Swing and the Initial Swing (phase E) RCF absorbs energy and decelerates the knee flexion. As there is no substantial positive power peak in phase F, no elastic energy of knee extensors is used to support leg extension during swing phase. In phase G, knee extension and thus the forward motion of the shank is decelerated by the hamstring muscles (BCF, SMT) and additionally the GSM in running (Fig. 3). A part of the energy could be saved and reused to flex the knee before touch down in phase A.

5.4.2 Optimizing SEA stiffness depending on speed and gait.

In Fig. 5, ER (right panel) and PP (left panel) are presented for SEA-E and the SEA-P configurations. Here spring stiffness was optimized individually for each walking and running speed. With such optimized SEA configurations, both ER and PP requirements can be clearly reduced in fast walking (2.1 m/s, 2.6 m/s) and running compared to the DD system. For slow walking (up to 1.6m/s) only energy reductions and no power reductions could be achieved.

Energy requirements: In walking, ER (Fig. 5) can be reduced (SEA-E) by 5% (0.5 m/s) to 29% (2.1 m/s). For running the benefit in energy is decreasing with speed (71% at 0.5 m/s

and 40% at 4 m/s). In comparison to SEA-P, ER can be further reduced with SEA-E by up to 11% in running and up to 25% in walking. For running above 1m/s only negative SEA work was predicted. Also in walking the negative work was dominating (e.g. 20% positive vs. 80% negative ER at 1.6m/s). This general behavior holds also for the DD.

Peak Power: In fast walking (2.1 m/s and 2.6 m/s), PP can be reduced (SEA-P) by 31%. For slower walking no or only little reductions (11% at 0.5 m/s) are found. In running, PP requirements are reduced between 78% (0.5 m/s) and 54% (4 m/s). The benefit is decreasing with speed. As compared to SEA-E, PP can be further reduced with SEA-P by up to 24% (1.6 m/s running). For all other running speeds and in walking the reduction is lower than 10%.

Optimal Stiffness (Tab. 2): For SEA-E, the stiffness increases with walking speed (122 kN/m-160 kN/m) except for 0.5 m/s (290 kN/m). In running, the stiffness is decreasing (162 kN/m-138kN/m) until 1.6 m/s and again increasing for higher speeds (147 kN/m-179 kN/m). In contrast, when optimizing PP (SEA-P), the stiffness first increases up to 2.6 m/s running and decreases for higher speeds. There is no such tendency in walking where stiffness values are widely spread (65 kN/m-363 kN/m). At 1.0 m/s and 1.6 m/s walking no PP reduction could be found.

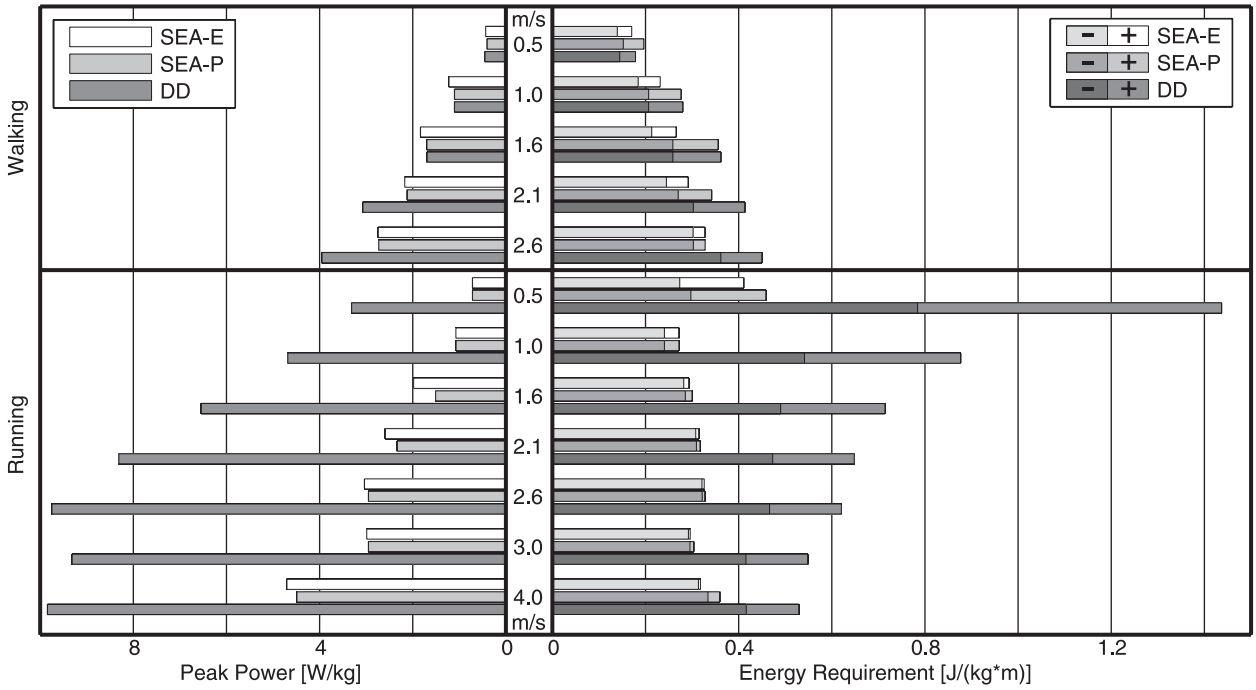

Figure 5: Knee PP and ER for different walking and running speeds with SEA stiffness optimized to minimize energy requirement (SEA-E), or peak power requirement (SEA-P), respectively. The amount of negative work is the darker left part of the ER bars, positive work is the brighter right part.

5.4.3 Constant SEA stiffness across speeds and gaits.

A constant SEA stiffness of around 155 kN/m can be used throughout all speeds and both gaits without substantial increases in ER and PP (Fig. 6). Especially lower stiffness values lead to

Table 2: Predicted optimal SEA stiffness values for minimizing ER (SEA-E) or PP (SEA-P) at different walking and running speeds.

Gait		Walking					Running						
Speed [m/s]		0.5	1.0	1.6	2.1	2.6	0.5	1.0	1.6	2.1	2.6	3.0	4.0
SEA Stiffness	SEA-E	290	122	142	157	160	162	146	138	147	153	167	179
in [kN/m]	SEA-P	65	rigid	rigid	363	176	143	144	154	155	156	153	135

increases in PP. Little or no increases in PP and ER are found when increasing SEA stiffness in walking.

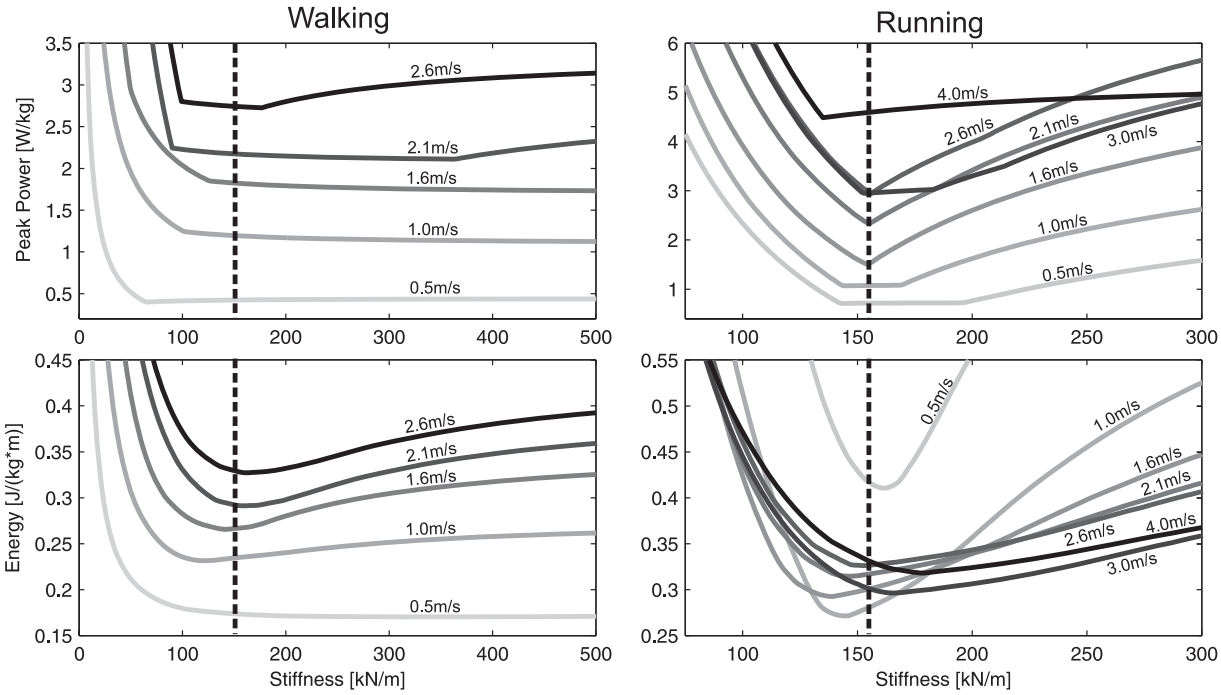

Figure 6: Peak power and energy requirements versus SEA spring stiffness for walking (left) and running (right) at different speeds. The dashed vertical line shows the preferred value (around 155 kN/m) for a constant stiffness.

5.5 DISCUSSION

5.5.1 Peak Power and Energy requirements.

In this study we investigated how tuning the spring stiffness of a serial elastic actuator (SEA) can lower both energy requirements (ER) and peak power (PP) of an actuated knee prosthesis at different walking and running speeds. In both gaits, large reductions in ER (up to 71% in running, up to 29% in walking) and PP were predicted (up to 78% in running, up to 31% in walking) by selecting appropriate stiffness values. During the gait cycle the SEA is mostly doing negative work (SEA-E and SEA-P) in running and also for some speeds in walking (SEA-E). This is in contrast to the ankle joint, where the net work was positive (Grimmer and Seyfarth, 2011).

For running, we found that adjusting the SEA stiffness for minimizing energy (SEA-E) results in almost no additional energy reductions compared to PP optimization (SEA-P) whereas for walking ER reductions with SEA-E are possible compared to SEA-P. In both gaits there is only a small increase of PP when optimizing for energy compared to SEA-P. Hence, it is equally appropriate to optimize for PP or for ER when designing the knee SEA. The results are different to similar calculations for the ankle joint (Grimmer and Seyfarth, 2011) in which optimizing PP was the better approach. As there is no optimal stiffness when optimizing PP for moderate walking speeds 1.0m/s and 1.6m/s, SEA-E should be preferred. Then ER benefits of up to 25% could be achieved during walking, the most frequently used gait pattern.

Surprisingly, it was not possible to reduce PP by tuning the SEA spring for walking at 1.0 m/s and 1.6 m/s. This can be explained using the power curve (1.6 m/s walking) in Fig. 2 where no PP reduction in phase E could be achieved by the spring. A PP reduction in phase E is also not possible for SEA-E (Fig. 4). Also for faster walking, PP can be reduced with SEA-P only to the maximum PP measured in phase E (DD). The observed knee flexion during this phase is not spring-like as there is no energy return during knee extension (phase F, see power curve in Fig. 2). To reduce ER or PP by tuning a serial spring, a synchronous increase and subsequent synchronous decrease of both SEA force and SEA length would be required (Fig. 2). Such a behavior occurs in phase B (loading) and C (undloading). Other examples are phase D and the transition from phase G (loading) to phase A (unloading). In contrast, in phase E the increase and decrease of SEA force is found in parallel to an on-going increase in length. This action can not benefit from a SEA spring.

At the knee joint, running above 1m/s could be realized even without a motor if the required negative work is performed by a damping mechanism (Fig. 4). For walking a small motor is required to provide the remaining positive energy, mainly for enforcing initial knee flexion after touch down (Fig. 4). These findings are comparable to results of (Martinez-Villalpando and Herr, 2009). The need for a knee motor in walking could further be reduced by considering coupling effects with other leg joints, e.g. by elastic or damping biarticular structures (Endo and Herr, 2009). Thus, in a knee prosthesis the knee motor could mainly manage joint damping and adjust SEA length to mimic human knee behavior.

5.5.2 Stiffness.

When optimizing for ER or PP, knee stiffness values for running are between 135 kN/m and 179 kN/m. At the ankle joint, this stiffness range is even smaller (Grimmer and Seyfarth, 2011). For walking, the knee stiffness increases with speed when optimizing for ER (except for 0.5 m/s). This is in contrast to the ankle joint (Grimmer and Seyfarth, 2011) where the SEA-E optimized stiffness decreases with speed. With SEA-P optimization, no benefits at the knee joint were predicted for 1.0 m/s and 1.6 m/s walking. This indicates that a DD would be sufficient with respect to required peak power. To keep the prosthetic system simple we would prefer to use one stiffness for the knee joint. Our results show that this is possible. With SEA-E optimization the optimal value for each walking and running speed can be determined. By averaging a mean stiffness value (in our model a stiffness around 155 kN/m) can be obtained that allows to handle all speeds with only little increases in PP or ER.

5.5.3 Passive prosthetic knee joints.

Passive prosthetic knee joints like the C-Leg (Ottobock), the Rheo-Knee or the Mauch SNS (both Ossur) cannot mimic human knee behavior in detail (Seroussi et al., 1996; Johansson et al.,

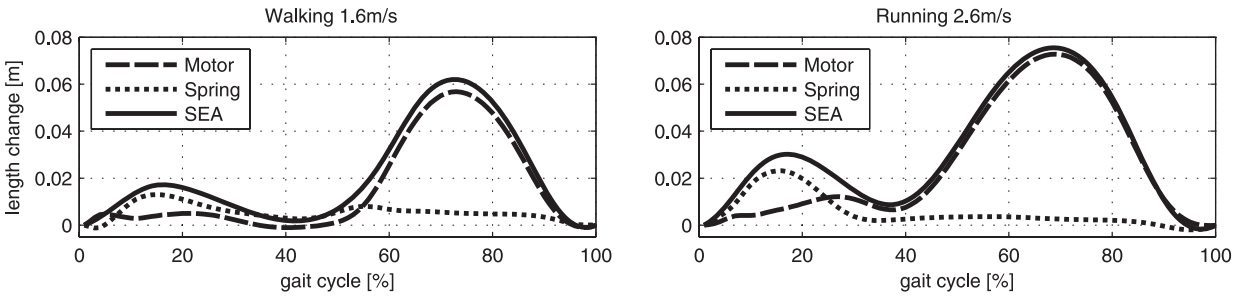

Figure 7: Desired length change of motor (dashed line), the spring (dotted line) and the whole SEA (solid line) during gait cycle in walking (left 1.6 m/s) and running (right, 2.6 m/s) to mimic the human knee behavior. In both cases the spring stiffness is optimized for energy (SEA-E).

2005; Segal et al., 2006). Especially in phase A (Fig. 2) knee flexion before touch down is missing as this requires positive work. This could be realized by a motor or by springs that store breaking energy in phase G and release it in phase A. Also, there is no negative and positive power in phases B and C, respectively (Seroussi et al., 1996; Johansson et al., 2005; Segal et al., 2006). The reasons are manifold. Some older prosthetic knee joints are not capable of performing knee flexion in the stance phase. The C-Leg provides this ability, however only few amputees are using it. One reason could be that the knee has no spring (tendons) and no motor (knee extensor) that could help to return to an extended position. Alternatively, hip extensors or an active foot (m. soleus) could support extension of the passive knee joint. This may cause side-effects such as gait asymmetries resulting in long-term sequelae (Robbins et al., 2009). In running, the knee SEA motor (Fig. 4) is mainly damping the spring and provides almost no positive energy during phase C. This negative work could equally be generated by a biarticular GSM structure (Fig. 3) as discussed in (Lipfert, 2010). The GSM would transfer the energy to the ankle joint in phases B and C for running and at the beginning of phase E in walking (Fig. 4). The positive power in phase D (Fig. 2) can be mimicked by a biarticular spring connected to the hip (m. sartorius, hip + knee flexor) or to the ankle joint (GSM). The damping (yielding) observed in phase E can be achieved in current knee prostheses. For instance, the Mauch SNS hydraulic knee joint (Seroussi et al., 1996) can mimic such a knee function during Pre-Swing and Initial Swing. However, according to Segal et al. (Segal et al., 2006) the C-Leg and the Mauch SNS generate nearly twice the negative energy that was found in the non amputee group. In some knee prostheses (e.g. Rheo-Knee) a torsion spring is supporting knee extension in Mid Swing (E to F), which is different to what is suggested by our experimental data (Fig. 2). With current knee prostheses, phase G can partially be reproduced, however different observations with respect to the breaking energy are found (Seroussi et al., 1996; Segal et al., 2006). One reason could be that joint deceleration of the swing leg is controlled only by monoarticular structures at the hip and the knee joint. In humans, the biarticular BCF, streched by hip flexion and knee extension, can decelerate the swing-leg (thigh + shank) very gradually. A similar process, caused by the biarticular RCF, can help to control the initiation of the swing phase in phase E by damping the knee flexion.

In summary, passive prosthetic knee joints without springs cannot generate positive power in phases A, C and D. With a passive knee, compensating mechanisms like an active ankle prosthesis or an adaptation in hip function can support a more functional gait. Knee damping by passive knee prostheses in phases E and G remains still challenging. This issue could be

resolved by improved adaptation strategies matching different walking patterns or by adding biarticular connections in prosthetic limbs.

5.5.4 Technical realization.

To mimic human knee behavior during walking and running, the SEA motor has to reproduce a defined profile (Fig. 7). Using a ball screw the rotation of the motor can be transferred to translation in a technical muscle. Considering the efficiency of the motor and the ball screw, motors can be selected that can handle the desired acceleration, speed and torque to reproduce positive and negative power without other damping mechanisms. Our calculations indicate that the motor requirements for walking with speeds up to 2.6 m/s are similar to those of the ankle joint (Grimmer and Seyfarth, 2011) and could be realized in a prosthetic system. For running, the torques requirements are more critical and could be achieved by temporarily overclocking actual brushless motors with high specific power.

5.6 ACKNOWLEDGMENTS

This work was supported by the DFG grant SE1042/8. The authors acknowledge S.W. Lipfert for providing human data.

5.7 AUTHOR CONTRIBUTIONS

Martin Grimmer is the main author of the article. He was responsible for the conception and design, analysis and interpretation of data and writing of the manuscript. André Seyfarth assisted for the revision of the article.

5.8 REFERENCES

Au, S., Weber, J., and Herr, H. (2009). Powered Ankle–Foot Prosthesis Improves Walking Metabolic Economy. *Robotics, IEEE Transactions on*, 25(1):51–66.

Endo, K. and Herr, H. (2009). A model of muscle-tendon function in human walking. In *Robotics and Automation, 2009. ICRA'09. IEEE International Conference on*, pages 1909–1915. IEEE.

Endo, K., Swart, E., and Herr, H. (2009). An artificial gastrocnemius for a transtibial prosthesis. In *Engineering in Medicine and Biology Society*, pages 5034–5037.

Grimmer, M. and Seyfarth, A. (2011). Stiffness adjustment of a series elastic actuator in an ankle-foot prosthesis for walking and running: The trade-off between energy and peak power optimization. In *Robotics and Automation, 2011. ICRA'11. IEEE International Conference on*.

Günther, M., Sholukha, V., Keßler, D., Wank, V., and Blickhan, R. (2003). Dealing with skin motion and wobbling masses in inverse dynamics. *Journal of Mechanics in Medicine and Biology*, 3(3-4):309–335.

Hitt, J., Sugar, T., Holgate, M., Bellman, R., and Hollander, K. (2009). Robotic transtibial prosthesis with biomechanical energy regeneration. *Industrial Robot: An International Journal*, 36(5):441–447.

Hollander, K. and Sugar, T. (2005). Design of the robotic tendon. In *Design of Medical Devices Conference (DMD 2005)*.

Johansson, J., Sherrill, D., Riley, P., Bonato, P., and Herr, H. (2005). A clinical comparison of variable-damping and mechanically passive prosthetic knee devices. *American Journal of Physical Medicine & Rehabilitation*, 84(8):563.

Lipfert, S. (2010). *Kinematic and dynamic similarities between walking and running*. Verlag Dr. Kovac, Hamburg. ISBN: 978-3-8300-5030-8.

Martinez-Villalpando, E. and Herr, H. (2009). Agonist-antagonist active knee prosthesis: A preliminary study in level-ground walking. *J Rehabil Res Dev*, 46:361–374.

Pratt, G. and Williamson, M. (2002). Series elastic actuators. In *Intelligent Robots and Systems 95.'Human Robot Interaction and Cooperative Robots', Proceedings. 1995 IEEE/RSJ International Conference on*, volume 1, pages 399–406. IEEE.

Robbins, C., Vreeman, D., Sothmann, M., Wilson, S., and Oldridge, N. (2009). A review of the long-term health outcomes associated with war-related amputation. *Military medicine*, 174(6):588–592.

Segal, A., Orendurff, M., Klute, G., McDowell, M., Pecoraro, J., Shofer, J., and Czerniecki, J. (2006). Kinematic and kinetic comparisons of transfemoral amputee gait using C-Leg® and Mauch SNS® prosthetic knees. *Journal of rehabilitation research and development*, 43(7):857.

Seroussi, R., Gitter, A., Czerniecki, J., and Weaver, K. (1996). Mechanical work adaptations of above-knee amputee ambulation* 1. *Archives of physical medicine and rehabilitation*, 77(11):1209–1214.

Seyfarth, A., Geyer, H., and Herr, H. (2003). Swing-leg retraction: a simple control model for stable running. *Journal of Experimental Biology*, 206(15):2547–2555.

Sup, F., Varol, H., Mitchell, J., Withrow, T., and Goldfarb, M. (2009). Self-contained powered knee and ankle prosthesis: Initial evaluation on a transfemoral amputee. In *Rehabilitation Robotics, 2009. ICORR 2009. IEEE International Conference on*, pages 638–644. IEEE.

Varol, H., Sup, F., and Goldfarb, M. (2009). Powered sit-to-stand and assistive stand-to-sit framework for a powered transfemoral prosthesis. In *Rehabilitation Robotics, 2009. ICORR 2009. IEEE International Conference on*, pages 645–651. IEEE.

Winter, D. (1983). Moments of force and mechanical power in jogging. *Journal of Biomechanics*, 16(1):91–97.

6 Manuscript IV: Energetic and Peak Power Advantages of Series Elastic Actuators in an Actuated Prosthetic Leg for Walking and Running

Authors:

Martin Grimmer, Mahdy Eslamy and André Seyfarth

Technische Universität Darmstadt

64289 Darmstadt, Germany

Published as a paper in

Actuators, Multidisciplinary Digital Publishing Institute, 2014

6.1 ABSTRACT

A monoarticular series elastic actuator (SEA) reduces energetic and peak power requirements compared to a direct drive (DD) in active prosthetic ankle-foot design. Simulation studies have shown that similar advantages are possible for the knee joint. The aims of this paper were to investigate the advantages of a monoarticular SEA driven hip joint and to quantify energetic benefit of an SEA driven leg (with monoarticular hip, knee and ankle SEAs) assuming that damping (negative power) is passively achieved. The hip SEA provided minor energetic advantages in walking (up to 29%) compared to the knee and the ankle SEA. Reductions in required peak power were observed only for speeds close to preferred walking speed (18 to 27%). No energetic advantages were found in running where a DD achieved the best performance when optimizing for energy. Using an SEA at each leg joint in the sagittal plane reduced positive work by 14 to 39% for walking and by 37 to 75% for running. When using an SEA instead of a DD, the contribution of the three leg joints to doing positive work changed: the knee contributed less, the hip contributed more positive work. For monoarticular SEAs the ankle joint motor did most of the positive work.

Keywords

series elastic actuator, prosthetics, human, walking, running, peak power, energy, joint work

6.2 INTRODUCTION

Powered prosthetics that actively support the amputee in movement tasks require a great battery capacity. While semi active (adjust damping) prosthetics such as the C-Leg (Ottobock) or the Rheo Knee (Ossur) have a runtime of 1 to 2 days the active Power Knee (Ossur) has a runtime of about 5 to 7 hours. Because longer charging intervals will improve amputees quality of life, prolonging runtime should be addressed in the development process. Adding batteries is not feasible due to weight constraints. The favorable approach should be to reduce energy requirements (ER) by improving system efficiency.

In addition to low energy consumption, the capability of the active prosthesis to reproduce human limb movements characterized by high angular acceleration, velocity and torque poses further important design goals. Finding an appropriate motor for mimicking the required joint profiles in prostheses is difficult. Direct drives (including appropriate transmission to comply with velocity and torque requirements) are a major contributor to system mass (Mathijssen et al., 2013). One way to reduce the motor's mass is to increase the mechanical efficiency of e.g. gear boxes or ball screws. Another way to achieve this goal is to reduce motor requirements by introducing elastic structures complementing the motor. For instance, design approaches using springs in series, in parallel or a mixture of both are utilized to exploit elastic recoil and decrease motor peak power requirements. Such bio-inspired solutions mimic the function of muscle fibers (motor), ligaments and tendons (springs). Several prosthetic foot designs based on elastic concepts have been developed (Cherelle et al., 2012; Ferris et al., 2012; Herr and Grabowski, 2012; Hitt et al., 2010; Sup et al., 2009; Suzuki et al., 2011; Zhu et al., 2010). However, complex elastic solutions with limited adaptability can decrease system variability, and solutions utilizing many mechanical parts can increase system weight, cost and failure rate. Hence, a compromise between design complexity to achieve energy and peak power requirements and system variability must be made.

A simple system design for mimicking muscle behavior is using series elastic actuators (SEA, (Pratt and Williamson, 2002)). Calculations for the ankle joint have shown that a linear spring in series (mimicking the Achilles tendon) can reduce energy requirements by 41% and peak power requirements by 69% for walking at normal speed compared to a direct drive (Hollander and Sugar, 2005). To validate the theoretical method, the results of calculations for the motor trajectory and optimal stiffness was included in a prosthetic foot design (Hitt et al., 2010). Walking tests showed that the method successfully overcame motor limitations. In another study, the same method including an SEA at the ankle joint was used for estimating energy and peak power requirements for a range of walking and running speeds (Grimmer and Seyfarth, 2011b). Especially in running high reductions could be identified when comparing SEA and direct drive. Results were almost comparable when using the same theoretical approach for a prosthetic knee (Grimmer and Seyfarth, 2011a). Including a hip SEA did not result in benefits in the sagittal plane (walking at 0.8m/s and 1.2m/s, (Wang et al., 2011)).

The authors of (Grimmer and Seyfarth, 2011a,b) calculated energy requirements as the sum of positive and the absolute of negative motor work and compared their values to those achieved with a direct drive. Negative joint work can be realized by passive damping mechanisms. This technology has been already implemented in several prosthetic knees (e.g., C-Leg or 3R80, Ottobock). The torque required for stopping knee extension before touch-down and for stopping knee flexion after take-off (TO) and after touch-down is generated by the integrated mechanical dampers (Johansson et al., 2005; Segal et al., 2006). When excluding this negative work, reducing energy beyond the values calculated in (Grimmer and Seyfarth, 2011b) and (Grimmer and Seyfarth, 2011a) should be possible. Moreover, during these breaking phases, the motor could also be used to harvest energy for charging the batteries. This approach has been implemented in a orthotic knee (Donelan et al., 2008) for walking and could be applied to further reduce battery requirements.

The current study addressed two specific aims. First, we investigated if energetic and peak power benefits observed for the ankle and knee SEA are also possible for a hip SEA. Energy and peak power requirements were compared between direct drive and SEA driven joints. The combination of an energy (hip, knee) or peak power (ankle) optimized series spring stiffness and motor angle change that best matches biological torque angle profiles was identified.

Second, results on reductions for the ankle (Grimmer and Seyfarth, 2011b) and knee (Grimmer and Seyfarth, 2011a) were combined with novel results for the hip to identify the energetic requirements necessary for an actuated prosthetic or orthotic leg with three degrees of freedom. Energy requirements were calculated for situations with only positive mechanical work. We assumed that negative joint work can be generated by passive dampers.

6.3 METHODS

6.3.1 Model Input Data

Previously collected data (Lipfert, 2010) was used as model input data. Subjects walked (experiment I) and ran (experiments I and II, Tab. 1) on a treadmill with integrated 3D force sensors (Kistler, 1000Hz) and synchronized high-speed infrared cameras (Qualisys, 240Hz). In experiment I, speeds were determined for each subject depending on the preferred transition speed (PTS). The mean PTS for all subjects was 2.07 m/s and represented 100%. Subjects walked and ran at 25, 50, 75, 100 and 125% PTS. In experiment II, subjects ran at fixed speeds of 3 m/s and

4 m/s. Although running speeds below 1.6 m/s are untypical in human gait, slower speeds and running-like motion in place can be performed. To analyze trends and to compare walking and running at the same speed we decided to include running speeds down to 0.5 m/s.

Table 1: Experimental and subject characteristics (mean ± std).

	number of subj.	age [yrs]	body height [m]	body mass [kg]	speeds [m/s]	leg length [m]
Exp. I	21	25.4 ± 2.7	1.73 ± 0.09	70.9 ± 11.7	0.52, 1.04, 1.55,2.07,2.59	0.96 ± 0.08
Exp. II	7	23.7 ± 1.1	1.80 ± 0.10	77.5 ± 8.8	3.0, 4.0	1.02 ± 0.07

For both experiments, hip, knee and ankle angles and corresponding torques (Fig. 1) were calculated from force and camera data (Günther et al., 2003; Lipfert, 2010). Torques were normalized to body mass and a resting leg length of 1 m defined as the distance between the center of mass (COM) and the center of pressure (COP) during stance. Joint angular velocities were calculated by numerical differentiation and multiplied by the torque to obtain reference joint power curves (Fig. 2).

6.3.2 Power and Energy Calculation

Actuator energy and peak power requirements were derived similar to (Grimmer and Seyfarth, 2011b; Hollander and Sugar, 2005). In contrast to previous studies, a rotational SEA model was used to model stiffness independent of geometry and lever arm. The specified motor power represents only the necessary mechanical work and did not include system efficiencies and inertia. It was assumed that the motor needs the same amount of energy for thrusting (positive work) and damping (negative work).

Motor power P_m was calculated as

$$P_m = M_m \cdot \dot{\theta}_m \tag{1}$$

Where M_m is the motor torque and $\dot{\theta}_m$ is the motor angular velocity. M_m is equal to the torsional spring torque M_s, and both are oppose of the external torque M_{ex}. $\dot{\theta}_m$ is the derivative of the motor angle θ_m calculated from total actuator angle θ_g and spring angle θ_s.

$$\theta_m = \theta_g - \theta_s \tag{2}$$

The spring angle was calculated based on the Hooke's law.

$$M_{ex} = K_s \cdot \Delta\theta_s \tag{3}$$

Where K_s is the spring constant. The deflection of the spring Δx_s was calculated by subtracting the instantaneous spring angle θ_s from the spring angle at rest θ_0.

$$\Delta\theta_s = \theta_0 - \theta_s \tag{4}$$

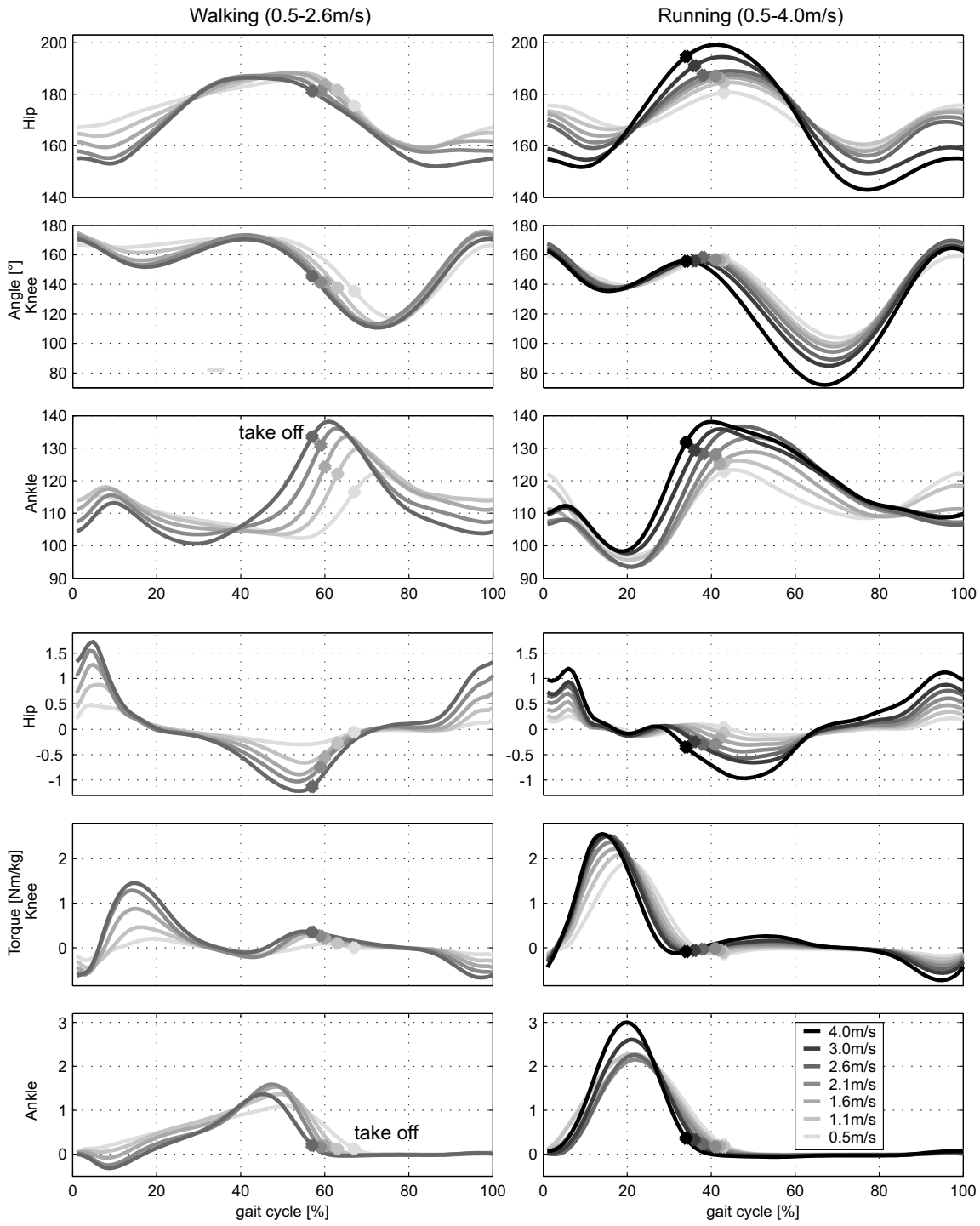

Figure 1: Hip, knee and ankle joint angle and joint torque for a gait cycle of human walking and running (mean of all subjects). Hip angle was calculated between the 7^{th} cervical vertebra, trochanter major and a assumed rotational point at the knee (2 cm proximal of the lateral joint space on the lateral femoral condyle). The knee angle was calculated as the angle between the line connecting the greater trochanter major and the rotational knee point and the line connecting the rotational knee point and the lateral malleolus. The ankle angle was calculated by the rotational point of the knee, the lateral malleolus and the 5^{th} metatarsophalangeal joint of the foot. Light grey lines represent slower speeds starting at 0.5 m/s. The black line represents maximum speed of 4 m/s (only running).

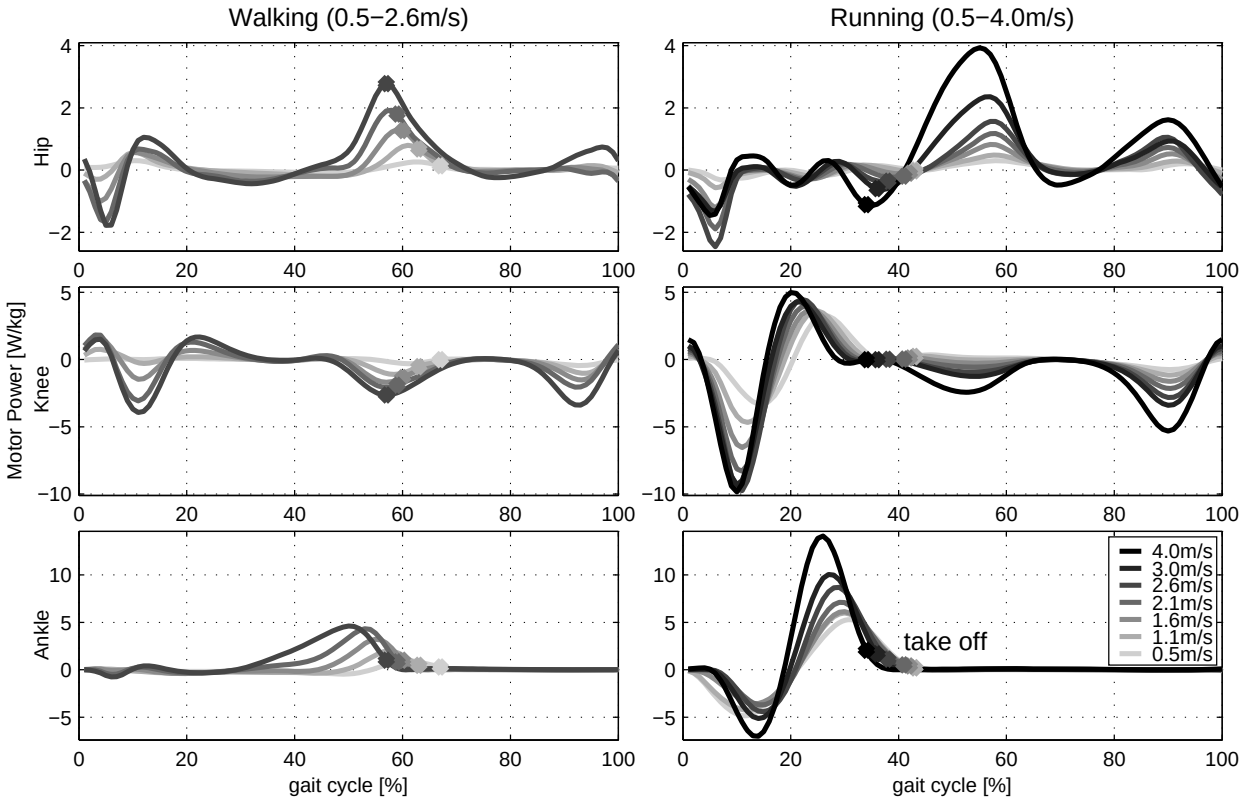

Figure 2: Hip, knee and ankle joint power for a cycle of human walking and running (mean of all subjects). The light grey line represents lower speeds starting at 0.5 m/s. The black line represents maximum speed of 4 m/s (only running). The measured joint power is similar to the power necessary for a direct drive system to mimic the torque angle profile of each joint. These curves were used as a reference for calculating possible reductions in energy and peak power when using an SEA.

Finally the equation for calculating spring angle θ_s is:

$$\theta_s = \theta_0 - \frac{M_{ex}}{K_s} \tag{5}$$

By using θ_s in Eq. 2, motor angle θ_m was calculated.

$$\theta_m = \theta_g + \frac{M_{ex}}{K_s} - \theta_0 \tag{6}$$

The derivation of Eq. 6 results in motor angular velocity $\dot{\theta}_m$.

$$\dot{\theta}_m = \dot{\theta}_g + \frac{\dot{M}_{ex}}{K_s} \tag{7}$$

The final equation for calculating motor power is:

$$P_m = M_m \cdot (\dot{\theta}_g + \frac{\dot{M}_{ex}}{K_s}) \tag{8}$$

In Eq. 8 and the figures no absolute values of motor power were used, to get a better understanding of the mechanical joint and the resulting motor function (thrusting, damping). For calculating the peak power, only absolute values are taken into account. Energy requirement was calculated as the sum of positive and the amount of negative work.

$$ER = E_+ + |E_-| = \int P_+(t)dt + \int P_-(t)dt \tag{9}$$

For the results of section 6.4.2 only positive motor work was considered and the second part of Eq. 9 was not taken into account. Because normalized torques were used, the estimated power and energy requirements were also normalized to body mass. In addition, energy requirements were normalized to distance traveled during the gait cycle representing the cost of transport related to the SEA.

It is important to note that the theoretical SEA model used in this paper can produce torques in both directions representing the function of both extensors and flexors of all three joints.

6.3.3 Finding the optimal stiffness

Optimal spring stiffness values K_s for minimizing energy or peak power requirements were determined by a brute-force search method for each walking and running speed. Stiffness values between 0.01 Nm/(rad·kg) and 100 Nm/(rad·kg) with 0.01 Nm/(rad·kg) increments were included in Eq. 8. Corresponding energy and peak power results were scanned for lowest values. The brute-force search method was used because computations require only some seconds to get a precise result from all possible solutions. Because normalized torque was used as an input, the results were normalized stiffness values (normalized to body mass).

For the hip and knee, joint stiffness was optimized for energy requirements. Grimmer et al. (Grimmer and Seyfarth, 2011b) have shown, that peak power optimization at the ankle results in similar energy requirements as those observed for minimizing energy. In contrast, optimizing for minimal energy results in clearly higher peak power requirements. Hence, the ankle SEA was optimized for peak power to find K_s. Minimum energy requirements and the corresponding peak power values of the SEA motor were compared to those for the direct drive.

6.4 RESULTS

The main results of this theoretical investigation can be found in Fig. 3 and 4. Fig. 3 shows the effect of series elastic elements on energy and peak power requirements for the hip, knee and ankle at various speeds for walking and running. Fig. 4 shows a comparison of positive motor work between SEA and direct drive motors. It was assumed that negative work can be performed by passive dampers. The sum of positive work performed at the hip, knee and ankle was used to investigate energy requirements of the leg in the sagittal plane.

6.4.1 Peak Power and Energy Requirements at Joint Level

Hip

When optimizing the hip SEA for minimum energy, benefits in peak power (18%-27%, Fig. 3) were identified only for speeds close to preferred walking speed (Dal et al., 2010). Peak power was drastically higher for the SEA than for the direct drive at very slow walking speed (172%). In addition, reductions in energy requirements of up to 29% were achieved for walking. For running, no considerable benefits in energy or peak power were found when using an SEA. Optimal stiffness for a hip SEA in running goes to infinity causing the second term of Eq. 8 to become zero. Consequently, $\dot{\theta}_m$ is equal to $\dot{\theta}_g$ resulting in identical power curves for SEA and direct drive motors (Fig. 6).

Knee

The stiffness of the knee SEA was optimized to minimize energy. Energy requirements were lower for the knee SEA compared to the direct drive for all walking (5%-28%) and running (39%-71%) speeds (Fig. 3). Peak power was lower for the SEA at all running speeds (51%-78%). For walking, peak power for the SEA was higher for preferred speeds (8%-11%) and lower for speeds equal or above than PTS (about 29%).

Ankle

The ankle SEA was optimized to minimize peak power. Using an appropriate stiffness reduced peak power by 21% to 68% for the ankle SEA compared to the direct drive for walking and by 70% to 86% for running. In addition, energy requirements were lower for the ankle SEA than the direct drive for all walking (3%-52%) and running speeds (56%-87%, (Fig. 3)).

6.4.2 Positive Sagittal Leg Work

Direct Drive

Positive work increased with increasing walking speed (0.32-0.55 J/(kg·m)). For running, positive work decreased with increasing speeds up to 2.6 m/s (2.04-0.66 J/(kg·m)) and increased slightly for speeds beyond (Fig. 4).

The main contribution to the required energy was generated by the ankle joint (47%-61%). For walking, the hip was a more important energy source than the knee, especially at lower and higher speeds. In contrast for running, the knee was a more important energy source than the hip for speeds up to 2.6 m/s while the hip played an increasingly role for speeds exceeding 2.6 m/s (Fig. 4).

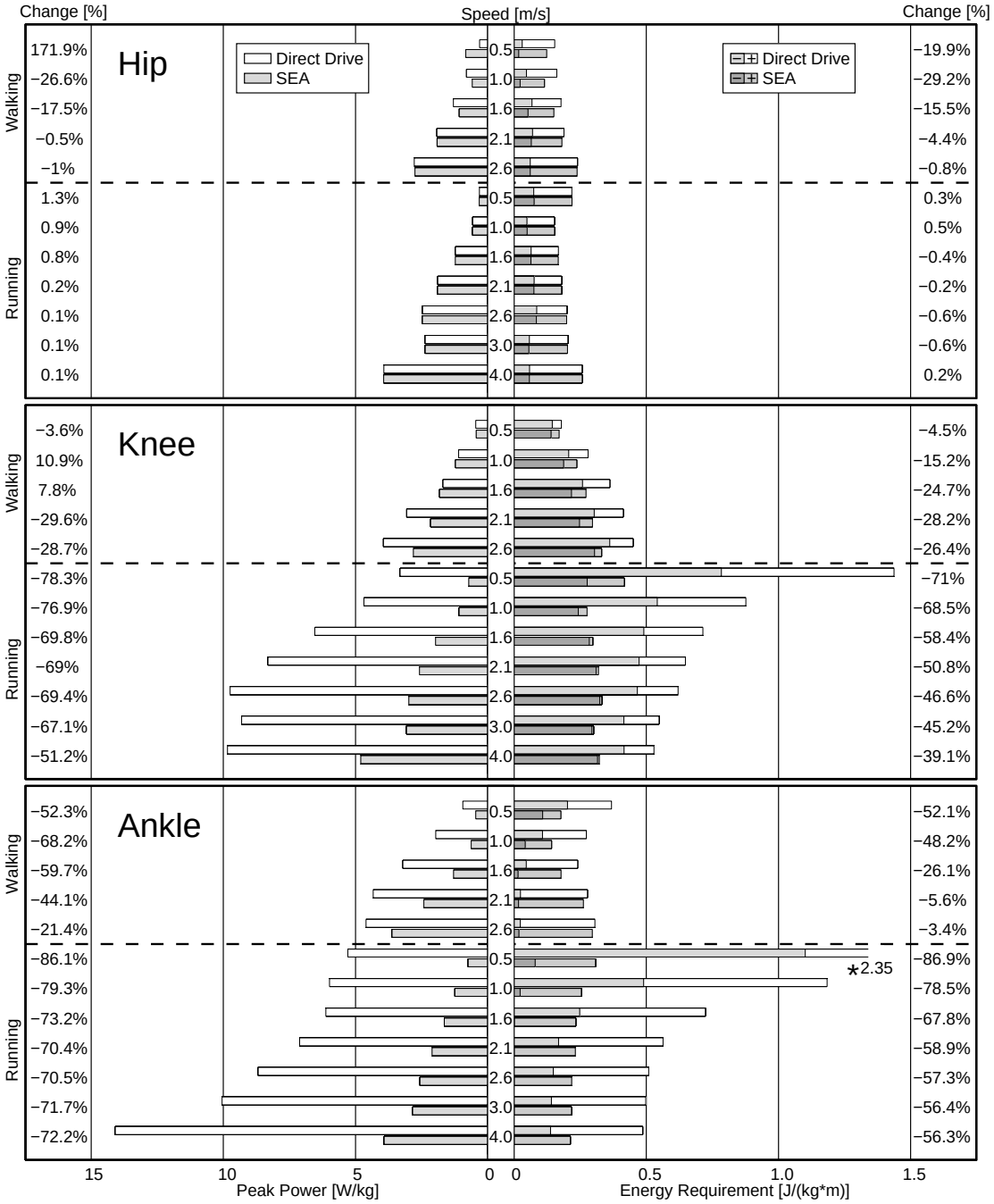

Figure 3: Hip, knee and ankle joint peak power (left side) and energy requirements (right side) for different walking and running speeds for SEAs and direct drives. SEA spring stiffness was optimized to minimize energy requirements at the hip and the knee. At the ankle, spring stiffness was optimized to minimize peak power. The amount of negative work is shown as darker parts of the energy requirement bars, and the amount of positive work is shown as lighter parts of the energy requirement bars. The outer columns list the difference in energy and peak power requirements between the SEA and the direct drive (SEA/DD*100; in percent). The middle column lists the corresponding walking or running speeds.

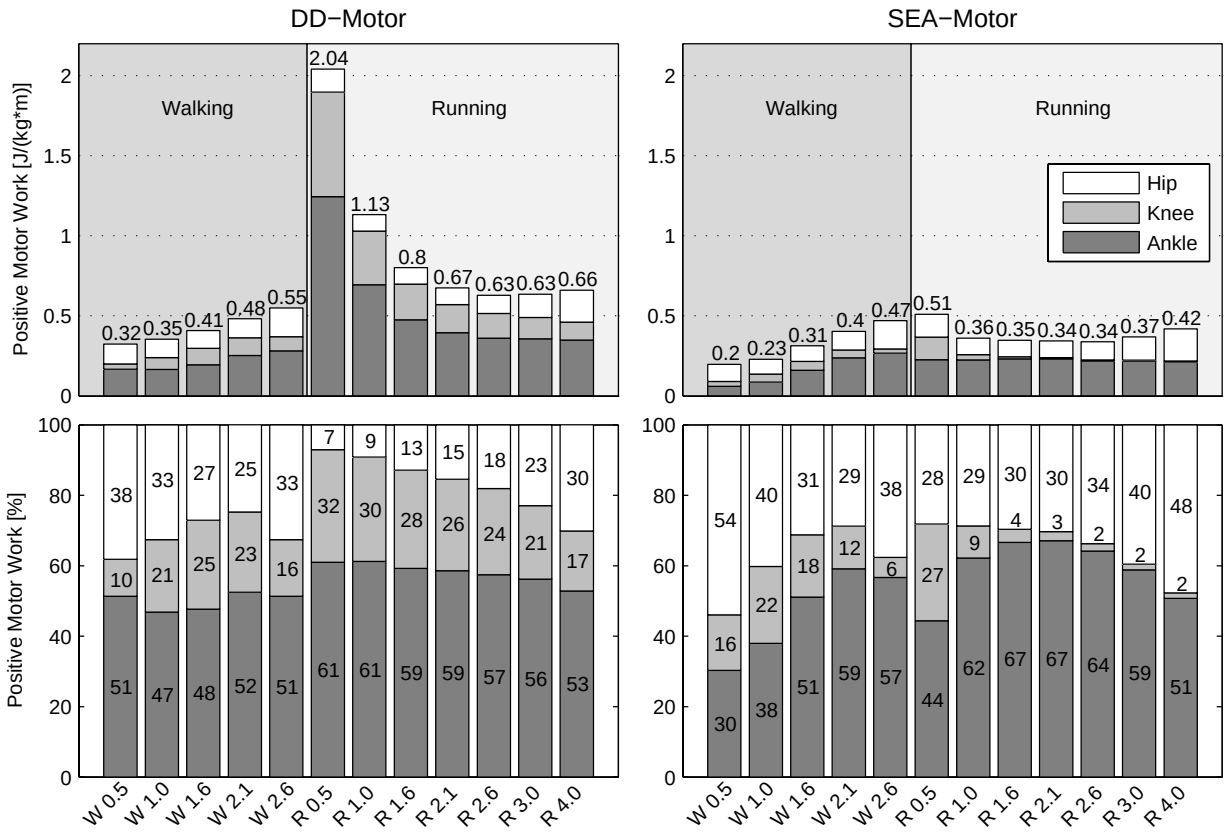

Figure 4: Absolute (top) and relative (bottom) positive motor work for a direct drive (DD, left) driven leg (hip, knee and ankle) compared to a series elastic actuator (SEA, right) driven leg for mimicking walking (W 0.5 m/s - W 2.6 m/s) and running (R 0.5 m/s - R 4.0 m/s). The preferred transition speed (PTS) where subjects typically change gait between walking and running was 2.1 m/s. Note that for some speeds, the total positive motor work does not add up to 100% because relative motor work values were rounded to integers.

Series Elastic Actuator

Compared to a direct drive, the total required positive motor work was lower for the SEA driven joints (14% to 39% walking) especially for running (37% to 75%, Fig. 4). For both walking and running, the differences in total required work between the SEA and the direct drive decreased with increasing speed. The main reduction in total required work for the SEA compared to the direct drive was observed at the ankle and knee. With an SEA knee, no positive work was required for running. The ratio for providing overall positive leg work increases drastically for the hip joint.

Beyond the preferred transition speed (PTS, 2.1 m/s), less positive work was required for running (0.34 J/(kg·m)) than for walking (0.4 J/(kg·m), Fig. 4).

6.4.3 Stiffness

For walking, hip SEA stiffness increased with speed (optimized to minimize energy, Tab. 2). Least energy consumption at highest walking and all running speeds was achieved using a rigid direct drive hip.

At the knee, joint stiffness increased with increasing walking speed above 0.5 m/s (optimized to minimize energy requirements). For running, joint stiffness decreased with increasing speeds up to 1.6 m/s and increased for speeds beyond 1.6 m/s up to 4 m/s.

At the ankle, joint stiffness increased with increasing speeds for walking (above 0.5 m/s) and running (optimized to minimize peak power). Compared to walking, joint stiffness remained relatively constant across running speeds.

Table 2: Predicted optimal SEA stiffness values K_r (Nm/(deg·kg)) for minimizing peak power at the ankle and minimizing energy requirements at the knee and the hip (Fig. 3) for walking and running at a wide range of speeds. Rotational stiffness values were normalized to body mass.

Gait	Walking					Running						
Speed [m/s]	0.5	1.0	1.6	2.1	2.6	0.5	1.0	1.6	2.1	2.6	3.0	4.0
Hip	.0712	.1817	.4238	.9821	rigid	rigid	rigid	rigid	rigid	rigid	rigid	rigid
Knee	.1848	.0873	.1058	.1215	.1274	.137	.1223	.1159	.1234	.1292	.141	.1508
Ankle	.1136	.0857	.1208	.1822	.2536	.0887	.0929	.0937	.0941	.0946	.1152	.1239

6.5 DISCUSSION

In this study, we estimated the reduction in motor requirements for monoarticular SEAs compared to direct drives at the hip, knee and ankle during walking and running. While large energy and peak power benefits were identified for the ankle and the knee, for the hip smaller benefits were observed for walking and none for running. Wang et al. (Wang et al., 2011) reported peak power reductions of up to 79% for slow to preferred walking speeds for a series spring at the ankle, which are higher than reductions predicted in our calculations (68%). Similar to our results, Wang et al. found no peak power benefits at the knee at these speeds. In contrast to our findings (27% reduction), no benefits in peak power at the hip were identified around preferred walking speed (Wang et al., 2011). Moreover, Wang et al. observed peak power benefits at the hip of up to 60% for abduction and adduction. Because both methods are similar, the observed differences are likely mainly caused by differences in the torque and angle input data. In our study, we observed large differences between subjects (see subsection 6.5.3), and hence it is possible that the differences in results between our study and Wang et al. are caused by differences in study cohorts (Wang et al., N=8 subjects; 24 yrs, 1.8 m, 69 kg).

6.5.1 Reason for the SEA benefits

Interestingly, peak power and energy requirements were not reduced by tuning the SEA spring at the hip at any running speed. In contrast to the ankle, for walking none or small reductions were observed for the hip and the knee. Especially running largely benefits from a serial spring at the knee and the ankle joint. Motor power is the product of required motor torque and motor velocity, and hence at least one of the parameters must be reduced to increase system efficiency. As discussed by Grimmer et al. (Grimmer et al., 2012), motor torque can be reduced by a parallel spring and motor velocity can be reduced by a series spring. Reductions in motor velocity are

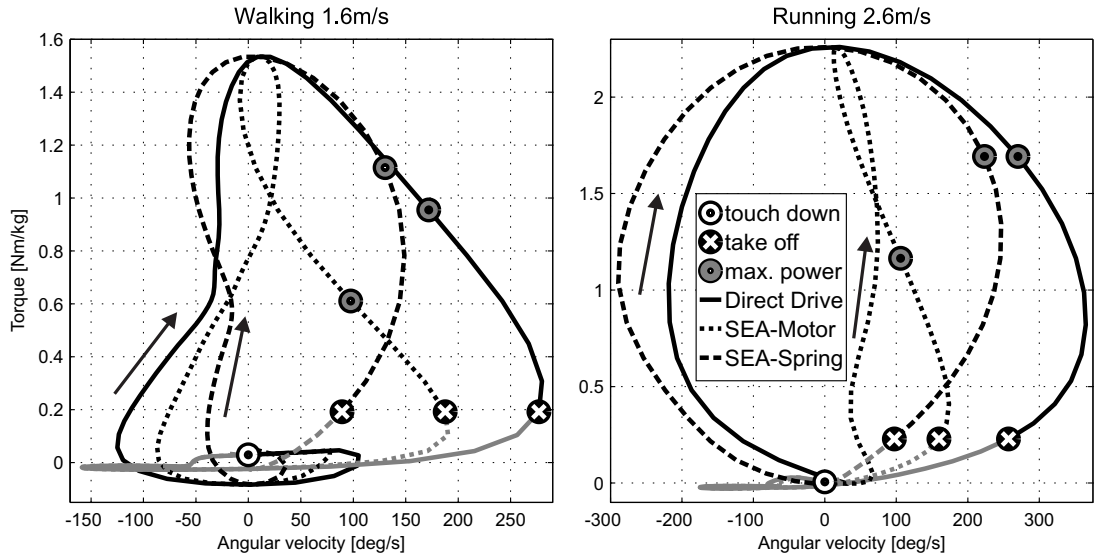

Figure 5: Ankle torque - angular velocity curves for walking at 1.6 m/s and running at 2.6m/s. The solid line represents human data, which is similar to that for a direct drive. The dotted line represents data for the SEA motor and the dashed line data for the SEA spring. Stance phase is indicated by a black line and flight phase by a grey line. Stance phase starts with touch down and ends with take off. Maximum power during push off is indicated for each case. Arrows indicate the path direction during the gait cycle. The series spring helps to reduce motor velocity resulting in lower peak power.

shown in Fig. 5 for an SEA at the ankle. Because the spring generates some of the joint rotation, the motor has a smaller range of motion to match joint torque-angle curves and motor velocity decreases. Using this effect, peak power and energy requirements can be reduced for the SEA motor as shown in Fig. 6. Both parameters benefit from the elastic properties of the spring: energy can be stored and released by spring deflection. For instance, for the ankle for walking, the spring is elongated between 30% and 50% of the gait cycle. Energy is saved in the spring to be released during push off to support the motor. Similar effects can be identified for the knee and the hip for walking. For running, only the ankle and the knee benefit from using a series spring.

The largest reductions in motor peak power and energy requirements are achieved when the series spring stiffness matches the slope of the torque-angle curves. The results of our optimization showed that stiffness values were within the ascending and descending parts of the torque-angle profiles (dashed lines, Fig. 7). For example, for running the ankle torque increases and ankle angle decreases in the first 20% of the gait cycle. During this phase, the spring is loaded which can be also observed for the power curves (Fig. 6). The opposite happens from 20% to 40% of the gait cycle where the torque decreases and the angle increases and the spring is unloaded and releases the energy for push off.

The stiffness results show that optimal joint stiffness can be approximated by estimating the mean slope of the joint torque-angle profile during the stance phase as illustrated by the dashed lines in Fig. 7. This stiffness closely resembles the smallest peak power and energy requirements. In contrast to an approximation, the optimization method used in our study provided a more accurate stiffness value because it is optimized for a selected criteria such as peak power or energy requirement.

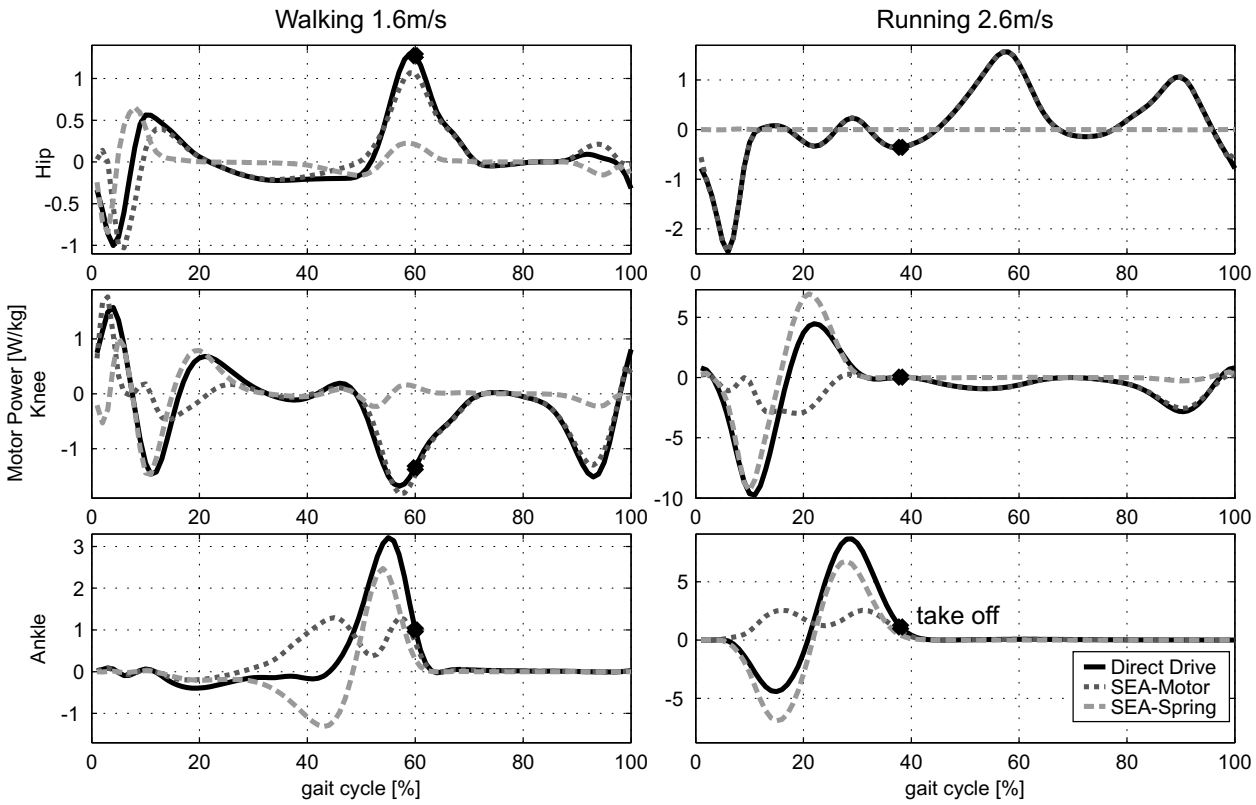

Figure 6: Hip, knee and ankle power for the gait cycle in human walking at 1.6 m/s and running at 2.6 m/s (mean of all subjects). The power is shown for the direct drive (black solid) and when an SEA drives the joint. For the latter, power is shared between SEA motor (dark grey dotted) and SEA spring (light grey dashed). The combination of the SEA motor and the SEA spring matches the direct drive situation. For the hip for running a rigid system without a spring requires the least energy. As a result the SEA motor matches direct drive behavior.

The brute-force method scanned only the positive stiffness region. However, we also identified optimal negative solutions for K for settings where a rigid system provided the best performance in the positive region (Tab. 2). While a spring with positive stiffness will first store the energy and release it later (Fig. 8), a spring with negative stiffness would first release the energy to the system and subsequently energy is required to return it to the original state. Because latter behavior is not realistic for a simple SEA, all negative stiffness solutions were not included in this investigation.

We believe that the mechanism of releasing energy first and subsequently returning it back may be realized through joint coupling. For instance, biarticular springs could be loaded by the knee, and this energy could be transferred to the hip. Hence, a resultant torque at the hip may behave similar to a spring with negative stiffness.

In addition to biarticular structures, non-linear elastic behavior, which is also found in nature, may contibute to the system's efficiency. Non-linear elastic behavior could be implemented by changing the length of the lever arm or introducing non-linear stiffness. A progressive spring behavior could help to use the same design (no tuning of stiffness) for mimicking speed dependent increases in optimal stiffness values identified for walking and running at all three joints (Tab. 2).

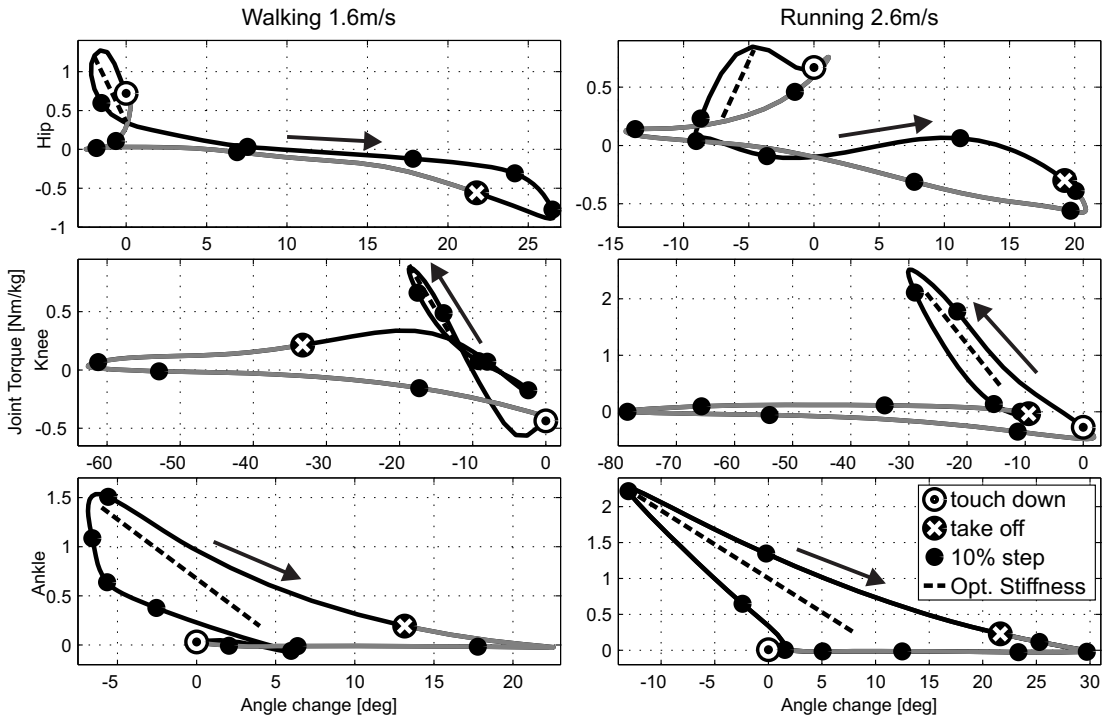

Figure 7: Hip, knee and ankle torque-angle curves for human walking at 1.6 m/s and running at 2.6 m/s (mean of all subjects). Arrows indicate the path direction during the gait cycle. The stance phase is shown in black and the swing phase is shown in grey. Touch down and take off are indicated by a big dot. Small dots characterize time increments of 10% gait cycle starting at touch down. The dashed line represents the slope of the optimal series stiffness listed in Tab. 2.

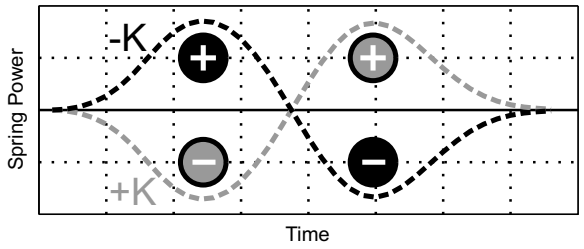

Figure 8: Power curves for positive (+K) and negative (-K) stiffness when a load is applied. Because negative stiffness can not be realized by an SEA, corresponding results were neglected. In these cases, a rigid direct drive resulted in the smallest energetic requirements (Tab. 2).

6.5.2 Positive Leg Work

The distribution of positive work necessary for driving the leg joints changes when using an SEA instead of a direct drive. Compared to the literature (Farris and Sawicki, 2012) our results for the direct drive indicate a smaller influence of the hip and greater influence of the ankle on positive work (about 10% for walking and running). Although Farris et al. (Farris and Sawicki, 2012) only analyzed speeds above 2 m/s, their data shows that with increasing running speed

the ankle and knee become less important contributors of positive energy and the hip becomes an increasingly important contributor of positive energy (32% at 2 m/s to 39% at 3.25 m/s).

Farris et al. (Farris and Sawicki, 2012) proposed in vivo studies to distinguish between the positive work done by the muscle fascicles and the positive work done by the tendons. Our approach may represent an alternative approach for estimating possible effects of work performed by the tendons. SEAs require up to 75% less absolute positive work than direct drives (Fig. 4).

In our model, all the elastic actuators are monoarticular. We assume that biarticular SEAs can further decrease positive work provided by motors, which is supported by simulations that use similar structures in principle (Van Den Bogert, 2003) and with a muscle-like arrangement (Sasaki et al., 2009).

For running with SEA the knee requires almost no positive work indicating that a damping mechanism combined with a spring can provide nearly all the work required for mimicking the knee torque angle behavior.

We observed an interesting phenomenon for the positive work at preferred transition speed (PTS) of 2.1 m/s. For direct drives running required more positive work than walking at all speeds (Fig. 4). However, for the SEAs, a change happens at PTS where running needs less positive mechanical energy than walking. This behavior was also observed for the total mechanical work of ankle and knee (Fig. 3). A similar phenomenon has been previously observed in oxygen consumption experiments (Hreljac et al., 2002) and for more complex humanoid models (Sasaki and Neptune, 2006). Hence, in agreement to (Sasaki and Neptune, 2006) the results of our study suggest that muscle mechanical energy expenditure may not be the only determinant but it could be one important determinant for the preferred gait mode at a given speed.

6.5.3 Sensitivity of results

Requirements for the joints were calculated from mean joint angle and mean joint torque data of up to 21 subjects (grand mean). For single subject mean torque and mean angle curves, an individual optimal K for minimizing peak power and energy requirements can be calculated. Exemplary results for the ankle of the 21 subject are presented in (Fig. 9). Similar results can be obtained for the knee and the hip. In the worst case, individual peak power at the ankle was more than twice (231%) the grand mean. Corresponding standard deviation (STD) for peak power was approximately 32% for walking at 1.6 m/s and approximately 27% for running at 2.6 m/s. The corresponding energy requirements could increase to approximately 145% (STD 18% for walking and running). In addition, stiffness varied between subjects, and the STD for optimal stiffnesses was 29% for walking and 16% for running.

The large STD of the overall mean stiffness indicates that peak power and energy requirements may be rather high for some amputees when using it. The V-shape of the power-stiffness curve compared to the energy-stiffness curve (Fig. 9) suggests that especially for running energy requirement is less sensitive to a suboptimal stiffness than peak power. Both energy and peak power are more sensitive to below than to above optimal stiffness values.

The predicted optimal SEA stiffness values (Tab. 2) depended on speed and gait. A simple mechanism suitable for all speeds for walking and running should ensure a constant stiffness. Grimmer et al. (Grimmer and Seyfarth, 2011b) showed how a constant stiffness influences peak power and energy requirements at the ankle and identified an optimal configuration that entailed only minor increases in peak power and energy requirements. Similar results have been reported for the knee (Grimmer and Seyfarth, 2011a).

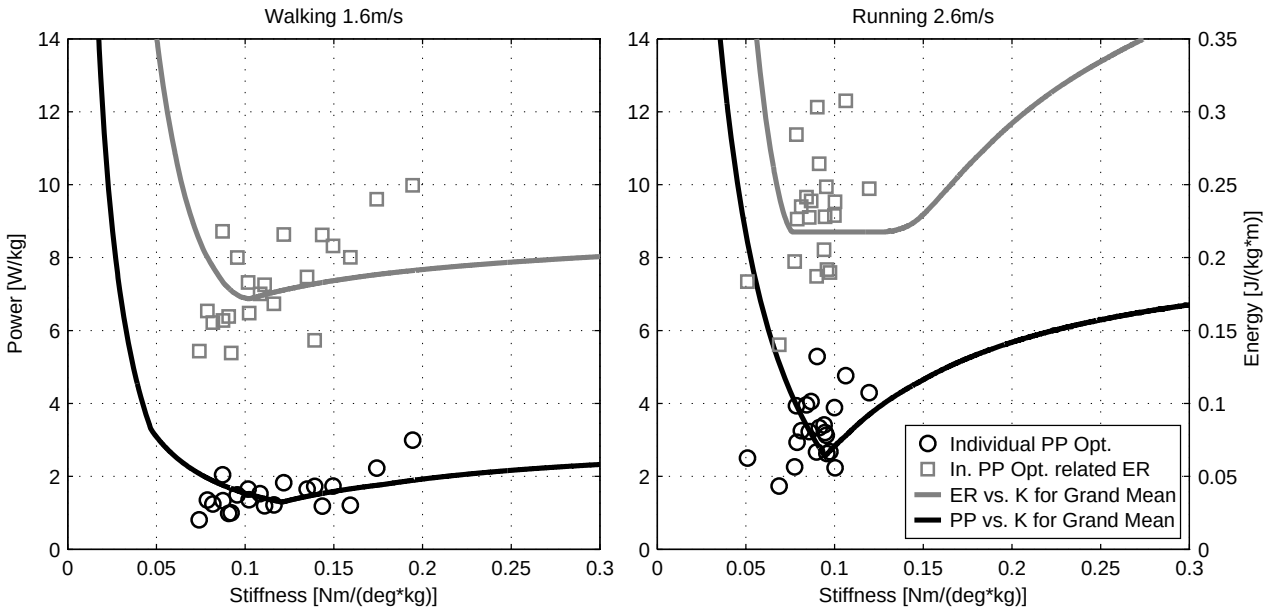

Figure 9: Peak power (black) and energy requirements (grey) in relation to spring stiffness K for walking at 1.6 m/s (left) and running at 2.6 m/s (right). The solid curves represent the values represent values for mean joint angle and mean joint torque as an input (21 subjects; grand mean). Single subject torque and angle curves were used to identify individual peak power optimum (small circles) and related stiffness. Corresponding individual energy requirement is indicated by a grey rectangle. In the worst case, peak power is more than two times the grand mean (231%) and energy requirement is up to 145% of the grand mean.

For powered prosthetic prototypes (Au et al., 2007; Sup et al., 2008) mean values of joint torque and joint angle are used to estimate required stiffness. Various studies (Ferris et al., 2012; Hitt et al., 2010) have shown remarkable gait performances using these values. We believe that performance could be further improved when using stiffness values optimized to individuals. Further investigating this paradigm would require a prosthetic foot design with changeable stiffness and a learning algorithm. Optimization criteria for the learning procedure could be leg symmetry to the healthy side combined with peak power or energy requirements. Joint behavior of the healthy side could be measured with sensors placed on a brace.

6.5.4 Methodological Considerations

For the results presented in Fig. 3, absolute peak power was minimized. By using a damping mechanism, only the peak power resulting from positive work should be considered. Especially at the knee this approach can change the peak power results dramatically.

Net joint torques shown in Fig. 1 may result from activation of antagonistic muscles which would lead to a systematic underestimation of energy comparing our results with values for human locomotion (Sasaki et al., 2009).

While in this paper we only considered the mechanical energy, the efficiency of the motor and the power train must be included for estimating the electrical energy. System characteristics including frictional losses, damping, heat, structural deflection and other power losses (Hitt et al., 2010) that are not considered will influence the estimation in addition. Depending on

the type of gait, motor speed and motor efficiency will change. A more detailed motor and mechanical system model and experimental results on powered prosthetics are required to make valid energetic predictions. As every prosthetic system uses different mechanical parts, gears and motors electrical requirements will be very design specific. The mechanical data presented in this work gives a good hint to what is possible for both gaits at various speed when using a series spring to assist the motor at the hip, knee and ankle joint.

6.6 CONCLUSIONS

In this paper we investigated the amount of reductions in energy and peak power requirements at the hip, knee and ankle for walking and running at various speeds with monoarticular series elastic actuators (SEAs) compared to a direct drive system. Large reductions in peak power and energy requirements were observed at the ankle. At the knee, comparable reductions were only observed for running. For walking, energy reductions were much smaller and peak power did not change at preferred speeds. At the hip, an SEA reduced energy requirements for all and peak power around preferred walking speeds. For running, there were no reductions. Based on these results, we recommend the use of elastic elements in artificial foot prostheses and for running a spring should be considered at the knee. In walking, including a series elastic spring at the knee and the hip would decrease energy requirements. In addition to the analyzed parameters, elastic structures may increase gait robustness to uneven terrain or sudden changes in ground. Also if the benefits in energy or peak power requirements are small, this could be a reason to consider the elastic structures for the system design.

When using an SEA instead of a direct drive, an interchange of providing positive work by the three leg joints was identified: the contribution of the knee decreased and the contribution of the hip increased. For monoarticular SEAs, the ankle motor generates most of the positive work. We assume that biarticular structures could shift the main contribution proximal towards the hip by coupling joints similar to what is achieved by human muscles. It is possible that the lack of these structures in our design resulted in small benefits in peak power and energy requirements with a monoarticular SEA at the hip. Hence, this inter-joint coupling should be considered in an extended analysis of leg function in human walking and running. Anticipated reductions in peak power and energy requirements could lead to advanced designs of prosthetic systems utilizing both monoarticular and biarticular SEAs. This concept could be realized with a prosthetic device extended by an orthosis to couple the intact joints via biarticular structures to the replaced joints in the prosthesis, resulting in a hybrid ortho-prosthesis.

6.7 ACKNOWLEDGMENTS

This work was supported by the DFG grant SE1042/8. The authors acknowledge S.W. Lipfert for providing human data.

6.8 AUTHOR CONTRIBUTIONS

Martin Grimmer is the main author of the article. He was responsible for the conception and design, analysis and interpretation of data and writing of the manuscript. Mahdy Eslamy was contributing on methodological questions, to the discussion of the results and for the revision of the article. André Seyfarth assisted for the revision of the article.

6.9 CONFLICT OF INTEREST

The authors declare no conflict of interest.

6.10 REFERENCES

Au, S. K., Herr, H., Weber, J., and Martinez-Villalpando, E. C. (2007). Powered ankle-foot prosthesis for the improvement of amputee ambulation. In *Engineering in Medicine and Biology Society, 2007. EMBS 2007. 29th Annual International Conference of the IEEE*, pages 3020–3026. IEEE.

Cherelle, P., Matthys, A., Grosu, V., Vanderborght, B., and Lefeber, D. (2012). The AMP-Foot 2.0: Mimicking intact ankle behavior with a powered transtibial prosthesis. In *4th IEEE RAS & EMBS International Conference on Biomedical Robotics and Biomechatronics (BioRob)*, pages 544–549. IEEE.

Dal, U., Erdogan, T., Resitoglu, B., and Beydagi, H. (2010). Determination of preferred walking speed on treadmill may lead to high oxygen cost on treadmill walking. *Gait & posture*, 31(3):366–369.

Donelan, J., Li, Q., Naing, V., Hoffer, J., Weber, D., and Kuo, A. (2008). Biomechanical energy harvesting: generating electricity during walking with minimal user effort. *Science*, 319(5864):807–810.

Farris, D. and Sawicki, G. (2012). The mechanics and energetics of human walking and running: a joint level perspective. *Journal of The Royal Society Interface*, 9(66):110–118.

Ferris, A. E., Aldridge, J. M., Rábago, C. A., and Wilken, J. M. (2012). Evaluation of a powered ankle-foot prosthetic system during walking. *Archives of physical medicine and rehabilitation*, 93(11):1911–1918.

Grimmer, M., Eslamy, M., Gliech, S., and Seyfarth, A. (2012). A comparison of parallel-and series elastic elements in an actuator for mimicking human ankle joint in walking and running. In *Robotics and Automation (ICRA), 2012 IEEE International Conference on*, pages 2463–2470. IEEE.

Grimmer, M. and Seyfarth, A. (2011a). Stiffness adjustment of a series elastic actuator in a knee prosthesis for walking and running: The trade-off between energy and peak power optimization. In *IEEE/RSJ International Conference on Intelligent Robots and Systems (IROS)*, pages 1811–1816. IEEE.

Grimmer, M. and Seyfarth, A. (2011b). Stiffness adjustment of a series elastic actuator in an ankle-foot prosthesis for walking and running: The trade-off between energy and peak power optimization. In *IEEE International Conference on Robotics and Automation (ICRA)*, pages 1439–1444. IEEE.

Günther, M., Sholukha, V., Keßler, D., Wank, V., and Blickhan, R. (2003). Dealing with skin motion and wobbling masses in inverse dynamics. *Journal of Mechanics in Medicine and Biology*, 3(3-4):309–335.

Herr, H. and Grabowski, A. (2012). Bionic ankle–foot prosthesis normalizes walking gait for persons with leg amputation. *Proceedings of the Royal Society B: Biological Sciences*, 279(1728):457–464.

Hitt, J., Sugar, T., Holgate, M., and Bellman, R. (2010). An active foot-ankle prosthesis with biomechanical energy regeneration. *Journal of Medical Devices*, 4:011003.

Hollander, K. and Sugar, T. (2005). Design of the robotic tendon. In *Design of Medical Devices Conference (DMD)*.

Hreljac, A., Parker, D., Quintana, R., Abdala, E., Patterson, K., and Sison, M. (2002). Energetics and perceived exertion of low speed running and high speed walking. *Facta Universitatis Series: Physical Education and Sport*, 1(9):27–35.

Johansson, J., Sherrill, D., Riley, P., Bonato, P., and Herr, H. (2005). A clinical comparison of variable-damping and mechanically passive prosthetic knee devices. *American Journal of Physical Medicine & Rehabilitation*, 84(8):563.

Lipfert, S. (2010). *Kinematic and dynamic similarities between walking and running*. Verlag Dr. Kovac, Hamburg. ISBN: 978-3-8300-5030-8.

Mathijssen, G., Cherelle, P., Lefeber, D., and Vanderborght, B. (2013). Concept of a series-parallel elastic actuator for a powered transtibial prosthesis. In *Actuators*, volume 2, pages 59–73. Multidisciplinary Digital Publishing Institute.

Ossur (2013). *www.ossur.com*.

Ottobock (2013). *www.ottobock.com*.

Pratt, G. and Williamson, M. (2002). Series elastic actuators. In *IEEE/RSJ International Conference on Intelligent Robots and Systems 95.'Human Robot Interaction and Cooperative Robots',Proceedings. 1995*, volume 1, pages 399–406. IEEE.

Sasaki, K. and Neptune, R. (2006). Muscle mechanical work and elastic energy utilization during walking and running near the preferred gait transition speed. *Gait & posture*, 23(3):383–390.

Sasaki, K., Neptune, R., and Kautz, S. (2009). The relationships between muscle, external, internal and joint mechanical work during normal walking. *Journal of Experimental Biology*, 212(5):738–744.

Segal, A., Orendurff, M., Klute, G., McDowell, M., Pecoraro, J., Shofer, J., and Czerniecki, J. (2006). Kinematic and kinetic comparisons of transfemoral amputee gait using C-Leg® and Mauch SNS® prosthetic knees. *Journal of rehabilitation research and development*, 43(7):857.

Sup, F., Varol, H., Mitchell, J., Withrow, T., and Goldfarb, M. (2009). Self-contained powered knee and ankle prosthesis: Initial evaluation on a transfemoral amputee. In *IEEE International Conference on Rehabilitation Robotics (ICORR)*, pages 638–644. IEEE.

Sup, F., Varol, H. A., Mitchell, J., Withrow, T., and Goldfarb, M. (2008). Design and control of an active electrical knee and ankle prosthesis. In *Biomedical Robotics and Biomechatronics, 2008. BioRob 2008. 2nd IEEE RAS & EMBS International Conference on*, pages 523–528. IEEE.

Suzuki, R., Sawada, T., Kobayashi, N., and Hofer, E. (2011). Control method for powered ankle prosthesis via internal model control design. In *International Conference on Mechatronics and Automation (ICMA)*, pages 237–242. IEEE.

Van Den Bogert, A. (2003). Exotendons for assistance of human locomotion. *Biomedical engineering online*, 2(17).

Wang, S., van Dijk, W., and van der Kooij, H. (2011). Spring uses in exoskeleton actuation design. In *IEEE International Conference on Rehabilitation Robotics (ICORR)*, pages 1–6. IEEE.

Zhu, J., Wang, Q., and Wang, L. (2010). Pantoe 1: Biomechanical design of powered ankle-foot prosthesis with compliant joints and segmented foot. In *IEEE/ASME International Conference on Advanced Intelligent Mechatronics (AIM)*, pages 31–36. IEEE.

7 Manuscript V: A powered prosthetic ankle joint for walking and running

Authors:

Martin Grimmer, Matthew Holgate, Robert Holgate, Alexander Boehler, Jeff Ward, Kevin Hollander, Thomas Sugar and André Seyfarth

Technische Universität Darmstadt

64289 Darmstadt, Germany

Submitted for publication in 2014

7.1 ABSTRACT

Current prosthetic ankle joints are either designed for walking or for running. With the aid of the powered prosthetic ankles, both walking and running can be done with the same device. In order to mimic the capabilities of a healthy ankle, a powered prosthetic ankle for walking and running was designed. In addition, a controller capable of transitions between standing, walking, and running with speed adaptations was developed. In a first test the system was mounted on an ankle bypass in parallel with the foot of a healthy subject. By this method the functionality of the hardware and the controller was proven. The Walk-Run ankle was capable of mimicking desired torque and angle trajectories in walking and running up to 2.6 m/s. At 4 m/s running, ankle angle could be matched while ankle torque could not. Limited motor power resulting from a suboptimal spring stiffness value was identfied as the main reason that torque could not be matched.

Keywords
prosthesis, walking, running, ankle, power, joint

7.2 INTRODUCTION

The current standard for prosthetic ankle joints are passive SACH (solid ankle cushioned heel) or carbon fiber ESAR (energy storage and return) feet. In contrast to the stiff SACH feet, ESAR feet are able to store energy during the stance phase and release it later during the push-off (Gitter et al., 1991; Czerniecki et al., 1991). By this they are able to mimic the function of the Achilles tendon (Farris and Sawicki, 2012). In contrast to the human muscles, carbon feet are not able to create net positive work for ankle plantar or dorsiflexion. To achieve healthy ankle behavior in the prosthetic ankles, actuation systems are required. Different approaches with pneumatics (Versluys et al., 2009) and electric motors (Cherelle et al., 2012; Ferris et al., 2012; Herr and Grabowski, 2012; Hitt et al., 2010; Sup et al., 2009; Suzuki et al., 2011; Zhu et al., 2010) have been developed during the last years. In order to support amputees in common daily life activities like walking on flat terrain (Ferris et al., 2012), stairs (Aldridge et al., 2012) or slopes (Sup et al., 2011), these activities were investigated and implemented in the active ankle joints.

In addition to the daily life movement requirements the amputees want to participate in social activities like sports. Cycling, swimming and running are some possible sportive activities, while running also being fundamental to multiple activities such as ball games. Some special prosthetic solutions for different sports have been designed (Bragaru et al., 2012; Radocy, 1987; Webster et al., 2001) such as waterproofed legs and arms for swimming, special programmable cycling or skiing modes for electronic controlled knee joints (C-Leg, Otto Bock) or also running and sprinting prostheses. As limited range of motion (ROM) of the existing prosthetic feet used for daily life make it hard to run, amputees now have to change prosthesis to perform running. The ankle prosthesis designs for running have no heel element to make it possible to roll over the foot, resulting in a gait similar to forefoot running. The missing heel element increases effort for standing and other tasks of daily life and therefore makes the feed designed for running less appropriate for the daily usage.

A powered prosthesis is not limited in ROM as it is able to inject energy to provide required plantarflexion and dorsiflexion. To inject the energy sufficient motor power especially for higher walking and running speeds would be required (Grimmer et al., 2014). Calculations show that

different arrangements of elastic elements can decrease these requirements, especially in running gait (Eslamy et al., 2012; Grimmer et al., 2012). When considering the assisting effect of a series elastic actuator (SEA) to mimic the ankle joint function, about 0.6 W/kg to 1.3 W/kg mechanical peak power should be provided for normal walking (1.1 m/s - 1.6 m/s) and 2.6 W/kg to 2.8 W/kg (Grimmer et al., 2014) for medium marathon running speeds of 2.6 m/s - 3 m/s (Leyk et al., 2007). A running speed of 4 m/s would require four times (3.9 W/kg) the peak power of the preferred walking speed.

Along with reduced power demands, the elastic elements can also reduce the energy requirements. Walking requires about 0.14 J/(kg·m) to 0.18 J/(kg·m) (1.1 m/s - 1.6 m/s) and running about 0.22 J/(kg·m) (2.6 m/s, 3 m/s and 4 m/s) (Grimmer et al., 2014) when using a series spring. This is an increase of about 22% to 57%. The system design should be adapted to these increased requirements for running.

In addition to the power and the energetic requirements, the control needs an adaptation to distinguish between walking and running as well as a measure of the desired speed. This could be critical when amputees want to run below or walk above preferred transition speed (2.1 m/s, PTS, (Lipfert, 2010)). Transitions from walking to running and running to walking must be realized quickly to support accelerating or decelerating during the transition process. Also, the transition between movement and standing is critical for the safety.

To investigate these topics, a powered prosthetic ankle was designed to be capable of walking and medium speed running. A controller to change between standing, walking, and running with speed adaptation was developed. For a first proof of concept the system was evaluated with one able bodied subject using a bypass system that is in parallel to the fixed healthy foot. Results are compared to healthy subject data and the corresponding prosthetic model estimations.

7.3 METHODS

7.3.1 Design of the Walk-Run ankle

The Walk-Run ankle (Fig. 1) is an active ankle prosthesis that is designed to perform walking and running in lab conditions. It is the first generation of a series of improved powered ankles for substantial load demands. The system uses a 200 W brushless DC motor as a power source and a spring to benefit from the elastic energy storage and release during walking and running gaits. The stiffness of the spring is about 445 kN/m and is optimized for a subject weight of 61 kg in a medium running speed of 2.6 m/s. To minimize the influence of the additional series elastic carbon foot the stiffest possible version of the Pacifica LP foot (Freedom Inovations) was selected.

The current design has a weight of 1.9 kg not including the battery and the electronics. Both the PC-104 for the control and the 4400 mAh 25.9 V battery (powering ankle and PC-104) are stationary on a test bench. For a subject (61 kg, 1.7 m height) with an amputation height of 0.31 m, the amputated limb mass is estimated to be about 2.3 kg according to calculations using the equation from (Grimmer and Seyfarth, 2014). Thus, the weight of the artificial foot, including adapters and socket, is only slightly higher compared to the healthy condition. A belt drive is used as a transmission between the motor and the roller-screw.

7.3.2 Control of the Walk-Run ankle

A controller for standing, walking, running, and transitions was designed using Simulink (MathWorks) to test the prosthetic prototype (Fig. 2). Two sensors, fixed at the upper part of the

Figure 1: Walk-Run Ankle (Springactive): A motor powered prosthesis to investigate on walking and running.

prototype, are implemented for the gait control. A rate gyro sensor ($\dot{\theta}_{\text{shank}}$), to measure shank velocity, is combined with a two axis accelerometer. For the accelerometer $\ddot{x}_{\text{shank}}$ is oriented forward and $\ddot{y}_{\text{shank}}$ is oriented vertically when the subject is standing. All the sensors measure motion in the sagittal plane.

All three signals (1000 Hz) where converted from voltage to acceleration or velocity in the *Raw Signal Processing* block. In addition all the data was filtered for *Gait Determination* with a 2nd order Butterworth filter using a cutoff frequency of 4.

Three parameters must be determined in order to calculate the appropriate motor position: the current gait mode, the gait speed, and the gait progression percent. To determine these parameters, first a *Gait Cycle Detection* is done. The beginning of the gait cycle is identified by rate gyro sensor data from the shank. When shank angular velocity crosses from negative (swinging forward) to positive velocity (swinging backward) the beginning of the gait cycle is defined (Fig. 3). At some walking and running speeds the same zero crossing can occur during the midstance. To avoid errors in the step detection a second condition was defined. During the swing phase, angular velocity reaches a maximum. For slower speeds the maximum value decreases. At 0.5 m/s walking the maximum was about -200 °/s. A hit crossing condition of -150 °/s needs to be fulfilled before the shank velocity zero crossing can be used to identify the beginning of a step. The output of the *Gait Cycle Detection* is the current frame and by this the start time of the gait cycle. In combination with the start time of the last gait cycle the time of the last step can be determined.

In the *Gait Determination* the incoming three sensor signals are compared to the sensor reference trajectories starting at the beginning of the gait cycle. The most similar reference is identified calculating a cumulative sum of error between the curves. This results in a measurement of the current gait mode and the movement speed.

The *Gait Percent Detection* block uses a lookup table of times, t_{cyc} (s), of gait cycles from different speeds of walking and running (Lipfert, 2010). The gait percent $G_{\%}$ is determined by dividing the current step time t_{cur} (s) by the reference step time t_{cyc} (s) from the lookup table.

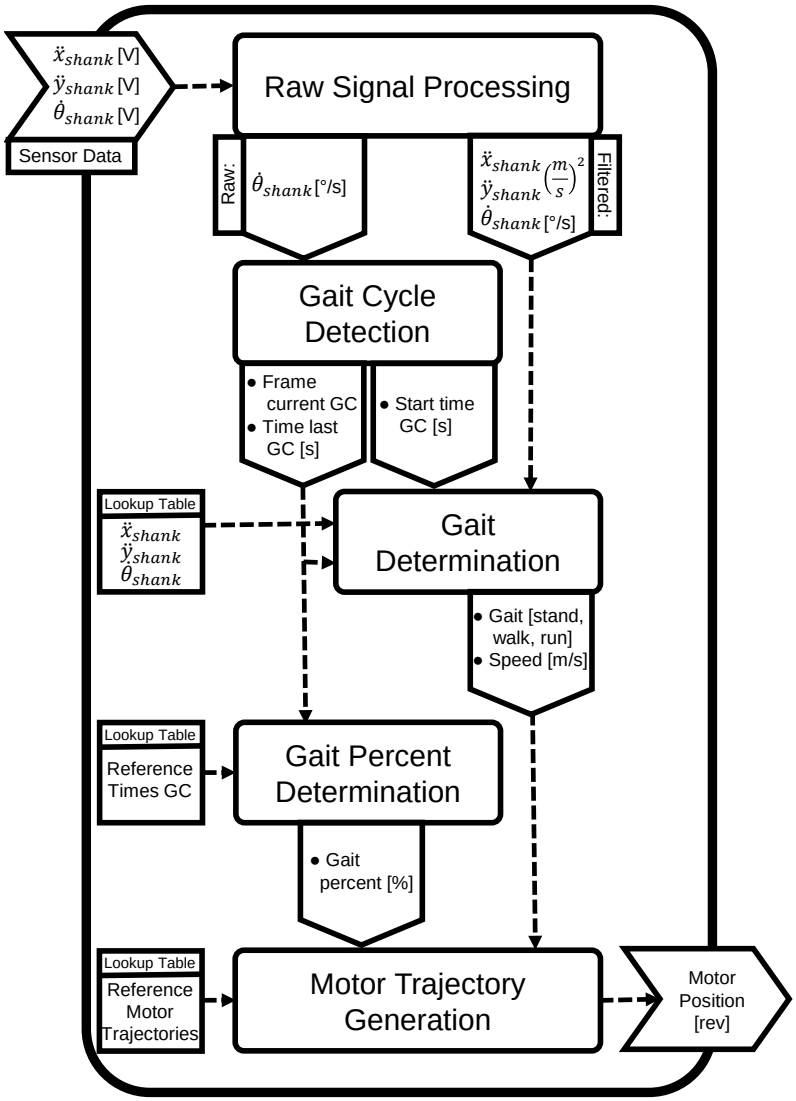

Figure 2: Controller Flowchart: Input for the control is shank angular velocity $\dot{\theta}_{\text{shank}}$ and shank acceleration $\ddot{x}_{\text{shank}}$ and $\ddot{y}_{\text{shank}}$. Five main steps of data processing are required to define the right motor pattern for the Walk-Run ankle. In addition three lookup tables from experimental gait studies are required. One as reference for detecting the gait, one for the calculating of gait percent and one as reference for the motor trajectories.

$$G_{\%} = (t_{\text{cur}}/t_{\text{cyc}}) \cdot 100\,\% \tag{1}$$

Due to individual differences in t_{cyc} from the reference lookup table, t_{cyc} of the last step is also taken into account as long as the gait mode and the speed are not changed. This results in more precise gait percent detection.

As a last step, the gait mode, the speed, and the gait percent are used in the *Motor Trajectory Generation* block to determine the motor trajectory using a reference lookup table.

The desired motor trajectory is followed by the implementation of PD control. As previously described, a belt drive is used in conjunction with a roller-screw to effect dorsiflexion or plantarflexion at the prosthetic ankle joint.

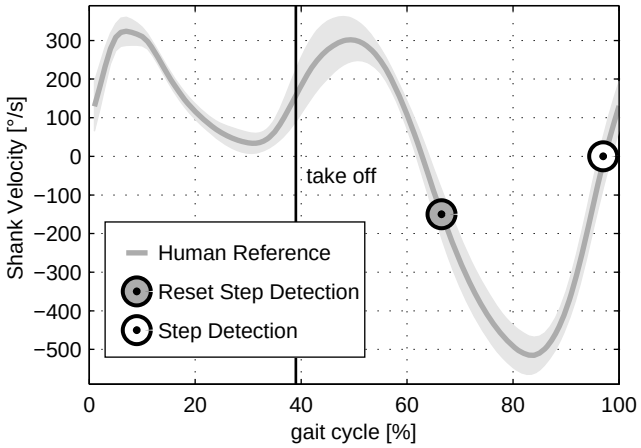

Figure 3: Step Detection: Human reference shank velocity for 2.6 m/s running used for step detection (mean of 21 healthy subjects). Zero crossing from negative to positive is used to determine the beginning of the next step. Step detection has a reset at -150 °/s to prevent errors that could occur by zero crossings at lower speeds during stance.

7.3.3 Control and Model Reference Data

Three different experiments were used to define reference data for the prosthetic control.

In a first experiment (Lipfert, 2010), healthy subjects (21 subjects) walked and ran (0.5 m/s to 2.6 m/s) on a treadmill with integrated 3D force sensors (Kistler, 1000 Hz). Kinematics were recorded by high-speed infrared cameras (Qualisys, 240 Hz). A second similar experiment (7 subjects), was repeated for higher running speeds (3 m/s and 4 m/s). Ankle angles and torques were calculated (Günther et al., 2003; Lipfert, 2010) and used to estimate the motor patterns corresponding to the Walk-Run ankle dimensions (Fig. 1). Calculation methods are similar to (Hollander and Sugar, 2005) and (Grimmer and Seyfarth, 2011). The reference times, used in the controller to determine the gait percent, were taken from both treadmill experiments.

In a third experiment, one subject (height: 1,73 m, mass: 63.5 kg, age: 23 years, male) walked and ran with the same speeds as in the previous experiments over level ground. The pace was set by a bicycle. A two axis accelerometer and a rate gyro sensor were mounted to a small wireless board. The board was affixed at the shank near the ankle joint to measure the reference values for all gait conditions. The fixation height of the system was similar to the height of the sensors of the Walk-Run ankle. About 40 steps were measured for each condition at the instrumented leg. Mean values for the gait cycle were created and filtered in like manner to the incoming data in the prosthetic controller (2nd order Butterworth filter, cutoff frequency 4).

All the experiments were in compliance with the Helsinki Declaration.

7.3.4 Evaluation of Walk-Run ankle

For the first evaluation of the Walk-Run ankle, one subject (similar to third preparation experiment) was tested on a treadmill using a bypass system (Fig. 4). The prosthesis is linked in parallel by an orthosis to a healthy subject. The leg length on the prosthetic side increased by about 5 cm. The shoe of the opposite leg was equipped with an additional 1.5 cm sole to reduce differences in leg length. Various walking and running speeds were tested. For this evaluati-

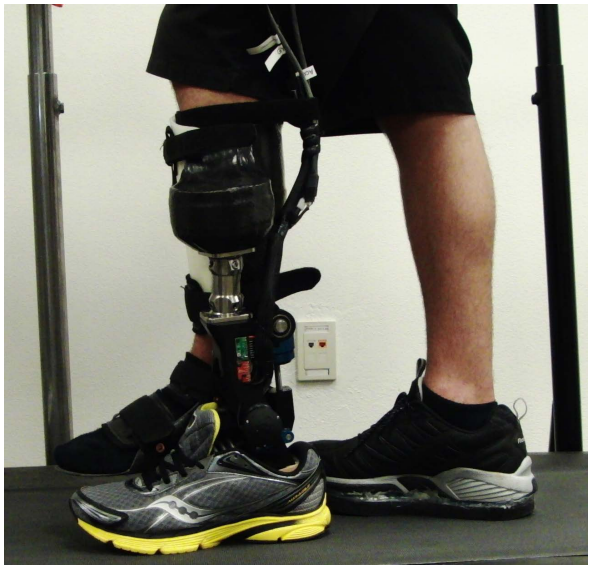

Figure 4: Bypass test orthosis: The Walk-Run ankle was mounted at an orthotic bypass to test it at healthy subjects

on, 44 continuous steps of 1.6 m/s walking, 60 continuous steps of 2.6 m/s running, and 37 continuous steps of 4.0 m/s running were used.

7.3.5 Calculation of biomechanical parameters

The biomechanical parameters of the Walk-Run ankle were calculated using the motor encoder and the ankle angle encoder. The length of the spring was determined by the position of the nut (motor) in combination with the ankle angle. Using Hooke's law, the spring force could be calculated. The spring and the nut velocity were determined by numerical differentiation. By using the lever arm of the spring towards the ankle joint, the ankle torque was calculated. The ankle torque could be related to the force applied by the nut using the lever arm of the ankle joint towards the roller screw. By multiplying the spring velocity and the spring force the mechanical power was calculated. The nut output power was calculated by multiplying the nut force and the nut velocity. The sum of the spring power and the nut power is equal to the ankle joint power.

The step length of the bypass site was calculated using the speed of the treadmill and the time required for the gait cycle.

7.4 RESULTS

7.4.1 Gait quality

Walking 1.6 m/s

The ankle angle sensor output and the calculated torque of the Walk-Run ankle were compared to the healthy subject data. We found that for walking at 1.6 m/s the controller identified a mean speed of 1.6 m/s during the gait cycle. Step length (1.72 m) on the prosthetic side was a little higher compared to the mean of the able body subjects (1.51 m). The angle and the torque matched almost perfectly (Fig. 5) to reference data. Power curves and related energy of the model calculations (0.17 J/(kg·m)) differ to some extent from the values measured by the

Walk-Run ankle (0.14 J/(kg·m)). During the loading phase we could identify small differences between the desired nut reference and the robotic nut trajectory (Fig. 6). As a result the peak power exerted by the motor to load the spring is smaller than in the model (Fig. 8 at 45%). As a consequence, the energy saved and released by the spring (0.11 J/(kg·m)) is also less compared to the model (0.15 J/(kg·m)).

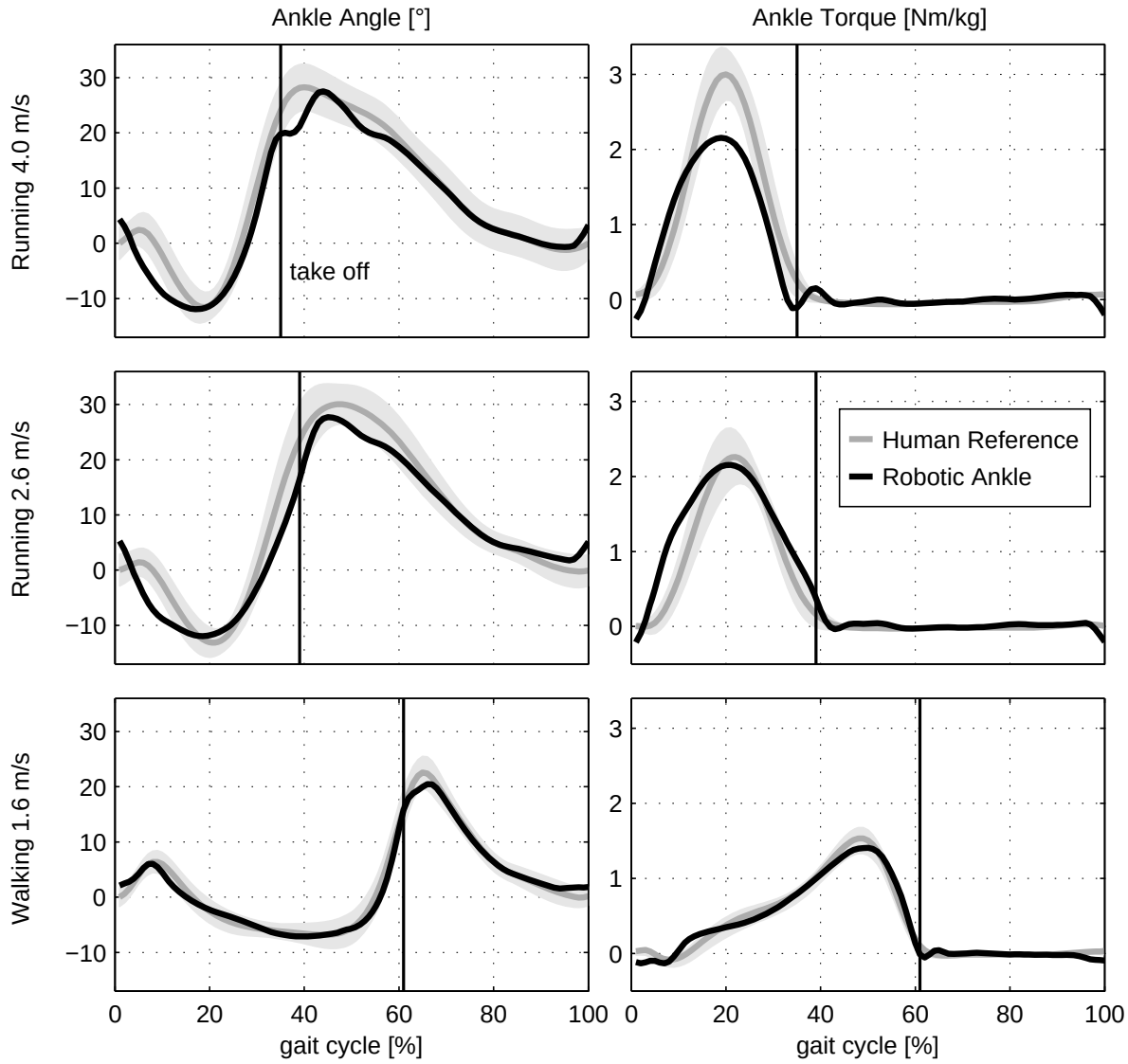

Figure 5: Angle and torque: Ankle angle (left) and ankle torque (right) for the mean of multiple steps using the Walk-Run ankle (black) and the mean of up to 21 health human reference subjects (gray). For the reference data also standard deviation is shown. Data is presented for the gait cycle of 1.6 m/s walking, 2.6 and 4.0 m/s running. The take off is indicated by a vertical line. An increase of the ankle angle implies plantarflexion.

The maximum power output of 3 W/kg is almost equal, but the timing of the maximum power of the Walk-Run ankle is later compared to the model curve.

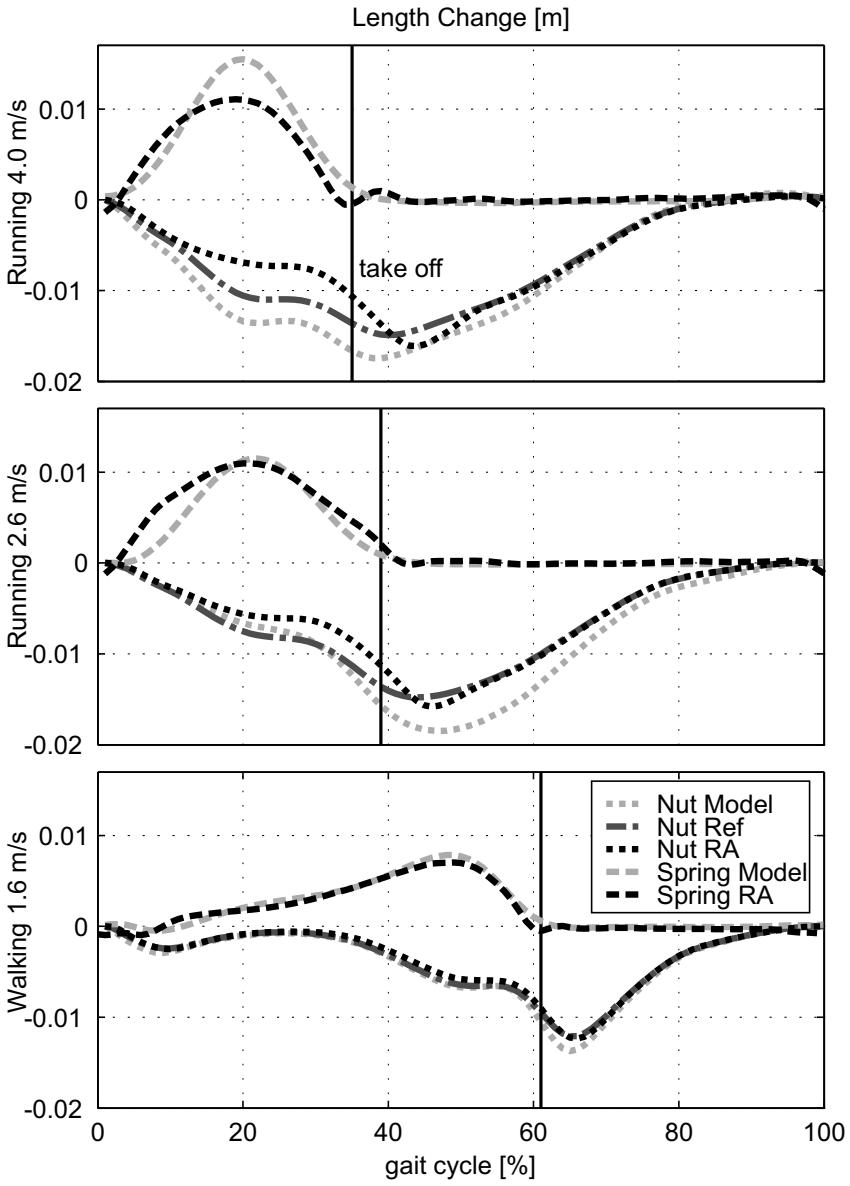

Figure 6: Nut and spring length change: Length change of the nut (dotted) and the spring (dashed) for the mean of multiple steps using the Walk-Run ankle (black) and the mean of up to 21 health human reference subjects (gray). Data is presented for the gait cycle of 1.6 m/s walking, 2.6 and 4.0 m/s running. The take off is indicated by a vertical line. Positive values imply lengthening. Light gray color indicates the pattern for the theoretical model. As detected locomotion speed is different from the desired model and the treadmill speed real nut reference (dark gray) curves differ from the model trajectory.

Running 2.6 m/s

While running at a treadmill speed of 2.6 m/s, the Walk-Run ankle identified a mean speed of about 2.8 m/s when using the bypass. The step length of the subject's prosthetic side was 1.92 m compared to 1.94 m for the reference data. When comparing the ankle angle and the torque to reference data from 2.6 m/s, especially at touch down and take off, differences could be identified. The ankle angle begins dorsiflexion earlier (0-10%) and plantarflexion later (30%-50%) compared to reference running data (Fig. 5). The difference in the shape of the torque

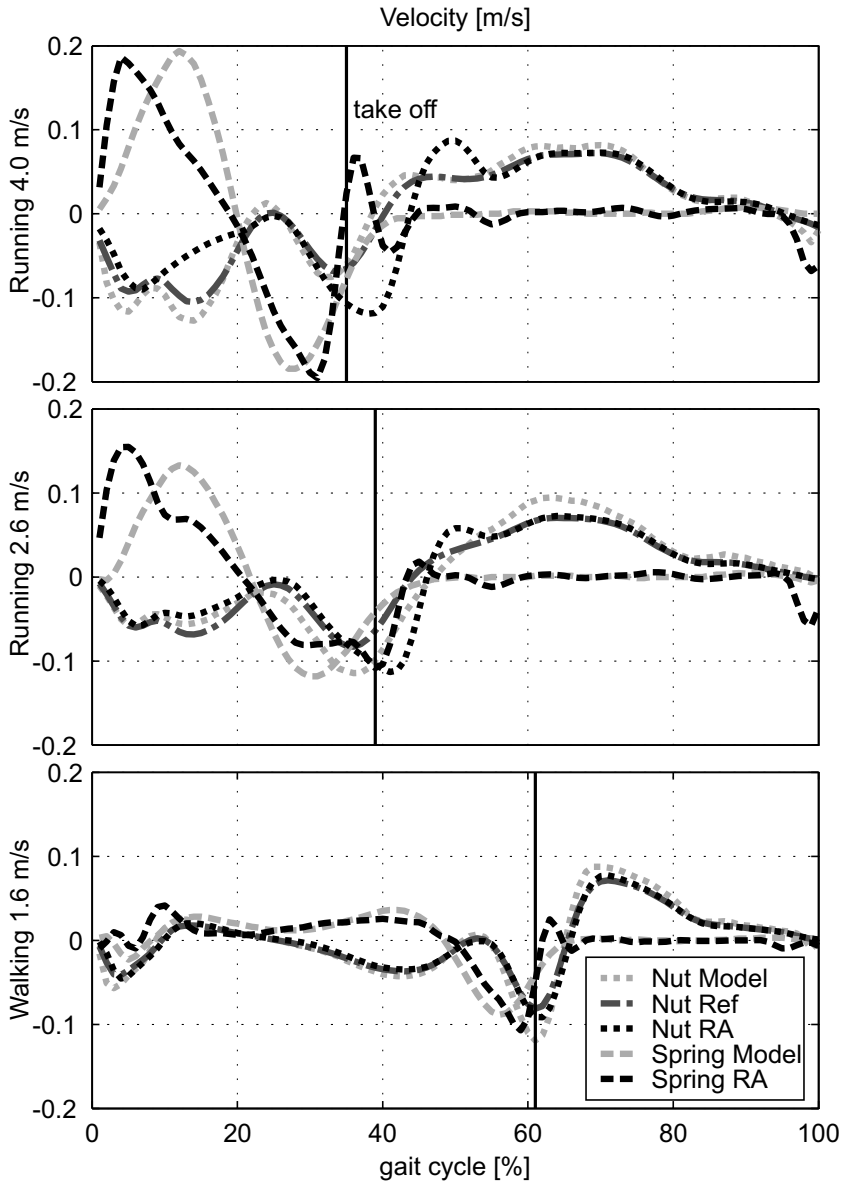

Figure 7: Nut and spring velocity: Velocity of the nut (dotted) and the spring (dashed) for the mean of multiple steps using the Walk-Run ankle (black) and the mean of up to 21 health human reference subjects (gray). Data is presented for the gait cycle of 1.6 m/s walking, 2.6 and 4.0 m/s running. The take off is indicated by a vertical line. Positive values imply lengthening. Light gray color indicates the pattern for the theoretical model. As detected locomotion speed is different from the desired model and the treadmill speed real nut reference (dark gray) curves differ from the model trajectory.

is in line with the observed changes in the ankle angle. The nut did not follow the reference trajectory closely during the stance phase (Fig. 6). The length of the spring increases earlier and decreases later compared to the reference data. This behavior is reflected also in the spring velocity (Fig. 7). The power curves differ in the shape from the model data. The amount of work provided by the robotic ankle motor (0.21 J/(kg·m)) and by the spring (0.23 J/(kg·m)) is similar but not exactly that of the model (0.22 nut output and 0.25 J/(kg·m) spring). The

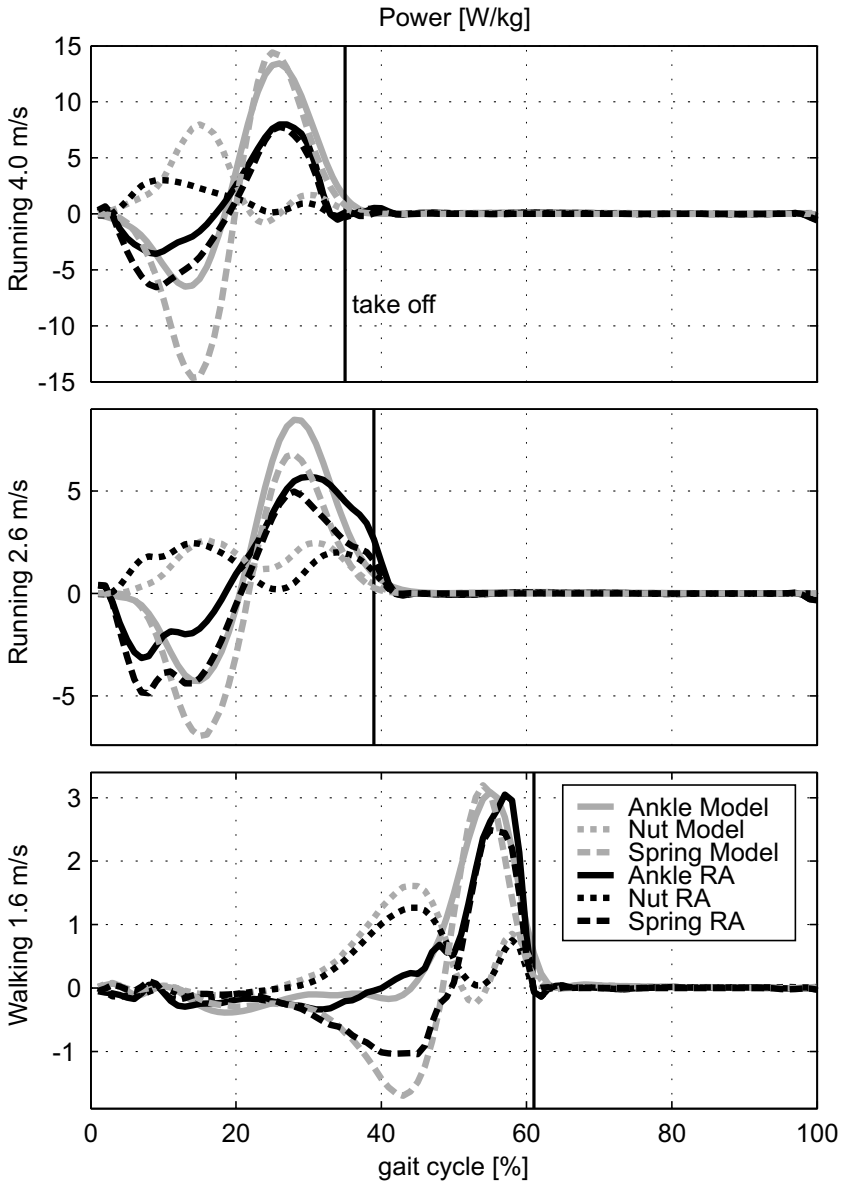

Figure 8: Nut, spring and ankle power: Mechanical power of the nut (dotted), the spring (dashed) and the ankle (solid) for the mean of multiple steps using the Walk-Run ankle (black) and the mean of up to 21 health human reference subjects (gray). Data is presented for the gait cycle of 1.6 m/s walking, 2.6 and 4.0 m/s running. The take off is indicated by a vertical line. As detected locomotion speed for running was different from the theoretical model and the treadmill speed, differences in power curves are to some extend caused by changes in the interpolated nut trajectories.

maximum power output is about 5.7 W/kg combining the effect of the spring and the motor. This maximum power output is much lower than the 8.5 W/kg of the model.

Running 4.0 m/s

For running at a treadmill speed of 4.0 m/s, the controller identified a speed of 3.7 m/s. The reference group used a step length of 2.81 m at 4 m/s running. The subject with the bypass had a mean step length of about 2.67 m on the bypass side. When comparing to the reference data

of 4.0 m/s, we identified the same ankle angle behavior as in 2.6 m/s running. The dorsiflexion happens earlier and the plantarflexion later compared to the model. After takeoff, a larger difference between the model and the system ankle angle occurs. Fluctuations in spring velocity are also seen after the takeoff. Similar fluctuations after takeoff with less amplitude can be found for 2.6 m/s running and 1.6 m/s walking. Similar to running at 2.6 m/s, there is a gap between the reference nut position and the real nut position in the the stance phase. The spring is not elongated in the same way as the model (Fig. 6). As a result of the nut position and the spring length, the ankle torque is less compared to the model values (Fig. 5). In addition, the peak power and the work (nut output: 0.12, spring: 0.17 J/(kg·m)) is less compared to the model data (nut output: 0.22, spring: 0.31 J/(kg·m)). The joint peak power should be about 13.4 W/kg. The robotic ankle can provide about 8 W/kg in total combining the effect of the spring and the motor.

7.5 DISCUSSION

7.5.1 Replication of human gait

The Walk-Run ankle could mimic the reference subject walking and running behavior when testing using a bypass system on a healthy subject. When comparing the reference and the real data only subtle differences could be identified in walking. For running, especially at 4.0 m/s, the behavior of the Walk-Run ankle differs from the model. To some extend this could be caused by the difference of the detected speed (2.8 instead of 2.6 m/s, 3.7 instead of 4.0 m/s) and the resulting difference in the desired motor trajectory. In running, a gap between the desired nut reference (Nut Ref) and the achieved nut position of the robotic ankle (Nut RA) between 10% and 43% of gait cycle exists.

As the motor current is not at its maximum (almost reached between 16% to 28%) during some part of this period, it could be possible to reduce the difference by an adaptation of the control parameters. During midstance (4 m/s), the motor was not able to deliver enough torque to move the nut. But motor torque was enough to hold position. It could be tested to which extent an earlier pretensioning of the motor, when less torque is applied, could improve the elastic recoil.

The differences in the nut trajectory during stance cannot explain the difference in ankle angle mainly caused by the spring deflection at the beginning of the stance phase. The spring is elongated faster than the model predicts. For a comparable joint torque, such a behavior could appear when the spring stiffness is too low. We assume that at 4 m/s, the stiffness could be a cause for differences in the slope of the ankle angle. Also, as the torque increases for the 2.6 m/s experiment, the same assumption cannot be made for this speed. The reason for the increase in the torque at 2.6 m/s running could be a subject specific pattern but also asymmetries caused by the bypass system. The shank velocity data and video shows that the subject is touching the ground while the shank is in forward rotation. This is in contrast to the natural pattern where at touch down the shank is already in backward motion. The so called leg retraction (Seyfarth et al., 2003) is used to avoid impacts. The longer leg (about 3.5 cm) of the bypass system seems to cause an increased impact that results in higher ankle torques compared to the reference data. For a more detailed analysis on the reason motion capturing and force measurements of both legs would be required.

7.5.2 Spring fluctuations after take off

After takeoff, fluctuations of the spring occurred. This was more distinctive for the higher speeds. It is unclear how much these fluctuations in the early flight phase affect the gait stability. It could be worthwhile to investigate if it is possible to reduce fluctuations by using the motor for damping. As a result of the fluctuations, the ankle angle after takeoff differs from reference data especially at 4.0 m/s running.

7.5.3 Touch down detection

For the ankle torque and the ankle angle in running, small changes happen slightly before the detected start of the gait cycle. This could indicate that the gait cycle is not detected correctly. The shank velocity is used as an indicator for detecting the beginning of each new step. For the reference data, the zero crossing of the shank velocity data happens 3% before the touch down (running 2.6 m/s, Fig. 3). As a result, the beginning of the gait cycle should be detected slightly before the ground contact. In the experimental data it seems to be the opposite. Ankle torque can be calculated before a new gait cycle is detected. The change in the ankle angle shortly before the detected touch down is about 3° for both running speeds. As the nut position is almost constant in this phase, the spring deflection (relative to change of the ankle angle sensor) causes the torque based on Hooke's law. As already discussed for subsection 7.5.1, the shank velocity and video indicate that the bypass touches the ground while the shank is still in forward rotation. Thus the control approach to use gyro data only for the step detection is inadequate. To avoid this phenomenon, future tests that include the bypass test bed should have a similar leg length. Another way to improve *Gait Cycle Detection* could be to use the calculated forces from the spring deflection as an indicator of the beginning of a gait cycle. In addition to the method of using only the gyro data, the stance and the swing phase can potentially be identified (Fig. 5).

7.5.4 Limitations of the Walk-Run ankle

The Walk-Run ankle nut was able to deliver about 3 W/kg mechanical peak power for a subject weight including bypass and prosthesis of about 67 kg. This 200 W maximum was almost reached for 2.6 m/s running. For running at 4.0 m/s the model predicted for the chosen stiffness a required nut peak power output of 8 W/kg. The motor was not able to deliver these 536 W. Using an optimal stiffness could reduce the requirements for running at 4 m/s to 3.9 W/kg (Grimmer et al., 2014). This could greatly improve the performance for the fastest running speed. Also while the motor desired and achieved trajectory for 4 m/s running were not matching, the final ankle angle was almost equal (neglecting angle caused by fluctuations after takeoff) to the reference data. Thus we assume there could be a better solution that is a compromise between following of the desired motor trajectory and the gait quality. The precise following will require a large amount of energy but the gait quality may only improve slightly. Investigations on this topic could be made by using a motion capture system and force plates to compare symmetry and by using a spiroergometry system to measure user effort.

7.6 CONCLUSION

For the first preliminary study on the Walk-Run ankle, we found that it is possible to mimic the human reference ankle joint behavior for walking and running up to a speed of 2.6 m/s.

Compared to the reference data, at 4 m/s running, the ankle torque from the prosthesis was not adequate. As the desired ankle angle was almost achieved even without the correct torque, the authors think that it is worthwhile to investigate the compromise between following the calculated optimal motor trajectories and the gait quality. The authors believe that there is a high potential to decrease the peak power requirements and the energy consumption when motor trajectories are manipulated in a way to have reduced acceleration and less changes in direction.

Some hardware and control issues, like the differences in motor desired and achieved trajectory, the fluctuations of the spring, and touch down detection, could be identified. Some of these may occur due to the bypass setup. Thus, the next step would be to test the ankle on an amputee to avoid larger differences in leg length or mass distribution in between the legs.

7.7 OUTLOOK

The data collected and presented in the paper was derived from the controller M. Grimmer developed for this system. This information is being used to influence the design of a ruggedized powered ankle that also has running capability. The new and improved design is being updated by Springactive to include weight reducing titanium springs that have a longer life, higher efficiency bearings that increased system efficiency, and embedded electronics.

7.8 ACKNOWLEDGEMENTS

Research reported in this publication was supported by the the DFG grant SE1042/8 and the Eunice Kennedy Shriver National Institute of Child Health & Human Development of the National Institutes of Health under award number R43HD072402. The content is solely the responsibility of the authors and does not necessarily represent the official views of the National Institutes of Health. The authors acknowledge S.W. Lipfert for providing human data.

7.9 AUTHOR CONTRIBUTIONS

M. Grimmer was responsible for programming the high and medium level gait control. In addition he was in the lead for drafting of the manuscript and experiments. M. Holgate was in the lead for project planing, prosthesis design specifications and organization. R. Holgate was responsible for the design of the Walk-Run ankle, sensor integration, wiring and assembling. A. Boehler was responsible for the setup of the PC-104 platform, including sensor and motor interfaces, used to control the robotic ankle. In addition he was programming the main framework for the prosthetic controller including the low level control. J. Ward provided supervision on control developments. In addition he assisted for interpretation on results to improve future prosthetic developments. M. Holgate, R. Holgate and A. Boehler and J. Ward assisted for experiments. A. Seyfarth assisted for the biomechanical analysis. Depending on there special field of knowledge, all authors including K. Hollander and T. Sugar participated in the critical discussion of the results and helped for revision of the manuscript.

7.10 CONFLICT OF INTEREST

Matthew Holgate, Alexander Boehler, Jeff Ward, Kevin Hollander and Thomas Sugar are owners of SpringActive. Robert Holgate was previously an employee of SpringActive. SpringActive, Inc.

supplied the Walk-Run ankle for this research and is currently developing commercial powered ankle prostheses. Martin Grimmer and Andre Seyfarth are with the Technical University of Darmstadt and have no competing interests.

7.11 REFERENCES

Aldridge, J. M., Sturdy, J. T., and Wilken, J. M. (2012). Stair ascent kinematics and kinetics with a powered lower leg system following transtibial amputation. *Gait & Posture*.

Bragaru, M., Dekker, R., and Geertzen, J. (2012). Sport prostheses and prosthetic adaptations for the upper and lower limb amputees: an overview of peer reviewed literature. *Prosthetics and Orthotics International*, 36(3):290–296.

Cherelle, P., Matthys, A., Grosu, V., Brackx, B., Van Damme, M., Vanderborght, B., and Lefeber, D. (2012). The amp-foot 2.0: A powered transtibial prosthesis that mimics intact ankle behavior. In *9th National Congress on Theoretical and Applied Mechanics*.

Czerniecki, J., Gitter, A., and Munro, C. (1991). Joint moment and muscle power output characteristics of below knee amputees during running: the influence of energy storing prosthetic feet. *Journal of biomechanics*, 24(1):63–65.

Eslamy, M., Grimmer, M., and Seyfarth, A. (2012). Effects of unidirectional parallel springs on required peak power and energy in powered prosthetic ankles: Comparison between different active actuation concepts. In *IEEE International Conference on Robotics and Biomimetics (ROBIO)*.

Farris, D. and Sawicki, G. (2012). Human medial gastrocnemius force–velocity behavior shifts with locomotion speed and gait. *Proceedings of the National Academy of Sciences*, 109(3):977–982.

Ferris, A. E., Aldridge, J. M., Rábago, C. A., and Wilken, J. M. (2012). Evaluation of a powered ankle-foot prosthetic system during walking. *Archives of physical medicine and rehabilitation*, 93(11):1911–1918.

Gitter, A., Czerniecki, J., and DeGroot, D. (1991). Biomechanical analysis of the influence of prosthetic feet on below-knee amputee walking. *American Journal of Physical Medicine & Rehabilitation*, 70(3):142.

Grimmer, M., Eslamy, M., Gliech, S., and Seyfarth, A. (2012). A comparison of parallel-and series elastic elements in an actuator for mimicking human ankle joint in walking and running. In *Robotics and Automation (ICRA), 2012 IEEE International Conference on*, pages 2463–2470. IEEE.

Grimmer, M., Eslamy, M., and Seyfarth, A. (2014). Energetic and peak power advantages of series elastic actuators in an actuated prosthetic leg for walking and running. In *Actuators*, volume 3, pages 1–19. Multidisciplinary Digital Publishing Institute.

Grimmer, M. and Seyfarth, A. (2011). Stiffness adjustment of a series elastic actuator in an ankle-foot prosthesis for walking and running: The trade-off between energy and peak power optimization. In *IEEE International Conference on Robotics and Automation (ICRA)*, pages 1439–1444. IEEE.

Grimmer, M. and Seyfarth, A. (2014). Mimicking human-like leg function in prosthetic limbs. In *Neuro-Robotics*, pages 105–155. Springer.

Günther, M., Sholukha, V., Keßler, D., Wank, V., and Blickhan, R. (2003). Dealing with skin motion and wobbling masses in inverse dynamics. *Journal of Mechanics in Medicine and Biology*, 3(3-4):309–335.

Herr, H. and Grabowski, A. (2012). Bionic ankle–foot prosthesis normalizes walking gait for persons with leg amputation. *Proceedings of the Royal Society B: Biological Sciences*, 279(1728):457–464.

Hitt, J., Sugar, T., Holgate, M., and Bellman, R. (2010). An active foot-ankle prosthesis with biomechanical energy regeneration. *Journal of Medical Devices*, 4:011003.

Hollander, K. and Sugar, T. (2005). Design of the robotic tendon. In *Design of Medical Devices Conference (DMD)*.

Leyk, D., Erley, O., Ridder, D., Leurs, M., Ruther, T., Wunderlich, M., Sievert, A., Baum, K., and Essfeld, D. (2007). Age-related changes in marathon and half-marathon performances. *International journal of sports medicine*, 28(6):513–517.

Lipfert, S. (2010). *Kinematic and dynamic similarities between walking and running*. Verlag Dr. Kovac, Hamburg. ISBN: 978-3-8300-5030-8.

Radocy, B. (1987). Upper-extremity prosthetics: Considerations and designs for sports and recreation. *Clin Prosthet Orthot*, 11(3):131–153.

Seyfarth, A., Geyer, H., and Herr, H. (2003). Swing-leg retraction: a simple control model for stable running. *Journal of Experimental Biology*, 206(15):2547–2555.

Sup, F., Varol, H., Mitchell, J., Withrow, T., and Goldfarb, M. (2009). Self-contained powered knee and ankle prosthesis: Initial evaluation on a transfemoral amputee. In *IEEE International Conference on Rehabilitation Robotics (ICORR)*, pages 638–644. IEEE.

Sup, F., Varol, H. A., and Goldfarb, M. (2011). Upslope walking with a powered knee and ankle prosthesis: initial results with an amputee subject. *Neural Systems and Rehabilitation Engineering, IEEE Transactions on*, 19(1):71–78.

Suzuki, R., Sawada, T., Kobayashi, N., and Hofer, E. (2011). Control method for powered ankle prosthesis via internal model control design. In *International Conference on Mechatronics and Automation (ICMA)*, pages 237–242. IEEE.

Versluys, R., Lenaerts, G., Van Damme, M., Jonkers, I., Desomer, A., Vanderborght, B., Peeraer, L., Van der Perre, G., and Lefeber, D. (2009). Successful preliminary walking experiments on a transtibial amputee fitted with a powered prosthesis. *Prosthetics and orthotics international*, 33(4):368–377.

Webster, J., Levy, C., Bryant, P., and Prusakowski, P. (2001). Sports and recreation for persons with limb deficiency. *Archives of physical medicine and rehabilitation*, 82(3):S38–S44.

Zhu, J., Wang, Q., and Wang, L. (2010). Pantoe 1: Biomechanical design of powered ankle-foot prosthesis with compliant joints and segmented foot. In *IEEE/ASME International Conference on Advanced Intelligent Mechatronics (AIM)*, pages 31–36. IEEE.

8 Manuscript VI: Simplified ankle control decreases powered prosthetic noise and improves performance and efficiency

Authors:

Martin Grimmer, Antje Grebel, Matthew Holgate, Jeff Ward, Alexander Boehler, Tobias Melz and André Seyfarth

Technische Universität Darmstadt

64289 Darmstadt, Germany

Submitted for publication in 2014

8.1 ABSTRACT

Powered ankle prostheses are demonstrated to be capable of performing kinematic and kinetic joint patterns similar to natural human biomechanics. For a better integration in amputees' daily life prosthesis operating times should be further increased and noise levels decreased. Motor assistance is designed in order to benefit from elastic structures. Model assumptions on the interaction of motor and springs do not necessarily represent the most preferred pattern of the amputee. The peak power optimized motor curves were filtered using a zero-lag second-order 4 Hz and a 2 Hz Butterworth low pass filter. The study shows the influence of these filtered motor patterns on the powered ankle noise, efficiency, and effects on 1.1 m/s walking kinematics. For ankle joint torque almost no differences could be observed between the optimized and the filtered patterns. The ankle angle showed reduced plantarflexion for the filtered curves in flight phase. Minor differences in both angle and torque caused highest push off peak power and efficiency for the 2 Hz filtered motor trajectory. Noise and electrical power consumption decreased when applying the filter. The subject felt most comfortable using the 2 Hz pattern.

Keywords

powered prosthesis, amputee walking, energy efficiency, gait performance, bionic limb, ankle angle, ankle torque

8.2 INTRODUCTION

Using passive prosthetic devices, transtibial amputees are not able to perform net positive work at the ankle joint (Czerniecki et al., 1991; Grimmer and Seyfarth, 2014). Resulting gait asymmetries may lead to long-term sequelae (Gailey et al., 2008; Robbins et al., 2009). Powered ankle prostheses allow the performance of joint patterns similar to natural human biomechanics. Current systems are able to mimic joint kinematics and kinetics of level walking and running but also of climbing stairs and walking inclines and declines (Aldridge et al., 2012; Au et al., 2009; Lawson et al., 2013; Sup et al., 2011; Ward et al., 2014). However, several user requests are left to improve on powered ankle acceptance and performance. To increase the operation time of the system, efficiency needs to be improved. Current designs are made to perform for about 5000 level walking steps per leg without charging the battery (Au et al., 2009). About 6500 steps a day are performed by healthy people in daily life using both legs (Tudor-Locke and Bassett, 2004). Powered systems should be able to cover at least one day, including also higher demanding activities like walking stairs and inclines. Next to the advancements in operating time, an improved efficiency (less friction) may cause less system noise. Amputees may perceive mechanical noise as annoying. They will be noticed to be an amputee when using such a system in daily life. Particularly, females reported the importance of preventing the prosthesis from making noise (Legro et al., 1999). Thus, improving the subjective user-experience should be one of the key elements for prosthetic developments (Beckerle, 2014).

To enhance powered ankle performance the efficiency of the drive (belt drive, bearings, roller screw, motor) can be increased. In addition dampers or springs are able to assist the power source (motor) to increase system efficiency. Simulations on various configurations showed the high potential of these structures (Eslamy et al., 2013; Grimmer et al., 2012, 2014). In (Grimmer et al., 2014), the stiffness of a series spring was optimized for minimum ankle motor peak power for different walking and running speeds. The outcome of the optimization are motor patterns that interact in a mechanically optimal way with the spring to reduce motor requirements. An

open question to these simulations is the reaction of the amputee to the given motor curves. As each subject is different and provided patterns are calculated based on subject group means of the joint angle and the joint torque, individual variations of the patterns may provide a better performance for the amputee. Next to an individualization, a generalization to main events in the gait cycle of the reference curves may also help to improve amputee acceptance. Optimized motor curves include, depending on speed and gait, several changes in motor direction that are required to match joint biomechanics. The motor complements the length change of the spring to achieve the reference ankle angle. Due to the inertia of motor and mechanics these changes in the sign of motor velocity may lead to increased power and energy demands.

In this study we will investigate to which extent smoother motor patterns, reducing peak acceleration and frequent changes in motor turning direction, can reduce power and energy demands of a powered ankle prosthesis in walking. By this approach, efficiency of the prosthesis should be increased and system noise decreased. As motor patterns change, amputee movement may differ. Using a motion capture system and an instrumented treadmill it will be proven to which extent the smoothing of the reference pattern affects the motion of a unilateral transtibial amputee.

8.3 METHODS

8.3.1 Walk-Run ankle design

The Walk-Run ankle (WRA, Fig. 1) is a powered ankle prosthesis that uses a 200 W brushless DC motor to perform walking and running. Next to the motor the system benefits from the elastic energy reuse of a spring that is optimized for a subject weight of 61 kg and a medium running speed of 2.6 m/s (Grimmer et al., 2014). The stiffest possible version of the Pacifica LP foot (Freedom Innovations) was selected to avoid further elasticity that is not included in the motor optimization model. A belt drive and a roller-screw are used to realize ankle dorsiflexion or plantarflexion.

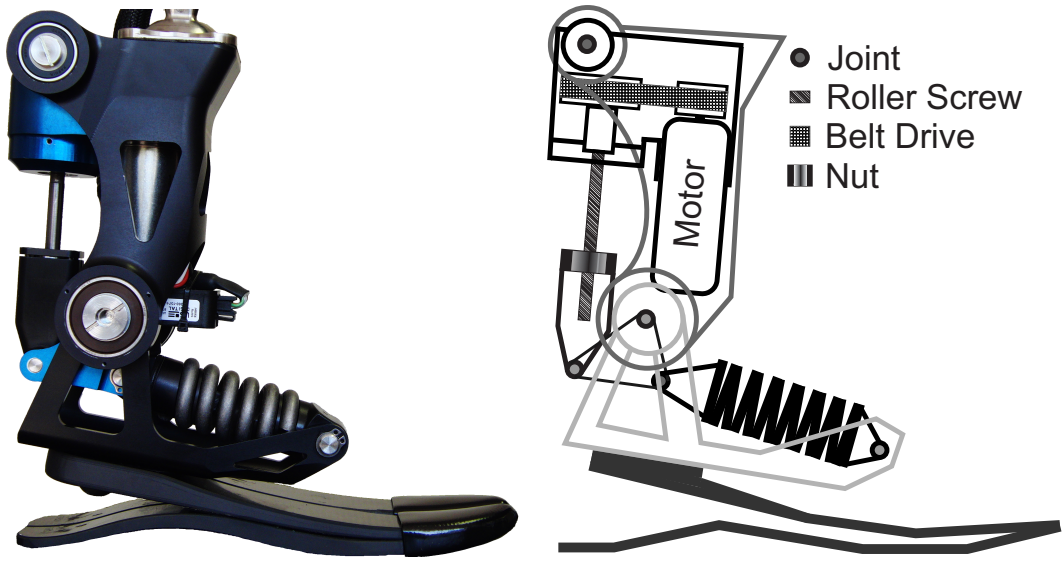

Figure 1: Walk-Run ankle (WRA) prosthesis (SpringActive)

For control an external PC-104 is used. The WRA has a weight of 1.9 kg not including the 25.9 V battery. The subject of this study (55 kg, 1.68 m height) has an amputation height of

0.34 m. The amputated limb mass is calculated to be about 2.3 kg (equation from (Grimmer and Seyfarth, 2014)). In combination with adapters (0.4 kg), socket and liner (0.75 kg) the weight of the lower limb prosthesis is above the healthy condition.

8.3.2 Walk-Run ankle control

An extended controller of the WRA was designed to distinguish between standing, walking, running, and transitions. A rate gyro sensor ($\dot{\theta}_{\text{shank}}$), to measure shank angular velocity, and a two-axis linear accelerometer ($\ddot{x}_{\text{shank}}$ is oriented forward and $\ddot{y}_{\text{shank}}$ vertically when the subject is standing) are used to mimic healthy ankle biomechanics. Sensors data is readout at 1000 Hz using Simulink (MathWorks).

For the performed experiments a simplified control algorithm was used that fixes gait mode to walking and gait speed to the treadmill speed of 1.1 m/s. Small differences in detected walking speed during the gait cycle normally cause adaptations of the motor trajectory. Avoiding this allows a better comparison to the model predictions. The beginning of the gait cycle is identified by rate gyro sensor data from the shank. When the shank angular velocity crosses from negative (swinging forward) to positive velocity (swinging backward) the beginning of the gait cycle is defined (Fig. 2). At some walking and running speeds the same zero crossing can occur during midstance. To avoid errors in step detection a second condition was defined. During the swing phase, angular velocity reaches a maximum. For lower speeds the maximum value decreases. At 0.5 m/s walking the maximum was about –200 °/s. A hit crossing condition of –150 °/s needs to be fulfilled before shank velocity zero crossing can be used to identify the beginning of a step. The output of the gait cycle detection is the step time and the start time of the current gait cycle. In combination with the start time of the last gait cycle the time of the last step can be determined.

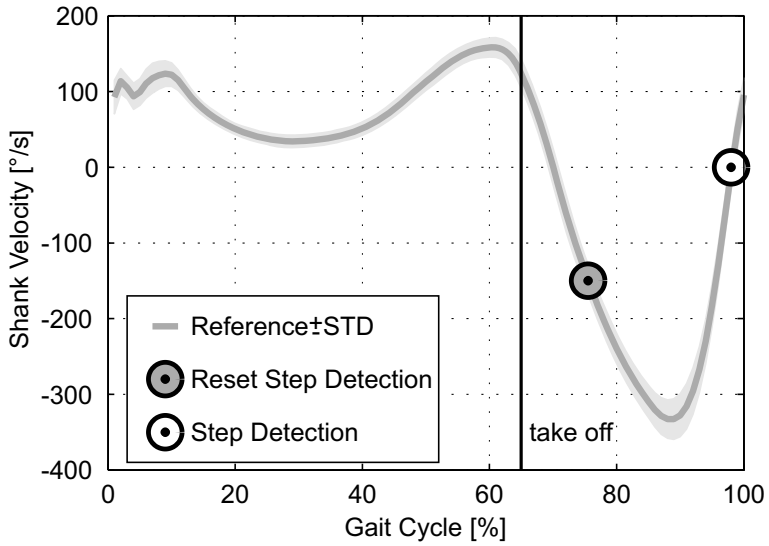

Figure 2: Human reference shank velocity curve (1.1 m/s walking, mean of 21 healthy subjects) used for step detection. Zero crossing from negative to positive is used to determine the beginning of the next step. Step detection starts below a threshold of –150 °/s to avoid errors that could occur by zero crossings at lower speeds during stance.

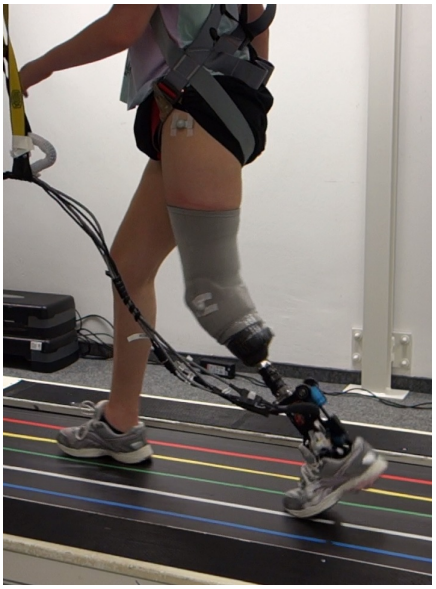

Figure 3: Unilateral transtibial amputee walking on an instrumented treadmill using the Walk-Run ankle (WRA).

The gait percent detection uses a lookup table of times of gait cycles from different speeds of walking and running (Lipfert, 2010). The gait percent $G_{\%}$ is determined by dividing the current step time t_{cur} (s) by the reference step time t_{cyc} (s) from the lookup table.

$$G_{\%} = (t_{\mathrm{cur}}/t_{\mathrm{cyc}}) \cdot 100\,\% \tag{1}$$

Due to individual differences in t_{cyc} from the reference lookup table, t_{cyc} of the last step is also taken into account. This results in more precise gait percent detection. Depending on gait percent, the optimized motor reference position is readout from a lookup table. The desired motor trajectory is achieved by PD control.

8.3.3 Control and model reference data

Reference data from healthy subjects (Lipfert, 2010) was used to calculate optimal motor trajectories and to perform WRA control. In the reference experiment 21 subjects walked and ran (0.5 – 2.6 m/s) on a treadmill with integrated 3D force sensors (Kistler, 1000 Hz). Kinematics were recorded by high-speed infrared cameras (Qualisys, 240 Hz). Ankle angles and torques were calculated (Günther et al., 2003; Lipfert, 2010) and used to estimate motor patterns corresponding to the WRA dimensions (Fig. 1). Calculation methods are similar to (Hollander and Sugar, 2005) and (Grimmer and Seyfarth, 2011). Reference times, used in the controller to determine the gait percent, were also taken from this experiment.

For this study only the data of 1.1 m/s walking is relevant.

8.3.4 Evaluation of Walk-Run ankle on an amputee

For the first evaluation of the WRA on an amputee, one female subject (55 kg, 17 years) was analyzed on an instrumented treadmill during walking at 1.1 m/s (Fig. 3). The subject has a unilateral transtibial amputation since birth.

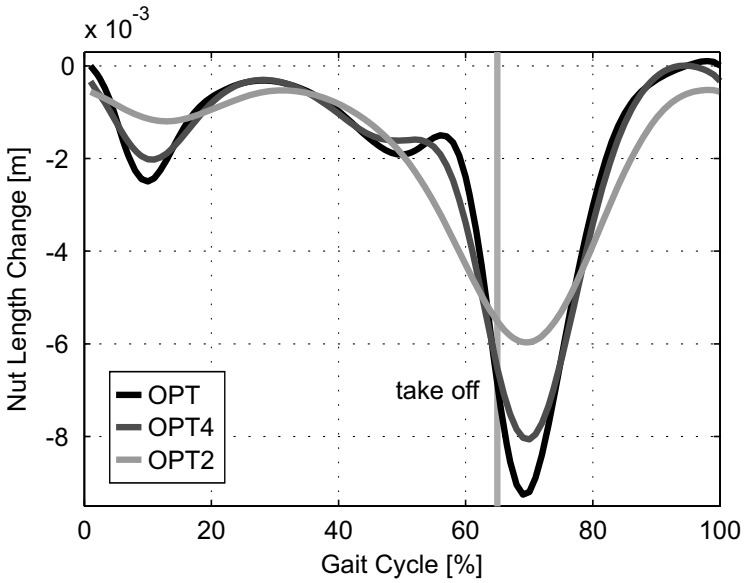

Figure 4: Using the calculation methods from (Grimmer and Seyfarth, 2011; Hollander and Sugar, 2005) a motor trajectory to actuate the powered ankle prosthesis can be calculated. This pattern is predicted to use the elastic properties of a spring in an optimized way to assist the motor (OPT, black). The calculated pattern was filtered with a 4 Hz (OPT4, dark gray) and a 2 Hz (OPT2, light gray) low pass filter. Take off is indicated by a vertical line.

Four different measurements, lasting 2 minutes each, were performed. In the first trial motor position was locked in neutral standing condition. Using this method, the powered prosthesis works purely passively (Passive). This trial is used for an estimation of the unpowered ankle performance. For the second trial a peak power optimized unfiltered motor pattern was used (OPT). It was determined using the methods presented in (Grimmer et al., 2014), to guarantee highest assistance of the series spring to power the artificial ankle joint. This motor pattern includes frequent changes in turning direction that are also reflected by the nut of the roller screw when moving the ankle joint (Fig. 4). In addition, acceleration values of the nut pattern are high. The nut pattern consists of 100 data points representing one gait cycle in percent. The time for this gait cycle is about 1.14 s. By smoothing the nut curve electrical energy consumption and system noise might be reduced. In a first approach a zero-lag second-order Butterworth low pass filter was used to simplify the pattern. The cut-off frequency was selected to avoid the little turn in the nut movement at 55% of gait cycle. This could be achieved using a cut-off frequency of 4 Hz. Next to the changes in this phase of the gait cycle also the nut movement after touch down and in the flight phase will be reduced. The resulting curve (OPT4) was used for the third experimental trial. To explore the limitations of the approach half of it (2 Hz, OPT2) was used for the fourth trial.

During the 2 minutes the subject performed between 80 to 97 valid steps that could be used for analysis. Ground reaction forces were measured at 1000 Hz by the Kistler sensors in the treadmill. Motion kinematics were captured at 250 Hz using a Qualisys system. The hip angle was calculated between the 7th cervical vertebra, trochanter major and an assumed center of rotation at the knee (2 cm proximal of the joint space on the lateral femoral condyle). The knee angle was calculated as the angle between the line connecting the greater trochanter

major, and the rotational knee point and the line connecting the rotational knee point and the lateral malleolus. The ankle angle was calculated by the rotational point of the knee, the lateral malleolus and the 5th metatarsophalangeal joint of the foot. All angles were calculated for the sagittal plane. Ankle joint torque was calculated using a static analysis (Günther et al., 2003). Joint angular velocities were calculated by numerical differentiation and multiplied by the joint torque to obtain joint power.

8.3.5 Walk-Run ankle parameter calculation

The motor encoder and the ankle angle encoder of the WRA provide the main input for further biomechanical calculations. Using both encoder positions the deflection of the spring can be determined. Hook's law and the spring deflection are used to calculate the spring force. The spring and nut (motor encoder) velocity were determined by numerical differentiation. The ankle torque is calculated by using the lever arm of the spring towards the ankle joint. The force at the nut is determined using ankle torque and the lever arm of the ankle joint towards the roller screw. The spring velocity and the spring force are multiplied to calculate the mechanical spring power. The nut velocity and the nut force are multiplied to calculate the nut output power. The sum of spring power and nut power is equal to the ankle joint power.

The mechanical energy requirement of the drive output at the nut was calculated as the sum of positive and the amount of negative work (Grimmer et al., 2014). Mechanical energy requirement of the system represents the total ankle joint work adding up the nut and spring power curve.

Power and torque are normalized to the body mass for the reference and the observed amputee data.

Electrical motor power P_{el} (W) is estimated using motor current I (A) and motor angular velocity ω (rpm). In addition the speed constant k_{n} of the Maxon EC 30 motor (710 $\mathrm{min}^{-1} \cdot \mathrm{V}^{-1}$) and its terminal resistance R (0.102 Ω) is required.

$$P_{\mathrm{el}} = \omega / k_{\mathrm{n}} \cdot I + R \cdot I^2 \,\mathrm{W} \tag{2}$$

8.3.6 Efficiency calculations

The system efficiency η_{system} describes the overall efficiency of the WRA including the effects of the elastic element. It is calculated by the electrical energy input $E_{\mathrm{electrical}}$ and the mechanical system output E_{system}.

$$\eta_{\mathrm{system}} = E_{\mathrm{system}} / E_{\mathrm{electrical}} \tag{3}$$

The drive efficiency η_{drive} describes the efficiency of the mechanical drive. It is calculated using the electrical energy input $E_{\mathrm{electrical}}$ and the mechanical energy output at the nut E_{nut} of the roller screw.

$$\eta_{\mathrm{drive}} = E_{\mathrm{nut}} / E_{\mathrm{electrical}} \tag{4}$$

8.3.7 Acoustical measurements

Young humans can hear sound in a frequency range of 20 Hz up to 20 kHz (Lerch et al., 2009). The ability to hear in the whole spectrum decreases with rising age (Frings and Müller, 2014). A time signal of a sound can be analyzed with respect to its frequency components by using a Fast Fourier Analysis (FFT) algorithm (Müller and Möser, 2013). Since the amplitude range between the hearing threshold and the pain threshold is very large, the logarithmic scale decibel (dB) is commonly used in acoustics. It expresses the ratio between the physical measurement data and the reference value (Rossing, 2007). As a sound pressure level, which can be easily measured with any sound level meter, always depends on the surrounding environment, sound power was taken for this investigation. Sound power is the rate of acoustic energy flow across a specified area emitted by a specific sound source and is absolutely independent of the surrounding environment. The sound power measurement was carried out in a hemi-anechoic room, which is a room with a hard reflecting floor and all other surfaces anechoic. The sound power level L_W can be calculated from sound pressure levels that are measured on positions on a hemisphere over the measurement object according to ISO 3745:2012 using

$$L_W = \overline{L_p} + 10 \cdot \lg\left(\frac{S_m}{S_0}\right) \text{dB}, \tag{5}$$

where $\overline{L_p}$ is the time-averaged and area-averaged sound pressure level, S_m is the surface of the measurement hemisphere, and S_0 is the reference surface of 1 m^2.

For sound power measurements the amputee walked on a treadmill (Schmidt Sportsworld, GM 2011) that was placed in the center of the hemi-anechoic chamber. The passive, the peak power optimized, and both filtered setups were tested. In the passive trial (Passive) the amputee walked without motor assistance. Thus, it represents the noise of the treadmill that can be used to calculate the sound power emitted by the prosthesis only for the powered trials.

8.4 RESULTS

8.4.1 General observations

Ankle angle and ankle torque of the WRA were calculated by two different methods. The first method used the sensors at the prosthesis (Sens. WRA), the second the kinematic data from the Qualisys motion capture system and the kinetics measured by the instrumented treadmill (Meas. WRA). When comparing both methods the motion capture system shows a larger Range of Motion (RoM) for the ankle angle. This is caused by the additional elasticities of the carbon foot and the shoe (Fig. 5, left). The ankle angle encoder cannot measure these deflections. On the other hand the torque calculation method by the WRA sensors shows a larger increase and higher peak values (Fig. 5, right). Due to these opposing trends, both methods result in almost equal mechanical power (Fig. 7, left). The peak mechanical power of the passive trial is lower compared to the powered trials.

Compared to the powered conditions (Org, Filter 4 Hz, Filter 2 Hz) the passive WRA trial (Passive) could not mimic the ankle joint kinematics of the reference data for the push off and the flight phase (Fig. 5, left). The ankle joint torque for the passive trial increased much later and is less compared to the powered trials. Both powered and passive trial did not reach the peak joint torque of the reference (Fig. 5, right). Times for the gait cycle increased when using

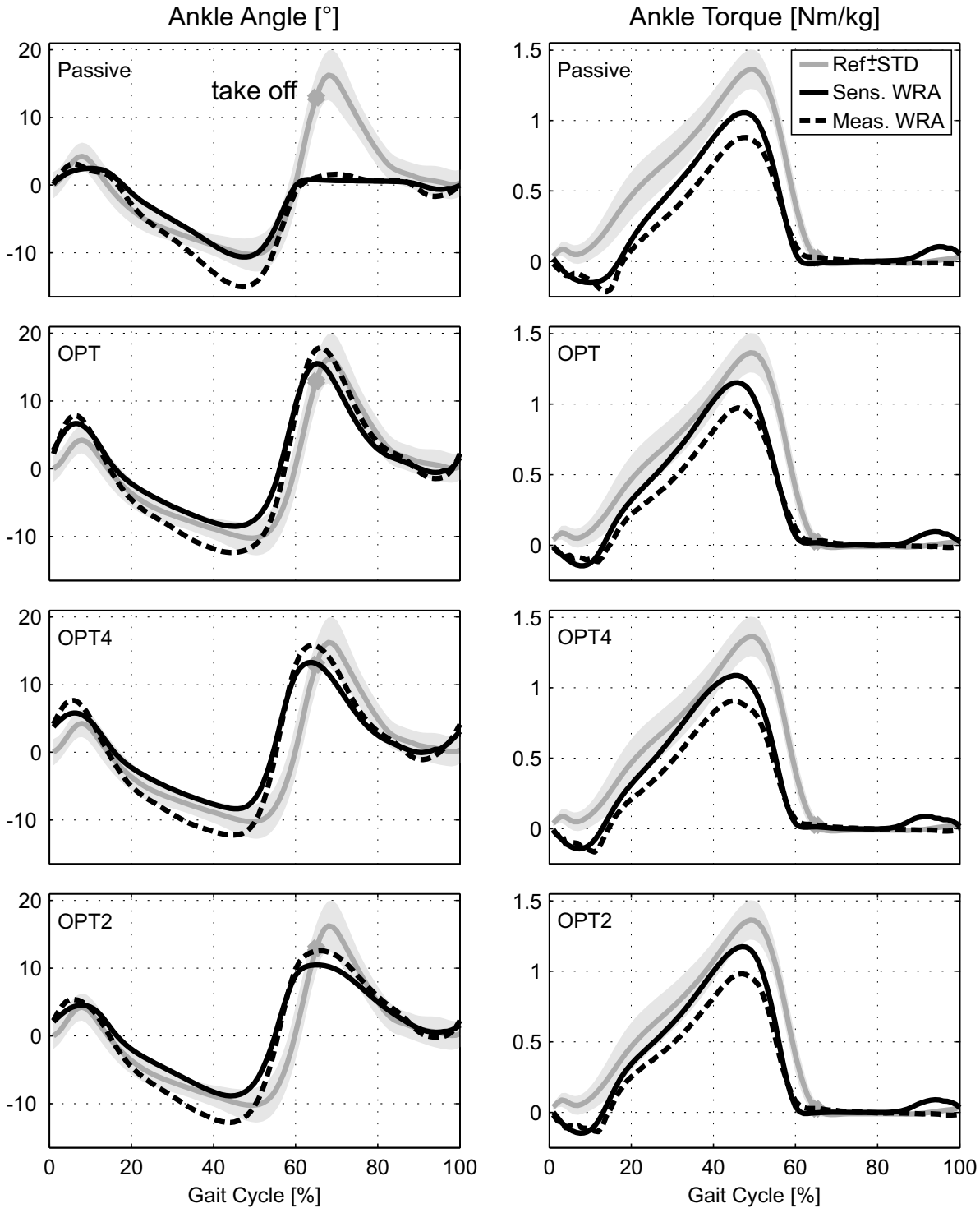

Figure 5: Ankle angle (left) and normalized ankle torque (right) for the mean of multiple steps using the Walk-Run ankle and the mean of healthy subjects as reference (gray). The data was determined using the sensors of the WRA (black, solid) and external measurement systems for kinematics and kinetics (black, dashed). For the reference data also the standard deviation is shown. Data is presented for the gait cycle of 1.1 m/s walking. The take off of the reference is indicated by a gray dot. An increase of the ankle angle implies plantarflexion.

the powered setups (Tab. 1) to values comparable to non-amputees. Only minor changes in intact and prosthetic limb duty factor can be observed (Tab. 1).

8.4.2 Model and experimental observation comparison

During the experiment the nut pattern was almost identical to the model reference (Fig. 6, left). Differences were observed for the spring length. After touch down the spring is shortened before elongation occurs. The maximum length is less compared to the model. Caused by the little change in spring deflection, the total length of the system also changes by this amount (Fig. 6, left). The shape of the mechanical power curves for the nut output, the spring, and the overall system are almost identical comparing model and experimental observations (Fig. 6, right). Peaks for spring loading and for push off power show reduced values for the experiment. The changed spring length at 10% of the gait cycle causes a difference in the experimental power curves compared to the model.

8.4.3 Effects of filtering the motor pattern

Ankle angle and torque

Due to the filtered motor pattern, peak plantarflexion angle shortly after take off is reduced and time of plantarflexion is prolonged. In stance, no major differences can be observed (Fig. 5, left). For the ankle joint torque, no trend could be identified caused by the filter (Fig. 5, right).

Ankle power

Peak ankle power is increasing with the reduction of cut-off frequency (Fig. 7, left). Comparing the duty factor of the prosthetic limb and the intact limb, only minor changes towards a more symmetric gait can be observed comparing powered and passive trials. Small reductions in intact limb peak power can be observed for an increased filter level (Fig. 7, left).

Nut acceleration

Maximum linear nut acceleration at the beginning of the flight phase (about 68% to 70% of gait cycle) is reduced from 2.36 m/s^2 (OPT) to 1.16 m/s^2 (OPT4) and to 0.37 m/s^2 (OPT2) when using the most filtered nut pattern (Fig. 8). Peak nut acceleration during the push off (about 54% to 60% of gait cycle) is reduced from –1.66 m/s^2 to –0.76 m/s^2 to –0.15 m/s^2 when increasing filter level.

Table 1: Time for one gait cycle (Time GC) and duty factors for the intact (DF IL) and the prosthetic (DF PL) limb. Data is shown for the healthy subject reference (Ref) and for passive and powered amputee walking trials.

Parameter	Ref	Passive	OPT	OPT4	OPT2
Time GC [s]	1.14	1.06	1.1	1.12	1.11
DF IL [%]	65	69	68	68	68
DF PL [%]	65	61	62	60	61

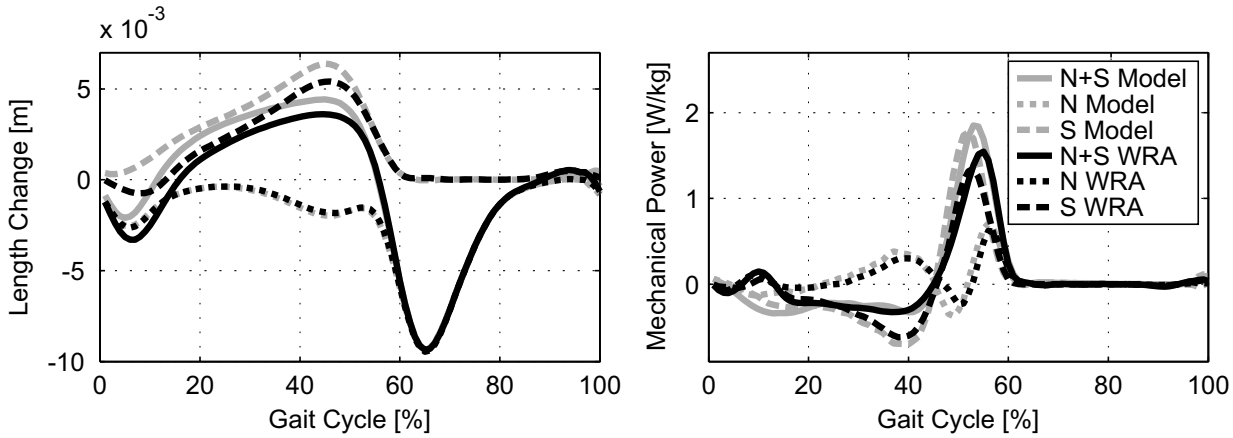

Figure 6: Length change (left) and normalized mechanical power (right) of the nut (N, dotted), the spring (S, dashed), and the combination of both (N+S, solid) for the Walk-Run ankle (black, mean of multiple steps) and the corresponding model prediction (gray, mean of 21 healthy human reference subjects). Data is presented for the gait cycle of 1.1 m/s walking for the unfiltered optimized motor pattern. As spring stiffness is sub-optimal for the amputee weight and the walking speed both model prediction and experimental observations differ from optimal model curves published in (Grimmer et al., 2014). Positive length values imply lengthening. For comparison the model reference values are shifted towards the left (3% of the gait cycle) to match the asymmetric gait pattern of the amputee.

Electrical power

The OPT motor pattern causes the highest peaks for the electrical power consumption (Fig. 7, right). Using the filtered curves these peaks can be reduced dramatically. Having the filter of 2 Hz the power peaks due to motor direction change after touch down and after take off can be almost eliminated. The double hump in the stance phase, originally observed for the mechanical and the electrical power, is converted to a single hump when applying the 2 Hz filter (Fig. 7, right).

Energy and efficiency

When using the filter of 4 Hz and 2 Hz, spring loading and mechanical energy output of the nut could be increased (Tab. 2). As a result the system output energy increased to values similar to the model. With the increase in mechanical output energy the electrical input decreased,

Table 2: Energy exchange [J/kg] and efficiencies

	Mech. Energy Spring			Mech. Energy Nut			Mech. Energy System			Elec. Energy Motor			Efficiency	
	Tot	Pos	Neg	Tot	Pos	Neg	Tot	Pos	Neg	Tot	Pos	Neg	Drive	System
Model	0.324	0.162	–0.162	0.138	0.103	–0.035	0.323	0.196	–0.127	-	-	-	-	-
Opt	0.24	0.12	–0.12	0.096	0.08	–0.016	0.243	0.154	–0.089	0.657	0.579	–0.078	0.146	0.37
Opt4	0.224	0.112	–0.112	0.113	0.109	–0.004	0.282	0.193	–0.088	0.559	0.536	–0.023	0.202	0.504
Opt2	0.25	0.125	–0.125	0.117	0.11	–0.006	0.299	0.202	–0.097	0.495	0.493	–0.002	0.235	0.603
Passive	0.206	0.103	–0.103	-	-	-	0.206	0.103	–0.103	-	-	-	-	-

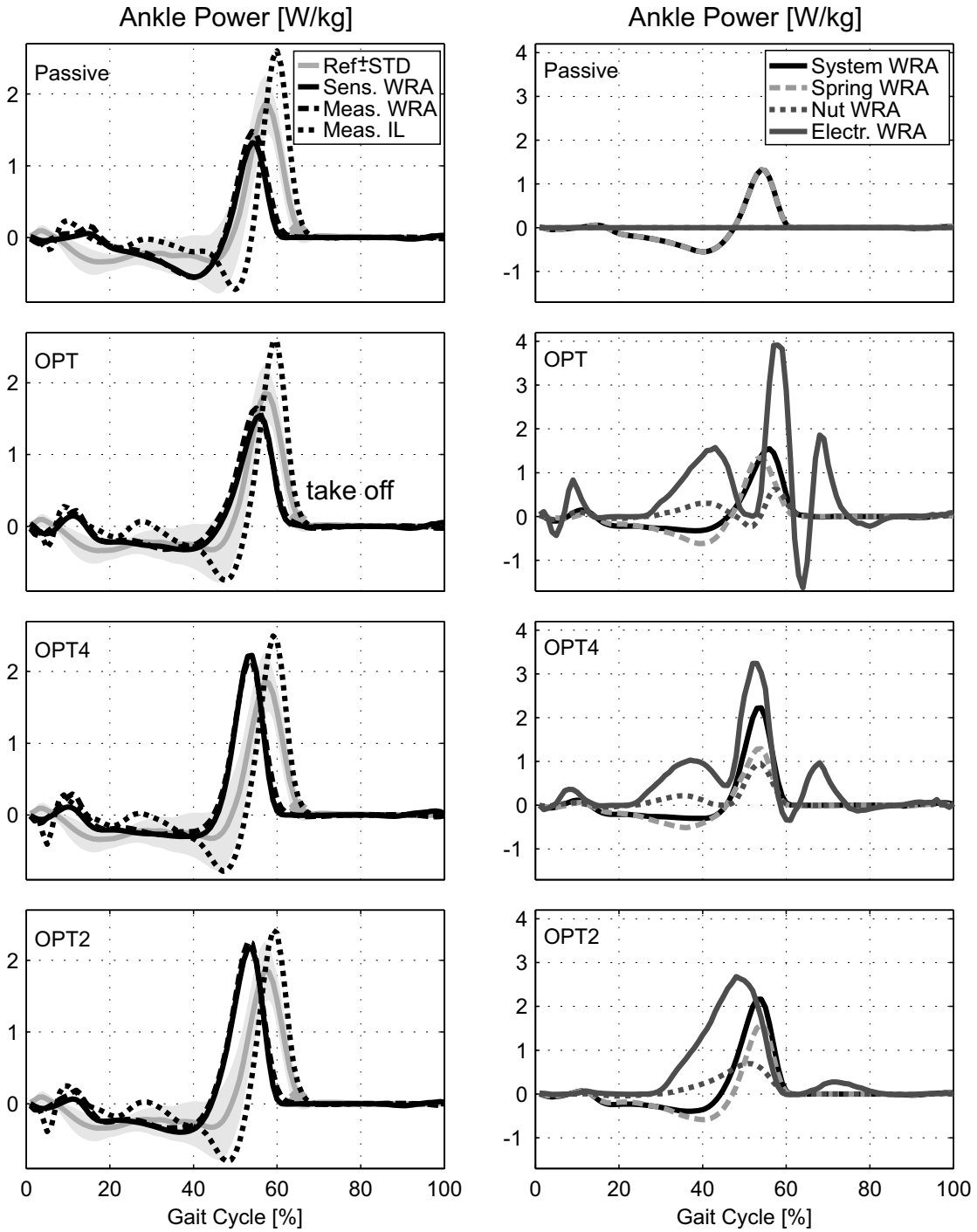

Figure 7: Mechanical and electrical power requirements for 1.1 m/s walking using the Walk-Run ankle. The passive trial is compared to the optimal (OPT) and the 4 Hz and 2 Hz filtered (OPT4, OPT2) pattern. On the left the reference (Ref+STD, gray solid) is compared to the mechanical output calculated by the sensors of the WRA (Sens. WRA, black solid) and the value calculated by measured kinematics and kinetics (Meas. WRA, black dashed). The mechanical output of the intact limb (Meas. IL) is displayed by the black dotted line. On the right the system mechanical output (Ankle WRA, black solid, similar to Sens. WRA), consisting of motor power (Motor WRA, black dotted) and spring power (gray dashed), is shown. Electrical energy consumption (Electr, WRA) is visualized by the dark gray solid line.

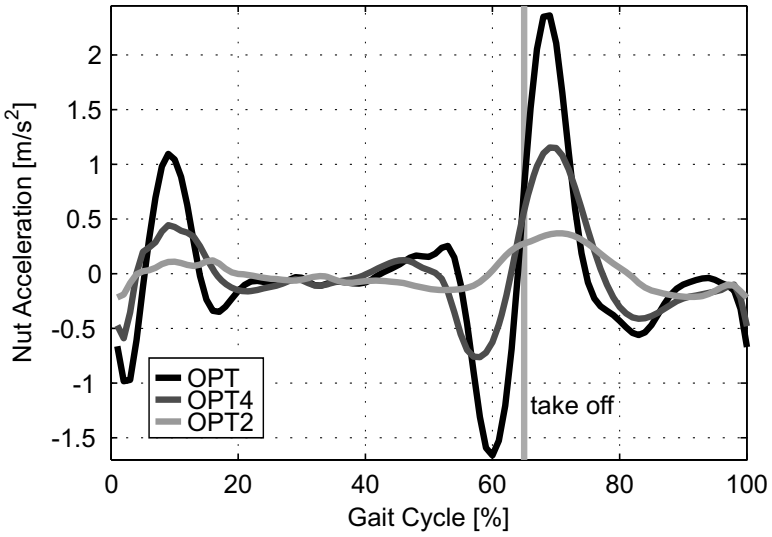

Figure 8: Measured nut acceleration of the peak power optimized (OPT, black), the 4 Hz filtered (OPT4, dark gray), and the 2 Hz filtered (OPT2, light gray) motor pattern (Fig. 4) of the Walk-Run ankle at 1.1 m/s walking. Take off is indicated by a vertical line.

which caused the efficiency of the WRA to increase from 37% to 60.3% when using the 2 Hz filter.

Hip and knee angle

No major differences for the OPT, the OPT4, and the OPT2 pattern could be identified. Also the passive trial results in almost similar joint angles (Fig. 9).

Acoustical measurements

Between 20 Hz and 1000 Hz no acoustical trends for the various powered trials can be observed (Fig. 10). Using the WRA passively showed a dominant treadmill sound at these frequencies.

In the high frequency range, starting in the 1000 Hz third-octave band, the differences in the prosthetic control can be clearly distinguished. The highest sound power levels are emitted by the optimized motor pattern (OPT), lower levels were observed when using the filtered control patterns. The lowest sound power levels were achieved with the 2 Hz filter (OPT2).

Sound power emitted from 20 Hz up to 20 kHz can be summed up to give a single value for noise evaluation. However, single values do not give any information about the composition of the emitted sound with respect to frequency. Furthermore an A-weighting (Müller and Möser, 2013) of the spectrum is able to represent human hearing ability.

The single values point out that the prosthesis with the 4 Hz filter in the controller and the treadmill emit approximately the same sound power level (Tab. 3). Emitted sound power can be reduced by 50% by applying the OPT4 control, since a reduction of 3 dB means halving the emitted sound power. In comparison the setup with the 2 Hz control emits only 20% of the sound power of the OPT trial.

As A-weighting does hardly affect high frequencies, the noise levels of the prosthesis are about the same as without the weighting. The sound power level of the treadmill is reduced from

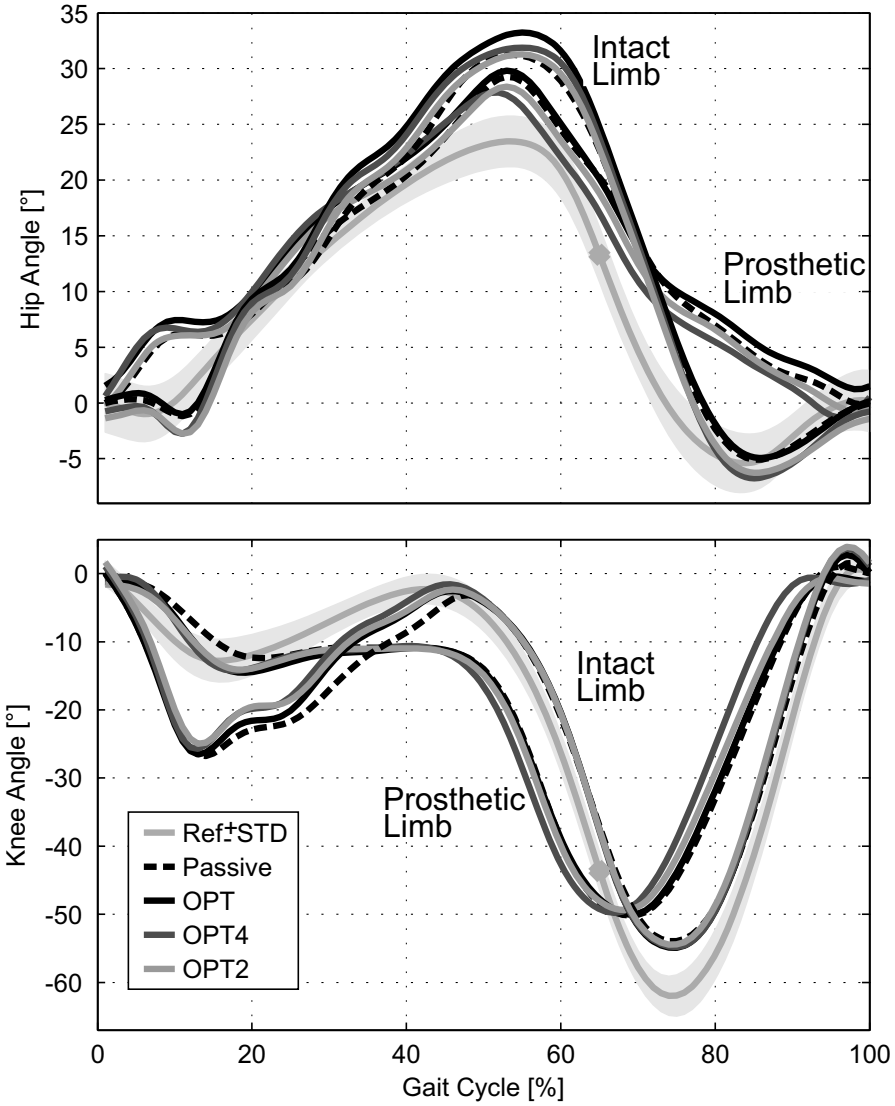

Figure 9: Hip (top) and knee (bottom) angle for the mean of multiple steps using the Walk-Run ankle in different control setups and the mean of healthy human reference subjects (gray). The WRA was used passively (passive, black dashed), with the optimized motor curve (Opt, black solid), with a 4 Hz filtered motor curve (Opt4, gray, solid), and with a 2 Hz filtered motor curve (Opt2, light gray, solid). For the reference data also standard deviation is shown. Data is presented for the gait cycle of 1.1 m/s walking. The take off of the reference is indicated by a gray dot. An increase of the hip and the knee angle imply extension.

81 dB(A) to 78 dB(A) because A-weighting especially reduces sound pressure levels at low frequencies (Morfey, 2000).

8.5 DISCUSSION

In this study it was analyzed how a simplification of a peak power optimized motor pattern affects the gait of a unilateral transtibial amputee. Using a filter of 4 Hz and 2 Hz the nut pattern of a powered ankle prosthesis was modified to include fewer changes in direction and reduced acceleration peaks. When applying these simplifications it was possible to increase the peak pu-

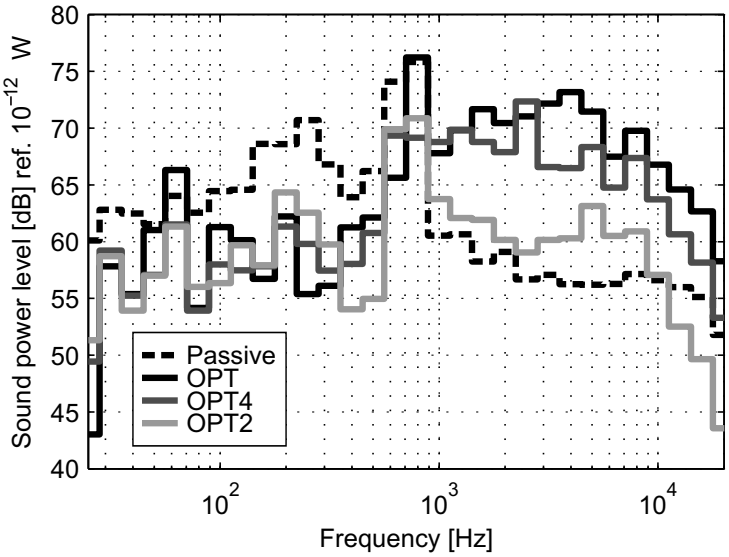

Figure 10: Spectrum of the emitted sound power level in third-octave bands for the peak power optimized (OPT, black solid), the 4 Hz filtered (OPT4, dark gray solid), and the 2 Hz filtered (OPT2, light gray) motor pattern. A passive walking trial (Passive, black, dashed) without motor assistance was used to evaluate sound power of the treadmill.

Table 3: Sound power levels unweighted and A-weighted for the passive trial (Passive + Treadmill), the peak power optimized (OPT) trial and two filtered (4 Hz, 2 Hz) motor patterns. The sound power of the passive trial mainly represents the sound power of the treadmill. Powered trials do not include treadmill sound power.

	Passive + Treadmill	OPT	OPT4	OPT2
unweighted dB(Z)	81	83	80	76
A-weighted dB(A)	78	83	80	75

sh off power at the powered ankle joint. Positive ankle joint work is increasing while electrical energy consumption is decreasing. Such an effect is caused by increased drive and system efficiency. Besides the positive effects on power and energy also the noise of the WRA decreases. As a result of all these improvements the amputee reported to feel most comfortable when using the smoothest nut pattern OPT2.

8.5.1 Gait performance

The peak power optimized nut pattern (OPT) was determined using the methods presented in (Grimmer et al., 2014). The approach uses the multiple steps mean of ankle angle and ankle torque curves from 21 subjects as input data. The determined nut curve must not necessarily provide the best performance for each individual subject. This study demonstrates that the basic model assumptions work well, as the comparison of model and experimental data shows high consistency (Fig. 6). For this study it was assumed that minor adaptations in the nut pattern allow improvements in WRA performance. Particularly the nut velocity change at about 50% to

60% of the gait cycle seems to cause the difference in powered push off for the OPT, the OPT4, and the OPT2 pattern (Fig. 4). The OPT curve is elongating the system by 0.5 mm in this phase. Such a behavior occurs because the stiffness of the spring is predicted to be too high for the required ankle angle change. As a result less energy is saved or already saved energy is released from the spring. In contrast, the OPT2 pattern increases spring loading already starting at 50%. As a consequence more mechanical energy is saved in the spring and less energy is wasted by the motor for damping.

The reduction in motor acceleration during push off provides benefits in electrical energy consumption. A similar effect can be observed during the flight phase. Inertia is less relevant using the filtered patterns, which leads to the increase in drive and system efficiency. Due to the change in nut pattern for the flight phase a clear difference can be observed for the reference and the WRA ankle angle. To which extent such a change influences gait is unknown. Future studies have to proove to which extend the model patterns can be changed without interfering the aimed amputee gait patterns. For the current study knee and hip motion stayed almost unchanged for all powered trials.

Almost similar hip and knee joint angle patterns were identified for the passive and the powered trials. Two reasons may cause this phenomenon. In contrast to most other published data (Grimmer and Seyfarth, 2014) push off peak power of the passive WRA is distinctive (Fig. 8). Provided positive energy is half of the reference (Tab. 2). Thus, the reduced enhancement may result in minor changes in angle patterns.

In addition training effects using the powered ankle may be a reason. The amputee walked 2 minutes with each configuration. No additional training was done before. For an exoskeleton it was shown that 3 days of 30 minutes training could stepwise reduce metabolic costs for walking (Wiggin et al., 2012). It is assumed that an immediate adaptation of the amputee might not occur due to steady biological motor patterns.

8.5.2 Electrical requirements for powered walking

Using the results of this study a first rough battery capacity and weight estimation for an autonomous prosthetic ankle can be performed. Using the 2 Hz filtered motor pattern a powered ankle would require about 37 J per step (1.1 m/s walking) for a 75 kg person. As only one ankle should be replaced, the powered system should be capable to cover half of the 6500 steps/per day (Tudor-Locke and Bassett, 2004). About 33 Wh (120 kJ) will be required to cover one day of level walking. Referring to an energy density of lithium polymer batteries of about 150 Wh/kg (Thackeray et al., 2012) a battery mass of about 0.22 kg would be required. As the preferred walking speed is about 0.2 m/s higher and inclines require increased energy support, an enlargement of the battery capacity should be considered.

8.5.3 Touch down detection and push off timing

For the experiment a very simple algorithm was used for gait control that could not adapt timing during stance. When touch down was identified, nut patterns followed the defined reference pattern depending on the current and the previous step time. Touch down is detected when zero crossing of the shank angular velocity occurs (Fig. 3). For our reference data this happened about 2% to 3% of the gait cycle before touch down. As it was not known how the amputee will behave, no adaptations were made for the control. The amputee walking trials identified zero crossing also early before the real touch down. 3% of gait cycle were observed for the passive

and the OPT, 6% for the OPT4, and 4% for the OPT2 pattern. As a result powered push off will happen 3% to 6% earlier compared to the reference data. Some part of the still existing difference between the time for intact limb push off and the time of prosthetic leg push off might result from this control issue. Malcolm et al. (Malcolm et al., 2013) demonstrated that push off timing is highly relevant to assist human walking gait using a powered exoskeleton. Further studies using the WRA should show how these results are in alignment with push off timing in powered prosthetic amputee walking. A reason for the gap of 6% may be the change in motor direction early before touch down in the OPT4 pattern (Fig. 4). It may cause the shank to change direction of angular velocity earlier than in the other trials.

To solve the control issue a phase shift adaptation of 3% should be included for follow up studies. To avoid gaps like the 6% for the OPT4 curve the adaptation of the motor curve around touch down must be proven. To get more independent of different amputee gait patterns an improved gait detection for experiments would be required. Next to the adaptation for the touch down event it could include an adaptation for the duty factor which is currently defined by the reference data set. Forces, calculated by the motor and the ankle angle encoder or also the accelerometers can provide required information for improvements.

8.5.4 Model stiffness

The optimal stiffness for the WRA was derived from human treadmill walking and running data. During the reference experiments the subjects used athletic footwear (Lipfert, 2010). Markers to determine reference ankle angle were placed at the shoe. The optimal motor pattern was calculated from these data. When including the pattern in the powered prosthesis the stiffness of the shoe and the carbon foot were not taken into account. The stiffness of the Pacifica LP foot was the maximum available to reduce possible effects on the overall system behavior. This study demonstrated that the difference between ankle angle encoder and the kinematic analysis is in the maximum 4° in stance and 3° during flight phase. Including the movement of the foot in the shoe and the shoe stiffness may result in lower differences between observed torques and angles. As a consequence, an adaptation of motor curves would be required when changing shoes in daily life.

By simplifying the motor patterns such an individual adaptation gets lost. The authors assume that a more general pattern is able to deal better with changed footwear but also changed ground stiffness conditions.

8.5.5 Acoustical measurements

Applying changes in the control of the active ankle prosthesis does highly influence the radiated sound power. The emitted sound of the active ankle prosthesis is dominated by frequencies over 1000 Hz. As the human ear is highly sensitive to theses frequencies it is important to find ways to reduce sound emissions in this frequency range. Our research demonstrates that it is possible to reduce sound power by 80% by reducing motor acceleration and changes in motor turning direction.

Future research needs to be done on the acoustics of controlled electric motors and also to identify sound emitted by mechanical parts (belt drive, roller screw drive). Another research area might be the psychoacoustics of active prostheses. Psychoacoustic metrics can give a measure for the annoyance of a sound.

8.6 CONCLUSION

The study on the Walk-Run ankle demonstrated that it is possible to improve powered push off by simplifying peak power optimized motor patterns. Changed nut curves lead to increased efficiency and decreased system noise. Study findings lead to an assumption for an opposing trend. On the one hand, a more general motor pattern, representing main events, improves powered ankle performance. On the other hand further individualization seems to be required for pattern timing. Additional research must show how push off timing can be used to improve amputees gait. Training with the prosthesis, including changing push off timing, may also help to retrain amputees knee and hip movements. In parallel to developments concerning the functionality of powered ankle prostheses, improvements for system noise are required. Modifications on noise producing mechanical parts and psychoacoustic analysis can help to enhance amputees acceptance.

8.7 ACKNOWLEDGEMENTS

Research reported in this publication was supported by the the DFG grant SE1042/8 and the Eunice Kennedy Shriver National Institute of Child Health & Human Development of the National Institutes of Health under award number R43HD072402. The content is solely the responsibility of the authors and does not necessarily represent the official views of the National Institutes of Health.

The authors acknowledge Kevin Hollander for applying the NIH grant. The authors acknowledge Robert Holgate for assisting with the Walk-Run ankle design, sensor integration, wiring, and assembling. The authors acknowledge S.W. Lipfert for providing human reference data.

8.8 AUTHOR CONTRIBUTIONS

Mechanical design: M. Holgate
Electrical design: A. Boehler
Study concept and design: M. Grimmer, A. Grebel
Acquisition of biomechanical and robotic data: M. Grimmer
Acquisition of acoustical data: A. Grebel
Analysis and interpretation of biomechanical data: M. Grimmer, A. Seyfarth, J. Ward, M. Holgate
Analysis and interpretation of electrical data: M. Grimmer, A. Boehler
Analysis and interpretation of acoustical data: A. Grebel, M. Grimmer
Drafting of manuscript: M. Grimmer, A. Grebel
*Revision:*A. Seyfarth, T. Melz, J. Ward, M. Holgate, A. Boehler

8.9 CONFLICT OF INTEREST

M. Holgate, A. Boehler, J. Ward are owners of SpringActive. SpringActive, Inc. supplied the Walk-Run ankle for this research and is actively researching and developing powered ankle prostheses. M. Grimmer, A. Seyfarth and A. Grebel are with the Technische Universität Darmstadt and have no competing interests.

8.10 INSTITUTIONAL REVIEW

The subject who participated in the study gave informed consent according to the guidelines of the ethic commission of the Technische Universität Darmstadt. Experiments were in compliance with the Helsinki Declaration.

The authors will notify the single study subject of the publication of this article.

8.11 REFERENCES

Aldridge, J. M., Sturdy, J. T., and Wilken, J. M. (2012). Stair ascent kinematics and kinetics with a powered lower leg system following transtibial amputation. *Gait & posture*, 36(2):291–295.

Au, S., Weber, J., and Herr, H. (2009). Powered Ankle–Foot Prosthesis Improves Walking Metabolic Economy. *IEEE Transactions on Robotics*, 25(1):51–66.

Beckerle, P. (2014). *Human-machine-centered design and actuation of lower limb prosthetic systems*. Shaker Verlag.

Czerniecki, J., Gitter, A., and Munro, C. (1991). Joint moment and muscle power output characteristics of below knee amputees during running: the influence of energy storing prosthetic feet. *Journal of Biomechanics*, 24(1):63–65.

DIN EN ISO 3745:2012-07 (2012). Acoustics – Determination of sound power levels and sound energy levels of noise sources using sound pressure – Precision methods for anechoic rooms and hemi-anechoic rooms (ISO 3745:2012), German version EN ISO 3745:2012.

Eslamy, M., Grimmer, M., Rinderknecht, S., and Seyfarth, A. (2013). Does it pay to have a damper in a powered ankle prosthesis? a power-energy perspective. In *IEEE International Conference on Rehabilitation Robotics (ICORR)*, volume 2013, pages 1–8.

Frings, S. and Müller, F. (2014). *Biologie der Sinne: Vom Molekül zur Wahrnehmung*. Springer-Verlag Berlin Heidelberg.

Gailey, R., Allen, K., Castles, J., Kucharik, J., and Roeder, M. (2008). Review of secondary physical conditions associated with lower-limb amputation and long-term prosthesis use. *Journal of Rehabilitation Research and Development*, 45(1):15.

Grimmer, M., Eslamy, M., Gliech, S., and Seyfarth, A. (2012). A comparison of parallel-and series elastic elements in an actuator for mimicking human ankle joint in walking and running. In *IEEE International Conference on Robotics and Automation (ICRA), St. Paul*, pages 2463–2470. IEEE.

Grimmer, M., Eslamy, M., and Seyfarth, A. (2014). Energetic and peak power advantages of series elastic actuators in an actuated prosthetic leg for walking and running. In *Actuators*, volume 3, pages 1–19. Multidisciplinary Digital Publishing Institute.

Grimmer, M. and Seyfarth, A. (2011). Stiffness adjustment of a series elastic actuator in an ankle-foot prosthesis for walking and running: The trade-off between energy and peak power optimization. In *IEEE International Conference on Robotics and Automation (ICRA), Shanghai*, pages 1439–1444. IEEE.

Grimmer, M. and Seyfarth, A. (2014). Mimicking human-like leg function in prosthetic limbs. In *Neuro-Robotics*, pages 105–155. Springer.

Günther, M., Sholukha, V., Keßler, D., Wank, V., and Blickhan, R. (2003). Dealing with skin motion and wobbling masses in inverse dynamics. *Journal of Mechanics in Medicine and Biology*, 3(3-4):309–335.

Hollander, K. and Sugar, T. (2005). Design of the robotic tendon. In *Design of Medical Devices Conference (DMD)*.

Lawson, B., Varol, H. A., Huff, A., Erdemir, E., and Goldfarb, M. (2013). Control of stair ascent and descent with a powered transfemoral prosthesis. *IEEE Transactions on Neural Systems and Rehabilitation Engineering*, 21(3):466–473.

Legro, M. W., Reiber, G., Aguila, M., Ajax, M. J., Boone, D. A., Jerrie, L., Smith, D. G., and Sangeorzan, B. (1999). Issues of importance reported by persons with lower limb amputations and prostheses. *Journal of Rehabilitation Research and Development*, 36(3).

Lerch, R., Sessler, G., and Wolf, D. (2009). *Technische Akustik: Grundlagen und Anwendungen*. Springer Berlin Heidelberg.

Lipfert, S. (2010). *Kinematic and dynamic similarities between walking and running*. Verlag Dr. Kovac, Hamburg. ISBN: 978-3-8300-5030-8.

Malcolm, P., Derave, W., Galle, S., and De Clercq, D. (2013). A simple exoskeleton that assists plantarflexion can reduce the metabolic cost of human walking. *PloS one*, 8(2):e56137.

Morfey, C. L. (2000). *Dictionary of acoustics*. Academic Press.

Müller, G. and Möser, M. (2013). *Handbook of engineering acoustics*. Springer-Verlag Berlin Heidelberg.

Robbins, C., Vreeman, D., Sothmann, M., Wilson, S., and Oldridge, N. (2009). A review of the long-term health outcomes associated with war-related amputation. *Military Medicine*, 174(6):588–592.

Rossing, T. D. (2007). *Springer handbook of acoustics*. Springer.

Sup, F., Varol, H. A., and Goldfarb, M. (2011). Upslope walking with a powered knee and ankle prosthesis: initial results with an amputee subject. *IEEE Transactions on Neural Systems and Rehabilitation Engineering*, 19(1):71–78.

Thackeray, M., Wolverton, C., and Isaacs, E. (2012). Electrical energy storage for transportationŮapproaching the limits of, and going beyond, lithium-ion batteries. *Energy & Environmental Science*.

Tudor-Locke, C. and Bassett, J. (2004). How many steps/day are enough?: Preliminary pedometer indices for public health. *Sports Medicine*, 34(1):1–8.

Ward, J., Schroeder, K., Vehon, D., Holgate, R., and Grimmer, M. (2014). A microprocessor controlled ankle-foot prosthesis that supports fill powered running. In *American Orthotic & Prosthetic Association (AOPA)*.

Wiggin, M., Collins, S. H., and Sawicki, G. S. (2012). A passive elastic ankle exoskeleton using controlled energy storage and release to reduce the metabolic cost of walking. In *Proceedings 7th Annual Dynamic Walking Conference*, pages 24–25.

9 Conclusion

The thesis *Powered Lower Limb Prostheses* aimed at improvements in lower limb prostheses. For this, biomechanical requirements to mimic the human ankle joint behavior in walking and running were analyzed. Models of elastic actuators were developed to mimic human joint behavior using mechanical structures. Different alignments of motors and springs were evaluated to represent the function of muscle fibers and tendons of the muscle-tendon complex. It was the aim to develop a controller for walking and running for testing the model predictions on the motor - spring interaction using a powered prosthetic ankle.

Next to the main targets, the thesis analyzed requirements for an artificial knee and hip joint. In addition, optimized walking control patterns were simplified to evaluate improvements on the powered ankle performance, the energy efficiency and the noise generation.

Modeling of elastic ankle actuation

Analyzes on human joint behavior in walking and running revealed that it is challenging to achieve required acceleration, velocity and torque with current motor technology. Thus the biologically inspired interaction of a motor and springs was investigated with respect to its ability to achieve human ankle gait biomechanics. Theoretical calculations demonstrated that series and parallel springs can help to decrease the peak power requirements and the energy consumption of a motor. Complex systems, including parallel and series springs, allow to achieve higher benefits for a single condition like walking at 1.6 m/s. However, if changes in the speed or the gait are required, complex mechanical solutions are less efficient and may cause disadvantages. Thus a simple actuation mechanism like a series elastic actuator seems to be preferable to achieve flexibility for human ankle requirements in daily life.

Experimental model evaluation

A powered ankle prosthesis prototype was used to evaluate the model predictions of the motor - spring interaction. It was tested if the user of the artificial ankle interacts with the system in the expected way. The spring stiffness may be inappropriate and the motor patterns may disturb dorsal flexion or plantar flexion of the foot. Also, the users' timing and the loading of the artificial ankle may differ from the values determined using healthy reference subject means. It was found that the optimized model behavior showed surprisingly good agreement with the experimental observations for walking gait. For a medium running speed, the joint angle and the torque tracings could be almost reproduced with the prosthesis. Higher running speeds could not be evaluated successfully due to suboptimal stiffness values and limitations in the motor power output. Results of the Manuscripts V and VI demonstrated that the model predictions on the assistance achieved by the spring worked quite well for walking and running. The use of springs makes it possible to assist the motor to achieve human-like ankle angle, power, and torque patterns in an artificial ankle.

Alignment of prosthesis actuators

In addition to the ankle, biomechanical requirements were also evaluated for artificial human knee and hip joints. The studies showed that a knee actuator can clearly benefit from a series spring, while a series spring for a hip actuator is less beneficial. The results for the hip series

elastic actuator raised the question on the alignment of the actuators. Current approaches used monoarticular actuators to mimic human like joint function for walking and running. In contrast, humans use both mono- and biarticular muscles coupling the hip, the knee and the ankle joint. It is assumed that these multi-joint linkages can further improve artificial leg function by reducing peak power and energy requirements, and by reducing the effort for locomotion control. Further analysis must resolve how these couplings may help to improve artificial leg efficiency for different gaits and speeds.

Prosthesis performance improvements

The peak power optimized motor patterns for the ankle actuator accomplish the deformation of the spring to match required joint ankle and torque behavior. The optimization is not including motor model parameters like electrical efficiency, friction, and inertia. Depending on the reference data (gait, speed) the motor trajectories can be unfavorable for the motor, e.g. changes in motor turning direction and high accelerations can be demanded. In Manuscript VI it was shown that by reducing these demands, improvements for the powered ankle are possible. A simplified motor walking control pattern can help to improve the powered ankle performance, the energy efficiency and to reduce the noise. The study also demonstrated that the hip and the knee angle tracings did not change considerably between the trial where the powered ankle was used actively or just passively. Also the gait asymmetry between the intact and the prosthetic limb of the amputee was not much affected by additional actuation of the WR ankle. It is assumed that changes in push off timing and training may further improve the amputee gait. Future studies need to be done to investigate if it is possible to retrain biological motor patterns of the proximal muscles actuating the knee and the hip joint. This was not possible during the short experimental trials in the gait lab. It may be realized by an increased time of usage. On the other hand it is possible that user movement patterns are fixed to the strategies used over several years with the passive daily life prosthesis. By varying push off timing of the artificial ankle it may be possible to retrain the locomotion motor patterns to reduce gait asymmetries. In combination with biarticular couplings differences of affected and unaffected leg kinematics and kinetics may be reduced.

Prosthesis weight, noise and user perception

Walking studies with the female amputee (55 kg) also brought up additional points for powered ankle improvements.

When walking through the lab after the measurements with her passive daily life prosthesis, the transtibial amputee reported to miss the powered push off with the Walk-Run ankle. On the other hand the amputee appreciated the reduced system weight of the passive carbon foot. In combination with the socket and the liner, the weight of the powered prosthesis is more than 1 kg above the biological leg. Including embedded electronics and a battery will further increase this difference. Thus an additional optimization for system weight should be included in upcoming designs. Alternatively, an improved fitting of the socket and the residual part of the shank may reduce this perception.

By smoothing the motor curves, the noise output of the prosthesis decreased dramatically. Further studies should analyze the components that mainly cause the noise. Improvements on efficiency and using insulation can further reduce the noise. If it is possible to modify occurring sound frequencies, psychoacoustic analyzes can help to identify less annoying frequencies to improve the amputee's acceptance.

Aside from the noise and the function also the design of the prosthesis was discussed with the 17 years old female amputee. The Walk-Run ankle prototype was perceived to appear to technical. Designs like the Odyssey ankle (Springactive), using a colored housing, may achieve higher acceptance. Apart from the visual effects, a full cover of the prosthesis can make such a system less noisy, more secure, and waterproof.

Prosthesis control

In the study of Manuscript V a controller for walking and running was developed. To perform the experiments and to guarantee a secure handling of the Walk-Run ankle also a standing mode was included in the control approach. The control makes it possible to change from walking to running at each desired speed up to a limit of 2.6 m/s. The motor assistance is adapted until 4 m/s running. Higher speeds only include an adaptation of the timing. To avoid jumps in the motor pattern, the gait changes from walking to running were not made directly when changing gait. The control waits until the touch down of the next step to adapt the motor trajectory. In contrast, stopping results in a direct response to ensure users safety. Further research and testing is required to improve the transitions between walking and running. Currently, the hip has to inject more than the usual energy for the gait transition to running. An improved assistance of the ankle joint for transition, but also changes in speed, would decrease the users' effort.

Improvements on the powered prosthetic control is one major field for upcoming research. Most of the lower limb prostheses use computational intrinsic control that works on the basis of force, angle, or inertial sensors at the prosthesis. The user intention is not directly distinguished from brain signals. The computational intrinsic control works well for continuous cyclic movements like walking or climbing stairs. Interactive extrinsic control would allow to use the prosthesis like a healthy part of the body. Voluntary powered ankle prosthesis movements, like pressing the gas pedal of a car, would be initiated by the users direct movement command. First steps to such a technology are tested using EMG sensors, similar to powered prosthetic hands (e.g. Michelangelo, Ottobock). Combining the methods, regarding intrinsic control for continuous locomotion and extrinsic control to adapt to a changing user intention, could bring the advantages of both control strategies together.

Research context

The thesis identified a huge potential for springs to assist motors to mimic the human lower limb joint kinematics and kinetics during gait. The results on the reductions of motor peak power requirements and energy consumption help to understand how human muscles may be used efficient to benefit as much as possible from the elastic tendon function.

The observed insights on the efficient cooperation can be used to improve the design and the control of powered lower limb prostheses. In contrast to passive prostheses, movement performance and thus amputees assistance and quality of life may improve.

Similar technologies can be used to improve exoskeleton design to assist elderly and subjects with mobility impairments. In addition elastic exoskeletons may augment human performance in daily life or workers environments.

Next to assisting human movement, the elastic actuators may advance the gait performance, the gait robustness, and the operation time of bipedal robots.

Thus the results of the thesis *Powered Lower Limb Prostheses* are not limited to the specific field of prosthetics but may also be useful for applications like exoskeletons and legged robots.

Martin Grimmer

Curriculum Vitae

Education

02/2015	Phd, Dr. rer. nat. at Technische Universität Darmstadt (D) Grade: summa cum laude - excellent
Dissertation:	Powered Lower Limb Prostheses
09/2008	Diploma in Sports Science at Friedrich Schiller Universität Jena Grade: very good
Thesis:	Biomechanik des Ganges bei Ober- und Unterschenkelamputation - Analyse und mechanische Intervention

Experience

03/2015 - 10/2015	Researcher at Harvard Biodesign Lab, Harvard University, School of Engineering and Applied Sciences, Cambridge (USA)
10/2011 - 03/2015	Researcher at Lauflabor Locomotion Laboratory and University Lecturer, Institute of Sports Science, Technische Universität Darmstadt (D)
07/2012 - 09/2012	Research Internship at Arizona State University and Springactive (USA)
02/2009 - 12/2011	Researcher at Lauflabor Locomotion Laboratory, Institute of Sports Science, Friedrich Schiller Universität Jena (D)
10/2008 - 01/2009	Research Assistant at Lauflabor Locomotion Laboratory, Institute of Sports Science, Friedrich Schiller Universität Jena (D)

Fellowships

03/2015 - 10/2015	Robert Bosch Fellowship on Aging Research at Harvard Biodesign Lab, Harvard University, School of Engineering and Applied Sciences, Cambridge (USA)